Tungsten Biochemistry in *Pyrococcus furiosus*

Tungsten Biochemistry in *Pyrococcus furiosus*

Proefschrift

ter verkrijging van de graad van doctor
aan de Technische Universiteit Delft,
op gezag van de Rector Magnificus Prof.dr.ir. J. T. Fokkema,
voorzitter van het College voor Promoties,
in het openbaar te verdedigen op maandag 10 maart 2008 om 15:00 uur

door

Loes Elizabeth BEVERS

doctorandus in de scheikunde
geboren te Nijmegen

Dit proefschrift is goedgekeurd door de promotor:
Prof.dr. W. R. Hagen

Samenstelling promotie commissie:

Rector Magnificus	voorzitter
Prof.dr. W. R. Hagen	Technische Universiteit Delft, promotor
Prof.dr. G. Schwarz	Universität zu Köln
Prof.dr. S. de Vries	Technische Universiteit Delft
Prof.dr. J. H. de Winde	Technische Universiteit Delft
Prof.dr. J. van der Oost	Wageningen Universiteit
Dr. A. Magalon	Laboratoire de Chimie Bactérienne, IBSM, CNRS, Marseille
Dr. P.L. Hagedoorn	Technische Universiteit Delft

This research has been financed by a grant from the Council for Chemical Sciences of the Netherlands Organization for Scientific research (NWO) (700.51.301).

Cover design by Esengül Yildirim

Contents

Aim and outline of thesis

This thesis describes a study on the role of the metal tungsten in the hyperthermophilic archaeon *Pyrococcus furiosus*. *P. furiosus* can be considered as a model system for hyperthermophilic archaea; its genome has been sequenced [1], the organism can be cultivated easily in a batch or continuous culture [2,3], and many of its proteins have been the subject of studies in recent years. *P. furiosus* can also be considered as a model system with respect to its tungsten metabolism. Cultivation studies showed a strong tungsten-dependent growth [2], and in the last decades four tungsten containing aldehyde oxidoreductases (AORs) were purified from *P. furiosus* cell-free extract [4-7].

The aim of this thesis project was to extend the knowledge on different aspects of tungsten metabolism in *P. furiosus* by trying to answer some fundamental questions: how do the cells take up the tungstate from the media? Can they also take up molybdate and incorporate the molybdenum in the active site of the AOR enzymes? To what extent is tungsten-cofactor (Wco) synthesis similar to molybdenum–cofactor (Moco) synthesis? And can we identify new tungsten-containing enzymes in *P. furiosus*?

The results of this study are presented in this thesis in the following order: **Chapter 1** provides a general introduction to the bioinorganic chemistry of tungsten. Repeatedly, reference is made to the homologous metal molybdenum, whose literature is generally more developed both for biological and model systems.

The presentation of the experimental data is divided into three parts representing different aspects of tungsten metabolism: uptake, incorporation, and catalytic action. **Part I** starts with the uptake of the metal from the media by describing the identification and characterization of the *P. furiosus* periplasmic tungstate binding protein (WtpA) (**chapter 2**). This protein, part of an ATP binding cassette (ABC) transport system, has an extremely low K_D for tungstate ($K_D = 17 \pm 7$ pM) but is also able to bind molybdate with a relatively high affinity ($K_D = 11 \pm 5$ nM).

Part II focuses on a subsequent step of tungsten metabolism; the incorporation of the metal into the pterin cofactor in order to tune its redox properties in a manner required for biological activity. In **chapter 3**, the hexameric *P. furiosus* MoaB protein is shown to catalyse the adenylylation of metal-binding pterin (MPT) as activation step prior to metal insertion. This finding shows that adenylylation of MPT is a conserved step in Wco/Moco biosynthesis in both prokaryotes and eukaryotes. The subsequent step of metal insertion catalyzed by the *P. furiosus* MoeA proteins is investigated in **chapter 4.**

Chapter 5 presents the *in vivo* incorporation of tungsten-homologous molybdenum into the cofactor of the *P. furiosus* AOR enzymes. So far, these enzymes had only been purified containing tungsten in their active site.

Part III focuses on the tungstoenzymes. **Chapter 6** describes the purification and biochemical characterization of a new AOR, tungsten oxidoreductase number five (WOR5), which completes the family of *P. furiosus* AORs. The gene adjacent to *wor5* (PF1479) encodes a putative four [4Fe-4S] clusters binding protein, which distinguishes WOR5 from

the other (monocistronic) AORs. **Chapter 7** provides a study on this PF1479 protein and proposes it to form a heterodimeric structure with WOR5, localized in the periplasmic space.

Chapter 8 describes the redox chemistry of the tungsten and iron-sulfur prosthetic groups in *P. furiosus* formaldehyde oxidoreductase (FOR). In addition, the K_M value for formaldehyde is suggested to be three orders of magnitude lower than previously reported, due to an unfavorable hydratation equilibrium which converts free formaldehyde into methylene glycol. Finally, **chapter 9** contains the concluding remarks and perspectives for future research, and is followed by **chapter 10**: a summary of all the results.

References

[1] F.T. Robb, D.L. Maeder, J.R. Brown, J. DiRuggiero, M.D. Stump, R.K. Yeh, R.B. Weiss, D.M. Dunn, Meth. Enzym. 330 (2001) 134.

[2] G. Fiala, K.O. Stetter, Arch. Microbiol. 145 (1986) 56.

[3] N. Raven, N. Ladwa, D. Cossar, R. Sharp, Appl. Microbiol. Biotech. 38 (1992) 263.

[4] S. Mukund, M.W. Adams, J. Biol. Chem. 270 (1995) 8389.

[5] S. Mukund, M.W. Adams, J. Biol. Chem. 266 (1991) 14208.

[6] R. Roy, S. Mukund, G.J. Schut, D.M. Dunn, R. Weiss, M.W.W. Adams, J. Bacteriol. 181 (1999) 1171.

[7] R. Roy, M.W.W. Adams, J. Bacteriol. 184 (2002) 6952.

Chapter 1

The Bioinorganic Chemistry of Tungsten

Loes E. Bevers
Peter-Leon Hagedoorn
Wilfred R. Hagen

Adapted from: Coordination Chemistry Reviews (2008) *in press*

Abstract

Tungsten is widely distributed in biology, however, the majority of the tungsten-containing enzymes purified to date, originates from anaerobic archaea and bacteria. Tungsten coordination complexes incorporated in these enzymes can be studied with similar analytical and spectroscopic techniques as tungsten model compounds. The metal is taken up by cells in the form of tungstate, and subsequently it is processed into a sulfur-rich coordination as part of a metal-organic cofactor referred to as tungstopterin, which is equivalent to the molybdopterin forms found as active centers in several molybdenum-containing enzymes. For biology tungsten is significantly different from molybdenum and this review focuses on the (bio)molecular basis of this differential cellular use of W compared to Mo in terms of their active transport, cofactor synthesis, and functioning as catalytically active sites.

Introduction

Tungsten is the bioelement with the highest atomic number, 74, and the only bioelement in the third transition row of the periodic table. Tungsten is widely distributed in biology, however, it is not a universal bioelement. For some species tungsten is essential: their life depends on the presence of the element; for other species tungsten is a facultative bioelement: they choose to make biological use of the element when they experience specific environmental constraints; for the remaining species tungsten is biochemically indifferent or possibly xenobiotic: they have not developed a functional use of the element, although, upon its inadvertent intake, their physiology may well be affected. Present knowledge places all eukaryotes, including man, in the last category. Two fundamental questions form the Leitmotif of this review; the first one is the 'why'-question: why do some cells go for tungsten chemistry and others not? The second is the 'how'-question: how do cells discriminate between tungsten and molybdenum.

Molybdenum is in many ways the twin element of tungsten. Also in biology the coordination chemistries of W and Mo are similar in structural and functional aspects. Molybdenum is the only bioelement in the second transition row. Like tungsten it is widely, though possibly not universally, distributed in biology. Its usage appears to be to a considerable extent the mirror image of that of tungsten. Some forms of life, e.g. humans, are strictly dependent on the availability of Mo while they are independent of W; other species, e.g. the archaeon *Pyrococcus furiosus*, have no apparent use for Mo, while they are strictly dependent on W; yet other species, e.g. the archaeon *Methanobacterium thermoautotrophicum*, appear to be able to choose between W and Mo as a function of a variable environment. And yet other species, e.g. the archaeon *Pyrobaculum aerophilum*, may have learned to employ the chemistries of Mo and W simultaneously for distinct functions. Mo-biochemistry and W-biochemistry are presently both very active areas of research, the latter in particular in relation to the fundamental why and how questions formulated above. Mo has been known to be a biological trace element for a long time, and the development of its biochemistry has commonly been taken to be an endeavor in its own right. The identification of tungsten as a bioelement is from a more recent date, and thus, it has come naturally to develop its biochemistry in comparison to that of molybdenum. Several aspects of Mo-biochemistry have been covered in recent reviews [1-4]. This review takes a tungsten vantage point and uses molybdenum for contrast. Early reviews on aspects of W-biochemistry can be found in [5-7].

Aqueous chemistry of tungsten

Since water is the only life-compatible solvent, the aqueous chemistry of tungsten is of relevance. The basic geochemical conditions for an element to qualify for general use in biology are a diffuse distribution over the surface of the earth and a reasonable solubility in

water. Both conditions hold for tungsten (and for molybdenum as well). Scheelite and wolframite are not unusual ores, and global leaching has resulted in an average tungsten concentration in the oceans of circa 10^{-4} ppm or ≈1 nM. It has been argued that a circa two orders-of-magnitude higher concentration of molybdenum in oceanic waters could be at the basis of a presumed preference for Mo over W in biology [8] [6], however, the oceanic concentration of cobalt, a universal bioelement, is of the same order, or less, of that of tungsten.

The dilute aqueous speciation of tungsten in water is presumably completely dominated by the tungsten(VI) oxoanion WO_4^{2-} over a wide range of pH and redox-potential values [9] that would cover conditions found in most of the terrestrial inhabitable environments, and so tungstate is likely to be the only molecule that cells in search of tungsten have to deal with. At increased concentrations a kinetically, and thermodynamically complex polyoxoanion chemistry evolves [10]. Thus the entry point of W-biochemistry is a stable, redox indifferent, highly soluble oxoanion; and it has a Mo congener of very similar properties including an anion radius of circa 1.74 Å [11].

Basics of tungsten biology

The top most systematic level of division of life on earth is into the three domains of eukaryotes, bacteria, and archaea (figure 1). The systematics of tungsten biochemistry is already significant at this level: there appears to be, respectively, no, occasional, and frequent usage of W in the three domains. It has been suggested that in an evolutionary sense tungsten is an ‘old’ element on its way to be replaced by ‘modern’ molybdenum (similarly nickel has been suggested to be in the course of being replaced by cobalt) [8]. This idea appears to be supported by the significant correlation between archaeal life and W-biochemistry. The name archaeon (previously: archaebacterium) is of course intended to transmit the notion that these forms of life are thought to be the most similar to ‘primitive’ life as it must have existed in early geological times not long after the appearance of the first living cell. It should, however, be realized that archaea, similar to bacterial or eukaryal monocellular organisms, typically have doubling times of the order of 10^{-1} to 10^{1} hours and, therefore, have a life span of the order of 10^{-2} year, i.e. a very brief moment on geological time scales. Archaea are modern organisms that live today and that do not show any sign of decreased fitness for survival at all. On the other hand, there appears to be a clear over-representation of archaea in ‘extreme’ habitats: e.g., the vast majority of hyperthermophiles (species with optimal growth temperature above 80 ˚C) consists of archaea. However, a link between W usage and extremophilicity is not immediately obvious, and the relation, if any, may well be a rather indirect one: most archaea are anaerobes (or perhaps microaerophiles) and the link may simply be one of mutual exclusion of molecular oxygen and tungsten biochemistry.

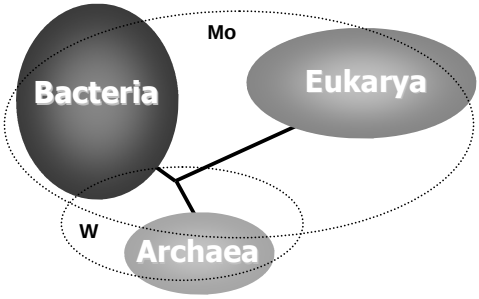

Figure 1. The tree of the three domains of life and the distribution of tungsten and molybdenum containing enzymes: molybdenum enzymes are found in all forms of life whereas the occurrence of tungsten enzymes appears to be restricted to archaea and some bacteria.

In general, the biochemistry of a metal in a monocellular organism encompasses several processes (figure 2): sequestering and transport over the cytoplasmic membrane, storage and release, metal-cofactor biosynthesis, metalloenzyme catalysis, and metal-controlled regulation of transcription and /or translation. Our present knowledge of these processes in relation to tungsten is not particularly balanced: tungsten-based biocatalysis is by far the best studied; the processes of tungsten transport and tungsten cofactor biosynthesis are emerging research areas; we are essentially ignorant on the remaining processes of storage and regulation. For the latter there is limited information from molybdenum biochemistry, and this may help in designing experiments to determine if comparable tungsten-related processes exist.

Tungsten is sequestered and transported into the cytoplasm as tungstate. It may then enter the biosynthetic machinery to be bound to a dithiolene-functionality of a tricyclic pterin moiety to form tungstopterin (W-MPT) (figure 2A) and eventually end up in tungstoenzymes in the form of a complex metal-organic cofactor: tungsto-bispterin (W-bis-MPT) or tungsto-bispterin guanine dinucleotide (W-bis-MGD) (figure 2B).

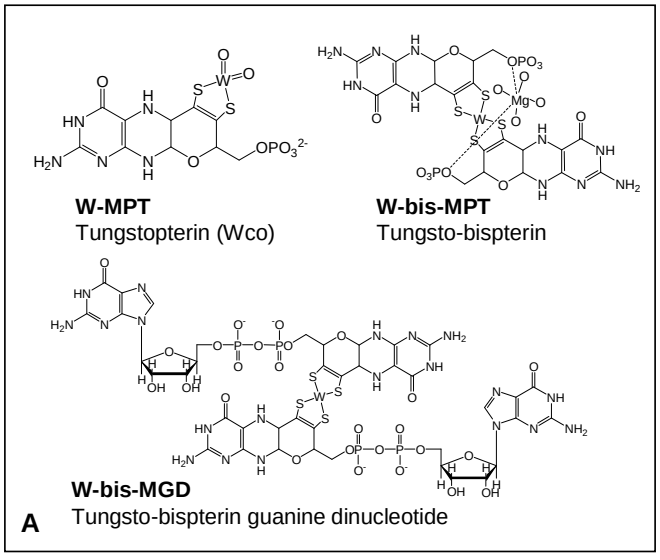

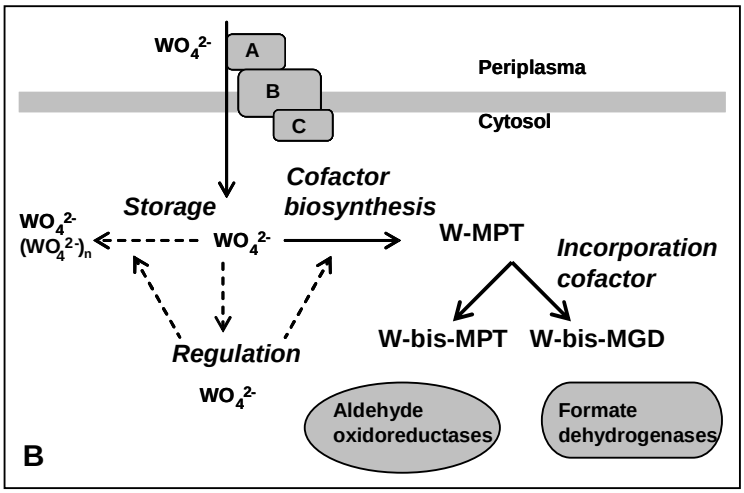

Figure 2. The structure of tungsten containing pterin cofactors and intermediates: tungsten containing metal binding pterin (W-MPT) (I), tungsto-bispterin (W-bis-MPT) (II), tungsto-bispterin guanine dinucleotide (W-bis-MGD) (III) (A). A schematic overview of the stages in cellular metabolism of tungsten (in various chemical forms): uptake, storage, regulation, cofactor biosynthesis, and incorporation in enzymes. Dashed arrows correspond to hypothetical processes based on cellular processes known for molybdate (B).

Spectroscopy of tungsten

The molecular spectroscopy of tungsten associated with biomolecules poses a number of considerable challenges, which find their origin not only in the physics of the methodology but also in practical biochemical problems. A key issue is the redox chemistry of the element, i.e. the availability of the three oxidation states +IV, +V, and +VI, over a relatively narrow potential window in combination with the tendency of W(V) to disproportionation. Tungstoenzyme preparations (and molybdoenzymes similarly) are frequently found to exhibit inhomogeneity in terms of oxidation state. Furthermore, they tend to be mixtures of holo- and apoenzyme (i.e. protein that has lost, or never received, the metal cofactor), and of active, inhibited (e.g., by substrate or product) and inactivated (e.g., by molecular oxygen) enzyme forms. Common as these problems may be at this time, they are presumably eventually solvable with careful protein production, purification, and characterization procedures. Unfortunately, this may not hold true for the problems of sensitivity and resolution intrinsic in tungsten spectroscopy.

NMR and Mössbauer spectroscopy

A decade ago we attempted an evaluation of the potential applicability of NMR and Mössbauer spectroscopy on W-proteins. It was then estimated that ^{183}W (I=1/2) NMR, in which a very high resolution is counterbalanced by an extremely low sensitivity, would be applicable to proteins only in a dedicated, very labour-intensive program [5]. Since then no papers have appeared on W-protein NMR, and, in fact, the literature on W-NMR in general is limited, and gives indications of a detection limit (e.g., > 0.1 M [12]) that would suggest it to be wise to exclude W-protein NMR for consideration in the foreseeable future.
In a similar vein, we considered ^{182}W ($I_{ground} = 0$; $I_{exited} = 2$; parent $t_{0.5}$ = 115 days) as a target for biological Mössbauer spectroscopy, and we suggested that W would be somewhat more difficult than Ni, a nucleus that was, at the time, actively explored for its potential in Mössbauer studies on nickel proteins [5]. Since then no papers have appeared on the Mössbauer effect in Ni- or in W-proteins, and the literature on tungsten Mössbauer in general over the last ten years is almost non-existent [13]. Again, one can fairly conclude that Mössbauer spectroscopy on tungstoproteins is not an advisable research subject at this time.

Optical spectroscopy

Fortunately, a somewhat brighter picture can be drawn now for optical spectroscopy on tungstoenzymes, which is another subject on which no primary literature existed ten years ago. Dimethyl sulfoxide reductase (DMSOr) is a member of a small subgroup of molybdoenzymes that do not carry any prosthetic group in addition to the molybdopterin active center. In the DMSOr from *Rhodobacter capsulatus* Mo can be replaced with W with retention of activity and without detectable change in the 3D structure of the rest of the molecule [14]. Both the Mo(VI) and the W(VI) version of this enzyme exhibit an optical spectrum with a number of absorption bands extending all the way into the IR and with extinction coefficients of the order of $\varepsilon \approx 2\ mM^{-1}cm^{-1}$ (figure 3 [14]).
The spectra have been qualitatively interpreted in terms of metal to sulfur charge transfer with reference to model compounds [14]. Also, considerable changes occur upon metal reduction during catalytic turnover, and this has been used as a monitor in a pre-steady-state kinetics study of the molybdoenzyme [15], however, a quantitative characterization of the complete spectra of any other form than the fully oxidized enzyme has not been reported yet.

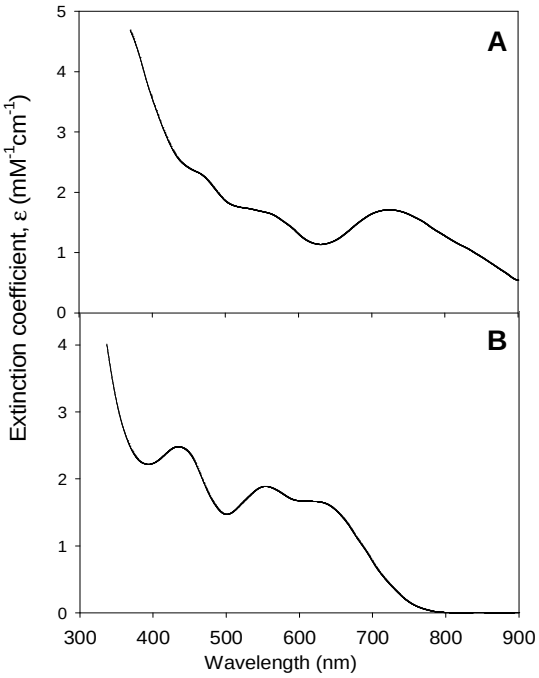

Figure 3. UV/visible absorption spectra, recorded at room temperature for molybdenum containing DMSOr (A) and tungsten containing DMSOr (B) (data reproduced from [14] with permission; the spectra have been re-plotted on an absolute absorption scale).

The typical molar extinction coefficient of 2 $mM^{-1}cm^{-1}$ implies a problem of sensitivity in optical studies of complex enzymes. The vast majority of tungstoenzymes and molybdoenzymes carry, in addition to their metallopterin active center, one or more cofactors for electron transfer. The collection of electron transfer cofactors can be quite complex in some molybdoenzymes where one can find combinations of Fe/S clusters with flavins and/or hemes resulting in a swamping by these strong absorbers of the relatively modest absorption spectrum of the metallopterin. Tungstoenzyme members of the aldehyde oxidoreductase (AOR) family (defined below) are a special case in that they carry, in addition to the tungsto-bispterin, only a single $[4Fe\text{-}4S]^{(2+;1+)}$ cluster. Although the extinction coefficient of the latter in its oxidized form is circa an order of magnitude greater than that of the tungstopterin, the shape of the spectrum is relatively simple with only a single, broad band peaking at circa 390-430 nm and gradually falling off to zero absorption towards circa 700 nm. The use of the relatively weak tungstopterin optical spectrum from these enzymes as a monitor in kinetic measurements has recently been employed in a study to delineate the redox intermediates in the reaction cycle of *P. furiosus* formaldehyde oxidoreductase (FOR) [16].

No resonance Raman data on tungsten enzymes have been reported in the primary literature. A peak at 874 cm^{-1} in the resonance Raman spectrum of *P. furiosus* FOR has been cited to be assignable to a W=O stretch frequency [17].

EPR spectroscopy

EPR spectroscopy of tungstoenzymes is relatively uncomplicated from the spectroscopist's point of view: oxidized W(VI) is diamagnetic, $[Xe]5d^0$; reduced W(IV) is d^2 and could in principle be high-spin, however, the spin state has not been determined in tungstoproteins or tungstopterin model compounds, and no paramagnetism has been reported for this oxidation state. The intermediate W(V) is $5d^1$ and S=1/2. From the positive sign of the spin orbit coupling constant for systems with less than half filled shells basic theory predicts the g-values to be less than that of the free electron value, g_e=2.0023, however, occasionally one can find one or two of the g-values to be greater than g_e possibly related to relativistic effects, and/or extensive charge transfer from S (or Se) ligands. Experimental g-values reported for tungstoenzymes are typically in the range 1.99 - 1.83 [7], and the deviation from g_e as well as the overall g-anisotropy are somewhat more pronounced than in molybdoenzymes. Natural tungsten consists of five isotopes, only one of which has a nuclear spin: ^{183}W occurs in a natural abundance of 14.4% and has a nuclear spin I=1/2. The isotope is frequently detectable in the S=1/2 spectra of W(V) in the form of small satellite lines with circa 7% relative intensity [18] (figure 4 [19]) and this is a unique fingerprint for the element. The hyperfine splitting along the principal g-tensor axes is some 30-80 Gauss, or approximately a few times the inhomogeneous line width [7], i.e. the pattern is frequently well resolved. Characteristically, for S=1/2 systems that lack extreme g-anisotropy the spin-lattice relaxation rate is relatively slow, and the spectra can be observed at least up to ~77 K without significant broadening. When a cryogenic He-flow system is in place (to detect heme or iron-sulfur prosthetic groups at low temperatures) tungsten S=1/2 signals are conveniently detected at circa 40-50 K. The relatively slow relaxation rate would seem to make W(V)-proteins quite suitable for high-resolution hyperfine spectroscopy through pulsed double resonance experiments (ESEEM, pulsed ENDOR). No data are available yet, but fruitful experiments on molybdoenzymes have been reported in particular by the Enemark group [20]. Finally, the ease of the EPR spectroscopy should perhaps be put into perspective by contrasting it to the complexities of the (bio)chemistry of W(V): multiple stable W(V) forms may well be enzyme dead-end products rather than catalytically competent intermediates [16,21,22].

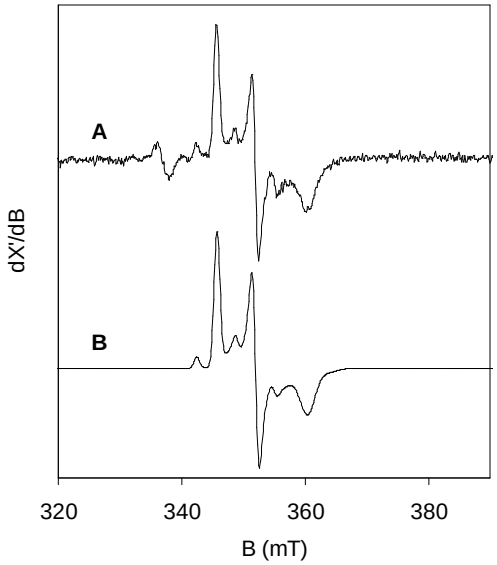

Figure 4. W(V) S=1/2 EPR from tungstoproteins is typically weak due to substoichiometry of the intermediate redox state, but is easily identified from the satellite hyperfine lines of the ^{183}W isotope (14.4%, I=1/2). This example, recorded at 9.43 GHz and 22 K, is from *Pyrobaculum aerophilum* AOR (A). The simulation has g_{xyz}= 1.948, 1.914, 1.870 (B) (reproduced from [19]).

If EPR is easy and optical spectroscopy (of enzymes with additional cofactors) is difficult, then what about their combination in the form of magnetic circular dichroism, MCD, of tungstoenzymes? Good quality, variable cryogenic temperature W(V) MCD data have been reported for *P. furiosus* AOR [21] and FOR [22] at reduction potentials where the iron-sulfur cluster is diamagnetic (at low temperatures) with multiple bands in the 300-800 nm range plus a near-IR band at 880 nm all assigned to S-to-W(V) charge transfer transitions. Unfortunately, cryogenic MCD detection requires high-quality transparent glasses, which means that glassing agents, typically 50% or more glycerol, have to be added to the sample, and this causes essentially complete inhibition of enzyme activity [21,22]. Sucrose may be used instead of glycerol to overcome this problem.

EXAFS spectroscopy

EXAFS spectroscopy at the L_{III}-edge of W (circa 10.2 eV or 1.22 Å) was initially explored by Cramer et al. on formate dehydrogenase (FDH) of *Clostridium thermoaceticum* [23], (now: *Moorella thermoacetica*) but this early work was hampered by low signal intensity and an ill defined redox state of the tungsten [24]. George et al. studied *P. furiosus* AOR with cryogenic W-EXAFS before high-activity preparations of this enzyme had become available. The W-coordination in the low-activity AOR, known as “red tungsten protein”, was proposed to be by three S, two oxo, and possibly one more N/O ligand [24]. The S/O

ratio is lower than in the X-ray structure that was later determined for the active *P. furiosus* AOR [25] suggesting that red-tungsten protein is an oxidative degradation product of AOR. A revisit of AOR EXAFS has not been reported yet. Metalloprotein EXAFS spectroscopy is most fruitfully applied when specific questions on coordination can be asked based on available X-ray structures, and the first example of such an approach is in the combined crystallographic and spectroscopic study of Stewart et al. on *R. capsulatus* W-substituted DMSO reductase [14]. The W(VI) data from oxidized enzyme were interpreted in terms of four equivalent dithiolene S ligands at 2.4-2.5 Å, the O^{γ} of Ser147 at 1.9 Å, a second O ligand at 1.9 Å, and possibly a third O close to one of the S. This coordination is consistent with X-ray structural data and is essentially identical to that previously determined for the native Mo(VI)-version of this enzyme, thus defining the protein as an excellent model to study intrinsic differences in redox properties between the two metals [26]. Tungsten oxidation state dependent EXAFS has been initially explored by Hagedoorn et al. on *P. furiosus* glyceraldehyde-3-phosphate oxidoreductase (GAPOR) poised at -645 mV versus -454 mV (using different substrate over product ratios) [27]. Data analysis afforded a six-coordination of four S and two O for both samples, with slightly longer distances in the more reduced sample, however these results should be considered preliminary with significant noise in the experimental data and in view of an observed mere 0.4 eV shift in edge position, which indicates that the two samples may not have been purely W(IV) and W(VI), respectively. All in all, EXAFS spectroscopy of tungstoproteins appears to have considerable potential for structure-function studies, but its exploration remains limited at this time.

Cellular transport of tungstate

The cellular transport system for oxoanions like tungstate, molybdate, sulphate and phosphate has been described for many organisms, in particular the molybdate uptake mechanism for *E. coli* [28]. All systems are members of the adenosine triphosphate (ATP) binding cassette (ABC) transporter family. The majority of these oxoanion transporters consist of three proteins; the ‘A’ protein is responsible for the recognition and binding of the substrate. This protein is located in the periplasm, which is the space between the cytoplasmic membrane and: (i) the cell wall in Gram-positive bacteria, (ii) the outer membrane in Gram-negative bacteria, or (iii) the S-layer in archaea. For some ABC transporters the first component is linked to the outer surface of the cellular membrane with a so called ‘lipotail’, which is a lipid-modified cysteine residue. The B component forms the transmembrane pore through which the substrate is transported into the cell, and this transport is facilitated by the ATP hydrolyzing activity of component C on the inner surface of the membrane. In figure 5 an overview is given of the general rules on gene and protein annotation, which are also used in this review [29].

The periplasmic molybdate binding protein in *E. coli*, referred to as ModA, specifically binds molybdate with an equilibrium constant for dissociation (K_D) of 20 nM. ModA is also able to bind tungstate with a similar affinity [30]. After binding to the periplasmic component the molybdate or tungstate is actively transported against a concentration gradient into the cell through the transmembrane unit ModB energized by the ATP hydrolyzing activity of ModC.

Genetic properties of organisms are described in terms of phenotypes and genotypes. **The genotype** refers to the genes present in the genome of an organism and the **phenotype** describes its observable properties, for example the expression of proteins.

An **operon** contains one or more structural genes which are transcribed as a single mRNA molecule that codes for more than one protein. The operon is designated by a three-letter, lower case, italicized symbol (e.g. *mod*). The structural genes are distinguished by italicized capital letters following the name of the operon (e.g. *modA modB modC*).

Proteins (i.e. gene products) are generally referred to with the three-letter symbol of the non italicized structural gene designation with the first letter of the symbol capitalized (ModA, ModB, ModC).

Figure 5. An overview of the annotation agreements for genes and proteins [29]

A tungsten-specific transporter: Tungsten uptake protein ABC (TupABC), was identified for the first time in the mesophilic bacterium *Eubacterium acidaminophilum* and was shown to bind tungsten with a dissociation constant (K_D) of 0.5 μM [31]. The K_D for molybdate was determined to be greater by several orders of magnitude. Recently, a second, structurally different tungsten specific ABC transporter system was discovered in the hyperthermophilic archaeon *P. furiosus* [32]. The periplasmic component: W-transport protein A (WtpA), was shown to bind tungstate specifically with a K_D in the picomolar range. Isothermal (displacement) titration calorimetry (ITC) of molybdate-saturated protein with tungstate showed clearly that tungstate replaces the molybdate in the binding pocket of the protein. These data indicate that the K_D for molybdate is several orders of magnitude greater than that for tungstate [32].
Based on a high sequence similarity with TupA (58%), the first high affinity vanadate transporter, Vanadate uptake protein ABC (VupABC), could be identified recently in *Anabaena variabil*s [33]. This organism requires vanadate for the expression of a vanadium-containing nitrogenase for the fixation of molecular nitrogen.
With the identification of these transporter systems that all have specific affinities, we can conclude that significant overall amino acid sequence similarities (ranging from 30% up to 60%) cannot be used to predict the type of oxoanion that is transported with the highest affinity. So which factors are determining the selectivity? Crystal structures of the periplasmic component in complex with the specific oxoanion could help to answer this

question. The three-dimensional structure can be used to identify essential amino acid ligands that play a role in determining the specificity of the protein. Subsequently mutational studies can confirm this role in *in vitro* binding experiments.

Crystal structures are available for ModA from *E. coli* [34] and ModA from *Azotobacter vinelandii* (ModA2) [35]. Both ModA proteins were crystallized in complex with tungstate or molybdate (figure 6AB). However, *in vitro* binding experiments showed that ModA was not able to discriminate between the two oxoanions, and therefore, these structures cannot be used to explain the specificity that was found for the tungstate transporters. Indeed, inspection of the structures confirms that the protein binds tungstate and molybdate in an identical way: in both ModA proteins, seven hydrogen bonds are formed between the tetrahedral oxoanion species and the amino acids of the protein. There are no (positively) charged residues and also no water molecules in both proteins within 8 Å of the oxoanion, and this determines the surface potential of the binding pocket to be neutral with an apolar character. Hu and co-authors have stated that it is energetically more favorable for an apolar pocket to bind a larger oxoanion, which could explain the selectivity for molybdate/tungstate compared to the smaller oxoanion sulfate [34]. This argument refers to simple electrostatic considerations based on Born charging energies. The authors add, however, that a more detailed analysis of the electrostatics of the anion binding, taking into account the locations and orientations of dipoles in the structure, is required to support this qualitative statement [34].
A very recent paper describes a third crystal structure of a ModA, namely, from *Archaeoglobus fulgidus* (figure 6C) [36]. The structure of this protein has been solved as part of the structure of the complete ABC transporter ($ModAB_2C_2$). However, in our opinion, the *A. fulgidus* protein should be referred to as WtpA homologue rather than ModA homologue. First of all, the sequence of the *A. fulgidus* periplasmic binding protein is significantly more similar to *P. furiosus* WtpA (44% identity, 64% similarity) than to *E. coli* ModA (27% identity, 45% similarity). Secondly, the crystal structure of the *A. fulgidus* protein shows a completely different coordination of the metal ion, namely an octahedral coordination, whereas the ModA of *E. coli* and *A. vinelandii* both show a tetrahedral coordination. The metal in the *A. fulgidus* protein is bound to the four oxygens of its oxoanionic structure and to one oxygen each of the carboxylate side groups of two amino acids Glu218 and Asp153, which are fully conserved only in WtpA homologues. The four oxygen atoms of the oxoanion are coordinated by eight hydrogen bonds, in a similar manner as in the ModA proteins (figure 6C). Finally, it is interesting to note that the genome of *A. fulgidus* contains several genes encoding putative tungsten containing aldehyde oxidoreductases, which also suggests that tungstate is the physiological ligand of this periplasmic binding protein. However, no affinity studies have been reported yet. In addition, the resolution of the crystal structures (1.5 Å - 1.6 Å) may conceal any differences between the tungstate and molybdate binding sites [36].

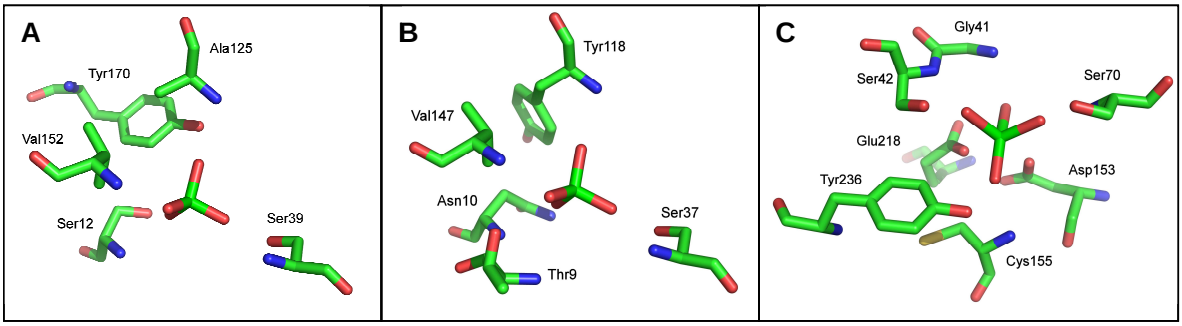

Figure 6. Crystal structure of the binding pocket of *E. coli* ModA binding molybdate (A) [34], *A. vinelandii* ModA binding tungstate (B) [35], and the periplasmic binging protein of *A. fulgidus* binding tungstate (C) [36].

Currently, no crystal structure is available of a periplasmic binding protein in complex with its ligand, for which a difference in affinity between molybdate and tungstate has been measured *in vitro*. In the coming years we expect to see crystal structures of the tungstate (and also vanadate) selective periplasmic binding proteins in complex with their ligands, and these might provide a basis to explain the molecular mechanism of the molybdenum and tungsten selectivity.
The presence of genes in the genome encoding one of these transporter systems: ModABC, TupABC or WtpABC, can explain the tungstate and molybdate uptake pathway in most bacteria and archaea. A recent paper reports the identification of the first eukaryal, high-affinity molybdate transporter in *Chlamydomonas reinhardtii* [37].

Cellular storage of tungstate

A way to insure a constant intracellular level of small essential compounds, such as metal ions, in cells is the operation of a (regulated) storage system. Proteins can act as storage units that are able to release the metal at specific locations in the cell when intracellular or local concentrations decrease. Proteins can also facilitate metal solubility or protect the cells against toxic levels of certain compounds by forming mineral cores, like in the case of ferritin. Free ferrous iron is potentially toxic to cells (notably in the presence of molecular oxygen) and therefore it is immobilized inside the ferritin protein as a mineral core of ferric iron combined together with phosphate and/or hydroxide ions. The resulting core is similar to the mineral ferrihydrite, and theoretically one protein molecule, consisting of 24 monomers, can store up to circa 3000 ferric ions [38].
So far, two classes of proteins have been described that play a role in the storage of molybdate and potentially also tungstate. The first class is formed by the so called ‘molbindin’ family. These proteins consist of one or two molybdate binding domains (Mop

domains) that are able to bind molybdate or tungstate [39]. They are found in bacteria and archaea, but not all organisms that use tungsten and/or molybdenum have copies of these 'Mop domain' encoding genes in their genome. Several molbindins have been crystallized: Mop from *Clostridium pasteurianum* [40], Mop from *Sporomusa ovata* [41] and di-mop (i.e. two mop domains in a single protein) ModG from *A. vinelandii* [42]. The crystal structures indicate that the mono-mop proteins form a trimer of dimers, and the di-mop proteins are trimeric, which in each case results in a native hexameric domain conformation. These hexameric molbindins can bind eight oxoanions per molecule at two different sites. Six oxoanions can bind to six high affinity sites, which are located between the faces of the dimers, and two can bind to lower affinity sites located along the trimeric symmetry axis in the middle of the three domains (figure 7).

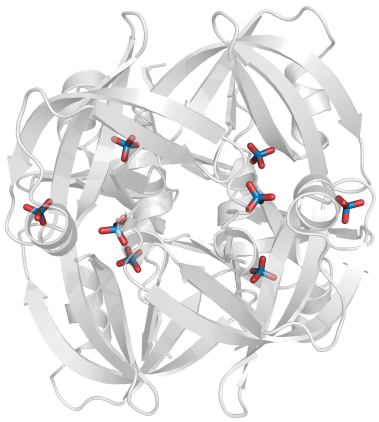

Figure 7. Crystal structure of the *S. ovata* molbindin protein, binding eight molecules of tungstate [41].

All three described Mop proteins were also crystallized with tungstate bound but no differences were observed in the coordination of the ligands compared to the protein complexed with molybdate [40-42] . In all cases the oxoanion was found to be coordinated by hydrogen bonds formed with the main chain and side chains of the protein. As in the ModA structures, there are no positively charged amino acids present within 8 Å of the binding sites.

Unfortunately, no quantitative *in vitro* binding experiments have been described for these three proteins that might have indicated a difference in affinity for tungstate or molybdate. The proteins were crystallized with both oxoanions and it was concluded that the higher binding affinity for molybdate and tungstate compared to an observed lower affinity for sulfate, was likely determined by the size of the binding pocket. Based on the apparently identical way in which the oxoanion is bound one would expect the Mop-domain proteins to bind tungstate and molybdate equally well.

However, so far only one molbindin protein has been described that was isolated from an organism for which we know that it actually uses tungsten: the Mop protein from *E. acidaminophilum* [43]. This organism expresses two tungsten containing enzymes [44] [45] and a specific tungsten uptake system [31] and therefore one can expect that this Mop protein serves as a tungstate storage protein *in vivo* with possibly a higher affinity for tungstate over molybdate. Unfortunately binding characteristics were determined only with a gel shift assay [43], which is not well suited for quantitative determination of the dissociation constant [32] .

In addition to the molbindin proteins, a second class of oxoanion storage proteins has been characterized that store tungstate and molybdate as a metal-oxygen cluster. The first protein identified in this category was the molybdenum storage (Mo/WSto) protein from *A. vinelandii* [46]. This protein has been isolated more than 20 years ago as a molybdate and tungstate binding protein [47]. Very recently, the structure of the protein loaded with tungstate could be determined [48]. The moly

bdate-binding counterpart of the protein could not be crystallized so far, because all the molybdate was released during the long-term incubation required for the crystal formation. The protein appeared to be a trimer of (αβ)-dimers resulting in a hexameric native structure. The α- and β-subunits have a molecular weight of 29 kDa and 28 kDa respectively. The protein can store up to circa 100 molybdenum or tungsten atoms per hexamer [46] as polynuclear tungsten- or molybdenum oxide aggregates. These polyoxotungstates and polyoxomolybdates are separated from each other within the protein complex in different cavity pockets [48]. Interestingly, the formation of the cluster differs for each type of pocket [48]. The α-subunit also harbors an ATP binding site, however the binding mode of ATP and its role in the formation or breakdown of the cluster is still a subject of study [48]. It should be noticed that so far no tungsten enzyme has been purified from *A. vinelandii* so it is possible that the binding of tungstate has no physiological function.

A sequence comparison by BLAST [49] studies against the non-redundant database reveals that the α- and β-subunit of the Mo/WSto protein are related to a family of uridine monophosphate kinases (UMKs) [46]. For most Mo/WSto homologues it is not clear whether the gene product encodes a Mo/WSto or a UMK. However, there are some other nitrogen-fixing bacteria for which the gene sequence homology with Mo/WSto is so high that the gene most likely encodes a Mo/WSto protein. Perhaps this is an indication that the Mo/WSto protein is somehow linked to the biosynthesis of the FeMo-cofactor of nitrogenases.

In addition to these two types of well characterized tungstate and molybdate storage proteins, a recent paper reports on a tungstate-binding protein isolated from *Acidithiobacillus ferrooxidans* strain AP19-3 [50]. This protein has yet to be characterized in detail: the amino acid sequence is not known, the form in which the tungsten is bound is unclear, and the protein has only been shown to bind tungstate after incubation in 1.0 mM sodium tungstate at pH 3.

A very different type of storage protein related to tungsten and molybdenum metabolism is the molybdenum cofactor carrier protein (MCP). This 16 kDa protein, which forms stable tetramers in solution, has been purified from the green alga *C. reinhardtii* [51,52]. In this protein the metal is stored *after* it has been incorporated in the pterin cofactor i.e. as a molybdenum cofactor (Moco) or a tungsten cofactor (Wco) (figure 2A). Synthesis of this cofactor is discussed in section 8 of this review, below. Recently, the crystal structure of the apo-MCP was solved [53]. Based on the conserved surface residues, charge distribution, shape, *in silico* docking studies, structural comparisons, and identification of an anion binding site, a prominent surface depression was proposed as a Moco-binding site [53]. Recombinant MCP containing tungsten or molybdenum, dependent on the medium composition, has been isolated from an *E. coli* host. In *C. reinhardtii*, only molybdenum-dependent enzymes have been described so far, suggesting that the binding of Wco to MCP has no physiological function.
However, BLAST studies against genome databases reveal that there are homologues of MCP in genomes that also contain homologues of tungsten-containing enzymes, indicating that MCP could also have a physiological role in storing Wco *in vivo*. The genome of *A. fulgidus* for example contains a gene that shares 56% similarity and 40% identity with the *C. reinhardtii* MCP. The *A. fulgidus* genome also contains genes encoding several putative tungsten-containing aldehyde oxidoreductases and the gene of the recently crystallized putative tungstate and molybdate selective transporter (see section 5).

In summary, two distinct molybdate and tungstate storage systems have thus far been identified: the molbindins and the Mo/WSto proteins. However they are only expressed in a small fraction of the organisms known to use one or both of the two metals. For well established molybdenum, respectively, tungsten users, like *E. coli* and *P. furiosus*, it is still not clear whether, and if so how, the metals are stored in the cell. Possibly, these cells have other proteins that function as a storage system. One can hypothesize that other proteins like ferritin might also play a role in tungstate or molybdate storage. There is experimental evidence that ferritin can incorporate vanadate, and molybdate [54] and tungstate (M.N. Hasan, personal communication) as phosphate analogues in the iron mineral core *in vitro*. However, any physiological relevance of this property has not been supported by *in vivo* data.

Cellular regulation of tungstate metabolism

In the framework of this review, cellular regulation concerns all the functions that cells carry out to maintain metal homeostasis. In the case of tungstate metabolism this includes regulation of the tungstate uptake, the storage, and the expression of both the cofactor synthesis proteins and the enzymes that contain the tungsten cofactor. Again, more data are available on the regulatory role of molybdate, especially in *E. coli*, and therefore we will

start to review those data and extrapolate these for tungstate. We will only consider metal induced regulations. Many molybdenum and tungsten containing enzymes are under metabolic control (product feedback); however these regulatory networks are not considered here.

It has been known for a long time that the internal cellular concentration of molybdenum in *E. coli* is maintained within a narrow range (0-10 μM) even when its external concentration varies widely [55,56]. Grunden et al [57] showed that this was mainly the result of a regulation of the transcription of the *modABC* operon which encodes the ABC transporter. A protein named ModE was found to be responsible for the molybdate dependent repression of the *modABC* operon, because in *modE* deficient mutant strains this regulation was absent [57]. The dimeric protein ModE binds tungstate or molybdate with the same affinity (K_D = 0.8 μM) [58], and the crystal structure of both complexes has been solved as well as the structure of the apo-protein [59]. The oxoanion ligands bind between the subunits at the dimerization interface, and an oxoanion-size selectivity is determined primarily by the size of the ligand-binding pocket as was previously concluded for the ModA and molbindin proteins [34,35,40-42]. Comparisons with the structure of the apo-protein have revealed a molybdate/tungstate dependent conformational rearrangement [59] which most likely creates a surface that has a high affinity for the DNA in the promoter region of the *modABC* operon [58]. These data indicate that the regulatory protein ModE does not seem to discriminate between tungstate and molybdate.

Only some organisms carry a *modE* homologous gene in their genome, which makes the ModE dependent regulation not universal among molybdenum and tungsten using organisms. BLAST studies against genome databases reveal that, for example, archaeal genomes do not contain *modE* homologues. Perhaps, these organisms have other regulatory systems for the uptake of molybdate and tungstate which still have to be identified.

Besides the regulation of the transcription of the genes encoding the ABC transporter, *E. coli* ModE also regulates the transcription of several other genes, namely: *dmsA*, which encodes the molybdenum containing subunit of the enzyme DMSO reductase [60], *hyc*, which encodes a hydrogenase [61], *narG*, the molybdenum containing subunit of nitrate reductase [61], and the *moa* operon [62], which encodes proteins involved in the first step of the molybdenum and tungsten cofactor synthesis (section 8).

The positive influence of ModE in the presence of molybdate on the transcription of the *moa* operon was detected in molybdenum cofactor deficient strains only (these cells have a defect in the cofactor synthesis and therefore no active cofactor is synthesized). Based on this observation it has been concluded that cofactor dependent repression of the transcription of the *moa* genes (in the presence of molybdate) is dominant over the ModE-molybdate activation [63]. *In vivo* data showed a similar positive effect of tungstate on the transcription of the *moa* operon. Surprisingly, this effect was independent of the presence of ModE or of the ability of cells to make the cofactor. Therefore, it has been suggested that the presence of tungsten results in the formation of a non-functional tungsten-containing

form of the cofactor, which is not able to cause the cofactor-dependent repression observed in the presence of molybdate [63].

Of specific interest is a group of organisms that express isoenzymes with molybdenum versus tungsten in the cofactor. An example is *M. thermoautotrophicum* which expresses a tungsten-containing formylmethanofuran dehydrogenase (FMDH) (operon *fwdHFGDACB*) and a molybdenum-containing FMDH (operon *fmdECB*) [64]. The subunits FwdB and FmdB were identified as harboring the redox active tungsten, respectively, molybdenum site. The largest subunit (FwdA) probably catalyses the formation of N-carboxymethanofuran from CO_2 and methanofuran [65]. Interestingly, the operon encoding the molybdenum-containing enzyme is lacking the gene encoding subunit A. Analysis revealed that subunit A in the Mo-containing FMDH has the same molecular mass and the same N-terminal amino acid sequence as subunit A of the W-containing enzyme. Therefore it was concluded that they are identical and encoded by the gene *fwdA* in the *fwd* operon. It was shown that the operon for the W-containing enzyme is constitutively transcribed, whereas the transcription of the Mo-operon appears to be induced by the presence of molybdate, independent of the presence or absence of tungstate [66]. However, later experiments showed a different effect of the tungsten concentration on the expression of the Mo containing FMDH. These experiments concerned also a small DNA binding protein (Tfx) that was identified to specifically bind to a DNA sequence downstream of the *fmd* operon. This protein was proposed to be a transcriptional regulator of the gene-encoding part of the Mo-containing FMDH [67]. Northern blot analysis (detection of mRNA) revealed that the transcription of this regulator was repressed during growth in the presence of tungstate rather than induced by molybdate. This result is not consistent with the previous findings which indicated that the Mo-operon is transcribed in the presence of molybdate, independent of the tungstate concentration [67].

Altogether the suggestion perspires that several factors may play a role in the molybdate and tungstate dependent regulation and homeostasis, and many questions remain to be addressed regarding their mechanisms.

Biosynthesis of the cofactor

Tungsten and molybdenum associated with enzymes, occur in a similar cofactor, which consists of one or two tricyclic pterin moieties usually referred to as ‘molybdopterin’ (MPT) (figures 2 and 8) [68]. The nomenclature is confusing because MPT seems to refer only to molybdenum, and, therefore the alternative name metal-binding pterin (MPT) was introduced [5]. For both types of cofactors (Moco and Wco) the metal is coordinated by the two dithiolene sulfurs of the pterin. In the case of tungsten there are always two pterin moieties resulting in a tungsten center coordinated by four dithiolene sulfurs in the tungsto-bispterin cofactor (figures 2 and 8).

The pathway of Moco biosynthesis has been extensively studied in prokaryotes (*E. coli*) as well as eukaryotes (*A. thaliana, Homo sapiens*) and appears to be highly conserved (figure 8) [69]. The pathway of Wco biosynthesis is thought to be similar to the pathway of Moco biosynthesis, at least up to the step of the metal insertion. The main ground for this assumption is that homologues of almost all genes that have an assigned function in the Moco biosynthetic pathway are also present in the genomes of organisms that use tungsten.
The first model of Moco synthesis was based on *E. coli* data [68]. Four operons have been identified to be involved in the Moco biosynthesis of this organism: *moaABCDE, mobAB, moeAB and mogA*. These operons encode ten proteins of which eight have an assigned function in the biosynthesis of Moco (figure 8). The names of the proteins follow the rules of the standard nomenclature (figure 5) and have no particular meaning except that Mo refers to molybdenum.

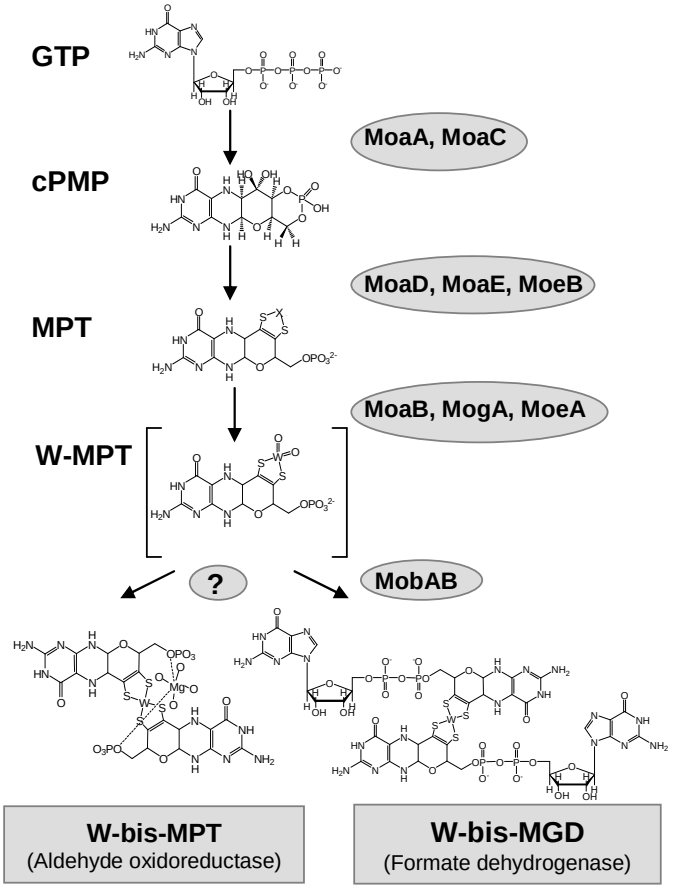

Figure 8. Schematic overview of the tungsten cofactor biosynthesis; modified figure from [4]. Abbreviations of the intermediates are written in bold on the left side of their structures, and the enzymes that catalyze the steps are depicted on the right side of the arrows. Note that the bracketed MPT structure is a hypothetical intermediate. The metal coordinating the dithiolene ligands in MPT is indicated by an X as this atom is not known. In the crystal structure of plant Cnx1G this metal was found to be a copper ion [133].

In *E. coli* the biosynthesis of Moco begins with the conversion of guanosine triphosphate (GTP) to a pterin intermediate called precursor Z or cyclic pyranopterin monophosphate (cPMP), catalyzed by two proteins: MoaA and MoaC [70]. The expression of these two proteins is regulated by ModE, described in section 7 [62]. Subsequently, metallopterin (MPT) is synthesized from cPMP by MPT synthase, which consists of the MoaD and MoaE proteins [4]. The next step involves the ligation of the metal atom to the dithiolene sulfurs of one or two MPT moieties. The proteins MoeA and MogA play a role in this step, and very recently also MoaB was found to be involved in this stage of the cofactor synthesis [71]. The proteins MogA and MoaB catalyze the activation of MPT by adenylylation with Mg-ATP [72,73]. The trimeric MogA proteins are commonly found in bacteria and eukaryotes whereas the hexameric MoaB proteins are mostly found in archaea and in some bacteria [71]. Subsequently, MoeA is thought to bind the adenylylated MPT (MPT-AMP), and in the presence of molybdate and/or tungstate the MPT-AMP complex is hydrolyzed, molybdenum or tungsten is incorporated through binding to the dithioleno sulfurs, and AMP is released. This proposed role for MoeA in *E. coli* is based on the activity of its plant homologue: Cnx1E (Cnx: Cofactor for nitrate reductase and xanthine dehydrogenase) from *A. thaliana* [74], which catalyses the hydrolysis of MPT-AMP in the presence of molybdate. When molybdate was replaced with tungstate, the hydrolysis catalyzed by Cnx1E was much less efficient [74], and this result suggests that Cnx1E, and homologues, may play a role in selectively incorporating either tungsten or molybdenum in MPT.

Interestingly, many bacterial genomes and all archaeal genomes sequenced so far, contain two different *moeA* genes which share approximately 40% sequence identity. It is tempting to speculate that perhaps one of the MoeA proteins is selective for molybdenum incorporation and the other for tungsten incorporation. The presence of these two MoeA's can then explain how organisms are able to regulate and express two enzymes, one with Moco and the other with Wco in the active center. For example, *Pyrobaculum aerophilum* expresses a W-containing AOR and a Mo-containing nitrate reductase [19,75]. However, *in vivo* and *in vitro* experiments are required to corroborate this hypothesis of selectivity by two different insertion catalysts.

As a final maturation step (only in bacteria and archaea), guanosine monophosphate (GMP) or cytosine monophosphate (CMP) can be attached (phosphoester condensation from GTP and CTP) to the MPT, forming a so called molybdopterin guanine/cytosine dinucleotide (MGD/MCD) cofactor. This reaction is catalyzed by MobA and MobB [76]. For some enzymes another maturation step is required: the coupling of two Wco's or two molybdenum- or tungsten-containing MGDs leading to the formation of the bis-pterin cofactor. The formation mechanism of this so called bis-pterin cofactor still needs to be established.

Tungsten enzymes

The first indication of a biological relevance of tungsten was obtained more than 30 years ago: Andreessen and co-authors showed that the growth of different *Clostridia* was positively influenced by the addition of tungstate to the growth media [77]. It took another decade before formate dehydrogenase could be purified from one of these acetogenic *Clostridia* as a naturally occurring tungsten containing enzyme [78]. In the years to follow, many tungstoenzymes have been purified and characterized [19,79]. The majority was believed that tungsten enzymes mainly occur in these extremophilic organisms. A relatively high concentration of tungstate compared to molybdate in certain extreme environments like hydrothermal vents and hot-spring waters would support this hypothesis. Furthermore, most isolated tungsten containing enzymes were very oxygen sensitive, and therefore it was also believed that they could only occur in anaerobes.
However, in the following years tungsten containing enzymes were also purified from (mesophilic) bacteria [44,80-83] and homologous genes are even found in the genomes of aerophilic organisms, suggesting that tungstoenzymes are present in a much wider range of microorganisms. There have been no reports yet on any tungsten enzyme in eukaryotes.
Tungsten and molybdenum enzymes have been classified in different families according to: (1) sequence homology, (2) composition of the cofactor, i.e. with or without nucleotide attachment, (3) the coordination of the metal by one or two pterins, and (4) axial ligands like oxygen, sulfide or cysteine (figure 9).
The tungsten-containing enzymes can be divided in two families: the aldehyde oxidoreductases (AORs) that contain a non-modified tungsto-bispterin cofactor, and the formate dehydrogenases which have a guanine monophosphate attached to each pterin moiety (figure 8).

	family-1	family-2	family-3	family-4
Mo-enzymes	Sulfite oxidase	Xanthine oxidase	DMSO reductase	
W-enzymes			Formate dehydrogenase	Aldehyde oxidoreductase

Figure 9. Schematic overview of the four families of molybdenum- and tungsten-containing enzymes with the names of example enzymes.

Aldehyde oxidoreductases

The enzymes in the AOR family catalyze the oxidation of aldehydes to carboxylic acids, and they use ferredoxin as redox partner protein. They are generally oxygen sensitive and typically have broad substrate specificities with partial overlap between enzymes from the same species. They all consist of mono-, di-, or tetramers of the catalytic subunit that contains the bis-pterin cofactor and an electron transferring [4Fe-4S] cluster. BLAST studies reveal that the genome of many organisms encodes multiple, different AOR enzymes [32]. The tungstoenzymes of *P. furiosus* have been intensively studied over the past two decades, and its complete AOR family has been purified and characterized (in some detail): aldehyde ferredoxin oxidoreductase (AOR) [79], glyceraldehyde-3-phosphate ferredoxin oxidoreductase (GAPOR) [84], formaldehyde ferredoxin oxidoreductase (FOR) [85], tungsten-containing oxidoreductase number four (WOR4) [86], and tungsten-containing oxidoreductase number five (WOR5) [87]. AOR and WOR5 have a broad substrate specificity; AOR appears to be most active on aldehydes derived from amino acids [79] whereas WOR5 has a high affinity for several substituted and non-substituted aliphatic and aromatic aldehydes with variable chain lengths (table 1) [87]. FOR has the highest activity on small C1-C3 aldehydes and semi- and di-aldehydes [85]. In contrast to these broad substrate specificities, GAPOR is only known to convert the substrate glyceraldehyde-3-phosphate (GAP). It functions in glycolysis where it converts GAP to 3-phosphoglycerate, and it replaces the couple glyceraldehyde-3 phosphate dehydrogenase plus phosphoglycerate kinase in an unusual Emden-Meyerhof pathway of glycolysis [84]. The fourth tungsten-containing enzyme, WOR4, could only be purified from *P. furiosus* grown in the presence of S^0 [86]. No activity has been identified yet for this enzyme.

The physiological function of this AOR family of enzymes is still not clear with the exception of GAPOR [84]. However, micro-array analysis in which levels of mRNA are determined under different growth conditions indicated possible physiological functions (table 2). In a first reported experiment *P. furiosus* was grown on peptides or on maltose [88]. Growth on peptides increased the mRNA levels of FOR and WOR4 significantly, whereas GAPOR mRNA levels increased, as expected, during growth on maltose, which is converted by glycolysis [88]. Furthermore, the cultivation temperature of the cells was dropped from their near-optimal growth temperature of 95 ˚C to 72 ˚C in order to elicit three different responses: an early shock response (1 to 2 hours at 72 ˚C) , a late shock response (5 hours at 72 ˚C), and an adapted response (occurring after many generations at 72 ˚C) [89]. WOR5 mRNA levels were significantly upregulated in the case of the early and late shock, whereas AOR mRNA levels decreased. For the adapted cells, in particular, WOR4 appeared to be upregulated [89]. The results of these micro-array experiments are perhaps not conclusive, but they do indicate that FOR and WOR4 might play a role in peptide fermentation, and that WOR4 and WOR5 are possibly involved in some kind of stress response, e.g., following a cold shock.

Table 1. An example of broad substrate specificity of W-containing AORs. Oxidation of various aldehydes at 60 °C by *P. furiosus* WOR5 with methylviologen as electron acceptor [87].

Substrate	Structure	V_{max} (U/mg)	K_M (mM)	K_{cat}/K_M($s^{-1}M^{-1}$)
Hexanal		15.6 ± 1.8	0.18 ± 0.02	80000
Hydratropaldehyde	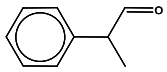	9.3 ± 0.7	0.12 ± 0.04	71500
2-Methylvaleraldehyde	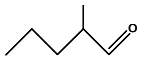	12.7 ± 1.3	0.27 ± 0.03	43400
2-Ethylhexanal	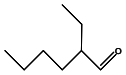	8.3 ± 1.5	0.17 ± 0.02	45100
3-Phenylbutyraldehyde	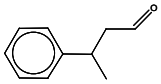	8.0 ± 0.6	0.42 ± 0.12	17600
2-Methylbutyraldehyde	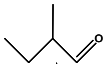	7.7 ± 0.4	0.43 ± 0.09	16500
Isobutyraldehyde		11.8 ± 0.9	0.79 ± 0.03	13800
2-Naphthaldehyde(β)	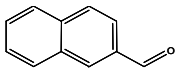	7.7 ± 0.8	1.3 ± 0.1	5500
Cinnamaldehyde	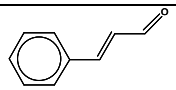	7.4 ± 1.6	1.6 ± 0.1	4600
2-Methoxybenzaldehyde	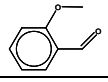	15.1 ± 0.6	4.8 ± 0.6	2900
Acetaldehyde		0.34 ± 0.05	1.5 ± 0.2	210
Formaldehyde		8.5 ± 1.0	45 ± 12	170
Glutaraldehyde		1.4 ± 0.1	9.4 ± 0.2	140
Crotonaldehyde	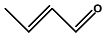	1.1 ± 0.1	46 ± 6	22
Glyceraldehyde-3-phosphate	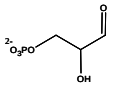	0.0	-	0

Table 2. The effect of different growth conditions on the mRNA levels of tungsten containing aldehyde oxidoreductases in *P. furiosus* [88,89]

	C-source		**Cold shock 72˚C**	
	Peptides	Maltose	1-5 hours	Adapted
AOR (PF0346)	- [a]	-	↓ [b]	-
FOR (PF1203)	↑ [c]	-	-	-
GAPOR (PF0464)	-	↑	-	-
WOR4 (PF1961)	↑	-	-	↑
WOR5 (PF1480)	-	-	↑	↑

a) - no significant difference
b) ↓ significant down-regulation
c) ↑ significant up-regulation

Formate dehydrogenases

The enzymes in the FDH family catalyze the oxidation of formate to carbon dioxide. They all have the same tungsto-bispterin-MGD cofactor in common and they often contain additional [4Fe-4S] or [2Fe-2S] clusters. For most of these enzymes the physiological redox partner is still unknown. The crystal structures of four FDH proteins have been reported: one tungsten-containing enzyme from *Desulfovibrio gigas* [90], two molybdenum-containing FDHs from *E. coli* [91,92], and recently, also a 2.6 Å resolution structure for the NADH-dependent FDH from *Pseudomonas sp. 101* was deposited (2GO1). The *D. gigas* W-containing FDH is a heterodimeric enzyme and contains a [4Fe-4S] cluster and a tungsto-bispterin-MGD cofactor in the large subunit [90]. Functional implications of the W-FDH structure will be discussed below.
A special case is acetylene hydratase from *Pelobacter acetylenicus*. Mechanistically, this enzyme does not fit into either class of tungsten enzymes because it apparently catalyzes a non-redox reaction: the hydration of acetylene to acetaldehyde [93]. The structure of this enzyme has recently been solved and encompasses a tungsto-bispterin-MGD cofactor and a [4Fe-4S] cluster [94]. The sequence and the overall structure are similar to the enzymes belonging to the FDH family.

Relationships with molybdenum-containing enzymes

The Moco-containing enzymes can be classified into three separate families based on the coordination of the molybdenum [69,95]. In the sulfite oxidase family (SOs), the molybdenum is covalently bound to a highly conserved cysteine residue. This cysteine is replaced by a non-protein sulfur atom in the family of xanthine oxidoreductases (XOs). The

DMSO oxidoreductases (DMSOrs) contain a bis-pterin cofactor modified with a nucleotide attachment, forming molybdo-bispterin-MGD.
Interestingly, no naturally occurring tungsten enzymes have been isolated that belong to the SO or XO family; conversely, also no molybdenum containing members of the AOR family are known to date. A very recent report describes the purification of active, molybdenum-containing *Methanococcus maripaludis* GAPOR recombinantly expressed in *E. coli* [96]. However, the physiological metal of the wild type enzyme has not been determined. The genome of *M. maripaludis* putatively encodes a molybdenum- and a tungsten-containing formylmethanofuran dehydrogenase and therefore the organism is likely able to process both metals into pterin cofactors. So far, only the families of the DMSOrs (molybdenum) and FDHs (tungsten) share significant sequence similarity and in addition, enzymes of both families contain the bis-MGD cofactor.

Exchange experiments

Many attempts have been made to substitute molybdenum with tungsten and vice versa in the cofactor of the various enzymes. These experiments show that not all enzymes can be synthesized with either metal. An overview of the attempts is given below.
The first substitution experiments were performed in rats that were fed with tungstate or molybdate and for which subsequently the metal content of the sulfite oxidase and xanthine oxidase was determined. It was found that both metals could be incorporated into the pterin cofactor of the enzymes, but the tungsten-containing enzymes were completely inactive [97]. In some enzymes of the DMSO reductase family, for example in the case of *R. capsulatus* DMSO reductase, expressed in *E. coli* [14], and in *E. coli* trimethylamine *N*-oxide (TMAO) reductase [98], replacing the molybdenum with tungsten afforded active enzyme. However, the activity profiles changed compared to the profile of the molybdenum-containing enzyme, presumably due to the lower reduction potential of the tungsten center [98]. Tungsten-containing DMSO reductase was found to be more active in reducing the DMSO but could not catalyze the reverse reaction, the oxidation of DMS [14]. The tungsten-containing TMAO reductase appeared to have a broader substrate specificity compared to the molybdenum enzyme because it was also able to reduce sulfoxides [98].
Not all enzymes of the DMSO reductase family could be synthesized with either tungsten or molybdenum to form a functional enzyme complex: no active tungsten substituted (prokaryotic) nitrate reductase has been obtained. Attempts have been made with nitrate reductase from *R. capsulatus* and *E. coli*, but both lead only to the formation of inactive apoenzyme [99,100].
These are all examples of naturally occurring molybdenum enzymes that were substituted with tungsten. The other way around appears to be less easy, as there is only one example of a naturally occurring tungsten enzyme, *P. acetylenicus* acetylene hydratase, in which the metal could be successfully substituted with molybdenum, leading to the formation of active

enzyme [101]. The molybdenum-containing enzyme exhibits 60% of the activity compared to the wild type tungsten enzyme [101].
Metal exchange experiments were also performed with the tungsten-containing AOR enzymes from *P. furiosus*. Adams and coworkers reported that *P. furiosus* cells selectively used the trace amounts of tungsten present in the media, and that they did not incorporate any molybdenum into the cofactor of these AORs [102]. On the contrary, similar experiments performed in our laboratory, with a 1000-fold excess of molybdate over tungstate in the growth media, resulted in a significant molybdenum incorporation in two AOR enzymes: FOR (5% Mo, 2% W, 93% apo) and WOR5 (23% Mo, 2% W, 75% apo) (our unpublished results). EPR spectra confirmed the incorporation of molybdenum into the pterin cofactor. The aldehyde oxidation activities of these proteins correlated with the tungsten content, indicating that the molybdenum containing AOR subunits are not catalytically active. Apparently, the AOR enzymes of *P. furiosus* are preferably synthesized with tungsten, despite the ability of the tungsten transporter (WtpABC) to take up molybdate from the medium [32,102].
An interesting category is formed by the isoenzymes (different genes encoding different enzymes, one with tungsten the other with molybdenum in the cofactor, which perform a similar reaction), for example, the above mentioned formylmethanofuran dehydrogenases in *M. thermoautotrophicum* [64]. Depending on the oxoanion that is available in the growth medium the organism expresses one or both isoenzymes. The metal dependent regulation of gene expression should be a subject of future research particularly in these organisms.
In summary, the activity (rate and specificity) of the enzyme is very much dependent on the metal present in the cofactor. Tungsten enzymes are generally faster in reducing substrates, however, in some cases they are unable to oxidize compounds, where the molybdenum counterpart can do the oxidation must faster, and, in its turn, might be unable (or less able) to catalyze the reduction. This is a result of the lower reduction potential of the W^{IV}/ W^{VI} redox couple compared to the reduction potential of the Mo^{IV}/ Mo^{VI} couple.

Selectivity

It is clear that the metal incorporation of W versus Mo in the cofactor of an enzyme does not only depend on the ability of the cells to take up the metal from the medium, as most organisms express either a ModA, TupA or WtpA homologue with high affinity for both oxoanions. Furthermore, selective incorporation is also not likely to be dependent on the ability of cells to insert only one of the two metals into the MPT cofactor, as we know that *E. coli* can make both Wco and Moco (e.g. TMAOr and recombinant *R. capsulatus* DMSOr [99,100])[14]) but can not incorporate a Wco in all enzymes (e.g. nitrate reductase [103]). There is also no clear relationship between the ability to incorporate the metals in the cofactor of an enzyme and the specific kind of cofactor present in the wild type enzyme. For example, the bis-MGD in TMAO reductase can contain molybdenum or tungsten [99,100,103], whereas the bis-MGD cofactor in prokaryotic nitrate reductase exclusively

contains molybdenum [99,100,103]. Perhaps the incorporation of the metal in the cofactor is mainly dependent on the structure of the apo-enzyme, possibly in combination with the occurrence of chaperone proteins that are specific for each organism and for each enzyme. So far, two chaperones have been characterized in *E. coli* that play a role in Moco incorporation in apo-molybdoenzymes: NarJ for the maturation of a nitrate reductase [104,105] and TorD for the maturation of TMAO reductase [106,107]. Recently, protein interaction assays revealed that NarJ and NarG do no longer interact with enzymes from the Moco biosynthesis pathway, MogA, MoeA and MobA, when *E. coli* strains are grown on tungstate instead of molybdate [105]. This is consistent with the above mentioned results that attempts to synthesize tungsten containing nitrate reductase in *E. coli* afforded only the isolation of apoenzyme. The enigmatic functioning of chaperones in the metal-insertion process calls for increased research efforts in the coming years.

Tungsten model chemistry

Synthetic model chemistry has helped biochemists to understand spectroscopic, structural, and mechanistic data of the molybdenum and tungsten enzymes. In general, the resolution of protein crystal structures is not high enough to determine the metal coordination by the cofactor and additional ligands in great detail. Therefore, synthetic models can aid to define accurate bond lengths and bond angles of the metals in different coordination geometries.
Due to the chemical similarity of Mo and W, nearly all W compounds have Mo counterparts. Recently the synthetic cofactor analogues of Mo and W enzymes have been thoroughly reviewed by Enemark and Holm [108]. Research efforts into the total synthesis of the molybdopterin cofactor have been reviewed in [109,110].

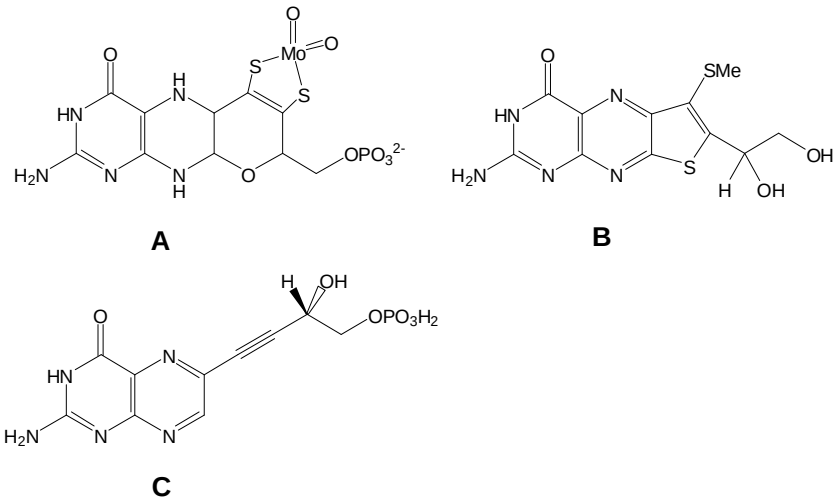

Figure 10. The molybdenum cofactor and derivatives: Molybdenum cofactor (Moco) (A), Urothione (B), FormA (C).

A Moco degradation product, urothione, and a Moco derivative, FormA, have been synthesized *de-novo* (figure 10) [111,112]. To date no one has been able to synthesize Moco. Recently, engineered *E. coli* strains have been developed that accumulate cyclic pyranopterin monophosphate (cPMP), a precursor of Moco. The compound cPMP can be applied as therapeutic for patients with genetic Moco biosynthesis deficiency [69,113]. Moco deficiency is a rare genetic disease causing severe physical and mental retardation and death in early childhood [114], giving an added significance to research efforts into synthetic or enzymatic approaches to produce Moco and cPMP.

One of the problems with synthesizing mononuclear oxomolybdenum and tungsten complexes is the usually irreversible μ-oxo "dimerization" reaction by which $Mo^{IV}O$ and $Mo^{VI}O_2$ react to form $Mo^{V}{}_2O_3$. Therefore, ligands have been used that sterically prevent this reaction. Since all tungsten enzymes contain either bis-MPT or bis-MGD cofactors, their synthetic models are much less prone towards dimerization than synthetic models of mono-MPT cofactors. W-dithiolene compounds with different functional groups have been synthesized (figure 11) [115]. For all W-complexes structurally similar molybdenum counterparts have also been synthesized.

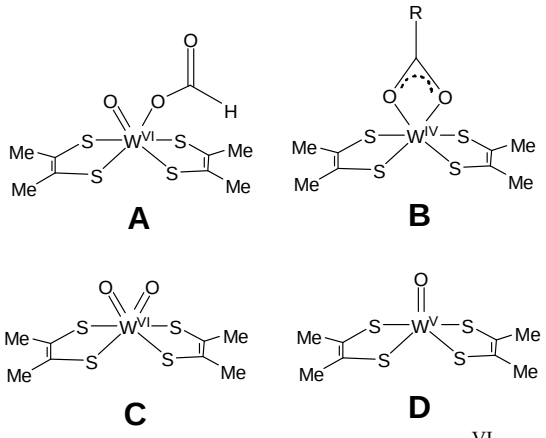

Figure 11. Examples of biologically relevant synthetic models: $[W^{VI}O(O_2CH)(S_2C_2Me_2)_2]^{1-}$ (A), $[W^{IV}O(O_2CR)(S_2C_2Me_2)_2]^{1-}$ (B), $[W^{VI}O_2(S_2C_2Me_2)_2]^{2-}$ (C), $[W^{V}O(S_2C_2Me_2)_2]^{1-}$ (D) [108].

Redox chemistry

The redox chemistry of tungsten model compounds has been extensively studied. Several factors that affect the tungsten reduction potentials have been identified and characterized. In general, the reduction potentials of tungsten complexes are lower than those of analogous molybdenum coordination complexes. This effect is due to larger relativistic effects in the heavy element W which cause increased shielding of the nucleus by the innermost orbitals and thus expansion and destabilization of the 5d orbitals making them less stable than the 4d-orbitals of Mo. As a consequence, bond ionicity is enhanced and higher oxidation states

are stabilized in the case of W [116]. The difference in reduction potential decreases as the bond covalency increases.

The effects of ligands on reduction potential and on electron transfer kinetics of Mo coordination complexes have been measured for compounds with different numbers of sulfur and oxygen ligands [117]. In general, replacing oxygen with sulfur increases the reduction potential of the $Mo^{V/IV}$ couple and increases the electron transfer rate. Furthermore, an aromatic framework of the ligands further increases the reduction potential, as compared to aliphatic frameworks. These observations are in line with the postulated function of the molybdopterin cofactor in modulating the reduction potentials of the metal center. Furthermore, the observations appear to be consistent with the fact that tungsten-containing enzymes always have a bis-MPT cofactor, with four dithiolene sulfurs. A mono-MPT coordination of tungsten would simply give the metal center too low reduction potentials for biologically relevant functions.

The coordination geometry also influences the reduction potentials, as has been measured for oxy Mo centers. In case of a mixed sulfur/oxo-coordination, the *cis*-oxo complex exhibits a 200 mV lower reduction potential that its *trans* counterpart [118].

Schulke has reported on the effects of temperature on the reduction potential of tungsten and molybdenum compounds (93). Tungsten compounds structurally similar to molybdenum counterparts were found to exhibit a different temperature dependence of the reduction potentials, leading to an inverse of the Mo/W reduction potential difference at high temperature (i.e. Mo lower that W) [119]. The author, however, only observed this behavior for $MO(fdt)_2$, and not for other W/Mo bis-dithiolene compounds. The reduction potential difference between $MoO(fdt)_2$ and $WO(fdt)_2$ was only 30 mV at ambient temperature, while the error in the measurements appears to be at least 50 mV. We would venture that the difference in temperature dependence that was found for Mo versus W, is probably not significant. The fact that $MoO(fdt)_2$ and $WO(fdt)_2$ have very close reduction potentials for the M^{IV}/M^{V} couple is interesting in its own right. It suggests that a conformational difference in the ligands coordinating the metals cancels out the normally found reduction-potential difference of at least 200 mV. Unfortunately, the crystal structures of the $MoO(fdt)_2$ and $WO(fdt)_2$ were not obtained.

Solvent effects on the reduction potentials of oxomolybdenum complexes with dendritic thiolate ligands are determined by the dielectric constant of the solvent and the donor number [120]. This qualitatively explains why a different local protein environment can lead to dramatically different reduction potentials of biological molybdenum and tungsten centers.

Related to the redox potential is the electron transfer kinetics. Biological Mo and W centers have to transfer electrons to or from other redox centers, such as iron-sulfur clusters. Apparently, the electron transfer kinetics is faster for coordination compounds with sulfur ligands, than for the ones with more oxo-ligands [117]. Furthermore, the metal-dithiolene fold-angle has been found to be important for electron transfer. The fold-angle of the dithiolene metallacycle along the S-S vector varies with the number of d-electrons of the

metal. In general, the fold angles are large for d^0 and small for d^2 configurations. Large fold angles are a consequence of the stabilizing interaction between the metal in-plane and the sulfur-π orbitals. This effect is important for electron transfer reactions for the regeneration of the Mo/W active site during catalysis. Additionally, encapsulation of the metal by bulky ligands, mimicking the buried metal center inside a protein, has been found to decrease the electron transfer kinetics of the metal center [120].

Mechanism of oxo transfer

Dithiolenes are well known to be non-innocent ligands, i.e. able to do undergo redox reactions themselves. An important question that has not been answered is to what extent the pterin dithiolenes participate in the redox reactions catalyzed by W (and Mo) enzymes. To date little evidence has been obtained for such involvement of the pterin dithiolenes, except for the observation of pterin-localized radicals in Mo-containing aldehyde dehydrogenases [121] and in W-containing AORs (our unpublished observation). Recently reported crystal structures of the Mo containing nitrate reductase A (NarGHI) from *E. coli* [122] and ethylbenzene dehydrogenase from *Aromatoleum aromaticum* [123] show that the bis-MGD cofactor can have an open pyran-ring structure for one of the two pterin moieties. The functional significance of these open-ring structures is not known. Only the closed pterin in both enzymes forms a feasible electron-transfer conduit from the Mo center to the iron-sulfur clusters. Although the precise functions of the pterin cofactor have not been completely resolved the consensus at present is that the (closed) pterin cofactor serves as a conduit for electron transfer and a modulator of the reduction potentials of the metal, and does not directly participate in the catalytic mechanism [123].
Since synthetic W model compounds have Mo analogues, it has been possible to compare their oxo-transfer capabilities and to look for metal-specific differences. Only a small number of analogue functional model systems has been synthesized compared to the number of structural analogues. Using these functional analogues a kinetic metal effect has been observed: Oxo transfer from substrate to metal ($M^{IV} \rightarrow M^{VI}O$) is faster with tungsten, while from metal to substrate ($M^{VI}O \rightarrow M^{IV}$) it is faster with molybdenum [124]. Thus, enzymes that physiologically should catalyze the reduction of a substrate (DMSO reductase, TMAO reductase) are faster with W than with Mo. Enzymes that preferably oxidize a substrate (like FMDH) are expected to be faster with Mo than W.
A recent DFT study of molybdenum- and tungsten-containing model complexes of Mo-dependent nitrate reductases reported differences in the reaction energies of the different steps during the catalytic mechanism [125]. W-complexes were found to have a lower activation energy for oxygen atom transfer (OAT) and a more negative reaction energy for the nitrate reduction half reaction. These calculations would suggest that nature has chosen an energetically unfavorable metal, since no tungsten has been found in any nitrate reductase. A possible explanation of this paradox can be the ease of reducing Mo^{VI} over

W^{VI} during the second half reaction which regenerates the metal center. However no calculations on this second half reaction were presented.
In summary, the metal-based differences between W and Mo that affect kinetics are: the metal-oxygen bond dissociation energies and the reduction potentials. Comparison of the catalytic properties of the W enzymes and their synthetic model compounds helps to define which factors give the enzymes their high turnover rates. In general, enzymes react orders of magnitudes faster than their synthetic model compounds.

Reaction mechanisms

Despite the considerable body of knowledge from synthetic model chemistry and structural and sequence information from biochemistry, it is still difficult to resolve the reaction mechanisms of tungstoenzymes. In order to prove a kinetic mechanism, it is essential to determine the reaction intermediates and kinetic parameters during a single turnover. Very recently we have reported the first pre-steady state kinetic data of a tungstoenzyme, FOR [16]. Most mechanisms presented below still await experimental substantiation, and are based on structural, spectroscopic, and inorganic-chemical knowledge. The structures of four naturally occurring W enzymes have been deposited in the Protein Data Bank: *P. furiosus* AOR (1aor) [25], *P. furiosus* FOR (1b25) [126], *D. gigas* FDH (1h0h) [90], and *P. acetylenicus* AH (2e7z) [94]. In all four cases the exact coordination by oxo- and/or sulfide ligands, other than the dithiolene sulfurs and the selenocysteine (in the case of FDH) is under debate. Detailed structural characterization of the first coordination sphere of the W center in defined oxidation states is still lacking.

Aldehyde oxidoreductases

The crystal structures of *P. furiosus* AOR [25] and FOR [126] indicate several important conserved amino acid residues in the active site region. Of these Glu308 (FOR numbering) has been proposed to be involved in the activation of a water molecule to attack the carbonyl group of the aldehyde bound to the tungsten center. A hydride of the carbonyl carbon is then thought to be transferred to the oxo-ligand of the tungsten center (figure 12). A hydrogen bond from Tyr416 to the carbonyl oxygen atom of the substrate may serve to activate the substrate for nucleophilic attack. Finally, Thr240 may facilitate proton transfer as part of the coupled electron proton transfer at the active site. Future mutagenesis studies may prove or disprove the proposed roles of these amino acid residues. The W(V) intermediate of this reaction should be detectable by EPR. It would be very interesting to measure this intermediate during a single turnover, e.g. by freeze-quench methods.
Recent stopped-flow experiments on the AOR-family member FOR from *P. furiosus* showed that an activation process from the fully oxidized form of the enzyme (W^{VI}; $[4Fe4S]^{2+}$) to the 2 electron reduced form of the enzyme (W^{IV}; $[4Fe\text{-}4S]^{2+}$) has to take place

before the enzyme reaches a fully active state. This activation can be achieved by reducing the enzyme with the substrate formaldehyde in the absence of an electron acceptor. During subsequent turnovers in the presence of redox partner ferredoxin, the enzyme shuttles between a 1-electron (W^{VI}; $[4Fe\text{-}4S]^{1+}$ or W^{V}; $[4Fe\text{-}4S]^{2+}$) and a 3-electron reduced state (W^{IV}; $[4Fe\text{-}4S]^{1+}$) compared to fully oxidized, resting enzyme [16].

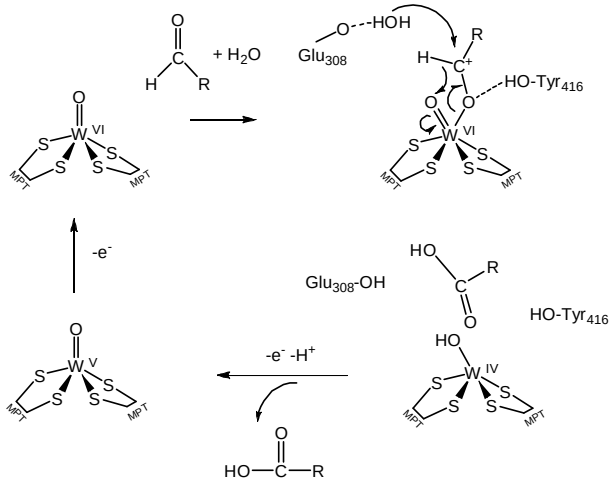

Figure 12. Proposed mechanism of W-AOR [126]. Glu308 (FOR numbering) activates a water molecule to attack the carbonyl group of the aldehyde bound to the tungsten center. A hydride of the carbonyl carbon is then transferred to the oxo-ligand of the tungsten center. A hydrogen bond from Tyr416 to the carbonyl oxygen atom of the substrate activates the substrate for nucleophilic attack. Finally, Thr240 facilitates proton transfer as part of the coupled electron proton transfer at the active site.

Formate dehydrogenases

The crystal structure of the tungsten-containing formate dehydrogenase from *D. gigas* has been determined to 1.8 Å resolution [90]. A positively charged substrate channel, a putative proton channel, and a hydrophobic CO_2 channel have been proposed in this structure. Electron transfer can take place from the pterin moiety via four [4Fe-4S] clusters, each circa 10 Å apart, offering an electron transfer conduit to the physiological redox partner, a monoheme cytochrome.

A recent re-evaluation of the crystal structure of the molybdenum-containing FDH-H from *E. coli*, together with the structure of the tungsten enzyme, suggests the following mechanism (figure 13) [127]. Formate binds to the tungsten center, displacing the selenocysteine ligand (SeCys158). The free selenocysteinate is stabilized by a nearby conserved arginine residue (Arg407). Subsequently, the alpha proton of the bound formate is transferred to a nearby conserved histidine residue (His159). During this step CO_2 is released and the tungsten center is reduced from VI to IV. Alternatively, the free

selenocysteinate may assist by forming a selenium-carboxylated intermediate as has been postulated previously [128]. As the final step two electrons are sequentially transferred from the tungsten center via the [4Fe-4S] cluster to an external redox partner protein, completing the catalytic cycle. This final step involves an EPR detectable W(V) intermediate. The mechanism of FDH, however, is still a subject of debate [129].

In the absence of a crystal structure of a formylmethanofuran dehydrogenase (FMDH), any proposed reaction mechanism remains highly speculative. FMDH catalyzes the reversible reductive carboxylation of methanofuran with CO_2 to *N*-formylmethanofuran. A three-dimensional structure of the enzyme would help to explain how both substrates can get into close proximity and may indicate the involvement of additional amino acid residues in the active site pocket.

Biochemical analysis and amino acid sequence comparison show that tungsten-containing FDMH contains a bis-MGD cofactor with an additional cysteine sulfur ligand to the tungsten center, and puts this enzyme into the DMSO reductase family [130,131].

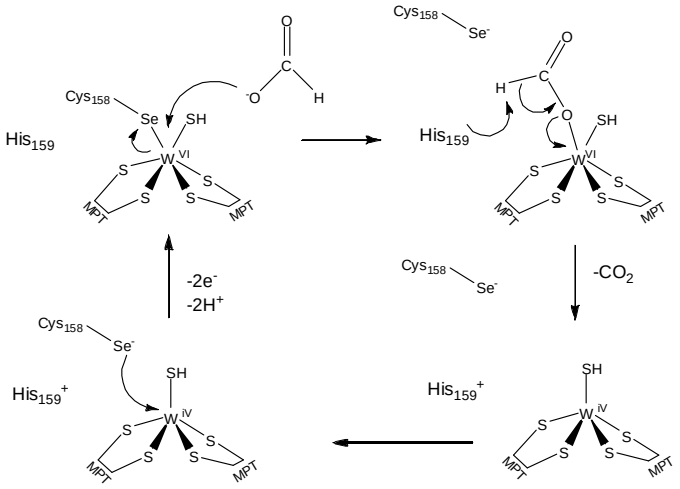

Figure 13. Proposed mechanism of W-FDH [127]. Formate binds to the tungsten center, displacing the selenocysteine ligand (SeCys158). The selenocysteinate is stabilized by a nearby conserved arginine residue (Arg407). Subsequently, the alpha proton of the bound formate is transferred to a nearby conserved histidine residue (His159). During this step CO_2 is released and the tungsten center is reduced from VI to IV. Alternatively, the free selenocysteinate may assist by forming a selenium-carboxylated intermediate. Finally, two electrons are sequentially transferred from the tungsten center via the [4Fe-4S] cluster to an external redox partner protein.

Acetylene hydratase

Acetylene hydratase is a unique tungsten-containing enzyme since it does not appear to catalyze a redox reaction. The structure has been determined at 1.26 Å resolution [132], and provides important clues on the catalytic mechanism and the roles of the W center and the [4Fe-4S] cluster (figure 14). The reactive species is either a hydroxo or a coordinated water

molecule. The hydroxo-ligand would act as a nucleophile with a vinyl-anion product that is able to deprotonate Asp13. Interestingly, the enzyme needs to be activated by reduction of the W center from W(VI) to W(IV). The [4Fe-4S] cluster is thought to facilitate this activation step. The coordinated water molecule could gain positive charge under the influence of the proximal Asp13. Subsequently, the electrophilic water can react with the acetylene triple bond in a Markovnikov-type electrophilic addition reaction. The tungsten center is regenerated by the binding of water to the W center and deprotonation by Asp13. Theoretical calculations suggests that the W(IV) active site favors coordination of water over hydroxo, supporting the electrophilic addition mechanism [132].

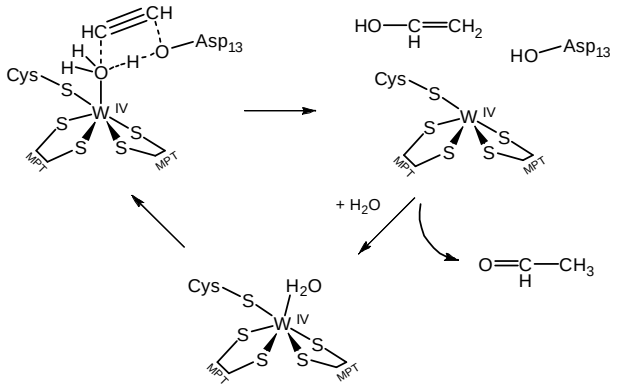

Figure 14. Proposed mechanism of W-Acetylene hydratase [132]. The reduced [4Fe-4S] cluster activates a coordinated water molecule, which gains positive charge under the influence of the proximal Asp13. Subsequently, the electrophilic water can react with the acetylene triple bond in a Markovnikov-type electrophilic addition reaction. The tungsten center is regenerated by the binding of water to the tungsten and deprotonation by Asp13. Alternatively, a hydroxo ligand would act as a nucleophile instead of a water molecule producing a vinyl-anion intermediate that is able to deprotonate Asp13.

Conclusions

In this review various aspects of the bioinorganic chemistry of the element tungsten have been considered. An overview was given of spectroscopic tools to study the metal either incorporated in proteins or as model coordination compound, followed by a description of relevant physiological processes, notably, the uptake and storage of the metal by cells and the incorporation into an organic cofactor in order to tune its redox properties required for biological activity. The two families of tungsten-containing enzymes were discussed: the aldehyde oxidoreductases containing a non-modified tungsto-bispterin cofactor, and the formate dehydrogenases which have a guanine monophosphate attached to each pterin. Understanding their mechanisms of action on a molecular level is a field of ongoing research, for which the use of spectroscopic techniques and the availability of synthetic mononuclear oxomolybdenum and tungsten complexes, are of high importance. Repeatedly, reference was made to the literature on molybdenum, which is generally more developed both for biological and for model systems.

In the introductory part two questions were raised to serve as Leitmotif for this review. The first question is: why do organisms use tungsten? At this time a full answer can not yet be given, although it has been shown that on an enzymatic level the presence of tungsten offers an advantage for the reduction of substrates with relatively low reduction potentials. Also, organisms that live in an environment with a relatively high tungsten over molybdenum concentration ratio and that have learned to exploit the tungsten, may have an advantage over the ones that are not able to do so, or for whom tungsten might even be xenobiotic [5-7].

The second question: ‘how do organisms discriminate between tungsten and molybdenum?’ also remains to be answered in full detail. However, it has become clear that the selection is not only made at the level of the transport proteins because these are all able to bind both oxoanions with affinities in the micromolar range or lower. A main act of selection must take place in the pathway of the cofactor synthesis and/or through specific enzymes that might only enable the incorporation of a specific metal-containing type of cofactor. In the coming years more experiments need to be designed and performed in order to solve the details of the selectivity process(es).

Finally, many issues are still to be addressed in the tungsten-biology fields of storage, regulation, and enzyme kinetics. Protein crystal structures of intermediates or intermediate analogues can help to solve reaction mechanisms of the tungstoenzymes. In addition, application of advanced spectroscopic techniques might contribute to a deeper insight into structure and mechanism. For these and other purposes, the synthesis of biomimetic tungsten complexes has an added importance.

References

[1] C.D. Brondino, M.J. Romao, I. Moura, J.J.G. Moura, Curr. Opin. Chem. Biol.10 (2006) 109.
[2] R. Hille, Chem. Rev. 96 (1996) 2757.
[3] J.J.G. Moura, C.D. Brondino, J. Trincao, M.J. Romao, J. Biol. Inorg. Chem. 9 (2004) 791.
[4] G. Schwarz, R.R. Mendel, Annu. Rev. Plant Biol. 57 (2006) 623.
[5] W.R. Hagen, A.F. Arendsen, Struct. Bond. 90 (1998) 161.
[6] A. Kletzin, M.W.W. Adams, FEMS Microbiol. Rev. 18 (1996) 5.
[7] M.K. Johnson, D.C. Rees, M.W.W. Adams, Chem. Rev. 96 (1996) 2817.
[8] J.R.R.Fraústo da Silva, R.J.P. Williams, The biological chemistry of the elements, Oxford University Press 1991
[9] M. Pourbaix, Atlas d'Equilibres Electrochimiques, Gauthier-Villars, Paris 1963.
[10] J.J. Cruywagen, I.F.J. Van der Merwe, J. Chem. Soc., Dalton Trans. (1987) 1701.
[11] F.H. Allen, J.E. Davies, J.J. Galloy, O. Johnson, O. Kennard, C.F. Macrae, E.M. Mitchell, G.F. Mitchell, J.M. Smith, D.G. Watson, J. Chem. Inform. and Comp. Sci. 31 (1991) 187.
[12] G. Lenoble, B. Hasenknopf, R. Thouvenot, J. Am. Chem. Soc. 128 (2006) 5735.
[13] R. Huang, B. Liu, J. Zhang, C. Liu, X. Gao, Chinese Sci. Bull. 46 (2001) 732.
[14] L.J. Stewart, S. Bailey, B. Bennett, J.M. Charnock, C.D. Garner, A.S. McAlpine, J. Mol. Biol. 299 (2000) 593.
[15] B. Adams, A.T. Smith, S. Bailey, A.G. McEwan, R.C. Bray, Biochemistry 38 (1999) 8501.
[16] E. Bol, N.J. Broers, W.R. Hagen, J. Biol. Inorg. Chem. (2007) DOI 10.1007/s00775-007-0301-3.
[17] M.K. Johnson, in Vibrational spectra of dithiolene complexes, Wiley, New York (2004) 213.
[18] J.L. Johnson, K.V. Rajagopalan, J. Biol. Chem. 251 (1976) 5505.
[19] P.L. Hagedoorn, T. Chen, I. Schroder, S.R. Piersma, S. de Vries, W.R. Hagen, J. Biol. Inorg. Chem. 10 (2005) 259.
[20] J.H. Enemark, A.V. Astashkin, A.M. Raitsimring, Dalton Trans. (2006) 3501.
[21] B.P. Koehler, S. Mukund, R.C. Conover, I.K. Dhawan, R. Roy, M.W.W. Adams, M.K. Johnson, J. Am. Chem. Soc. 118 (1996) 12391.
[22] I.K. Dhawan, R. Roy, B.P. Koehler, S. Mukund, M.W. Adams, M.K. Johnson, J. Biol. Inorg. Chem. 5 (2000) 313.
[23] S.P. Cramer, C.L. Liu, L.E. Mortenson, J.T. Spence, S.M. Liu, I. Yamamoto, L.G. Ljungdahl, J. Inorg. Biochem. 23 (1985) 119.
[24] G.N. George, R.C. Prince, S. Mukund, M.W.W. Adams, J. Am. Chem. Soc. 114 (1992) 3521.
[25] M.K. Chan, S. Mukund, A. Kletzin, M.W.W. Adams, D.C. Rees, Science 267 (1995) 1463.
[26] P.-L. Hagedoorn, W.R. Hagen, L.J. Stewart, A. Docrat, S. Bailey, C.D. Garner, FEBS Lett. 555 (2003) 606.
[27] P.L. Hagedoorn, PhD thesis, Delft University of Technology (2002) http://repository.tudelft.nl/file/80698/007489
[28] S. Rech, U. Deppenmeier, R.P. Gunsalus, J. Bacteriol. 177 (1995) 1023.
[29] M. Demerec, E.A. Adelberg, A.J. Clark, P.E. Hartman,Genetics 54 (1966) 61.
[30] J. Imperial, M. Hadi, N.K. Amy, Biochim. Biophys. Acta 1370 (1998) 337.
[31] K. Makdessi, J.R. Andreesen, A. Pich, J. Biol. Chem. 276 (2001) 24557.
[32] L.E. Bevers, P.-L. Hagedoorn, G.C. Krijger, W.R. Hagen, J. Bacteriol. 188 (2006) 6498.
[33] S. Pratte Brenda, T. Thiel, J. Bacteriol. 88 (2006) 464.
[34] Y. Hu, S. Rech, R.P. Gunsalus, D.C. Rees, Nat. Struct. Biol. 4 (1997) 703.
[35] D.M. Lawson, C.E.M. Williams, L.A. Mitchenall, R.N. Pau, Structure 6 (1998) 1529.
[36] K. Hollenstein, D.C. Frei, K.P. Locher, Nature 446 (2007) 213.

[37] M. Tejada-Jimenez, A. Llamas, E. Sanz-Luque, A. Galvan, E. Fernandez, Proc. Natl. Acad. Sci. USA 104 (2007) 20126.
[38] N.D. Chasteen, P.M. Harrison, J. Struct. Biol. 126 (1999) 182.
[39] D.M. Lawson, C.E. Williams, D.J. White, A.P. Choay, L.A. Mitchenall, R.N. Pau, J. Chem. Soc., Dalton Trans. (1997) 3981.
[40] A.W. Schuttelkopf, J.A. Harrison, D.H. Boxer, W.N. Hunter, J. Biol. Chem. 277 (2002) 15013.
[41] U.G. Wagner, E. Stupperich, C. Kratky, Structure 8 (1993) 1127.
[42] L. Delarbre, C.E. Stevenson, D.J. White, L.A. Mitchenall, R.N. Pau, D.M. Lawson, J. Mol. Biol. 308 (2001) 1063.
[43] K. Makdessi, K. Fritsche, A. Pich, J.R. Andreesen, Arch. Microbiol. 181 (2004) 45.
[44] D. Rauh, A. Graentzdoerffer, K. Granderath, J.R. Andreesen, A. Pich, Eur. J. Biochem. 271 (2004) 212.
[45] A. Graentzdoerffer, D. Rauh, A. Pich, R. Andreesen Jan, Arch. Microbiol. 179 (2003) 116.
[46] D. Fenske, M. Gnida, K. Schneider, W. Meyer-Klaucke, J. Schemberg, V. Henschel, A.-K. Meyer, A. Knochel, A. Müller, ChemBioChem. 6 (2005) 405.
[47] P.T. Pienkos, W.J. Brill, J. Bacteriol. 145 (1981) 743.
[48] J. Schemberg, K. Schneider, U. Demmer, E. Warkentin, A. Müller, U. Ermler, Angew. Chem. 46 (2007) 2408.
[49] S.F. Altschul, T.L. Madden, A.A. Schaffer, J. Zhang, Z. Zhang, W. Miller, D.J. Lipman, Nucleic Acids Res. 25 (1997) 3389.
[50] T. Sugio, H. Kuwano, Y. Hamago, A. Negishi, T. Maeda, F. Takeuchi, K. Kamimura, J. Biosci. Bioeng. 97 (2004) 378.
[51] M. Aguilar, K. Kalakoutskii, J. Cardenas, E. Fernandez, FEBS Lett. 307 (1992) 162.
[52] C.-P. Witte, M.I. Igeno, R. Mendel, G. Schwarz, E. Fernandez, FEBS Lett. 431 (1998) 205.
[53] K. Fischer, A. Llamas, M. Tejada-Jimenez, N. Schrader, J. Kuper, F.S. Ataya, A. Galvan, R.R. Mendel, E. Fernandez, G. Schwarz, J. Biol. Chem. 281 (2006) 30186.
[54] J. Polanams, A.D. Ray, R.K. Watt, Inorg. Chem. 44 (2005) 3203.
[55] D. Scott, N.K. Amy, J. Bacteriol. 171 (1989) 1284.
[56] J.H. Glaser, J.A. DeMoss, J. Bacteriol. 108 (1971) 854.
[57] A.M. Grunden, R.M. Ray, J.K. Rosentel, F.G. Healy, K.T. Shanmugam, J. Bacteriol. 178 (1996) 735.
[58] L.A. Anderson, T. Palmer, N.C. Price, S. Bornemann, D.H. Boxer, R.N. Pau, Eur. J. Biochem. 246 (1997) 119.
[59] D.G. Gourley, A.W. Schuttelkopf, L.A. Anderson, N.C. Price, D.H. Boxer, W.N. Hunter, J. Biol. Chem. 276 (2001) 20641.
[60] P.M. McNicholas, R.C. Chiang, R.P. Gunsalus, Mol. Microbiol. 27 (1998) 197.
[61] W.T. Self, A.M. Grunden, A. Hasona, K.T. Shanmugam, Microbiol. 145 (1999) 41.
[62] P.M. McNicholas, S.A. Rech, R.P. Gunsalus, Mol. Microbiol. 23 (1997) 515.
[63] L.A. Anderson, E. McNairn, T. Leubke, R.N. Pau, D.H. Boxer, J. Bacteriol. 182 (2000) 7035.
[64] P.A. Bertram, R.A. Schmitz, D. Linder, R.K. Thauer, Arch. Microbiol. 161 (1994) 220.
[65] J.A. Vorholt, R.K. Thauer, Eur. J. Biochem. 248 (1997) 919.
[66] A. Hochheimer, R. Hedderich, R.K. Thauer, Arch. Microbiol.170 (1998) 389.
[67] A. Hochheimer, R. Hedderich, R.K. Thauer, Mol. Microbiol. 31 (1999) 641.
[68] K.V. Rajagopalan, J.L. Johnson, J. Biol. Chem. 267 (1992) 10199.
[69] G. Schwarz, Cell. Mol. Life Sci. 62 (2005) 2792.
[70] M.M. Wuebbens, K.V. Rajagopalan, J. Biol. Chem. 270 (1995) 1082.
[71] L.E. Bevers, P.-L. Hagedoorn, J.A. Santamaria-Araujo, A. Magalon, W.R. Hagen, G. Schwarz, Biochemistry (2007) *in press*.

[72] A. Llamas, R.R. Mendel, G. Schwarz, J. Biol. Chem. 279 (2004) 55241.
[73] J.D. Nichols, K.V. Rajagopalan, J. Biol.Chem. 280 (2005) 7817.
[74] A. Llamas, T. Otte, G. Multhaup, R.R. Mendel, G. Schwarz, J. Biol.Chem. 281 (2006) 18343.
[75] S. Afshar, E. Johnson, S. de Vries, I. Schroder, J. Bacteriol. 183 (2001) 5491.
[76] T. Palmer, I.P. Goodfellow, R.E. Sockett, A.G. McEwan, D.H. Boxer, Biochim. Biophys. Acta (1998) 135.
[77] J.R. Andreesen, L.G. Ljungdahl, J. Bacteriol. 116 (1973) 867.
[78] I. Yamamoto, T. Saiki, S.M. Liu, L.G. Ljungdahl, J. Biol. Chem. 258 (1983) 1826.
[79] S. Mukund, M.W. Adams, J. Biol. Chem. 266 (1991) 14208.
[80] M.J. Almendra, C.D. Brondino, O. Gavel, A.S. Pereira, P. Tavares, S. Bursakov, R. Duarte, J. Caldeira, J.J.G. Moura, I. Moura, Biochemistry 38 (1999) 16366.
[81] C.M. Hensgens, W.R. Hagen, T.A. Hansen, J. Bacteriol. 177 (1995) 6195.
[82] B.M. Rosner, B. Schink, J. Bacteriol. 177 (1995) 5767.
[83] C.D. Brondino, M.C.G. Passeggi, J. Caldeira, M.J. Almendra, M.J. Feio, J.J.G. Moura, I. Moura, JBIC, J. Biol. Inorg. Chem. 9 (2004) 145.
[84] S. Mukund, M.W.W. Adams, J. Biol. Chem. 270 (1995) 8389.
[85] R. Roy, S. Mukund, G.J. Schut, D.M. Dunn, R. Weiss, M.W.W. Adams, J. Bacteriol. 181 (1999) 1171.
[86] R. Roy, M.W.W. Adams, J. Bacteriol. 184 (2002) 6952.
[87] L.E. Bevers, E. Bol, P.-L. Hagedoorn, W.R. Hagen, J. Bacteriol. 187 (2005) 7056.
[88] G.J. Schut, S.D. Brehm, S. Datta, M.W.W. Adams, J. Bacteriol. 185 (2003) 3935.
[89] M.V. Weinberg, G.J. Schut, S. Brehm, S. Datta, M.W.W. Adams, J. Bacteriol.187 (2005) 336.
[90] H. Raaijmakers, S. Macieira, J.M. Dias, S. Teixeira, S. Bursakov, R. Huber, J.J.G. Moura, I. Moura, M.J. Romao, Structure 10 (2002) 1261.
[91] J.C. Boyington, V.N. Gladyshev, S.V. Khangulov, T.C. Stadtman, P.D. Sun, Science 275 (1997) 1305.
[92] M. Jormakka, S. Tornroth, B. Byrne, S. Iwata, Science 295 (2002) 1862.
[93] R.U. Meckenstock, R. Krieger, S. Ensign, P.M.H. Kroneck, B. Schink, Eur. J. Bioch. 264 (1999) 176.
[94] G.B. Seiffert, G.M. Ullmann, A. Messerschmidt, B. Schink, P.M.H. Kroneck, O. Einsle, Proc. Natl. Acad. Sci. USA 104 (2007) 3073.
[95] R.R. Mendel, Dalton Trans. (2005) 3404.
[96] M.O. Park, T. Mizutani, P.R. Jones, J. Bacteriol. (2007).
[97] H.J. Cohen, R.T. Drew, J.L. Johnson, K.V. Rajagopalan, Proc. Natl. Acad. Sci. USA 70 (1973) 3655.
[98] J. Buc, C.-L. Santini, R. Giordani, M. Czjzek, L.-F. Wu, G. Giordano, Mol. Microbiol. 32 (1999) 159.
[99] S. Siemann, K. Schneider, M. Oley, A. Mueller, Biochem. 42 (2003) 3846.
[100] V.V. Pollock, R.C. Conover, M.K. Johnson, M.J. Barber, Arch. Biochem. Biophys. 403 (2002) 237.
[101] M. Boll, B. Schink, A. Messerschmidt, P.M.H. Kroneck, J. Biol. Chem. 386 (2005) 999.
[102] S. Mukund, M.W.W. Adams, J. Bacteriol. 178 (1996) 163.
[103] A.J. Gates, R.O. Hughes, S.R. Sharp, P.D. Millington, A. Nilavongse, J.A. Cole, E.-R. Leach, B. Jepson, D.J. Richardson, C.S. Butler, FEMS Microbiol. Lett. 220 (2003) 261.
[104] A. Vergnes, J. Pommier, R. Toci, F. Blasco, G. Giordano, A. Magalon, J. Biol. Chem. 281 (2006) 2170.
[105] A. Vergnes, K. Gouffi-Belhabich, F. Blasco, G. Giordano, A. Magalon, J. Biol Chem. 279 (2004) 41398.

[106] J. Pommier, V. Mejean, G. Giordano, C. Iobbi-Nivol, J. Biol. Chem. 273 (1998) 16615.
[107] M. Ilbert, V. Mejean, M.-T. Giudici-Orticoni, J.-P. Samama, C. Iobbi-Nivol, J. Biol. Chem. 278 (2003) 28787.
[108] J.H. Enemark, J.J.A. Cooney, J.-J. Wang, R.H. Holm, Chem. Rev. 104 (2004) 1175.
[109] D. Collison, C.D. Garner, J.A. Joule, Chem. Soc. Rev. 25 (1996) 25.
[110] B. Fischer, S.J.N. Burgmayer, Met. Ions Biol. Syst. 39 (2002) 265.
[111] E.C. Taylor, L.A. Reiter, J. Am. Chem. Soc. 111 (1989) 285.
[112] E.C. Taylor, P.S. Ray, I.S. Darwish, J.L. Johnson, K.V. Rajagopalan, J. Am. Chem. Soc. 111 (1989) 7664.
[113] G. Schwarz, R. Mendel, J. Santamaria, J. Reiss, PCT Int. Appl. WO200573387.
[114] J. Reiss, M. Bonin, H. Schwegler, J.O. Sass, E. Garattini, S. Wagner, H.-J. Lee, W. Engel, O. Riess, G. Schwarz, Mol. Gen. Metab. 85 (2005) 12.
[115] J. Jiang, R.H. Holm, Inorg. Chem. 43 (2004) 1302.
[116] M. Kaupp, Angew. Chem. Int. Ed. 43 (2004) 546.
[117] D. Uhrhammer, F.A. Schultz, Inorg. Chem. 43 (2004) 7389.
[118] S.R. Davie, N.D. Rubie, B.S. Hammes, C.J. Carrano, M.L. Kirk, P. Basu, Inorg. Chem. 40 (2001) 2632.
[119] C. Schulke, Dalton Trans. (2005) 713.
[120] P. Basu, V.N. Nemykin, R.S. Sengar, Inorg. Chem. 42 (2003) 7489.
[121] D.M.A.M. Luykx, J.A. Duine, S.de Vries, Biochemistry 37 (1998) 11366.
[122] M.G. Bertero, R.A. Rothery, N. Boroumand, M. Palak, F. Blasco, N. Ginet, J.H. Weiner, N.C.J. Strynadka, J. Biol. Chem. 280 (2005) 14836.
[123] D.P. Kloer, C. Hagel, J. Heider, G.E. Schulz, Structure 14 (2006) 1377.
[124] J.H. Enemark, J.J. Cooney, J.J. Wang, R.H. Holm, Chem. Rev. 104 (2004) 1175.
[125] M. Hofmann, J. Biol. Inorg. Chem. 12 (2007) 989.
[126] Y. Hu, S. Faham, R. Roy, M.W.W. Adams, D.C. Rees, J. Mol. Biol. 286 (1999) 899.
[127] H. Raaijmakers, M.J. Romao, J. Biol. Inorg. Chem. 11 (2006) 849.
[128] J. Heider, A. Boeck, Adv. Microb. Physiol. 35 (1993) 71.
[129] M.G. Rivas, P.J. Gonzalez, C.D. Brondino, J.J.G. Moura, I. Moura, J. Inorg. Biochem. 101 (2007) 1617.
[130] P.P. Schmidt, R. Lange, A.C.F. Gorren, E.R. Werner, B. Mayer, K.K. Andersson, J. Biol. Inorg. Chem. 6 (2001) 151.
[131] A. Hochheimer, R.A. Schmitz, R.K. Thauer, R. Hedderich, Eur. J. Biochem. 234 (1995) 910.
[132] G.B. Seiffert, G.M. Ullmann, A. Messerschmidt, B. Schink, P.M.H. Kroneck, O. Einsle, Proc. Natl. Acad. Sci. USA 104 (2007) 3073.
[133] J. Kuper, A. Llamas, H.-J. Hecht, R.R. Mendel, G. Schwarz, Nature 430 (2004) 803.

Part I

Uptake of tungstate

Chapter 2

Tungsten transport protein A (WtpA) in *Pyrococcus furiosus*: first member of a new class of tungstate and molybdate transporters

Loes E. Bevers
Peter-Leon Hagedoorn
Gerard C. Krijger
Wilfred R. Hagen

Adapted from: Journal of Bacteriology 188 (2006) 6498-6505

Abstract

A novel tungstate and molybdate binding protein has been discovered from the hyperthermophilic archaeon *Pyrococcus furiosus.* This tungstate transport protein A (WtpA) is part of a new ABC transporter system selective for tungstate and molybdate. WtpA has very low sequence similarity with earlier characterized transport proteins ModA for molybdate and TupA for tungstate. Its structural gene is present in the genome of numerous archaea and some bacteria. The identification of this new tungstate and molybdate binding protein, clarifies the mechanism of tungstate and molybdate transport in organisms that lack the known uptake systems associated with the ModA and TupA proteins, like many archaea. The periplasmic protein of this ABC transporter, WtpA (PF0080), was cloned and expressed in *Escherichia coli*. Using isothermal titration calorimetry (ITC), WtpA was observed to bind tungstate (K_D of 17 ± 7 pM) and molybdate (K_D of 11 ± 5 nM) with a stoichiometry of 1.0 mole oxoanion per mole of protein. These low K_D values indicate that WtpA has a higher affinity for tungstate compared to ModA and TupA, and a similar affinity for molybdate compared to ModA. A displacement titration of molybdate-saturated WtpA with tungstate, showed that the tungstate effectively replaced the molybdate in the binding site of the protein.

Introduction

Molybdenum and tungsten have similar ionic radii and chemical properties. Tungsten is the heaviest atom and the only third transition row element that exhibits biological activity in enzymes. Molybdenum is the only second transition row metal that exhibits biological activity when it is present in a cofactor of a metalloenzyme. Both metals are present mainly in enzymes that catalyse oxygen atom transfer reactions. In these enzymes they are coordinated by the two dithiolene sulfur atoms of a pterin molecule, called a molybdopterin cofactor (MPT) [1]. In the case of tungsten, the metal is always coordinated by two pterin moieties, forming a so called bis-pterin cofactor (Wco) [2,3]. Molybdenum is an essential trace metal for many forms of life whereas tungsten is found mostly in archaea and in some bacteria. The Moco-containing enzymes can be divided into three families depending on the coordination chemistry of the Mo ligand: the sulfite oxidases (SOs), the xanthine oxidoreductases (XORs), also including the aldehyde oxidases, and the dimethyl-sulfoxide (DMSO) reductases, which are only found in prokaryotes [4,5]. The Wco-containing enzymes only consist of the aldehyde oxidoreductases (AORs), formate dehydrogenases (FDHs), and an acetylene hydratase [3]. Based on sequence comparison the FDHs and acetylene hydratase are part of the molybdenum containing DMSO reductase family.

The transport of molybdate has been well characterized in particular for *Escherichia coli*, which expresses a high affinity ABC transporter for molybdate encoded by the ModABC genes [6]. The periplasmic molybdate binding protein ModA binds specifically molybdate and tungstate and not sulfate or other anions [6]. Crystal structures of the *E. coli* and the *Azotobacter vinelandii* ModA indicate that the specificity for molybdate and tungstate is mostly determined by the size of the binding pocket. The Cambridge Structural Database [7] gives 1.75 +/- 0.04 Å and 1.76 +/- 0.02 Å for molybdate and tungstate respectively and 1.47 +/- 0.02 Å for sulfate. The ModA proteins cannot discriminate between molybdate and tungstate. The first tungsten specific ABC transporter was identified in *Eubacterium acidaminophilum* [8]. The periplasmic tungsten uptake protein (TupA) was cloned and expressed in *E. coli* and was shown to bind only tungstate with a high affinity. A crystal structure of TupA is not yet available, and it is not clear what the structural basis is of the specificity for tungstate over molybdate. Recently, a high affinity vanadate transporter, which was highly selective for vanadate compared to tungstate, was identified in the cyanobacterium *Anabaena variabilis ATCC 29413* based on the sequence similarity with the TupA protein from *E. acidaminophilum* (58% sequence similarity) [9]. *A. variabilis ATCC 29413* expresses an alternative V-dependent nitrogenase for the fixation of nitrogen and therefore it requires vanadate [9]. The specificity of this transporter for vanadate indicates that high sequence similarities are not conclusive for the selectivity of the transporter.

Our goal was to study tungstate transport in an organism that is strictly dependent on tungstate, the hyperthermophilic archaeon *Pyrococcus furiosus.* This organism grows optimally at 100 ºC under strict anaerobic conditions [10]. In the last decade five tungsten containing aldehyde oxidoreductase enzymes were purified and characterized from *P.*

furiosus. Aldehyde oxidoreductase (AOR) [11], formaldehyde oxidoreductase (FOR) [12] and tungsten containing oxidoreductase 5 (WOR5) [13] all have a broad substrate specificity for aldehydes varying from shorter chains, and C4 to C6 semialdehydes (FOR) to longer, aromatic and aliphatic backbones (AOR, WOR5). These broad substrate specificities do not immediately imply a clear physiological function for these proteins; micro array experiments indicate that they might play a role in peptide fermentation or in stress response [14,15]. In contrast, glyceraldehyde-3-phosphate oxidoreductase (GAPOR) is known only to convert the substrate glyceraldehyde-3-phosphate (GAP) [16]. It is the only W-containing aldehyde oxidoreductase with an assigned function, namely, in the Embden Meyerhof-type of glycolysis where it converts GAP to 3-phosphoglycerate, replacing glyceraldehyde-3-phosphate dehydrogenase (GAPDH) and phosphoglycerate kinase (PGK). Tungsten oxidoreductase 4 (WOR4) was purified from *P. furiosus* grown in the presence of elemental sulfur (S^0) [17]. No substrate has been identified yet for WOR4. Besides these five tungsten containing enzymes of the AOR family, the genome of *P. furiosus* also encodes two genes for putative tungsten or molybdenum containing formate dehydrogenases (FDHs) [18].

Cultivation experiments indicated that *P. furiosu*s has a highly specific tungstate uptake mechanism. When molybdate was added to the growth media in a 1000-fold excess, the cells were able to selectively scavenge the traces of tungstate from the media and used it for the incorporation in the cofactor of the AOR enzymes [19].

The genome of *P. furiosus* does not carry a *tupA* homologue, however a putative sulfate/thiosulfate/molybdate transporter is present that has 30% sequence similarity with the ModA protein from *E. coli* (PF0080/PF0081/PF0082)) (18% sequence identity). The other components of this putative transporter, WtpB and WtpC, have a high sequence similarity to ModB/TupB (53% and 50% similarity) and ModC/TupC (51%/56%), respectively. Besides this putative sulfate/thiosulfate/molybdate transporter, the only ABC transporter encoded in the genome with some similarity (28%) to ModA is annotated as a putative phosphate transporter (PF1003/PF1006/PF1007/PF1008). However the sequence identity is much lower, only 11%.

Since no molybdenum enzymes have been identified yet from *P. furiosus*, we hypothesized that the operon that contains the PF0080, PF0081 and PF0082 genes encodes for a tungstate selective ABC transporter. An mRNA fragment coding for the PF0080 gene has previously been detected in micro array experiments [15], indicating that the protein is expressed *in vivo*.

In this paper we describe the cloning, expression and binding characteristics of this new tungstate transport protein (WtpA).

Materials and Methods

Materials - All chemicals used were of the highest quality available. Prepacked strep-tag columns were used as recommended by the supplier (IBA).

Cloning of the WtpA gene - The WtpA gene (PF0080) was amplified by PCR using *Pfx* polymerase (Invitrogen), sense (WtpA_F_Bsa1) and antisense (WtpA_R_Bsa1) primers (Thermohybaid) 5'-ATGGTACGTCTCAAATGCGAGAGGG-3' and 5'-ATGGTACGTCTCAGCGCTCTTTTCAAT-3' and chromosomal DNA from *P. furiosus* as a template. Extraction of the chromosomal DNA was performed with phenol/chloroform/isoamylalcohol [20]. The PCR product was treated with *Taq* polymerase (Amersham Bioscience) for 10 minutes at 72 °C to obtain single 3'adenine overhangs for sub-cloning into the pCR®2.1-TOPO® vector (Invitrogen). This TOPO-construct was transformed into competent *E. coli* TOP10 cells (Invitrogen) and plasmid was isolated from an overnight culture. Both primers contain a Bsa1 restriction site and they were used to clone the *wtpA* gene into the Bsa1 site of the pASK-IBA2 expression vector (IBA), resulting in a WtpA fusion protein with an N-terminal OmpA *E. coli* signal peptide and a C-terminal strep-tag. This construct was transformed into competent *E. coli* BL21- CodonPlus®-(DE3)-RIL cells (Stratagene) and sequenced for confirmation.

Protein expression and purification - *E. coli* BL21(DE3) cells that contained the plasmid encoding the WtpA fusion protein were grown on LB medium containing 100 µg/ml ampicilin. Protein synthesis was induced with 200 µl of an anhydrotetracyclin solution (2 mg/ml in dimethyl-sulfoxide) per litre culture, when the absorbance of the culture reached 0.5 at 600 nm. Cells were induced for 4 hours at 30 °C and harvested by centrifugation. The cells were washed with 100 mM Tris-HCl, pH 8.0, and were broken in the same buffer (1 g of cells per 5 ml buffer) with a cell disruptor system (Constant systems). Cell-free extract was obtained by centrifugation for 20 minutes at 15.000 x g at 4 °C. As a first purification step the supernatant was heated for 30 minutes at 60 °C. Precipitated protein was removed by centrifugation and the remaining cell-free extract was applied to a 1 ml strep-tactin column (IBA) equilibrated with buffer W (100 mM Tris-HCl, pH 8.0, 150 mM NaCl, 1 mM EDTA). The column was washed with 5 ml buffer W and the protein was eluted in 3 ml buffer W containing 2.5 mM desthiobiotin.

Gel-shift assay - The gel shift assay developed by Rech et al. [21] was used to qualitatively observe the binding of different oxoanions to the protein. Samples of 10 µl containing 25 µM of purified WtpA in 10 mM Tris-HCl pH 8.0, were incubated in 50 mM potassium acetate (pH 5.0) and 10 mM of one of the oxoanions: sulfate, phosphate, chlorate, molybdate, and tungstate for 30 minutes on ice. Samples were analysed on a high density (20%) native polyacrylamide gel on a Phast System (GE Healthcare). The electrophoresis was performed at a voltage of 150 V, at 4 °C for approximately 4 hours.

Size exclusion chromatography - Size exclusion chromatography was performed using an analytical HR10/30 Superdex-200 column (GE Healthcare) equilibrated with 20 mM Tris-HCl pH 8.0, 150 mM NaCl. WtpA (35 µM) was incubated with different concentrations of tungstate and/or molybdate in a total volume of 100 µl for 30 minutes at room temperature.

The protein was separated from unbound oxoanion with a flow rate of 0.5 ml/min. Fractions were collected and the molybdenum and tungsten content was determined by catalytic adsorptive stripping voltammetry [22].

Radioactive labelled tungstate experiments - ^{187}W (half-life 23.8 h) was produced by irradiation of 10 mg Na_2WO_4 in a thermal neutron flux of 4 x 10^{16} m^{-2} s^{-1} for 10 hours. The specific activity was 8 x 10^{12} Bq ^{187}W per mole W. The target material was dissolved in 1.0 ml 20 mM Tris-HCl pH 8.0.
0.5 µM WtpA was incubated with varying concentrations (25 nM – 20 µM) of radioactive labelled sodium tungstate for 5 minutes in 20 mM Tris-HCl pH 8.0 at room temperature in a total volume of 250 µl. Dowex AG-1X8 (100-200 mesh, Cl^- form, Fluka), 50 mg, was added as a slurry (1 vol. water/vol. resin) to remove unbound tungstate from the protein solution. The Dowex was allowed to settle for 5 minutes and the ^{187}W in 200 µl of the supernatant was determined in a Wallac (Turku, Finland) 1480 Automatic 3'' gamma counter. The amount of ^{187}W in the Dowex and the residual supernatant was also determined in this gamma counter.

Isothermal titration calorimetry (ITC) - Prior to all ITC experiments WtpA was extensively dialyzed against large volumes of ITC buffer (10 mM Tris-HCl, 50 mM NaCl, pH 8.0) at 4° C. Tungstate and molybdate stock solutions (1 M) were prepared in H_2O and diluted to 0.1 – 0.4 mM final concentration using ITC buffer. Tungstate and molybdate were titrated as ligand into the sample cell (1.42 ml) containing 7-15 µM WtpA. Tungstate and molybdate were injected in 2-4 µl injections to reach a final molar ratio of ligand to WtpA ranging from 2:1 to 4:1 at the end of the experiment. Blank injections of titrant into the buffer were performed to estimate the heat of injection, mixing and dilution, which was similar to the heat release that was seen at the end of each titration after reaching saturation. At least three experiments were performed with tungstate and molybdate, and two displacement titrations with tungstate were done using molybdate saturated WtpA (containing 1.5 fold molar excess of molybdate). All experiments were performed at 25° C using a VP-ITC Microcalorimeter (Microcal, Northhampton, USA). For every injection the binding enthalpy was calculated by integration of the peak area using the ORIGIN software. The heat change after each injection is related to the calorimetric enthalpy of binding ΔH_{cal} and is also dependent on the stoichiometry of the WtpA/anion complex. The association constant K_a and additional binding parameters (binding stoichiometry, enthalpy and entropy) were obtained through curve fitting with ORIGIN. Baseline subtraction was performed manually by averaging the last 5-10 injections after reaching saturation and subtracting from the ΔH_{cal}.

Protein assays. Protein concentration was determined using the bicinchoninic acid assay method with bovine serum albumin as the standard. Molecular weight and degree of purity

was determined with SDS-polyacrylamide gel electrophoresis on a Phast System (GE Healthcare) in 8-25% gradient SDS-PAGE gels.

Results

Cloning and purification of WtpA

The N-terminal amino-acid sequence of WtpA (PF0080) starts with a putative lipobox of a lipoprotein signal peptide. The consensus sequence for a lipobox in bacteria is [I/L/G/A]-[A/G/S]-C [23] and in the case of WtpA it is AGC (figure 1). Furthermore, significant homology was found with leader peptides from other periplasmic components of anion ABC transporters in archaea with the putative motif: KK-X_{14}-GC (GC is part of lipobox sequence, figure 1) [23]. The cysteine is always conserved in this motif. In bacteria it has been shown that this residue is lipid modified prior to cleavage by type II signal peptidases [23].

These lipoproteins have not yet been identified in archaea. Some archaeal solute-binding proteins have been characterized that also contain a typical lipobox motif (SGC), e.g. the maltotriose binding protein of *P. furiosus* [24]. However these proteins were N-terminally blocked and therefore the presence of the lipid moiety could not be confirmed. The leader peptides are split at the N-terminal side of the cysteine in the case of bacteria; the cleavage site in archaea is unknown. In bacteria the mature lipoprotein remains anchored in the cytoplasmic membrane after cleavage.

For the TupA gene of *E. acidaminophilum* a similar leader sequence was found [8]. When the TupA protein was expressed in *E. coli* containing its native leader peptide, 90% of the recombinant protein was found associated with the cytoplasmic membrane of *E. coli* and only a small fraction of soluble protein was obtained. Therefore the WtpA (PF0080) protein from *P. furiosus* was cloned without its native leader sequence into the pASK-IBA2 vector. This vector contains an N-terminal *E. coli* leader sequence, encoding for the OmpA leader peptide that causes the protein to be exported across the cytoplasmic membrane. The WtpA gene was cloned into the pASK-IBA2 vector and expressed as a C–terminal strep-tag fusion protein. Purification resulted in a yield of approximately 5 mg WtpA per litre of induced *E. coli* culture. The protein remained stable and soluble during the purification step in which the *E. coli* cell-free extract was heated for 30 minutes at 60 ºC. The heat stability of WtpA was tested more thoroughly on the purified protein; The 280 nm absorption remained constant for at least 6 hours after incubation of the protein at 80 ºC, and there was no precipitation observed (data not shown).

Purified WtpA showed multiple bands of apparent molecular weights between 35-45 kDa (data not shown) on native polyacrylamide gel electrophoresis, which was also observed for the TupA protein from *E. acidaminophilum* [8]. These different forms of WtpA are obtained because they are processed differently by the signal peptidases of *E. coli*. The major band was observed around 40 kDa, which is in agreement with the gene PF0080 encoding for a

37 kDa protein (without the leader sequence), suggesting that the WtpA protein occurs as a monomer in its native form.

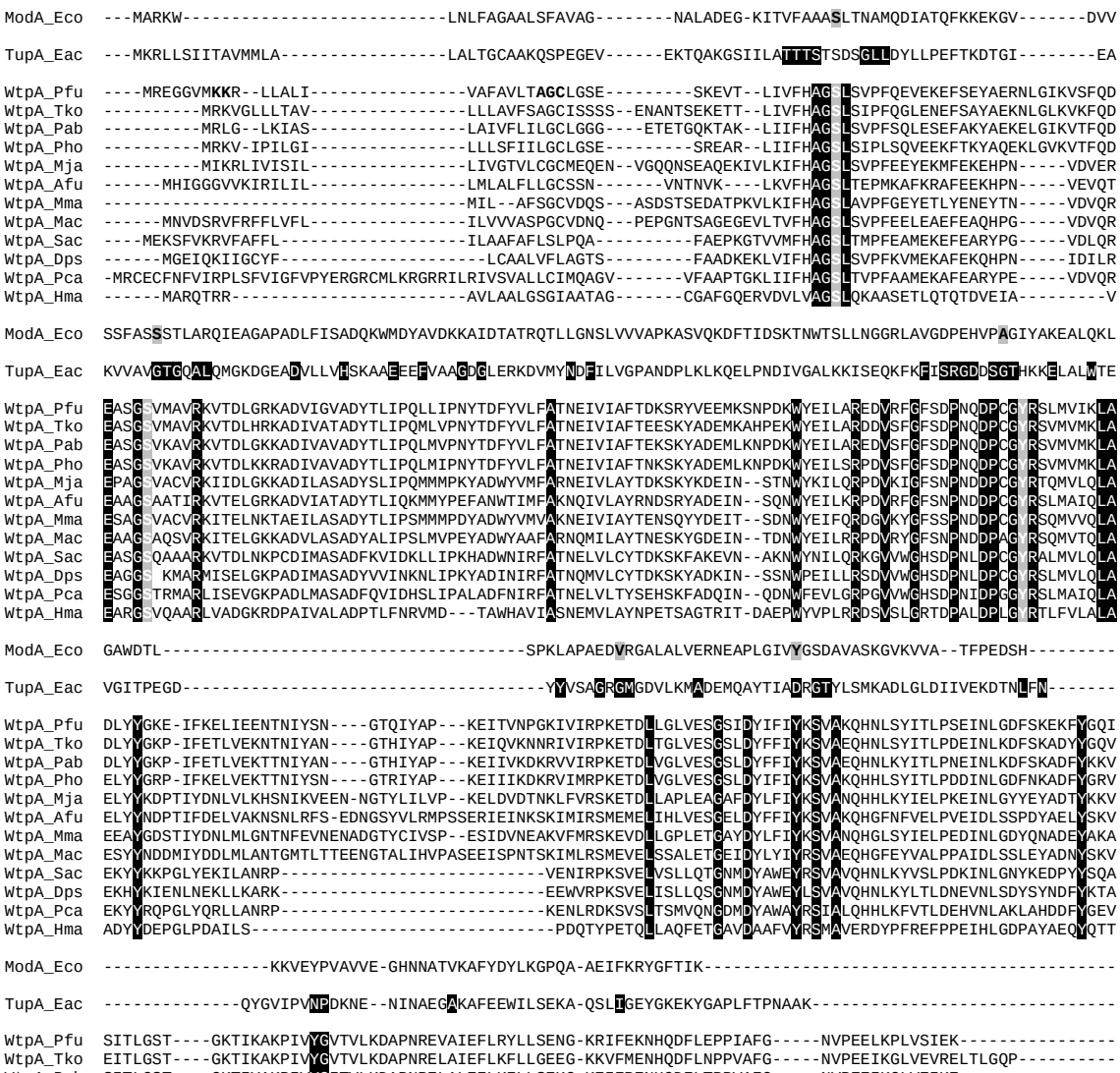

Figure 1. Amino acid sequence alignment of periplasmic binding proteins: *E. coli* ModA, *E. acidaminophilum* TupA, *P. furiosus* WtpA and the 11 WtpA homologues. The sequence alignment was performed with all the protein sequences that were also used to create the phylogenetic tree (figure 4). The bold residues (shaded grey) in the ModA protein are involved in the binding of the molybdate, based on the resolved crystal structures [25,26]. The bold residues in the WtpA protein indicate the lipobox consensus sequence and the ones postulated to play a role in binding of the oxoanion are printed in white (shaded grey). The residues printed in white (shaded black) in the TupA and WtpA sequences are conserved amongst their homologues.

Qualitative binding experiments

WtpA (35 μM) was incubated with 50 μM tungstate or molybdate and the protein was subsequently separated from the unbound salt with size exclusion chromatography. The presence of the oxoanions did not change the elution profile of the monomeric protein. The metal content of the protein fraction and the low molecular weight fraction (unbound oxoanion) was determined by catalytic adsorptive stripping voltammetry [22]. It was found that molybdate and tungstate co-eluted with the protein (figure 2) and the excess of oxoanion eluted in the low molecular weight fraction. The molar ratio of tungstate and/or molybdate and protein was determined to be less than one in all experiments. This can be explained by a loss of bound oxoanion during the time course of the experiment of approximately 30 minutes. Still 20% of the tungstate or molybdate was bound to the protein at the end of the chromatography run, which indicates an off-rate in the order of 10^{-3} per second.

To qualitatively examine the preference for either tungstate or molybdate, the protein was incubated with a mixture of the two oxoanions. In all experiments both metals were detected in the protein fraction. However the amount of bound tungstate was significantly higher, even in the presence of an excess of molybdate during the incubation (figure 2). These data demonstrate that WtpA is able to bind tungstate and molybdate, with a preference for tungstate, without changing the oligomeric state of the protein.

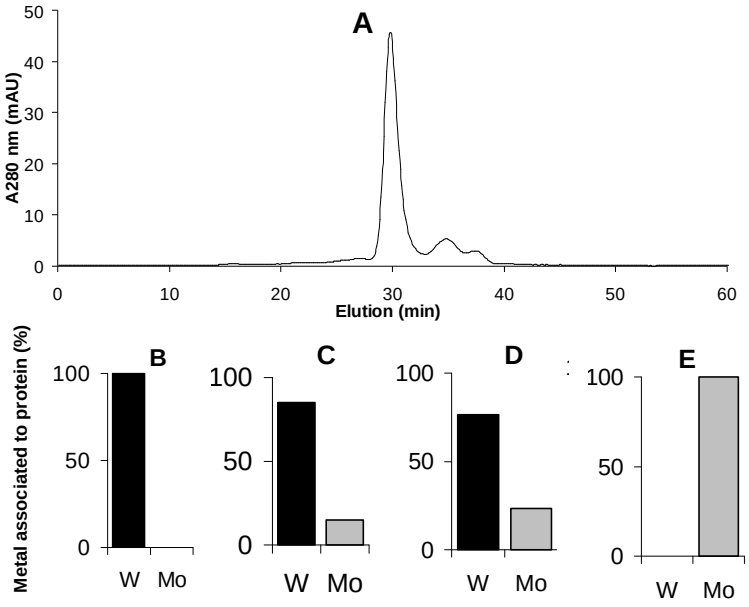

Figure 2. (A) Size exclusion chromatography of WtpA (35 μM, 100 μl sample volume, 0.5 ml/min). (B,C,D,E) Percentage of total metal, tungstate (black) or molybdate (grey), detected in the protein fraction after incubation of 30 minutes at room temperature with: 50 μM sodium tungstate (B), a mixture of 46 μM sodium tungstate and 92 μM sodium molybdate (2-fold excess of molybdate) (C), a mixture of 44 μM sodium tungstate and 222 μM sodium molybdate (5-fold excess of molybdate) (D), 50 μM sodium molybdate (E).

To test the affinity for other oxoanions, a ligand-dependent protein gel-shift assay was performed with reference to the migration rate of the uncomplexed protein in native polyacrylamide gels [21]. The protein was incubated with a 400-fold molar excess of sulfate, phosphate, chlorate, molybdate and tungstate. Only the tungstate incubated samples showed a slight but significant mobility shift compared to the non-incubated protein and to the samples incubated with the other anions (data not shown). A similar gel-shift assay has been used before to estimate the dissociation constant (K_D) for tungstate to be 0.5 μM for the *E. acidaminophilum* TupA [8] (table 1). In the present case, the sensitivity of this gel-shift mobility assay was not sufficient to determine dissociation constants of *P. furiosus* WtpA for tungstate or molybdate.

Table 1. Dissociation constants (K_D) for the binding of tungstate and molybdate to periplasmic binding proteins.

Protein	Tungstate	Molybdate	Method
ModA *E. coli* [27]	20 ± 8	20 ± 8	Radioactive Dowex assay
TupA *E. acidaminophilum*	500	not determined	Gel shift assay
WtpA *P. furiosus*	0.017	11 ± 5	ITC

Ligand dependent spectral changes have also been used to estimate values for the apparent K_D for the binding of molybdate or tungstate to periplasmic binding proteins. In the case of the ModA protein, binding of tungstate or molybdate has been shown to cause a slight change in the spectrum in the far UV wavelengths range; also the intrinsic fluorescence spectrum of ModA changes upon molybdate binding [21,27]. However, for *P. furiosus* WtpA these spectral differences were not significant enough to make a valid estimation for the K_D (data not shown).

An isotopic binding method provided the most accurate K_D value of 20 +/- 8 nM for molybdate binding of ModA (table 1) [27]. Therefore, a similar experiment was carried out for determining the K_D of *P. furiosus* WtpA for tungstate. However, the determined ligand-to-protein stoichiometry was much lower than unity; this indicates that this experimental setup is not reliable, as it is likely to result in a serious overestimation of the magnitude of K_D. Most likely, the Dowex resin was able to strip bound tungstate from the protein.

In summary, the above mentioned assays which were all used in previous reports to determine the K_D for periplasmic binding proteins, were not sensitive and/or accurate enough to determine the K_D in the case of WtpA. However they qualitatively confirm the ability of the WtpA protein to bind tungstate.

Isothermal titration calorimetry

ITC of WtpA showed that the protein endothermically binds tungstate and molybdate with a stoichiometry of one mole oxoanion per mole of protein, as deduced from the heat consumption upon addition of tungstate or molybdate to the protein solution (figure 3). The

obtained binding curve for molybdate was used to determine the K_D value to be 11 ± 5 nM. The extremely high affinity of the protein for tungstate resulted in a very steep binding curve, and this precluded an accurate fit to determine the K_D value of the protein for tungstate. It was not possible to significantly decrease both the protein concentration or the amount of titrated tungstate to obtain more data points in the steep region in view of the signal to noise ratio. However an upper limit for the K_D of 1 nM was estimated from the data.

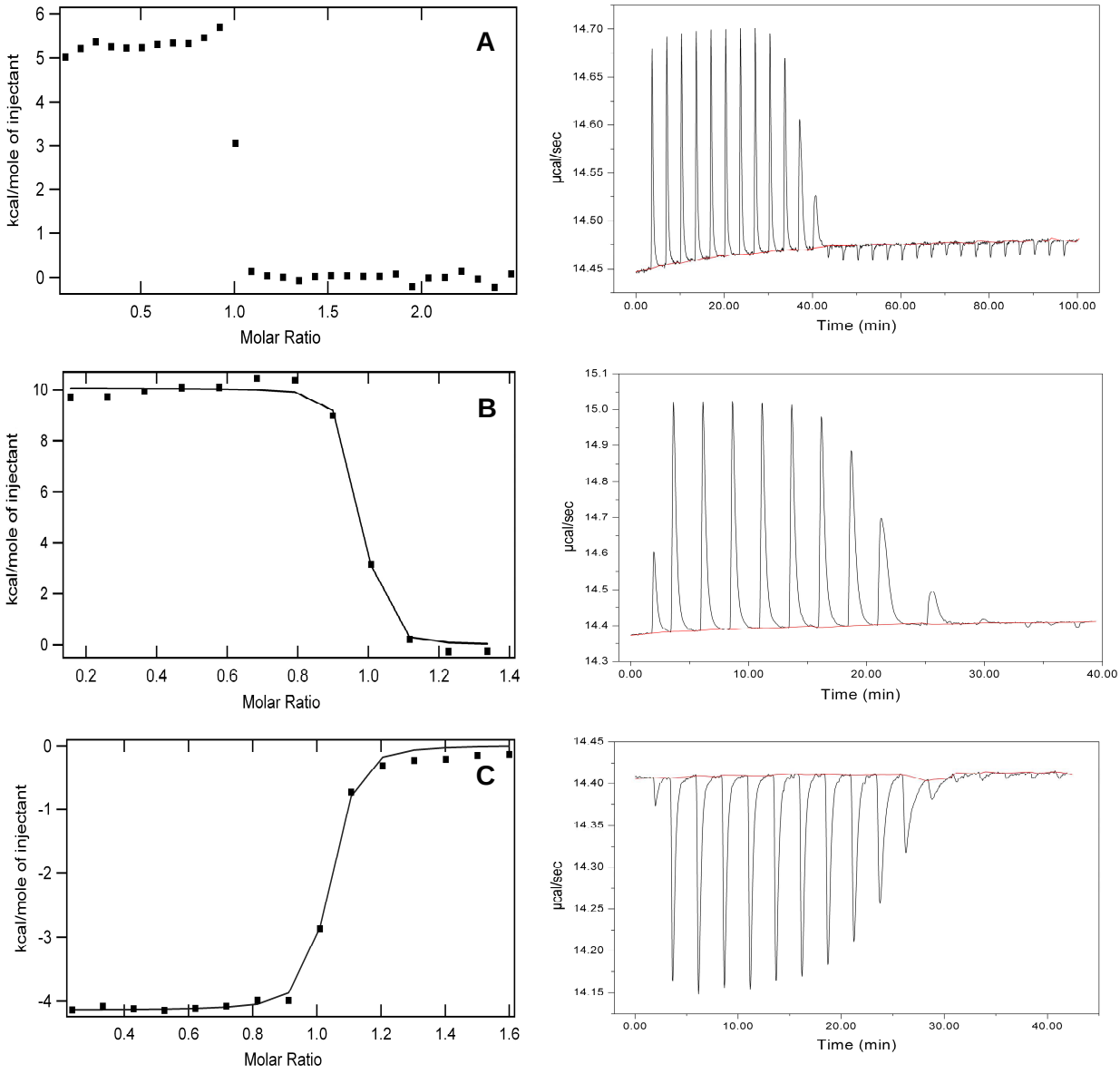

Figure 3. ITC of 10 µM WtpA titrated with injections of 0.8 µM tungstate (A), and 1 µM molybdate (B). (C) Displacement titration of 10 µM WtpA incubated with 15 µM molybdate, with injections of 1 µM tungstate. Data were fitted (continuous line in figure B and C) with the ORIGIN software. The raw ITC data are shown in the right graphs.

Binding of molybdate resulted in a greater heat consumption (ΔH_{cal} = 9.9 ± 0.5 kcal/mole of injectant) compared to the heat consumption upon the binding of tungstate (ΔH_{cal} = 5.3 ± 0.2 kcal/mole of injectant). These numbers were calculated by taking the average heat consumption of the first data points of the curve where all the ligand was directly bound to the protein.

A displacement titration of the molybdate-saturated protein with tungstate showed a heat release, which corresponds to the difference in heat release between the two oxoanions (ΔH_{cal} = -4.1 ± 0.4 kcal/mole of injectant) (figure 3C). This shows clearly that the protein favors the binding of tungstate, even when the binding site is occupied by a molybdate molecule. The *apparent* K_D for tungstate when the protein is saturated with molybdate was determined to be 15 ± 4 nM (figure 3C). The K_D value of a displacement titration in combination with the K_D value for the inhibiting ligand in the absence of strong binding ligand, can be used to calculate the actual K_D for the strong binding ligand with the following competition equation: $K_{app} = K_A/(1 + K_B[B])$ [28] where K_A is the binding constant for the strong binding ligand (tungstate) and K_B for the competitively inhibiting ligand (molybdate). The apparent binding constant depends on the concentration of free molybdate [B], which changes during the experiment between 5 μM and 15 μM. An average value of 10 μM was used in the equation to calculate a K_D of 17 ± 7 pM of WtpA for tungstate (K_A) [28], which is the lowest K_D value determined for any tungstate or molybdate periplasmic binding protein. The displacement titration and the extremely low K_D value for tungstate indicate the latter to be the physiological substrate for WtpA.

Sequence alignments

WtpA (PF0080) - The highest similarities with the PF0080 gene were found with hypothetical proteins from *Thermococcus kodakarensis KOD1* (YP_182428) (87%), *Pyrococcus abyssi GE5* (NP_125843) (87%) and *Pyrococcus horikoshii OT3* (NP_142154) (90%). They are all included in operons encoding putative ABC transporters and represent the periplasmic binding protein. WtpA has only weak similarity with the ModA protein of *E. coli* (17.6% identity, 30% similarity) and the TupA protein of *E. acidaminophilum* (15.6% identity, 30.7% similar) (figure 1,4) and therefore it forms a new class of tungstate and molybdate binding proteins (figure 4). A BLAST search of the WtpA sequence against the non-redundant database (NCBI) resulted in the identification of 11 homologues (P-value < 10^{-20}) (figure 1, 4). These homologues of the *P. furiosus* WtpA protein and the five closest homologues, each of the *E. coli* ModA protein, the *E. acidaminophilum* TupA protein, and the two *A. vinelandii* ModA1 and ModA2 proteins were used to make the alignment in figure 1.

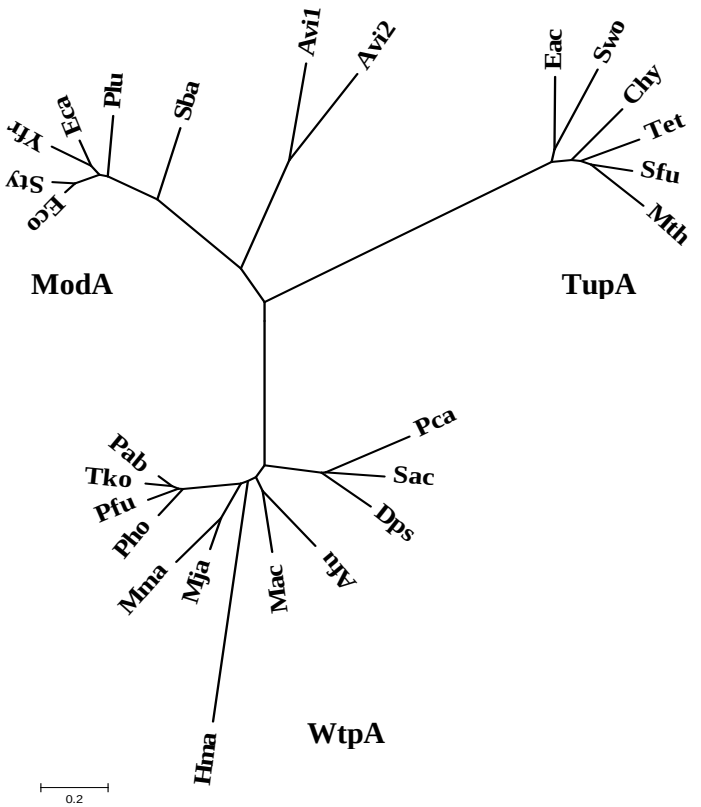

Figure 4. Unrooted phylogenetic tree of molybdate and tungstate periplasmic binding proteins. The alignment was made with the 11 homologues (P-value < 10^{-20}) of the *P. furiosus* WtpA protein and the five closest homologues, each of the *E. coli* ModA protein, the *E. acidaminophilum* TupA protein, and the two *A. vinelandii* ModA1 and ModA2 proteins. ModA homologues: *Salmonella typhimurium LT2* (accession number: AE008732.1, identity 86%, similarity 91%), *Erwinia carotovora subsp. atroseptica SCRI1043* (BX950851.1, 69%, 80%) *Yersinia frederiksenii ATCC 33641* (NZ_AALE01000012.1, 70%, 80%), *Photorhabdus luminescens subsp. laumondii TTO1* (BX571864.1, 61%, 75%), *Shewanella baltica OS155* (NZ_AAIO01000008.1, 50%, 71%). TupA homologues: *Syntrophomonas wolfei str. Goettingen* (NZ_AAJG01000003.1, 51%, 67%), *Thermoanaerobacter ethanolicus ATCC 33223* (NZ_AAKQ01000001.1, 50%, 70%), *Carboxydothermus hydrogenoformans Z-2901* (CP000141.1, 50%, 65%), *Syntrophobacter fumaroxidans MPOB* (NZ_AAJF01000122.1, 48%, 66%), *Moorella thermoacetica ATCC 39073* (NC_007644.1, 46%, 64%). WtpA homologues: *Thermococcus kodakarensis KOD1* (AP006878.1, 75%, 87%), *Pyrococcus abyssi GE5* (AJ248283.1, 74%, 87%), *Pyrococcus horikoshii shinkaj OT3* (BA000001.2, 73%, 90%), *Methanococcus jannaschii DSM2661* (L77117.1, 49%, 69%), *Archaeoglobus fulgidus DSM4304* (NC_000917.1, 46%, 67%), *Methanococcus maripaludis S2* (BX957223.1, 46%, 63%), *Methanosarcina acetivorans C2A* (AE010299.1, 43%, 63%), *Syntrophus aciditrophicus SB* (NC_007759.1, 39%, 60%), *Desulfotalea psychrophila LSv54* (CR522870.1, 40%, 56%), *Pelobacter carbinolicus DSM 2380* (CP000142.1, 36%, 55%), *Haloarcula marismortui ATCC 43049* (AY596297.1, 29%, 47%).

The crystal structure of the ModA protein of *E. coli* and the ModA2 protein of *A. vinelandii* have been solved to high resolution [25,26]. The residues that bind molybdate through hydrogen bonds in the ModA proteins are S12, S39, A125, V152 and Y170 in *E. coli* ModA (figure 1) and T9, N10, S37, Y118 and V147 in *A. vinelandii* ModA2. Unfortunately, there is no crystal structure of TupA available yet and therefore it is not known which residues play a role in the binding of tungstate in this protein. A structural homology model was made for WtpA based on the amino acid sequence and a homologue of a known structure [29]. The protein 1AMF (*E. coli* ModA) was selected by the program from the PDB database as parental structure to which the WtpA structure could be modelled with an e-value of 10^{-139}. This indicates a significant structural similarity and therefore we use the obtained structure to hypothesize which residues might play a role in the binding of tungstate or molybdate. Three of the five amino acids that bind molybdate in *E. coli* ModA have identical residues at identical positions in the modelled structure of WtpA. The S42, S75 and Y164 residues in the WtpA protein are positioned homologously to the S12, S39 and Y170 residues in ModA. Furthermore, these residues are completely conserved among all WtpA homologues and this is an additional indication that they might play a role in the binding of the molybdate or tungstate (figure 1). The ModA residues A125 and V152 that bind the molybdate through their backbone NH group show no obvious similar residues in the WtpA model. A crystal structure of the WtpA protein is required for the confirmation of these residues being involved in binding of the oxoanion. Crystallisation studies with WtpA are currently in progress in our laboratory.
The sequence similarity of the other components of the novel tungstate ABC transporter, between WtpB and ModB/TupB (53% and 50% similarity, respectively) and between WtpC and ModC/TupC (51% and 56%, respectively) are much higher than the similarities between the A components. WtpB and WtpC both exhibited highest similarity with the permease and ATP-ase components from the putative ABC transporters in *T. kodakarensis KOD1* (87%/90%), *P. abyssi GE5* (87%/86%) and *P. horikoshii OT3* (89%/90%) whose binding protein component also exhibited the highest similarity with the periplasmic WtpA component.

WtpB (PF0081) - Analysis of the WtpB sequence by using the Goldman, Engelman and Steitz (GES) hydrophobicity scale [30], identified the presence of 5 transmembrane helices. This indicates that WtpB is located in the membrane. The conserved C-terminal region EAA-X2-G-X9-I-X-LP, which is generally present in permease components of ABC transporters, was identified to be VARTLG-X9-I/V-X-LP in the case of the WtpB proteins. This conserved sequence is thought to be the recognition site for the C component of the transporter [31].

WtpC (PF0082) - Sequence analysis of the WtpC component of the tungstate transporter identifies the presence of characteristic motifs that are responsible for binding nucleotides [32]. These so-called Walker A (GPSGAGKT) and Walker B motifs (LDEPF) and a Q-loop

(LSGGEQQ) are conserved in WtpC as in ModC and TupC. Hung et al. have postulated a role in nucleotide binding for a conserved histidine residue, which is also present in ModC, TupC and WtpC [33]. Sequence analysis of the WtpC protein in the InterPro database for domains and functional sites [34], identifies an ATPase domain (IPR003593/SM00382). Therefore WtpC is proposed to be the ATPase part of the ABC transporter. Besides the ATPase domain, also a transport associated oligonucleotide/ oligosaccharide binding domain, TOBE-domain (IPR005116/PF03459) [35] and a molybdate/tungstate binding domain, MOP-domain (IPR008995/SSF50331) are recognized. These two domains are also found in *E. coli* ModC immediately after the ATPase domain. Probably the TOBE and MOP domains are involved in the recognition of the molybdate and tungstate.

Additional BLAST searches confirm that this new class of tungstate transporters clarifies the uptake mechanism of many organisms that express tungsten-containing enzymes, or encode putative tungsten containing enzymes on the genome. To corroborate this proposal, a group of organisms that most likely use tungstate in their metabolism was obtained by performing a BLAST search [36] of the sequence of the *P. furiosus* aldehyde oxidoreductase (AOR) against the non-redundant database (NCBI). AOR is the only enzyme known thus far that can only use tungsten and not molybdenum. This search resulted in 33 organisms that have a gene encoding for a putative tungsten containing aldehyde oxidoreductase ($P < 10^{-30}$) and therefore most likely require a tungstate uptake mechanism. Subsequently, BLAST searches of the sequences of *E. acidaminophilum* TupA, *E. coli* ModA and *P. furiosus* WtpA were performed against these genomes ($P < 10^{-20}$) (table 2). The discovery of WtpA as a new class of tungstate transporters identifies the tungstate uptake system of a significant number of archaea, and some bacteria (see below), that do not express homologues of the *E. acidaminophilum* TupA or the *E. coli* ModA. Some of the archaea and bacteria have homologue genes for more than one transporter system. There are no WtpA, TupA or ModA homologues found in eukaryotic organisms even though they do express molybdenum enzymes.

Table 2. Organisms containing a putative member of the tungsten containing aldehyde: ferredoxin oxidoreductase family encoded in the genome ($P < 10^{-30}$).

Organism	Anaerobic	TupA homologue	ModA homologue	WtpA homologue
Archaea				
Pyrococcus furiosus	Yes	-	-	+
Pyrococcus abyssi	Yes	-	-	+
Pyrococcus horikoshii	Yes	-	-	+
Thermococcus kodakarensis	Yes	-	-	+
Thermoplasma volcanium	Facultative	-	-	+[1]
Thermoplasma acidophilum	Facultative	-	-	+[1]
Archaeoglubus fulgidus	Yes	-	-	+
Methanosarcina acetivorans	Yes	-	+	+
Methanosarcina mazei	Yes	+	+	-
Methanocaldococcus jannaschii	Yes	-	-	+
Methanococcus maripaludis	Yes	-	+	+
Haloarcula marismortui	No	+	-	+
Pyrobaculum aerophilum	Facultative	+	-	-
Aeropyrum pernix	No	-	+[1]	-
Termoproteus tenax[2]	Yes			
Termococcus litoralis[2]	Yes			
Bacteria				
Eubacterium acidamoniphilum[2]	Yes	+		
Cloistridium acetobutylicum	Yes	-	+[1]	-
Geobacter sulfurreducens	Yes	+	+	-
Geobacter metallireducens	Yes	+	+	-
Desulfuromonas acetoxidans	Yes	+	+	-
Desulfovibrio vulgaris	Yes	+	+	-
Desulfovibrio desulfuricans	Yes	+	-	-
Desulfotalea psychrophila	Yes	+	+[1]	+
Wolinella succinogenes	No	+	+[1]	-
Magnetospirillum magnetotacticum	Facultative	+	+	-
Rhodospirillum rubrum	Facultative	-	-	-
Azoarcus sp. EbN1	Facultative	+	+[1]	-
Rubrivivax gelatinosus	Facultative	+	+	-
Shigella flexneri	Facultative	-	+	-
Escherichia coli	Facultative	-	+	-
Thermus thermophilus HB8	Facultative	+	-	-
Thermus thermophilus HB27	No	+	-	-
Symbiobacterium thermophilum	No	+	+	-

[1] These homologues have P-values higher than the threshold of 10^{-20}; however they still exhibit significant homology with the protein in the corresponding column (between 10^{-8} and 10^{-16}).

[2] The *E. acidaminophilum, T. tenax and T. litoralis* genomes have not been completely sequenced yet or are not freely accessible. However they are known to contain W containing AORs [37], [38], [39].

Discussion

The discovery of the tungstate specific ABC transporter from *P. furiosus*, WtpABC, uncovers a new class of tungstate and molybdate transporters given the low sequence similarity between WtpA and the earlier characterized periplasmic binding proteins ModA and TupA, which are part of the ABC transporters ModABC [21] and TupABC [8]. BLAST searches of WtpA against the non-redundant database (NCBI) indicate that WtpA is an archaeal tungstate transporter, whereas TupA (and homologue VupA) and ModA occur predominantly in bacteria. Homologues of the *wtpA* gene are found in the genomes of only three bacteria; *Syntrophus aciditrophicus, Desulfotalea psychrophila and Pelobacter carbinolicus. D. psychrophila* encodes a tungsten-containing AOR homologue (table 2), but for the other two bacteria it is not known if they use tungsten in their metabolism. They might also use the WtpABC transporter for the uptake of molybdate. The bacterium, *Rhodospirillum rubrum* is identified with BLAST to contain a tungsten-containing AOR homologue; however there is no putative ModA, TupA or WtpA protein present in its genome. This might indicate that there are still other tungstate and/or molybdate uptake systems that not have been identified yet. However, with the discovery of the WtpABC transporter, together with the earlier characterized ModABC and TupABC, the tungstate and molybdate uptake system of most bacteria and archaea can be identified.
The discovery of the very high affinity WtpABC transporter explains the earlier observed ability of *P. furiosus* cells to scavenge traces of tungstate from growth media [19]. However, it does not explain the highly selective incorporation of tungstate in the cofactor of the AOR enzymes in the presence of a 1000-fold excess of molybdate in the growth medium (chapter 5) [19] because the WtpABC transporter also has a high affinity for molybdate. As a consequence, this indicates the existence of an additional intracellular mechanism that determines the selective incorporation of tungstate in the pterin cofactor of these AOR enzymes.

Acknowledgements

This research was supported by a grant from the Council for Chemical Sciences of the Netherlands Organization for Scientific Research (700.51.301).

References

[1] K.V. Rajagopalan, J.L. Johnson, J. Biol. Chem. 267 (1992) 10199.
[2] R. Hille, Trends Biochem. Sci. 27 (2002) 360.
[3] A. Kletzin, M.W.W. Adams, FEMS Microbiol. Rev. 18 (1996) 5.
[4] G. Schwarz, Cell. Mol. Life Sci. 62 (2005) 2792.
[5] R.R. Mendel, Dalton Trans. (2005) 3404.
[6] S. Rech, U. Deppenmeier, R.P. Gunsalus, J. Bacteriol. 177 (1995) 1023.
[7] F.H. Allen, J.E. Davies, J.J. Galloy, O. Johnson, O. Kennard, C.F. Macrae, E.M. Mitchell, G.F. Mitchell, J.M. Smith, D.G. Watson, J. Chem. Inform. Comp. Sci. 31 (1991) 187.
[8] K. Makdessi, J.R. Andreesen, A. Pich, J. Biol. Chem. 276 (2001) 24557.
[9] S. Pratte Brenda, T. Thiel, J. Bacteriol. 188 (2006) 464.
[10] G. Fiala, K.O. Stetter, Arch. Microbiol. 145 (1986) 56.
[11] S. Mukund, M.W. Adams, J. Biol. Chem. 266 (1991) 14208.
[12] R. Roy, S. Mukund, G.J. Schut, D.M. Dunn, R. Weiss, M.W.W. Adams, J. Bacteriol. 181 (1999) 1171.
[13] L.E. Bevers, E. Bol, P.-L. Hagedoorn, W.R. Hagen, J. Bacteriol. 187 (2005) 7056.
[14] G.J. Schut, S.D. Brehm, S. Datta, M.W.W. Adams, J. Bacteriol. 185 (2003) 3935.
[15] M.V. Weinberg, G.J. Schut, S. Brehm, S. Datta, M.W.W. Adams, J. Bacteriol. 187 (2005) 336.
[16] S. Mukund, M.W.W. Adams, J. Biol. Chem. 270 (1995) 8389.
[17] R. Roy, M.W.W. Adams, J. Bacteriol. 184 (2002) 6952.
[18] F.T. Robb, D.L. Maeder, J.R. Brown, J. DiRuggiero, M.D. Stump, R.K. Yeh, R.B. Weiss, D.M. Dunn, Methods Enzym. 330 (2001) 134.
[19] S. Mukund, M.W.W. Adams, J. Bacteriol. 178 (1996) 163.
[20] J. Sambrook, Fritsch, E. F., and Maniatis, T., Molecular cloning: A laboratory Manual 2nd Ed. (1989) Cold Spring Harbor Laboratory.
[21] S. Rech, C. Wolin, R.P. Gunsalus, J. Biol. Chem. 271 (1996) 2557.
[22] P.L. Hagedoorn, P. van't Slot, H.P. van Leeuwen, W.R. Hagen, Anal. Biochem. 297 (2001) 71.
[23] S.-V. Albers, A.J.M. Driessen, Arch. Microbiol. 177 (2002) 209.
[24] S.M. Koning, M.G.L. Elferink, W.N. Konings, A.J.M. Driessen, J. Bacteriol. 183 (2001) 4979.
[25] Y. Hu, S. Rech, R.P. Gunsalus, D.C. Rees, Nat. Struct. Biol. 4 (1997) 703.
[26] D.M. Lawson, C.E.M. Williams, L.A. Mitchenall, R.N. Pau, Structure 6 (1998) 1529.
[27] J. Imperial, M. Hadi, N.K. Amy, Biochim. Biophy. Acta 1370 (1998) 337.
[28] B.W. Sigurskjold, Anal. Biochem. 277 (2000) 260.
[29] P.A. Bates, L.A. Kelley, R.M. MacCallum, M.J. Sternberg, Proteins Suppl 5 (2001) 39.
[30] D.M. Engelman, T.A. Steitz, A. Goldman, Annu. Rev. Biophys. Biophysical Chem.15 (1986) 321.
[31] M. Mourez, M. Hofnung, E. Dassa, EMBO J. 16 (1997) 3066.
[32] L. Schmitt, R. Tampe, Curr. Opin. Struct. Biol.12 (2002) 754.
[33] L.W. Hung, I.X. Wang, K. Nikaido, P.Q. Liu, G.F. Ames, S.H. Kim, Nature 396 (1998) 703.
[34] E.M. Zdobnov, R. Apweiler, Bioinformatics 17 (2001) 847.
[35] E.V. Koonin, Y.I. Wolf, L. Aravind, Adv. Prot. Chem. 54 (2000) 245.
[36] S.F. Altschul, T.L. Madden, A.A. Schaffer, J. Zhang, Z. Zhang, W. Miller, D.J. Lipman, Nucl. Acids Res. 25 (1997) 3389.
[37] D. Rauh, A. Graentzdoerffer, K. Granderath, J.R. Andreesen, A. Pich, Eur. J. Biochem. 271 (2004) 212.

[38] B. Siebers, B. Tjaden, K. Michalke, C. Doerr, H. Ahmed, M. Zaparty, P. Gordon, C.W. Sensen, A. Zibat, H.-P. Klenk, S.C. Schuster, R. Hensel, J. Bacteriol. 186 (2004) 2179.
[39] S. Mukund, M.W. Adams, J. Biol. Chem. 268 (1993) 13592.

Part II

Tungsten cofactor synthesis

Chapter 3

The function of MoaB proteins in the biosynthesis of the molybdenum and tungsten cofactors

Loes E. Bevers
Peter-Leon Hagedoorn
José A. Santamaria-Araujo
Axel Magalon
Wilfred R. Hagen
Guenter Schwarz

Adapted from: Biochemistry 47 (2008) 949-956

Abstract

Molybdenum (Mo) and tungsten (W) enzymes catalyze important redox reactions in the global carbon, nitrogen, and sulfur cycles. Except in nitrogenases both metals are exclusively associated with a unique metal-binding pterin (MPT) that is synthesized by a conserved multistep biosynthetic pathway, which ends with the insertion and thereby biological activation of the respective element. While the biosynthesis of Mo-cofactors has been intensively studied in various systems, the biogenesis of W-containing enzymes, mostly found in archaea, is poorly understood. Here, we describe the function of the *Pyrococcus furiosus* MoaB protein that is homologous to bacterial (such as MogA) and eukaryotic proteins (such as Cnx1) involved in the final steps of Mo-cofactor synthesis. MoaB reconstituted the function of the homologous *Escherichia coli* MogA protein and catalyzes the adenylylation of MPT in a Mg^{2+} and ATP-dependent way. At room temperature reaction velocity was similar to that of the previously described plant Cnx1G domain but it were increased up to 20-fold at 80°C. Metal and nucleotide specificity for MPT adenylylation is well conserved between W- and Mo-cofactor synthesis. Thermostability of MoaB is believed to rely on its hexameric structure while homologous mesophilic MogA-related proteins form trimers. Comparison of *P. furiosus* MoaB to *E. coli* MoaB and MogA revealed that only MogA is able to catalyze MPT adenylylation while *E. coli* MoaB is inactive. In summary, MogA, Cnx1G, and MoaB proteins exhibit the same adenylyl transfer activity essential for metal insertion in W- or Mo-cofactor maturation.

Introduction

Tungsten and molybdenum are transition metals with very similar properties. They both have an essential role in biology as they are present in cofactors of enzymes that mainly catalyze oxygen atom transfer reactions. Mo-enzymes are ubiquitous in all forms of life [1], whereas W-containing enzymes have only been identified in prokaryotes (predominantly archaea) so far [2]. Both metals are bound to the same type of cofactor, which consists of one or two tricyclic pyranopterin moieties originally described as molybdopterin [3] but now called metal-binding pterin (MPT) [4]. The metals are coordinated by the dithiolene sulfurs in the pyranoring of MPT. In case of tungsten, there are always two pterin moieties present resulting in the four sulfur-coordinated tungsten bis-pterin cofactor (Wco) [5].

Mo-cofactor (Moco)-containing enzymes can be classified into three separate families based on the coordination of the molybdenum [6]. Dimethyl sulfoxide oxidoreductases (DMSORs) contain a bis-pterin cofactor modified by nucleotide monophosphates covalently attached to the terminal phosphate of each MPT molecule. The DMSOR-type cofactors of Mo-enzymes are directly related to one of the two families of Wco-containing enzymes, which comprises formate dehydrogenases (FDHs) found in *Pyrococcus furiosus* [7] and other archaea. The other class of Wco-dependent enzymes comprises unique enzymes that form the family of W-containing aldehyde oxidoreductases. Five of these enzymes have been identified from the hyperthermophilic archaeon *Pyrococcus furiosus*: aldehyde oxidoreductase [8], formaldehyde oxidoreductase [9], glyceraldehyde-3-phosphate oxidoreductase [10], tungsten-containing oxidoreductase 4 [11] and tungsten-containing oxidoreductase 5 [12] that all share a bis-pterin Wco without nucleotide modification.

The biosynthetic pathway of MPT cofactors has been extensively studied for Moco in bacteria as well as in higher eukaryotes and appears to be highly conserved [4]. In brief, GTP is converted in an S-adenosyl methionine-dependent reaction to cyclic pyranopterin monophosphate. In the second step two sulfur atoms are transferred by the heterotetrameric MPT synthase, which consists of two large and two small subunits. Only recently, details on the third, metal insertion step have been obtained by the characterization of plant Cnx1 protein that combines functions of two homologous bacterial proteins (MoeA and MogA) in a single two-domain protein (E and G). Cnx1G binds MPT with high affinity [13] and catalyzes an adenylyl transfer to the MPT phosphate yielding MPT-AMP [14,15]. The product of Cnx1G is subsequently transferred in a molybdate-dependent manner to the adjacent Cnx1E domain where MPT-AMP is hydrolyzed in the presence of Zn^{2+} or Mg^{2+} and Moco is released [16].

While eukaryotic mono-pterin cofactor maturation by Cnx1 is well-studied, the mechanism for the synthesis of bis-pterin cofactors of the DMSOR type is less understood. As Cnx1G reconstitutes *E. coli* MogA function [17] one can assume that a similar chemistry involving formation of MPT-AMP is performed in bacteria. In addition, the Cnx1E homologous MoeA protein has been demonstrated to function in Mo-insertion [18] but the lack of Cnx1E reconstitution in *moeA* mutants indicates significant differences in the metal insertion

mechanism between bacteria and eukaryotes [19]. Furthermore, attachment of nucleotides is required to complete the synthesis of bis-pterin guanine Mo-cofactors in *E. coli* [20]. In *E. coli*, out of the ten products of four operons (*moaABCDE, mobAB, moeAB and mogA*) eight proteins were found to be essential for the biosynthesis of Moco. For two proteins, MoaB and MobB, a functional requirement in this pathway is unproven as none of the available nitrate reductase-deficient mutants were associated with their loci [3].
In contrast to that of Moco, synthesis of Wco has not been studied so far. However, it is likely that the basic mechanisms of Wco and Moco synthesis are similar as almost all genes that have an assigned function in the Moco biosynthetic pathway are also present in the genome of organisms that use tungsten in their metabolism. Main differences should occur in the metal insertion step as here a specific discrimination between Mo and W is required. For example, recent work on the assembly of the Mo-dependent nitrate reductase in *E. coli* showed that cofactor insertion into apo-nitrate reductase is lost in the presence of tungsten, indicating that a W-substituted nitrate reductase does not exist in *E. coli* [21]. However, the molybdenum in *E. coli* trimethylamine *N*-oxide (TMAO) reductase, could be replaced with tungsten resulting in an active form of the enzyme [22]. TMAO reductase and nitrate reductase both contain a bis-MGD cofactor and therefore the type of cofactor is apparently not determining the metal specificity. The selective metal incorporation is also not strictly dependent on the transporter system as molybdate (ModA) and tungstate transporters (TupA and WtpA) are known to bind both oxoanions, be it with different affinities. For example, the recently identified tungstate transporter from *P. furiosus* selectively binds tungstate with a 1000-fold higher affinity over molybdate [23].
MogA and MoeA are known to be important for *E. coli* Mo insertion, however in *P. furiosus* and other archaea only the MogA-homologous MoaB proteins are found. In addition, two different MoeA orthologs a present in these genomes. We have chosen the hyperthermophilic archaeon *P. furiosus*, which is strictly dependent on tungstate and grows optimally at 100 ºC under anaerobic conditions [24], as model organism to study Wco biosynthesis. Here we report that *P. furiosus* MoaB as well as *E. coli* MogA catalyze MPT adenylylation, a finding that demonstrates the universal existence of MPT-AMP in the biosynthesis of both tungsten as well as molybdenum cofactors.

Materials and Methods

Plasmids, bacterial strains - The following *E. coli* mutant strains were used: RK5206 (*mogA)* [RK4353 chlG206::Mu cts *mogA*] and RK4353 [27] that were cultured at 30 ˚C.

Cloning of *P. furiosus* and *E. coli moaB* and *mogA* genes - The *moaB* genes, PF00372 (*P. furiosus*) and b0782 (*E. coli*) were amplified by PCR using Pfx polymerase (Invitrogen) and chromosomal DNA from *P. furiosus* or *E. coli* DH5α as a template, respectively. Extraction of the chromosomal DNA was performed with phenol/chloroform/isoamylalcohol. PCR

products were treated with Taq polymerase (Amersham Bioscience) for 10 min at 72 °C to obtain single 3'adenine overhangs for sub-cloning into the pCR®2.1-TOPO® vector (Invitrogen). TOPO-constructs were transformed into competent *E. coli* TOP10 cells (Invitrogen), plasmids were isolated and after sequencing positive fragments were cloned into the Nde1 and BamH1 sites of the pET15b (Novagen), resulting in MoaB fusion proteins with an N-terminal his-tag. These constructs were transformed into competent *E. coli* BL21- CodonPlus®-(DE3)-RIPL cells (Stratagene). *E. coli mogA* was PCR-cloned into the NdeI/XhoI sites of pET22b plasmid (Novagen) and transformed into BL21 (DE3) cells (Stratagene). Site directed mutagenesis was performed by PCR on the expression plasmid pET15b-PfMoaB using the QuickChange® Site-Directed Mutagenesis kit (Stratagene).

Determination of nitrate reductase activity in *E. coli* - The λDE3 lysogenization procedure (Novagen) was used to integrate the gene for T7 polymerase into the chromosome of the RK5206 *mogA* strain. The resulting strain RK5206(DE3) was transformed with the corresponding pET15b constructs containing PfMoaB variants or EcMoaB. The cells were cultured as described and nitrate reductase activity was determined spectrophotometrically using reduced benzyl viologen as electron donor [28].

Protein production and purification of PfMoaB and homologous E. coli proteins - *E. coli* BL21(DE3) cells containing pET15b-PfMoaB or pET15b-EcMoaB were grown aerobically in Luria-broth medium containing 100 µg/ml ampicillin. Protein synthesis was induced with a final concentration of 0.5 mM IPTG, when the absorbance of the culture reached 0.5 at 600 nm. Cells were induced for 5 h at 30 °C, harvested by centrifugation, washed with buffer A (20 mM Tris-HCl, pH 8.0, 10 mM imidazole, 500 mM NaCl and 10% glycerol) and lysed in the same buffer (1 g of cells per 5 ml buffer) using a cell disruptor system (Constant systems). Cell-free extract was obtained by centrifugation for 20 min at 15.000 x g at 4 °C. In the case of the PfMoaB, the supernatant was heated for 30 min at 70 °C as a first purification step. Precipitated protein was removed by centrifugation and the supernatant was applied to a Ni-sepharose 6 fast flow resin (GE healthcare) equilibrated with buffer A, washed with the same buffer and eluted with buffer B (20 mM Tris-HCl, pH 8.0, 500 mM Imidazole, 500 mM NaCl and 10% glycerol). Protein-containing samples were dialyzed against buffer C (20 mM Tris, pH 8.0, 250 mM NaCl and 10% glycerol), concentrated and applied to a Superdex-200 HR27/60 column equilibrated with buffer C. Fractions eluting under the main peak were pooled, concentrated (10 mg/ml) and stored at -80 ˚C. Overproduction of EcMogA was performed in Luria-broth medium supplemented with 0.2 mM IPTG at 37 °C under aerobic conditions. Protein extracts were prepared as described above using 20 mM Tris/HCl, pH 7.6, 500 mM NaCl, 5 mM imidazole buffer and applied to a Ni^{2+} affinity column (HiTrap, GE Healthcare) equilibrated with the same buffer. After washing the column, the EcMogA was eluted with 200 mM imidazole and protein containing fractions were pooled, dialyzed against 20 mM Tris/HCl, pH 7.6, 0.1 M NaCl buffer, frozen in liquid nitrogen and stored at -80 °C until used.

In vitro synthesis and analysis of MPT and MPT-AMP - MPT was synthesized in vitro using purified cyclic pyranopterin monophosphate (cPMP) [29], as well as purified *E. coli* MPT synthase [30] or *E. coli* MoaE and *E. coli* thiocarboxylated MoaD that were purified and assembled into active MPT synthase as described before [30]. Standard in vitro MPT synthesis was performed in MPT buffer (100 mM Tris, pH 7.2) containing: 1000 pmol cPMP, 250 pmol MoaB, 20 pmol MoaE and 100 pmol MoaD in an assay volume of 140 µL per point of measurement and incubated at room temperature for 30 min to saturate MPT synthesis. Subsequently, the mixture was incubated for 2 min at the temperature required for the adenylylation, which was 65 ˚C under standard conditions for PfMoaB. The adenylylation reaction was initiated upon addition of nucleotide and divalent cations. At different time points, samples (140 µL) were taken directly from the reaction mixture and the reaction was stopped by the addition of 17.5 µL of 1% I_2, 2% KI, 1 M HCl. MPT and MPT-AMP were determined by HPLC formA (i.e. MPT iodine oxidized product) analysis as described [15] with the variation that 200 µL Q-sepharose columns (GE healthcare) were used to purify formA and formA-AMP prior HPLC analysis.

Results

Expression and purification of MoaB variants

PfMoaB shows high homology at the primary sequence level to EcMoaB, MogA and Cnx1G (figure 1A). Superimposition of Cnx1G-MPT-AMP complex structure [14] with the available crystal structures of *E. coli* MogA [31] and *E. coli* MoaB [25,26] demonstrates a high degree of structural conservation surrounding the hypothetical active sites of all three proteins (figure 1B). The sequence alignment of MoaB- and MogA-homologous proteins confirms the conservation of residues that have been shown to be important for substrate (MPT) binding and catalysis (adenylyl transfer) in Cnx1G. Therefore, we have replaced three hypothetical active residues in PfMoaB in order to generate variants that are proposed to be affected in their MPT-binding site (S112A), nucleotide-binding site (D32A) and catalysis (D56A) (figure 1A, black arrows). Adjacent to D56, D57 seems to be less conserved (figure 1A) as some proteins including *E. coli* MogA contain a glutamate. In order to generate a protein more similar to the active site of *E. coli* MogA we also generated the PfMoaB variant D57E. Wild type PfMoaB, its variants, and EcMoaB and MogA were recombinantly expressed in *E. coli* as N-terminally His-tagged proteins and purified to homogeneity (see Materials and Methods). For all variants average yields of 10-15 mg per liter culture were obtained.

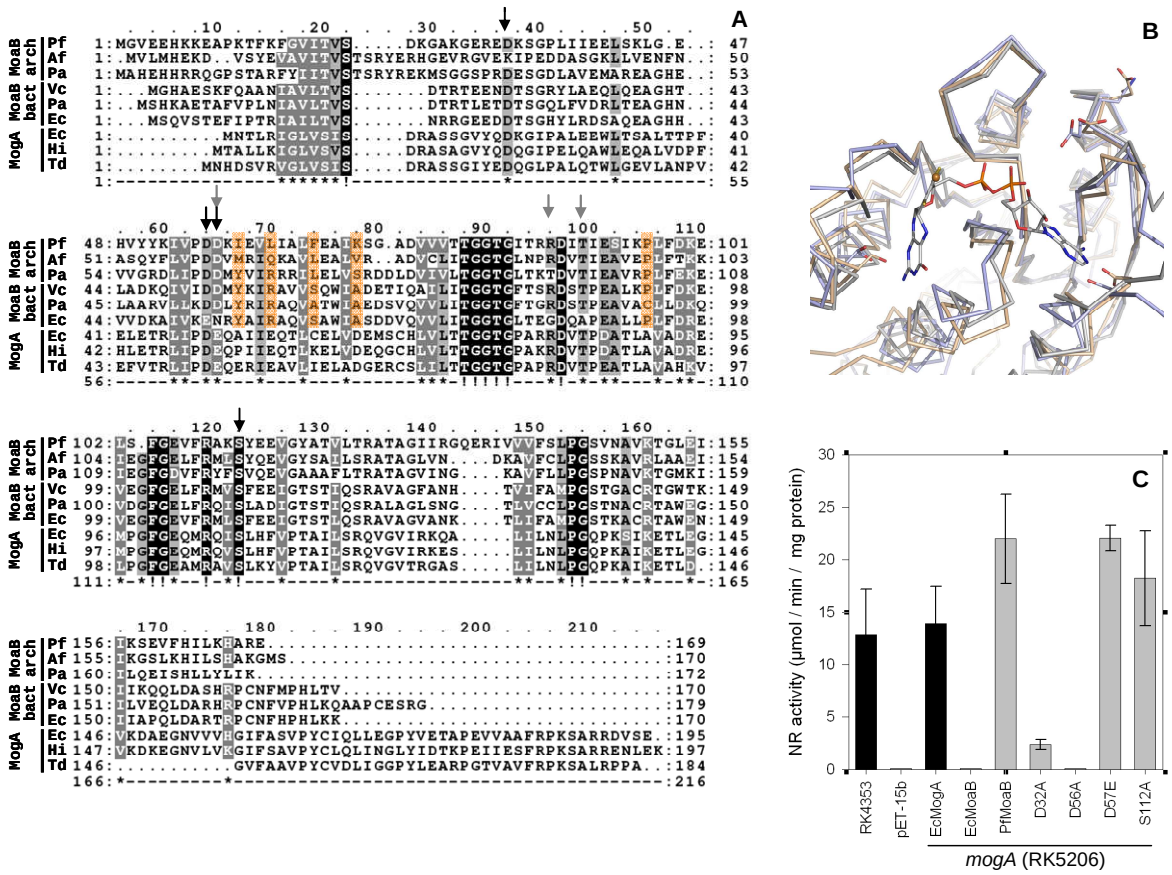

Figure 1. Sequence and structural comparison of MoaB, MogA and Cnx1G. (A) Multiple sequence alignment of *P. furiosus* MoaB (PF0372), *Archaeoglobus fulgidus* MoaB (AF0265), *Pyrobaculum aerophilum* MoaB (PAE0969), *Vibrio cholerae* MoaB (VC1025), *Pseudomonas aeruginosa* MoaB (PA3029), *E. coli* MoaB (b0782), *E. coli* MogA (b0009), *Haemophilus influenzae* MogA (NTHI0454), and *Thiobacillus denitrificans* MogA (Tbd2143) listed in the order of appearance. The alignment was generated with ClustalW, consensus sequence calculation and shadings were performed using a threshold of 75% for conserved residues. Completely conserved residues show an exclamation mark (!) in the consensus line and are printed in white letters (shaded dark). Highly conserved residues (white letters) and low conserved residues (black letters) are shaded in gray. Residues subjected to mutagenesis are marked with a black arrow while residue positions that are specifically altered in EcMoaB are highlighted with a gray arrow. Residues forming contacts in the EcMoaB trimer are overlayed with an orange box. (B) Structural comparison of Cnx1G (S583A variant, shown in gray) with bound MPT-AMP (1UUY) and *E. coli* proteins MogA (1DI6, blue) and MoaB (1MKZ, orange). Corresponding residues that were mutated in PfMoaB are highlighted in the structure of EcMogA as well as EcMoaB. The figure was generated with COOT (www.ysbl.york.ac.uk/~emsley/coot) and rendered with POVRAY (www.povray.org). (C) Functional reconstitution of nitrate reductase activity in *E. coli mogA* mutants upon production of *E. coli* MogA and MoaB as well as wild type and mutant PfMoaB variants. The *E. coli* RK4353 strain was used as positive control, and RK5206 (*mogA*) strains transformed with the empty vector was taken as negative control.

Reconstitution of *E. coli* Moco biosynthesis

In view of the conservation at the primary sequence level between PfMoaB and MogA proteins, we investigated whether an *E. coli mogA* (RK5206) mutant could be complemented by PfMoaB, EcMoaB or by positive control *E. coli* MogA. Production of wild type PfMoaB in *mogA* deficient cells restored Moco synthesis, which was monitored by the reconstitution of nitrate reductase activity (figure 1C). In contrast, EcMoaB did not show any complementation, while EcMogA restored activity to the level of the wild type. This observation showed that (i) PfMoaB can replace MogA in bacterial Moco biosynthesis and that (ii) the thermophilic PfMoaB is also able to function at 30 ˚C, which was the growth temperature of the *E. coli mogA* mutant. The variant D56A expected to be impaired in catalysis [17], showed a complete loss of function, as nitrate reductase activity was similar to cells transformed with control plasmid (figure 1C). Variants with changes in the hypothetical substrate binding site for MPT (S112A) and the nucleotide binding site (D32A) retained their activity or showed only a partially reduced activity, respectively. The PfMoaB D57E variant mimicking the active site structure of MogA also restored nitrate reductase activity completely.

MPT binding

Successful reconstitution of Moco synthesis in *E. coli* demonstrated that PfMoaB participates in a similar reaction as catalyzed by MogA in bacterial Moco biosynthesis. Therefore we investigated the ability of PfMoaB to bind MPT, the starting molecule for the adenylyl transfer reaction.

First, size exclusion chromatography of PfMoaB was performed. Wild type PfMoaB (figure 2A) as well as all variants (data not shown) eluted at a molecular weight of circa 120 kDa. As monomeric PfMoaB has a theoretical mass of 20.7 kDa we conclude that it forms hexamers as main oligomeric form. A smaller peak eluted before the main PfMoaB peak, which was found to contain also PfMoaB protein that formed higher ordered oligomers (ca. 300 kDa). No significant absorption at 375 nm was observed, which was consistent with MPT determinations (data not shown) that showed no co-purification of MPT with PfMoaB upon overproduction in *E. coli*.

Next, MPT was synthesized in vitro using purified MPT synthase [30] and excess purified cPMP [29] and co-incubated with PfMoaB. We used 2 nmol MPT synthase and 10 nmol cPMP to synthesize MPT, which was subsequently co-incubated under anaerobic conditions with 30 nmol PfMoaB. The reaction mixture was separated by size exclusion chromatography and no change in the oligomeric state of PfMoaB was detectable (figure 2B). However, upon coincubation with the MPT synthase reaction a strong absorption at 375 nm was detectable under the hexameric as well as under the high molecular weight peak of PfMoaB. The hexameric PfMoaB peak was collected and concentrated to 314 µM. HPLC FormA analysis revealed that 11 µM MPT (1650 pmol) was bound to the PfMoaB

hexamer while only trace amounts of MPT retained on MPT synthase (data not shown). Substoichiometric saturation with MPT was due to the excess of PfMoaB.

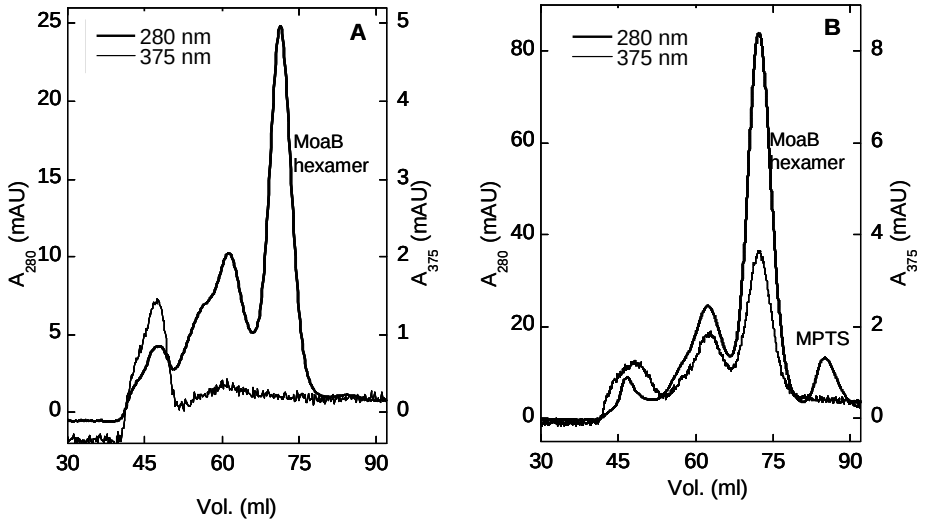

Figure 2. Transfer of MPT to purified PfMoaB. (A) Size exclusion chromatogram of purified PfMoaB (10 nmol) indicating its hexameric structure (B) Size exclusion chromatogram of PfMoaB (30 nmol) and MPT synthase (2 nmol) showing efficient transfer of MPT from MPT synthase to PfMoaB.

P. furiosus MoaB catalyzes MPT adenylylation

Having shown MPT binding to PfMoaB we investigated its ability to catalyze a similar nucleotidyl transfer reaction as previously described for plant Cnx1G [15]. For all subsequent functional studies of PfMoaB we used purified *E. coli* MoaE protein (large subunit of MPT synthase) and thiocarboxylated MoaD protein (small subunit of MPT synthase) that were in vitro assembled to form fully active MPT synthase converting cPMP into MPT in vitro [30]. MPT synthesis was performed in the presence of excess cPMP (2,000 pmol) and 250 pmol PfMoaB for 60 min to ensure quantitative MPT synthesis and transfer to PfMoaB.

First, we investigated the ability of PfMoaB to catalyze MPT adenylylation under similar conditions as previously used for plant Cnx1G [15]. The reaction was initiated with 1 mM ATP and 10 mM $MgCl_2$. MPT-AMP formation and MPT consumption were monitored by HPLC formA and formA-AMP analysis (figure 3). At room temperature we found an almost complete conversion of MPT (50 pmol) into MPT-AMP (70 pmol) within 120 min (figure 3A). The increase in MPT-AMP in comparison to the starting amount of MPT is due to ongoing MPT synthesis by the MPT synthase. The velocity of MPT adenylylation at room temperature was comparable to previous results with Cnx1G, where most of the MPT-AMP was synthesized within the first 60 min of the reaction (in the absence of inorganic pyrophosphatase) [15]. Prolonged incubation (above 180 min) caused progressive degradation of MPT-AMP (figure 3A).

As PfMoaB derives from a hyperthermophilic organism, we also studied the temperature dependence of MPT adenylylation. It is important to note that Moco and MPT are extremely unstable even when they are bound to different (eukaryotic) Mo-dependent enzymes: they can be rapidly released and oxidized by heat denaturation [13]. The initial MPT synthesis reaction including binding of MPT to PfMoaB was performed at room temperature. Subsequently the reaction mixtures were heated to the indicated temperatures, and incubated for 2 min before adenylylation was started by the addition of Mg-ATP. A strong acceleration in MPT-AMP synthesis was observed with increasing temperatures with a maximum at 80 °C (figure 3B). In the range of 50 to 80 °C quantitative conversion of MPT into MPT-AMP was indicated by saturation of MPT-AMP formation and depletion of MPT (data not shown), while at 25 °C the reaction was not completed within the investigated time frame. Additionally, with prolonged reaction time MPT-AMP levels rapidly decreased at higher temperature, probably due to degradation of the compound or degradation of PfMoaB and/or both. Subsequent experiments were performed at 65 °C because PfMoaB remained stable at that temperature and the velocity of the reaction enables accurate kinetic determinations.

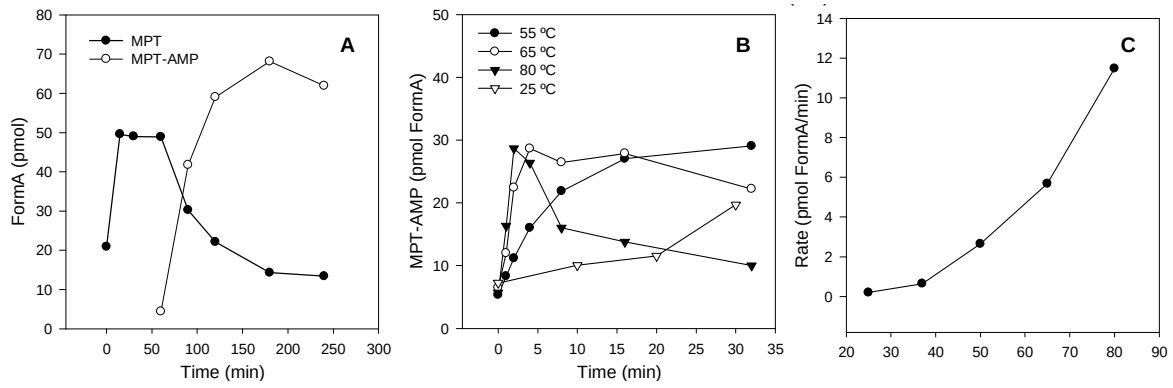

Figure 3. Adenylylation of MPT by PfMoaB. MPT was in vitro synthesized by using purified *E. coli* MoaE and thiocarboxylated MoaD proteins and purified cPMP. After 60 min MPT synthesis adenylylation was started by adding 1 mM ATP and 10 mM $MgCl_2$. MPT and MPT-AMP were determined by HPLC formA and formA-AMP analysis. (A) MPT adenylylation at room temperature by monitoring MPT depletion and MPT-AMP formation. (B) Temperature-dependent MPT-adenylylation kinetics (MPT-AMP synthesis). (C) Initial reaction velocities at different temperatures.

Finally, we analyzed MPT-AMP formation (taken from the initial velocity) as a function of reaction temperature (figure 3C), which followed a typical activity profile of a thermo-stable enzyme. A maximal synthesis of 12 pmol MPT-AMP per min was found at 80 °C, which is more than 20 times higher than the corresponding velocity of PfMoaB at room temperature.
Next we determined the kinetic parameters of PfMoaB using MPT and Mg-ATP as substrates (figure 4AB). We recorded MPT adenylylation velocities for four different ATP concentrations (30-1000 µM) resulting in a K_M value of 220 µM ATP and a maximal

velocity of 18.6 pmol MPT-AMP/min. In comparison to Cnx1G [15], the K_M and V_{max} are respectively 4 and 20 times higher for PfMoaB.

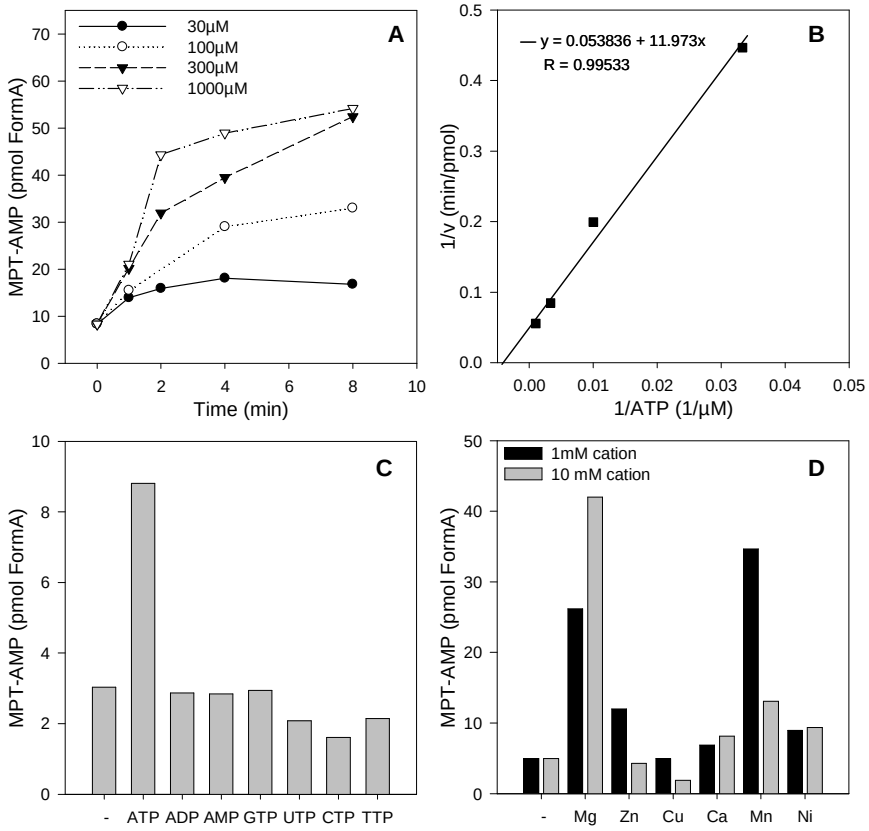

Figure 4. Nucleotide- and metal-dependent PfMoaB activity. (A) ATP-dependent adenylylation of MPT at 65 °C and (B) reciprocal plot of the obtained reaction velocities. (C) PfMoaB-catalyzed formation of MPT-nucleotidylylates with different nucleotides (1 mM) in the presence of 10 mM $MgCl_2$ at 65 °C. (D) Cation-dependent adenylylation of MPT in the presence of 1 mM ATP at 65 °C at 1 and 10 mM of the respective cation.

Substrate specificity of PfMoaB

In view of the unusual growth conditions of *P. furiosus*, we tested alternative substrates and co-substrates that might be used for nucleotidylylation of MPT. For example, some hyperthermophilic enzymes are known to use ADP as substrate in contrast to their mesophilic homologues that operate with ATP, and this is thought to be related to a higher thermostability of ADP [32]. However, no other nucleotide was found to exhibit significant activity in the formation of nucleotidylylated MPT (figure 4C). Apparently, adenyl transfer to MPT represents an evolutionary conserved mechanism important for the maturation of both molybdenum and tungsten cofactors. Regarding the specificity of PfMoaB for different divalent cations as co-substrates, Mg^{2+} and Mn^{2+} exhibited comparable activity with Mn^{2+} being even more active at lower concentrations (figure 4D).

Characterization of PfMoaB variants

Next, we investigated the functional properties of the PfMoaB variants previously studied by functional reconstitution of *E. coli mogA* mutants. Variants with no (D56A) or strongly reduced (D32A) activity in *E. coli* were also inactive in MPT-AMP synthesis (figure 5A). However, D57E, which was expected to be as active as wildtype PfMoaB (figure 1C) showed somewhat less activity under the experimental conditions while variant S112A with hypothetically impaired MPT binding was even more active than wild type PfMoaB (figure 5A) indicating that this residues does not contribute significantly to MPT binding in PfMoaB.

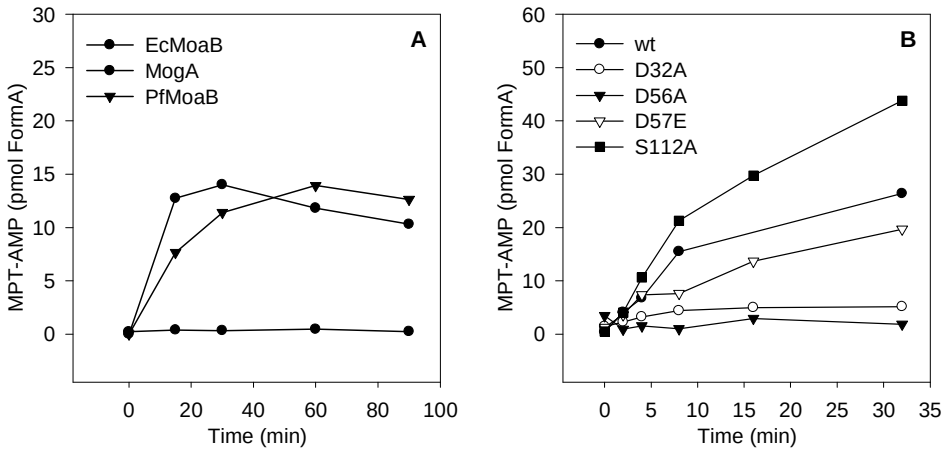

Figure 5. Functional characterization of PfMoaB variants and *E. coli* MogA and MoaB. (A) MPT adenylylation by PfMoaB variants under standard conditions with 1 mM ATP and 10 mM $MgCl_2$ at 65 °C (B) MPT adenylylation by PfMoaB, *E. coli* MogA and *E. coli* MoaB under standard conditions at 37 °C.

Comparison of PfMoaB to its bacterial homologues *E. coli* MogA and MoaB

The fact that PfMoaB as well as Cnx1G reconstitutes *E. coli mogA* mutants strongly suggests that MogA catalyzes the same reaction as Cnx1G and PfMoaB. Therefore we expressed and purified *E. coli* MogA and subjected it to standard adenylyl transfer experiments (figure 5B). MogA was able to catalyze MPT adenylylation even more efficiently than PfMoaB at 37 °C. These results confirm unequivocally that all protein members of the MoaB/MogA/Cnx1G family catalyze the same MPT activation reaction essential for metal transfer into different pterin cofactors.

A final experiment addressed the functional properties of *E. coli* MoaB (EcMoaB) in vitro. The fact that *mogA* mutants are Moco deficient suggests that EcMoaB is unable to replace MogA function in *E. coli*, which was further strengthened by the inability of EcMoaB to complement *mogA* mutants even after over-expression (figure 1C). In order to prove this proposal we purified EcMoaB as His-tagged protein and subjected it to MPT-AMP synthesis experiments (figure 5B). The results clearly demonstrated that *E. coli* MoaB is not

able to perform an adenyl transferase reaction (figure 5B) although it is able to bind MPT in vitro (data not shown). Our results show for the first time that the *E. coli* representative of the family of MoaB proteins has no catalytic function in Mo-cofactor biosynthesis although it is expressed in the *moa*-operon encoding four other proteins involved in bacterial Moco biosynthesis.

Discussion

Mo- and W-containing enzymes share the same pterin-based scaffold chelating the reactive metals to ene-dithiolate groups. The basic physico-chemical properties of these metals are very similar and it is therefore likely that a common, probably highly conserved mechanism has evolved to transform both transition metals into biocatalyst [33]. At the same time very restrictive reactions should enable a clear discrimination between these related metals as they are both bio-available and known to often represent antagonists for each other. While Mo-containing enzymes are found in all kingdoms of life, W-dependent enzymes are restricted to prokaryotes and are mostly found in archaea [5].

Analyses of archaeal genomes identified a complete set of genes homologous to genes encoding proteins involved in the biosynthesis of Moco. Therefore, a general conservation in the biosynthesis of the MPT pterin backbone has been proposed [33]. However, little is known about how organisms discriminate between molybdenum and tungsten. Recent studies regarding tungstate uptake in *P. furiosus* showed high substrate specificity of WtpA [23], the periplasmic oxoanion-binding protein of the high-affinity ABC-type tungstate uptake system for which recently a crystal structure has been determined from a related organism [34]. In order to uncover common and metal specific processes in Moco and Wco biosynthesis we investigated the function of *P. furiosus* MoaB, a protein of hitherto unknown function but with clear homology to the Cnx1G domain [35]. As Cnx1G was the first and so far only protein for which a novel MPT adenylylation function has been described [14,15] it was crucial to know if this reaction is common for Moco biosynthesis and if similar or even identical mechanisms are important for Wco biosynthesis.

We have shown here that *P. furiosus* MoaB and *E. coli* MogA catalyze the same adenylylation reaction as plant Cnx1G in order to activate the MPT for metal insertion. Therefore, MPT-AMP synthesis is not only crucial for eukaryotic Moco biosynthesis, but it represents a common and well-conserved reaction intermediate essential for the synthesis of Mo- and W-cofactor in all kingdoms of life. As a result, MogA and MoaB proteins can be classified as pterin adenyl transferases similar to Cnx1G (figure 6).

Interestingly, *E. coli* MoaB was found to be inactive in MPT adenylylation. When comparing EcMoaB to different MogA and MoaB proteins a few but very specific changes of otherwise conserved residues (N53, G84, A87) are observed (figure 1A, gray arrows). Similar to *E. coli* MoaB such changes are also found in other orthologs that are co-expressed with a (hypothetically) active MogA protein in the same organism such as in

Salmonella enterica choleraesuis, *Klebsiella pneumoniae*, or *Erwinia carotovora atroseptica*.

In conclusion, EcMoaB is not directly involved in *E. coli* Moco synthesis but it might have other yet unknown functions related to this pathway. For example the ability to bind MPT (data not shown) might point to a regulatory role in sensing the pterin and/or Mo-cofactor status of the cell. A key regulatory site in bacterial Moco synthesis is the *E. coli moa*-operon, which is controlled by molybdate as well as by levels of active cofactor [36].

Genomic inspections showed that the functionally inactive sequence of *E. coli* MoaB forms the exception and that most other MoaBs are expected to be active adenyl transferases like PfMoaB. These adenyl transferases are most abundant amongst archaea, as no archaeal genome sequenced so far contains a gene for a MogA homologue. As *E. coli* MogA and other homologous proteins such as plant [19] and Chlamydomonas Cnx1G [37] as well as gephyrin G domain form trimers in solution [38], one can conclude that these proteins represent an unique family of trimeric adenyl tranferases. Regarding MoaB, structural information is limiting, as only EcMoaB has been determined so far. Therefore, PfMoaB represents the second characterized hexameric MoaB protein and more studies are needed to confirm that MoaB proteins are in general hexameric. However, inspection of the trimer interface in EcMoaB reveals that at least three (Tyr55, Arg58, Pro92) out of the five residues that mediate contacts between the two MoaB trimers are conserved in MoaB-homologous proteins (figure 1A). It is even more important that in MogA like proteins these residues are replaced by residues with either opposite charge or different character (EcMogA Ala52, Glu55, Ala90). The non-existence of archaeal trimeric adenyl transferases combined with the abundance of MoaB proteins in archaeal (hyper)thermophiles leads to the hypothesis that thermostability of PfMoaB relies in part on its hexameric structure. As the hexamer interface does not interfere with the active site of MoaB proteins, future experiments should allow detailed structure-function studies to uncover the molecular basis of thermal stability. Furthermore, the trimeric and hexameric adenyl transferases might contribute differently downstream in the pathway such as in bis-pterin formation or metal insertion (figure 6).

Based on our results MPT-AMP represents the last common intermediate of Moco and Wco biosynthesis, and selective metal incorporation should therefore rely on the oxyanion-dependent hydrolysis of MPT-AMP, as described for plant Cnx1E domain [16]. Therefore, Cnx1E-homolgous MoeA proteins from bacteria or archaea should also hydrolyze MPT-AMP in a molybdate- and/or tungstate-dependent manner. The fact that eukaryotic Cnx1E cannot replace the function of *E. coli* MoeA [1] suggests different mechanisms in metal insertion, possibly due to the formation of bis-metal-pterin cofactors in prokaryotes (including W-cofactors). The finding that in *P. furiosus* and in many other archaeal genomes two different MoeA (PfMoeA1 and PfMoeA2) proteins are expressed might either contribute to metal selectivity or to the formation of the two different tungsten cofactors known so far (figure 6). Uncovering these mechanisms and how they differ between Moco and Wco synthesis is a main challenge for the future.

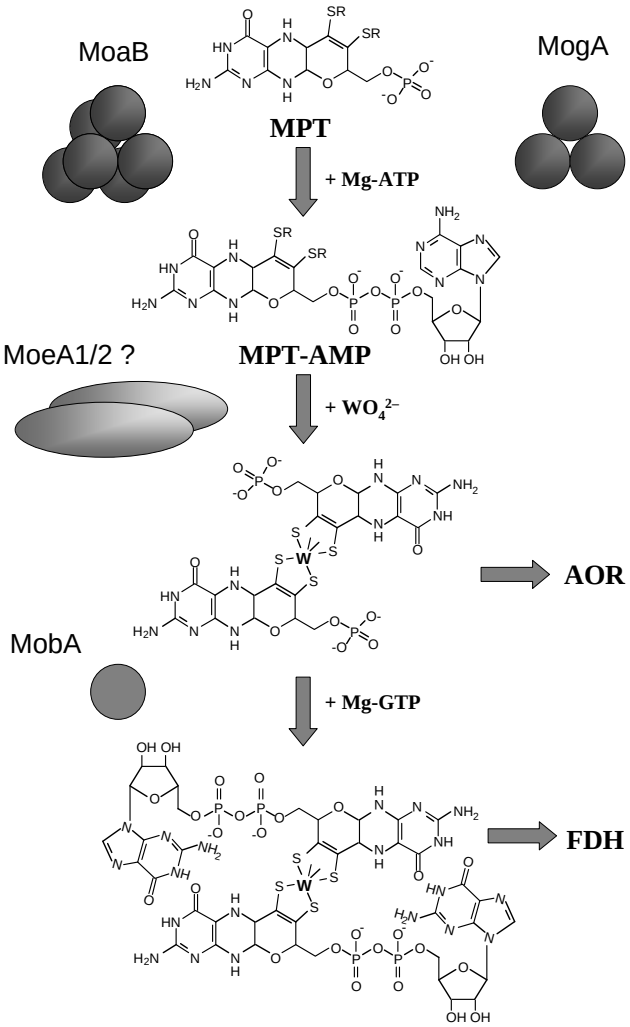

Figure 6. Model for the last steps in tungsten cofactor biosynthesis of *P. furiosus*. Shown are the steps following MPT synthesis in *P. furiosus* leading to the formation of W- bispterin-cofactor as found in enzymes of the aldehyde oxidoreductase (AOR) family and W- bispterin-containing guanine dincleotide cofactor found in formate dehydrogenase (FDH). First, MPT is adenylylated by the action of the hexameric MoaB, a function which is identical to the trimeric MogA protein found in *E. coli*. Next, the metal is inserted by MoeA1 or MoeA2 or both. Finally, guanylylation has to be catalyzed by the MobA protein. In MPT and MPT-AMP both dithiolene ligands are indicated by an R as the ligand is not known so far.

Acknowledgements

We thank Simona Cerrone and Sarah Nicklas (University of Cologne) for technical assistance. This work was supported by grants from the Council for Chemical Sciences of the Netherlands Organization for Scientific Research (700.51.301 to WRH), the Deutsche Forschungsgemeinschaft (GS), the Bundesministerium für Bildung und Forschung (GS) and Fonds der Chemischen Industrie (GS).

References

[1] R. Hille, Chem. Rev. 96 (1996) 2757.
[2] A. Kletzin, M.W. Adams, FEMS Microbiol. Rev. 18 (1996) 5.
[3] K.V. Rajagopalan, J.L. Johnson, J. Biol. Chem. 267 (1992) 10199.
[4] G. Schwarz, Cell. Mol. Life Sci. 62 (2005) 2792.
[5] R. Hille, Trends Biochem. Sci. 27 (2002) 360.
[6] R. Hille, Arch Biochem Biophys 433 (2005) 107.
[7] F.T. Robb, D.L. Maeder, J.R. Brown, J. DiRuggiero, M.D. Stump, R.K. Yeh, R.B. Weiss, D.M. Dunn, Methods Enzymol. 330 (2001) 134.
[8] S. Mukund, M.W. Adams, J. Biol. Chem. 266 (1991) 14208.
[9] R. Roy, S. Mukund, G.J. Schut, D.M. Dunn, R. Weiss, M.W.W. Adams, J. Bacteriol. 181 (1999) 1171.
[10] S. Mukund, M.W. Adams, J. Biol. Chem. 270 (1995) 8389.
[11] R. Roy, M.W.W. Adams, Met. Ions Biol. Syst. 39 (2002) 673.
[12] L.E. Bevers, E. Bol, P.-L. Hagedoorn, W.R. Hagen, J. Bacteriol. 187 (2005) 7056.
[13] G. Schwarz, D.H. Boxer, R.R. Mendel, J. Biol. Chem. 272 (1997) 26811.
[14] J. Kuper, A. Llamas, H.J. Hecht, R.R. Mendel, G. Schwarz, Nature 430 (2004) 806.
[15] A. Llamas, R.R. Mendel, G. Schwarz, J. Biol. Chem. 279 (2004) 55241.
[16] A. Llamas, T. Otte, G. Multhaup, R.R. Mendel, G. Schwarz, J. Biol. Chem. 281 (2006) 18343.
[17] J. Kuper, T. Palmer, R.R. Mendel, G. Schwarz, Proc. Natl. Acad. Sci. USA 97 (2000) 6475.
[18] J.D. Nichols, K.V. Rajagopalan, J. Biol. Chem. 280 (2005) 7817.
[19] G. Schwarz, J. Schulze, F. Bittner, T. Eilers, J. Kuper, G. Bollmann, A. Nerlich, H. Brinkmann, R.R. Mendel, Plant Cell. 12 (2000) 2455.
[20] C.A. Temple, K.V. Rajagopalan, J. Biol. Chem. 275 (2000) 40202.
[21] A. Vergnes, J. Pommier, R. Toci, F. Blasco, G. Giordano, A. Magalon, J. Biol. Chem. 281 (2006) 2170.
[22] J. Buc, C.L. Santini, R. Giordani, M. Czjzek, L.F. Wu, G. Giordano, Mol. Microbiol. 32 (1999) 159.
[23] L.E. Bevers, P.L. Hagedoorn, G.C. Krijger, W.R. Hagen, J. Bacteriol. 188 (2006) 6498.
[24] G. Fiala, K.O. Stetter, Arch. Microbiol. 145 (1986) 56.
[25] R. Sanishvili, S. Beasley, T. Skarina, D. Glesne, A. Joachimiak, A. Edwards, A. Savchenko, J. Biol. Chem. 279 (2004) 42139.
[26] G. Bader, M. Gomez-Ortiz, C. Haussmann, A. Bacher, R. Huber, M. Fischer, Acta Crystallogr. D. Biol. Crystallogr. 60 (2004) 1068.
[27] V. Stewart, C.H. MacGregor, J. Bacteriol. 151 (1982) 788.
[28] R.W. Jones, P.B. Garland, Biochem. J. 164 (1977) 199.
[29] J.A. Santamaria-Araujo, B. Fischer, T. Otte, M. Nimtz, R.R. Mendel, V. Wray, G. Schwarz, J. Biol. Chem. 279 (2004) 15994.
[30] G. Gutzke, B. Fischer, R.R. Mendel, G. Schwarz, J. Biol. Chem. 276 (2001) 36268.
[31] M.T. Liu, M.M. Wuebbens, K.V. Rajagopalan, H. Schindelin, J. Biol. Chem. 275 (2000) 1814.
[32] S. Ito, S. Fushinobu, I. Yoshioka, S. Koga, H. Matsuzawa, T. Wakagi, Structure 9 (2001) 205.
[33] G. Schwarz, P.L. Hagedoorn, K. Fischer, Mol. Microbiol. Heavy Metals, Microbiology Monographs, Springer, 2007.
[34] K. Hollenstein, D.C. Frei, K.P. Locher, Nature 446 (2007) 213.
[35] B. Stallmeyer, A. Nerlich, J. Schiemann, H. Brinkmann, R.R. Mendel, Plant J. 8 (1995) 751.
[36] L.A. Anderson, E. McNairn, T. Lubke, R.N. Pau, D.H. Boxer, J. Bacteriol. 182 (2000) 7035.

[37] A. Llamas, M. Tejada-Jimenez, D. Gonzalez-Ballester, J.J. Higuera, G. Schwarz, A. Galvan, E. Fernandez, Eukaryot. Cell 6 (2007) 1063.
[38] G. Schwarz, N. Schrader, R.R. Mendel, H.J. Hecht, H. Schindelin, J. Mol. Biol. 312 (2001) 405.

Chapter 4

Metal incorporation into the metallopterin cofactor by MoeA proteins

Loes E. Bevers
Wilfred R. Hagen
Guenter Schwarz

Abstract

The biosynthesis of the molybdopterin cofactor has been studied intensively in various organisms. The majority of these reports are focused on molybdenum cofactor (Moco) synthesis. A recent study on the function of *Pyrococcus furiosus* MoaB protein has shown that adenylylated MPT is the last common intermediate in Moco and Wco biosynthesis (Bevers, L.E. et al, Biochemistry 47, 2008, 949-456). The main difference in the synthesis of both cofactors is expected to be found in the step of metal insertion. This step has been studied already in plants, where Cnx1E catalyses the molybdate-dependent hydrolysis of MPT-AMP upon the insertion of molybdenum into the metallopterin (Llamas et al., 2006, JBC 281, 18343-50). Interestingly, many bacterial and archaeal genomes, including the *P. furiosus* genome, harbor two copies of these Cnx1E-homologous genes referred to as MoeAs. In this study, the two Cnx1E-homologous genes in *P. furiosus*, MoeA1 and MoeA2, were cloned, and the proteins were purified. *In vivo* reconstitution studies of nitrate- and trimethylamine-*N*-oxide reductase activity in an *E. coli moeA* mutant showed that the MoeA2 protein was able to complement the mutant strain up to 30% of the activity of the wild type, however, only at high molybdate concentrations. High cPMP levels (an intermediate in Moco/Wco synthesis) were detected in this MoeA2-complemented strain, which indicates only a partial complementation. Both MoeA proteins were able to catalyze the hydrolysis of MPT-AMP *in vitro* in the presence of tungstate or molybdate. Based on these results, a model is proposed for the function of MoeA1 and MoeA2 in tungsten- and molybdenum-cofactor synthesis.

Introduction

Tungsten and molybdenum are both associated with enzymes in a similar type of cofactor consisting of one or two tricyclic pterin moieties, referred to as molybdenum cofactor (Moco) or tungsten cofactor (Wco) [1,2]. The biosynthesis of these molybdo- and tungsto-pterin cofactors has been extensively studied in prokaryotes and eukaryotes (Chapter 1, figure 8) and appears to be conserved amongst all kingdoms of life at least until the step of metal insertion. In the first three steps of the biosynthesis in *Escherichia coli*, GTP is converted into cyclic pyranopterin monophosphate (cPMP) by the enzymes MoaA and MoaC [3]. Subsequently, cPMP is sulfurated by MPT-synthase (MoaE and MoaD) [1] and the resulting MPT is adenylyated by the trimeric MogA protein (chapter 3) [4]. In archaea and some bacteria, the adenylylation of the MPT is catalyzed by the homologous MoaB protein (chapter 3) [4]. The existence of this adenylylated biosynthetic intermediate was firstly identified in the crystal structure of plant *Arabidopsis thaliana* Cnx1G protein (plant homologue of MogA/MoaB). The protein was co-crystallized with its product: adenylylated molybdopterin. An additional surprising observation was the identification of a bound copper atom between the two sulfurs of the pterin moiety [5]. The role of this copper atom is still under investigation, but it might be involved in protecting the dithiolene sulfurs from oxidation and/or forming a suitable leaving group for subsequent molybdenum or tungsten insertion. These investigations also include the examination of other metals that might fulfill the same role as copper, for example, in anaerobic organisms in which copper is expected to be low or absent. Studies on the adenylylation activity of bacterial *E. coli* MogA [4], archaeal *Pyrococcus furiosus* MoaB [4], plant *A. thaliana* Cnx1G [5], and algal *Chlamydomonas reinhardtii* Cnx1G [6] have now confirmed unequivocally that the MPT activation by adenylylation is essential for the subsequent step of metal insertion into the different pterin cofactors.

This subsequent step of metal insertion is catalyzed by the MoeA protein and its homologues. The mechanism of the metal insertion catalyzed by the plant homologue Cnx1E has been elucidated recently [7]: MPT-AMP is transferred from Cnx1G to Cnx1E in the presence of molybdate, and subsequently, upon addition of a divalent cation like Mg^{2+}, MPT-AMP is hydrolysed and the metal is inserted between the dithiolene sulfurs. The authors proposed the formation of a transient adenylylated molybdate intermediate, because the depletion of MPT-AMP was observed to be 1.5 fold faster than the rate of release of AMP, indicating an intermediate step. Interestingly, the transfer of MPT-AMP from Cnx1G to Cnx1E also occurred in the presence of tungstate, however, this complex showed only very low hydrolysis activity [7]. This last result indicates that Cnx1E and its homologues could play a role in metal specificity.

Recently, Magalon and coworkers have shown that the metal specificity can also be dependent on the type of apoenzyme and its chaperones. They have detected interactions between nitrate reductase subunit NarH and MogA, MoeA and MobA, *in vivo*, in *E. coli* cells grown on molybdate [8]. In tungstate-supplemented cells these interactions between

NarH and the proteins of the biosynthesis pathway were absent, which explains why nitrate reductase could not been synthesized with a tungsten containing bis-MGD cofactor [9]. It should be noted that the interactions between MogA, MoeA and MobA did not change during the tungstate supplementation [10], indicating that the cofactor synthesis itself is not inhibited. *E. coli* has already been shown to be able to synthesize the tungsten-bisMGD containing trimethylamine-*N*-oxide (TMAO) reductase [11] implying that, for the nitrate reductase, the metal selective incorporation is directed by the apo-enzyme and its chaperones [8] more likely than by the metal selective hydrolysis of MoeA.

Mutant strains also gave more insight in the functional roles of the MoeA protein *in vivo*. For example, the *moeA* deficient mutant of *Rhodobacter capsulatus* [12] could be complemented by high levels of molybdate with respect to the synthesis of Moco-containing xanthine dehydrogenase. On the contrary, enzyme activities of MGD-containing enzymes like DMSO reductase or nitrate reductase could not be restored. A similar observation was done in an *in vitro* assay where molybdenum was ligated into MPT in the presence of MoeA, and the formation of active Moco was monitored by restoration of apo-sulfite oxidase (SO) activity [13]. In absence of MoeA the restored SO activity was low, however, this could be increased by addition of high concentrations of molybdate [13]. These results altogether suggest to assign two functions to MoeA: (i) catalysis of the metal insertion into MPT at low concentrations of molybdate or tungstate, and (ii) forming a surface to enable the interaction between Moco and MobA, which is the protein that catalyses the nucleotide attachment leading to the formation of MGD cofactors.

Interestingly, all archaeal genomes and a significant number of bacterial genomes harbor two copies of these *moeA*-encoding genes. At this moment it is unclear whether these two proteins have different functions. It is tempting to speculate that one of the MoeAs is selective for the hydrolysis of MPT-AMP in the presence of molybdate and the other in the presence of tungstate. An alternative hypothesis involves the interaction between the MoeA and the MobA protein, which is responsible for the nucleotide attachment. One of the two MoeAs might have a stronger interaction with MobA, processing the cofactor to its final form of MGD, whereas the other MoeA protein prevents Moco from being further modified by not bringing it in close proximity of MobA.

Several crystal structures have been determined for MoeAs from different organisms: the *E. coli* MoeA structure (1G8L) [14], the two MoeAs from *Pyrococcus horikoshii* MoeA1 (1UZ5) and MoeA2 (1WU2), and *P. furiosus* MoeA2 (1XI8). The *P. furiosus* proteins are very homologous to the proteins of *P. horikoshii*: MoeA1 (79% identity, 89% similarity) and MoeA2 (74%/89%). Compared to each other, the *P. fusiosus* proteins share 40% identity and 58% similarity and compared to *E. coli* MoeA the numbers are: 35%/53% for MoeA1 and 32%/50% for MoeA2.

Previously performed mutational studies on the *E. coli* MoeA protein have identified several residues that are important for the activity of the enzyme. The activity of the mutants was monitored by the ability to complement nitrate reductase activity in an *E. coli moeA* mutant [15], and the ability to restore apo-sulfite oxidase activity in (i) *moeA*- crude cell extract or

(ii) in an assay with purified components [13]. All residues that appeared crucial for the *E. coli* MoeA activity are conserved in *P. furiosus* MoeA1 and MoeA2: D59, T100, E188, D228, D259, P298, and P301, respectively, suggesting similar mechanisms and functionalities for these bacterial and archaeal 'metal insertases'.
We have chosen *P. furiosus* as a model system for tungsten cofactor synthesis, because the organism's growth is dependent on the presence of tungsten and it is known to express five tungsten containing aldehyde oxidoreductase enzymes. Initial studies were focused on the adenylylation step catalyzed MoaB (chapter 3), and these are now followed-up by a study on the step of metal insertion. In this chapter we describe the cloning, expression and purification of the two MoeAs from *P. furiosus*, and we report the activity of these enzymes in different *in vivo* and *in vitro* assays.

Materials and methods

Plasmids, bacterial strains – The following *E. coli* mutant strain was used: SE1578 (*moeA)* [*mutD5 ara-14 ArgE3(Oc) galK2 hisG4(Oc) kdgK51 lacY1 leuB6 mgl-51 mtl-1 rac rfbD1 rpsL31 supE44 thi-1 thr-1 tsx-33 xyl-S*] [16]. *E. coli* MC4100 was used as wild type strain.

Cloning of *P. furiosus* moeA1 and moeA2 genes – The *moeA1* gene (PF0542) and the *moeA2* gene (PF1783*)* were amplified by PCR using *Pfx* polymerase (Invitrogen) and chromosomal DNA from *P. furiosus* as a template, subcloned into the pCR®2.1-TOPO® vector (Invitrogen). Plasmids were isolated and after sequencing positive fragments were cloned into the *Nde1* and *BamH1* sites of the pET15b (Novagen), resulting in MoeA fusion proteins with N-terminal his-tag. These constructs were transformed into competent *E. coli* BL21- CodonPlus®-(DE3)-RIPL cells (Stratagene).

Protein expression and purification of PfMoaB and homologous *E. coli* proteins – *E. coli* BL21(DE3) cells containing pET15b-MoeA1/2 were grown aerobically in Luria-broth medium containing 100 μg/ml ampicillin. Protein synthesis was induced with a final concentration of 0.2 mM IPTG, when the absorbance of the culture reached 0.5 at 600 nm. Cells were induced for 5 h at 30 °C, harvested by centrifugation, washed with buffer A (20 mM Tris-HCl, pH 8.0, 10 mM Imidazole, 500 mM NaCl and 10% glycerol) and lysed in the same buffer (1 g of cells per 5 ml buffer) using a cell disruptor system (Constant systems). Cell-free extract was obtained by centrifugation for 20 min at 15.000 x g at 4 °C. The supernatant was heated for 30 min at 70 °C as a first purification step. Precipitated protein was removed by centrifugation and the supernatant was applied to a Ni-sepharose 6 fast flow resin (GE healthcare) equilibrated with buffer A, washed with the same buffer and eluted with buffer B (20 mM Tris-HCl, pH 8.0, 500 mM Imidazole, 500 mM NaCl and 10%

glycerol). Protein-containing samples were dialyzed against buffer C (20 mM Tris, pH 8.0, 150 mM NaCl and 10% glycerol), concentrated and stored at -80˚C.

Determination of nitrate reductase/trimethylamine-n-oxide activity in *E. coli* – The λDE3 lysogenization procedure (Novagen) was used to integrate the gene for T7 polymerase into the chromosome of the SE1578 *moeA* strain. The resulting strain SE1578(DE3) was transformed with the pET15b-MoeA1 and MoeA2 constructs. The cells were grown for 7 hours under anaerobic conditions in LB-media containing 0.1% trimethylamine-*N*-oxide (TMAO). Nitrate reductase and TMAO reductase activity were determined spectrophotometrically using reduced benzyl viologen as electron donor [17,18].

Detection of cPMP in *E. coli* cell free extract – the cells were grown for 7 hours under anaerobic conditions in 50 ml LB-media containing 0.1% TMAO. The cells were freeze dried and subsequently resuspended in 0.5 ml 100 mM Tris, pH 7.2. Cells were broken by sonification, 2 times 10 seconds at an amplitude of 45%, and CFE was obtained by centrifugation. Cyclic pyranopterin monophosphate (cPMP) levels were determined by HPLC as described [19].

In vitro hydrolysis of MPT-AMP – MPT was synthesized *in vitro* using purified cPMP [20], and *E. coli* MoaE and *E. coli* thiocarboxylated MoaD that were purified and assembled into active MPT synthase as described before [21]. Subsequent MPT adenylylation to obtain MPT-AMP by *P. furiosus* MoaB was performed as described in [4]. Standard *in vitro* hydrolysis was performed in buffer (100 mM Tris, pH 7.2) containing: 250 pmol MoaB-MPT-AMP and 500 or 5000 pmol molybdate/tungstate in an assay volume of 140 µL per point of measurement. Subsequently, the mixture was incubated for 2 min at the temperature required for the hydrolysis, which was 65 ˚C under standard conditions. The hydrolysis reaction was initiated upon addition of 500 pmol MoeA1 or MoeA2. At different time points, samples (140 µL) were taken directly from the reaction mixture and the reaction was stopped by the addition of 17.5 µL of 1% I_2, 2% KI, 1 M HCl. MPT and MPT-AMP were determined by HPLC analysis of formA (i.e. MPT iodine oxidized product) analysis as described [19] with the variation that 200 µL Q-sepharose columns (GE healthcare) were used to purify formA and formA-AMP prior HPLC analysis.

Results

Expression and purification of the MoeAs

The *moeA1* and *moeA2* genes were cloned into the pET15b vector and expressed as N–terminal his-tag fusion protein. Purification resulted in a yield of approximately 20 mg MoeA1 or MoeA2 per liter of induced *E. coli* culture. The purified proteins were analyzed by size exclusion chromatography and both proteins eluted at a molecular weight of 90 kDa

indicating a dimeric native conformation (data not shown) as seen for the *E. coli* MoeA [14].

In vivo reconstitution of *E. coli moeA* mutants by *P. furiosus* MoeAs

Initially, the activity of the protein was tested by its ability to restore nitrate reductase- and TMAO reductase-activity in a *moeA* mutant under different molybdate and tungstate concentrations (figure 1). Interestingly, the mutants expressing the MoeA2 protein were partly complemented for their TMAO- and nitrate reductase activity. The complementation increased when the concentration of molybdate in the growth medium increased. On the contrary, MoeA1 was not able to restore TMAO- or nitrate reductase activity. It should be noted that these cells were grown without any nitrate supplementation to induce the expression of nitrate reductase.

Previous studies have shown that wild type *E. coli* (strain MC4100) is able to produce active, tungsten-containing TMAO reductase [11]. In our experiments, TMAO reductase activity was indeed detected in tungsten-supplemented cells of the wild type strain, however, this activity was very low. The addition of tungstate clearly inhibited the TMAO reductase activity that was detectable in non-supplemented wild type cells. None of the *P. furiosus* MoeA proteins could reconstitute TMAO reductase activity in the tungsten-supplemented cells.

In summary, these data show that *P. furiosus* MoeA2 is able to complement the *E. coli moeA* mutant, especially at high molybdate concentration.

.

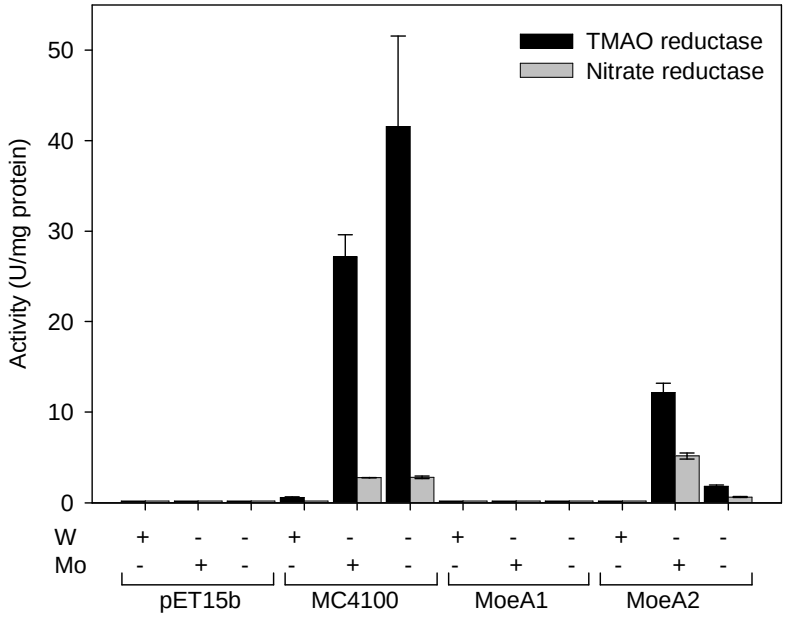

Figure 1. Functional reconstitution of TMAO reductase and nitrate reductase activity in *E. coli moeA* mutants upon expression of *P. furiosus* MoeA1 and MoeA2 proteins, and under supplementation of 1 mM tungstate (+), 1 mM molybdate (+), or without supplementation (-). The *E. coli* MC4100 strain (wild type) was used as positive control, and SE1581 (*moeA)* transformed with the empty vector (pET15b) was taken as negative control.

Levels of cPMP in reconstituted *E. coli moeA* mutants

The levels of the Moco-biosynthesis intermediate cPMP in the complemented mutant cells were measured (figure 2) in order to determine to what extent the *P. furiosus* MoeA proteins were able to complement, as previous studies have described an upregulated cPMP synthesis in cells containing low levels of active cofactor [22].

In non-supplemented and molybdate-supplemented wild type cells, no cPMP could be detected. However, significant levels of cPMP were found in the wild type strain grown on tungstate. All the *moeA* cell lysates contained high levels of cPMP independent of their type of supplementation and complementation (only the average cPMP concentration in these cell lines is depicted in figure 2). Indeed, less active cofactor was formed in the tungsten supplemented wild type cells as their TMAO and nitrate reductase activity decreased compared to the non-supplemented cells (figure 1). High cellular cPMP levels in the non-complemented mutants, could also be explained due to the absence of active cofactor. However on the contrary, similar high levels of cPMP were detected in the mutant strain complemented by *P. furiosus* MoeA2, which was expected to contain active cofactor. This finding indicates that *P. furiosus* MoeA2 is able to complement the activity of *E. coli* MoeA only partially.

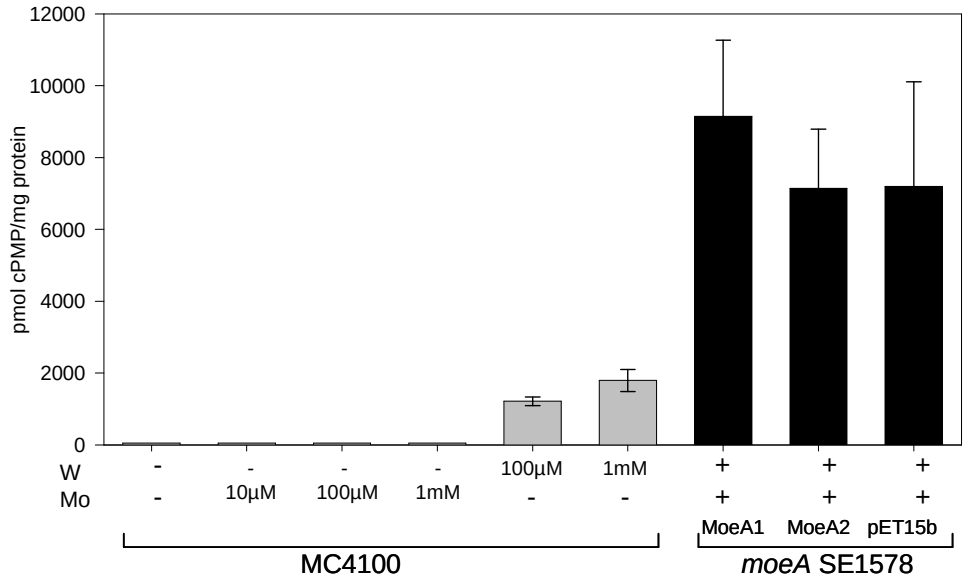

Figure 2. Levels of cPMP detected in cell lysates of MC4100 (wild type) under different supplementation conditions, and in cell lysates of *moeA* SE1578 expressing *P. furiosus* MoeA1 or MoeA2, or transformed with the empty vector averaged for the same, set of supplementation conditions.

Analyzing the activity of these *P. furiosus* MoeA proteins *in vivo* in *E. coli*, has two intrinsical problems: (i) a non-optimal temperature (the growth temperature of *E. coli* is 37 ˚C, whereas the optimal activity of *P. furiosus* proteins is 100 ˚C), and (ii) a different substrate donor, as MogA transfers MPT-AMP to MoeA in *E. coli*, whereas MoaB is the MPT-AMP donor in *P. furiosus*.

To avoid these issues and to use a more defined system, the activity of the two MoeA proteins was also investigated in an *in vitro* assay using purified proteins and cPMP. In this assay (at 60 ˚C), *P. furiosus* MoaB adenylylates MPT and subsequently, upon co-incubation with the MoeAs and molybdate or tungstate, the hydrolysis of MPT-AMP was monitored (figure 3AB). The results show that both MoeA1 and MoeA2 were able to hydrolyze MPT-AMP in the presence of tungstate and molybdate, at a 10-fold excess of the respective oxoanion over the MoeA protein concentration. No differences were observed in the rate of hydrolysis between the samples with tungstate or molybdate. No MPT-AMP hydrolysis was observed in the absence of MoeA protein (figure 3C). In the absence of oxoanion, however, also a decrease of MPT-AMP was detected, approximately 20% of the decrease detected in the presence of either tungstate or molybdate (data not shown). This observation might point to the presence of trace amounts of molybdate or tungstate in the MoeA preparations. This background activity in the absence of added oxoanion was also observed in measurements with plant Cnx1E [7] and *E. coli* MoeA (unpublished results G. Schwarz).

In order to study metal specific hydrolysis of MPT-AMP, the ratio between the oxoanion and the protein should be approximately unity. These experiments were executed; however, the rate of hydrolysis was of the same order-of-magnitude as the background decrease of MPT-AMP (data not shown). Therefore, at this time, no conclusions can be made regarding the metal-specific hydrolysis for the two MoeA proteins.

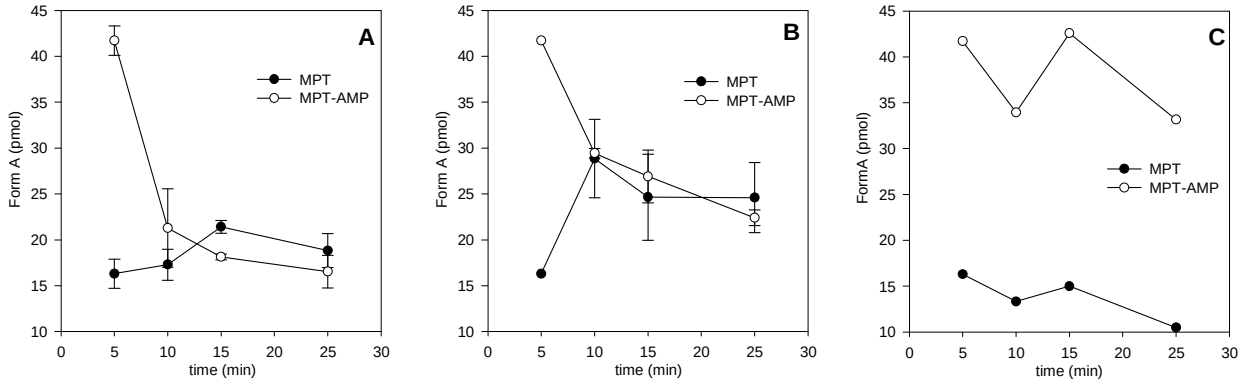

Figure 3. *In vitro* hydrolysis of MPT-AMP by *P. furiosus* MoeA1 (A), MoeA2 (B), no protein (C), incubated with a 10-fold excess of tungstate. Similar results were obtained with molybdate (data not shown).

Conclusion and discussion

Initial studies on tungsten cofactor synthesis in *P. furiosus* were focused on the adenylylation of MPT by MoaB (chapter 3). Preliminary results on the subsequent step of MPT-AMP hydrolysis and metal insertion catalyzed by MoeA proteins are described in this chapter. Like all sequenced archaeal and many bacterial genomes, the *P. furiosus* genome harbors two copies of MoeA-encoding genes. The results from this study clearly show that both *P. furiosus* MoeA proteins are able to catalyze the hydrolysis of MPT-AMP, previously synthesized by MoaB *in vitro*. Complementary to these data, future experiments are required to confirm the formation of active Moco or Wco by including, for example, apo-enzymes as acceptor sites for the produced cofactor by using a defined *in vitro* assay.
Furthermore, the reconstitution assay of TMAO- and nitrate-reductase activity in the *E. coli moeA* mutant showed that the *P. furiosus* MoeA2 protein is able to complement the mutation in a molybdate-dependent manner. On the contrary, no reconstitution of TMAO- or nitrate reductase activity was observed in cells expressing the MoeA1 protein.
The complementation by *P. furiosus* MoeA2 indicates that this protein catalyzes a similar reaction as *E. coli* MoeA, however, a high, non-physiological molybdate concentration was required. In addition, high intracellular cPMP levels were detected in cells complemented by *P. furiosus* MoeA2, suggesting a remaining impaired Moco synthesis. Both observations imply that there are differences between the mechanism of MPT-AMP hydrolysis catalyzed by *P. furiosus* MoeA and *E. coli* MoeA.
From the literature it is known that the MoeA protein is somehow involved in the regulation of the the *moaA* operon, which encodes the proteins that catalyse the synthesis of cPMP [23]. The protein itself does not show binding affinity towards DNA and, therefore, a product of the reaction catalyzed by MoeA was speculated to acts as regulator [23]. The data obtained in the present study indicate that *P. furiosus* MoeA2 cannot complement *E. coli* MoeA's regulatory function, as the cellular cPMP levels in the complemented mutant remained high.
Previous studies have shown that high levels of molybdate can complement the *Rhodobacter capsulatus moeA* mutant for the formation of non-nucleotide modified cofactor [12]. This means that, at high molybdate concentrations, Moco can be formed independently of the presence of any MoeA homologue. Taking this into account, we propose a model for the complementation of the *E. coli moeA* mutant by *P. furiosus* MoeA2 (figure 4). It proposes that the MPT-AMP generated by MogA is non-specifically hydrolyzed in the presence of a high molybdate concentration, and that the released Moco is subsequently able to bind to *P. furiosus* MoeA2. This MoeA2-Moco complex is proposed to have an affinity to interact with *E. coli* MobA, thereby bringing the Moco in close proximity to this nucleotide attaching protein. In the case of low molybdate concentrations, there will be no non-specifically formed MoeA2-Moco complexes. As a result, there will be no 'interaction' between MoeA2-Moco and MobA, which is required for nucleotide attachment [12] and, therefore, no reconstitution of the nitrate- or TMAO- reductase activity will be detected.

Previous studies have shown that *E. coli* MobA has no affinity to bind Moco, and it was proposed to only bind Moco in the presence of MoeA [12].
Reasons for the absence of complete reconstitution by the *P. furiosus* proteins might be the non-physiological trimeric substrate donor MogA, the non-physiological temperature, or any other physiological condition that is different in *E. coli* compared to *P. furiosus*.

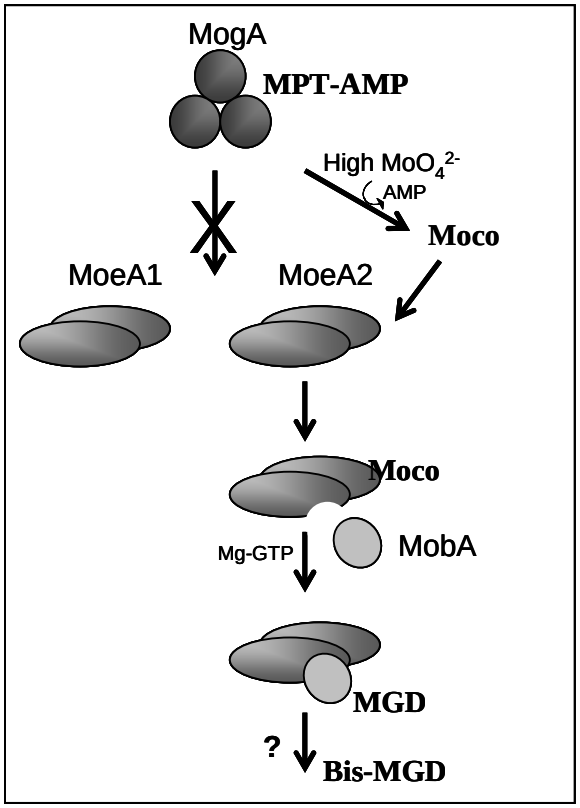

Figure 4. Proposed model for the complementation of *E. coli moeA* mutant with *P. furiosus* MoeA1 and MoeA2 proteins; upon addition of high molybdate, Moco is non-specifically synthesized and binds to MoeA2, which changes conformation and will become susceptible to interact with MobA. Subsequently the nucleotide is attached and nitrate- and TMAO-reductase activity can be measured. MoeA1 is not able to bind free Moco and/or will not obtain a high affinity for MobA. The mechanism of bis-cofactor formation is still unknown.

In line with the proposed model for the complementation of the *E. coli moeA* mutant, the main difference between MoeA1 and MoeA2 in *P. furiosus* is likewise proposed to be at the level of interaction with MobA (figure 5). In this very speculative model, these different interactions are proposed to serve as a mechanism to selectively process part of the Moco and/or Wco for the synthesis of MGD in the following manner: Moco and/or Wco bound to MoeA1 will end up as a MPT or a bis-MPT type of cofactor (AORs) and Moco and/or Wco bound to MoeA2 will be modified with a nucleotide attachment in order to obtain a MGD type of cofactor (FDHs) (figure 4). The issue regarding the metal specificity remains to be

elucidated. In order to analyze the metal-dependent hydrolysis, it is important to improve the established *in vitro* set-up and to decrease the observed background hydrolysis (figure 3).

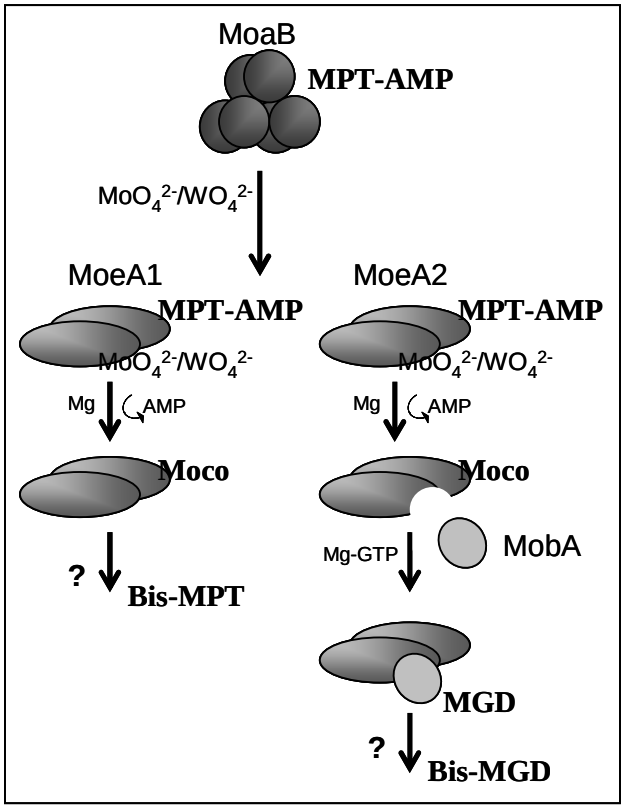

Figure 5. Proposed model for the physiological pathway in *P. furiosus*; MPT-AMP is transferred from MoaB to MoeA1 and MoeA2 and Wco/Moco is formed in the presence of low amounts of tungstate and/or molybdate. MoeA2 subsequently binds to MobA and Wco/Moco is further processed to form MGD. The molecular mechanism of bis-cofactor formation is still unknown.

Furthermore, it should be noted that, so far, no *P. furiosus* enzymes have been purified yet that contain a MGD-type of cofactor. However, they are likely to exist as the genome contains two genes annotated as putative MGD-containing formate dehydrogenases, and also two genes encoding MobA and MobB homologues proteins (PF0618 and PF1954).
Further research is required to confirm the expression of these MGD containing proteins. Micro-array studies might help to validate the model (figure 5) by showing a co-regulation in mRNA levels of MoeA1 and MPT containing proteins versus MoeA2 and MGD containing proteins.

Acknowledgements

This research was supported by a grant from the Council for Chemical Sciences of the Netherlands Organization for Scientific Research (700.51.301).

References

[1] G. Schwarz, R.R. Mendel, Annu. Rev. Plant Biol. (2006) 623.
[2] R. Hille, Chemical Reviews (Washington, D. C.) 96 (1996) 2757.
[3] M.M. Wuebbens, K.V. Rajagopalan, J. Biol.Chem. 270 (1995) 1082.
[4] L.E. Bevers, P.-L. Hagedoorn, J.A. Santamaria-Araujo, A. Magalon, W.R. Hagen, G. Schwarz, Biochemistry 47 (2008) 949.
[5] J. Kuper, A. Llamas, H.-J. Hecht, R.R. Mendel, G. Schwarz, Nature 430 (2004) 803.
[6] A. Llamas, M. Tejada-Jimenez, D. Gonzalez-Ballester, J.J. Higuera, G. Schwarz, A. Galvan, E. Fernandez, Eukaryot. Cell 6 (2007) 1063.
[7] A. Llamas, T. Otte, G. Multhaup, R.R. Mendel, G. Schwarz, J. Biol.Chem. 281 (2006) 18343.
[8] A. Vergnes, K. Gouffi-Belhabich, F. Blasco, G. Giordano, A. Magalon, J. Biol.Chem. 279 (2004) 41398.
[9] R.A. Rothery, J.L. Simala Grant, J.L. Johnson, K.V. Rajagopalan, J.H. Weiner, J. Bacteriol. 177 (1995) 2057.
[10] A. Magalon, C. Frixon, J. Pommier, G. Giordano, F. Blasco, J. Biol.Chem. 277 (2002) 48199.
[11] J. Buc, C.-L. Santini, R. Giordani, M. Czjzek, L.-F. Wu, G. Giordano, Mol. Microbiol. 32 (1999) 159.
[12] S. Leimkuhler, S. Angermuller, G. Schwarz, R.R. Mendel, W. Klipp, J. Bacteriol. 181 (1999) 5930.
[13] J.D. Nichols, K.V. Rajagopalan, J. Biol.Chem. 280 (2005) 7817.
[14] S. Xiang, J. Nichols, K.V. Rajagopalan, H. Schindelin, Structure 9 (2001) 299.
[15] C. Sandu, R. Brandsch, Biol. Chem. 383 (2002) 319.
[16] V. Stewart, C.H. MacGregor, J. Bacteriol. 151 (1982) 788.
[17] R.W. Jones, P.B. Garland, Biochem. J. 164 (1977) 199.
[18] M. Takagi, T. Tsuchiya, M. Ishimoto, J. Bacteriol. 148 (1981) 762.
[19] A. Llamas, R.R. Mendel, G. Schwarz, J. Biol. Chem. 279 (2004) 55241.
[20] J.A. Santamaria-Araujo, B. Fischer, T. Otte, M. Nimtz, R.R. Mendel, V. Wray, G. Schwarz, J. Biol. Chem. 279 (2004) 15994.
[21] G. Gutzke, B. Fischer, R.R. Mendel, G. Schwarz, J. Biol. Chem. 276 (2001) 36268.
[22] L.A. Anderson, E. McNairn, T. Leubke, R.N. Pau, D.H. Boxer, J. Bacteriol.182 (2000) 7035.
[23] A. Hasona, W.T. Self, R.M. Ray, K.T. Shanmugam, FEMS Microbiol. Lett. 169 111.

Chapter 5

Replacing tungsten by molybdenum in aldehyde oxidoreductases in *Pyrococcus furiosus*

Loes E. Bevers
Emile Bol
Wilfred R. Hagen

Abstract

The hyperthermophilic archaeon *Pyrococcus furiosus* expresses five aldehyde oxidoreductases (AORs) all containing a non-modified tungsto-bispterin cofactor. The growth of this organism is fully dependent on the presence of tungsten in the media. Previous attempts by Adams and coworkers to incorporate molybdenum or vanadium in the active site of these AOR enzymes were unsuccessful (Mukund, S., Adams, M.W.W., 1996, J. Bact.178, 163-170). On the contrary, we describe here the incorporation of molybdenum in formaldehyde oxidoreductase (FOR) and tungsten containing oxidoreductase number five (WOR5), with efficiencies up to one quarter holo-protein formation. The quantity of the metal was determined with catalytic adsorptive stripping voltammetry and the nature of its coordination was studied with EPR spectroscopy. It is concluded that *P. furiosus* can internalize molybdenum and insert it in a pterin cofactor. Aldehyde oxidation activity correlated with the tungsten content indicates that the molybdenum analogue is inactive.

Introduction

Tungsten and the chemically analogous molybdenum are always associated with enzymes in an unique metal-binding pterin (MPT) cofactor, except in nitrogenases [1]. Tungsten containing enzymes can be divided in two families: the aldehyde oxidoreductases (AORs) that contain a non-modified tungsto-bispterin cofactor, and the formate dehydrogenases (FDHs) which have a guanine monophosphate attached to both pterin moieties.

Because of the chemical similarities, many attempts have been made to substitute molybdenum with tungsten and vice versa in the cofactor of various enzymes. These experiments have shown that not all enzymes can be synthesized with either metal and that successful substitution does not always lead to the formation of active enzyme. Experiments with rat sulfite- and xanthine oxidase showed that both metals could be incorporated into the pterin cofactor, but the tungsten-containing enzymes were completely inactive [2]. Replacing the molybdenum with tungsten in the case of *Rhodobacter capsulatus* DMSO reductase, heterologously expressed in *Escherichia coli* [3], and *E. coli* trimethylamine *N*-oxide (TMAO) reductase [4] resulted in active enzyme. However, the activity profiles changed compared to the profile of the molybdenum containing enzyme, presumably due to the lower reduction potential of the tungsten center [4].

These were examples of naturally occurring molybdenum enzymes substituted with tungsten. The other way around appears to be less easy, as there is so far only one example of a naturally occurring tungsten enzyme, *Pelobacter acetylenicus* acetylene hydratase, in which the metal could be successfully substituted with molybdenum [5]. The molybdenum containing enzyme exhibits 60% of the activity compared to the wild type tungsten enzyme [5]. Acetylene hydratase is also exceptional because it catalyses a non-redox reaction (the hydration of acetylene to acetaldehyde) and therefore it does not fit in either of the two classes of tungsten enzymes [6]. A very recent study reports the incorporation of molybdenum in an active glyceraldehyde-3-phosphate oxidoreductase (GAPOR) from *Methanococcus maripaludis* heterologously expressed in *E. coli* grown on molybdate supplemented media [7]. *M. maripaludis* is a mesophilic organism, whose genome contains genes encoding putative tungsten- and molybdenum formylmethanofuran dehydrogenases (MMP1249, respectively, MMP1249) [8]. Its GAPOR protein shares high homology with *P. furiosus* GAPOR in amino residues involved in pterin cofactor binding, therefore, the protein most likely contains the same unmodified bis-pterin cofactor. In that case, this is the first active enzyme of the AOR family containing molybdenum. However, it is not known if the wild- type GAPOR also contains molybdenum [7].

Tungsten metabolism in the hyperthermophilic archaeon *Pyrococcus furiosus* has been a research topic in our laboratory for many years. The growth of this anaerobic organism is strictly dependent on the presence of tungsten in the media [9]. Five tungsten containing aldehyde oxidoreductases have been purified from this organism. Aldehyde oxidoreductase (AOR) [10], formaldehyde oxidoreductase (FOR) [11], and tungsten containing oxidoreductase number 5 (WOR5) [12] all catalyze the oxidation of a wide variety of

aldehydes whereas the previously mentioned GAPOR is only known to convert the substrate glyceraldehyde-3-phosphate [13]. WOR4 was purified by monitoring column fractions of proteins that contained tungsten and no activity has been determined yet for this protein [14]. Except for GAPOR, with its assigned role in glycolysis, the physiological function of these AORs is still unknown. In addition to the five genes encoding AOR proteins, the *P. furiosus* genome encodes two putative formate dehydrogenases, which might contain either molybdenum or tungsten. So far, no physiological function has been established for molybdenum in *P. furiosus*.

Adams and coworkers have made an attempt to substitute tungsten with molybdenum and vanadium in the AOR enzymes of *P. furiosus* by growing the organism on an excess of molybdate or vanadate [15]. They purified enzymes by monitoring aldehyde oxidation activity and they subsequently determined their metal content. No incorporation of molybdenum or vanadium was detected in the AORs within the detection limits of the plasma emission spectroscopy used for the metal analysis. On the contrary, low sub-stoichiometric amounts of tungsten were found, and it was concluded that the cells had scavenged the traces of tungstate from the medium in the presence of a 1000-fold excess of molybdate or vanadate, and had used only the tungsten for incorporation in the cofactor of the AOR enzymes [15]. An inability of *P. furiosus* cells to efficiently take up the molybdate from the medium could be a possible explanation for the absence of molybdenum in the active site of the enzymes. However, more recently, a tungsten binding protein WtpA from the tungstate ABC transporter (WtpABC) from *P. furiosus* has been characterized in our laboratory and was shown to bind both oxoanions with a high affinity (chapter 2). The transporter was found to be very selective for tungstate with a K_D of 17 pM [16] but was also able to bind molybdate with a K_D of 11 nM [16]. This result would exclude the transporter system as a selective barrier in favor of tungstate over molybdate when present in a 1:1000 ratio. *P. furiosus* should be able to take up molybdate from the media with the WtpABC transporter. This was a first reason to repeat the molybdenum-substitution experiments in *P. furiosus* AOR proteins. Additionally, our laboratory developed a very sensitive method to determine sub-nanomolar concentrations of molybdenum and tungsten in protein samples [17]. This method, based on catalytic adsorptive stripping voltammetry, forms an excellent tool to measure sub-stoichiometric amounts of molybdate incorporated in proteins, and is more sensitive than the plasma emission spectroscopy that was used in previous work.

In this chapter we describe the actual incorporation of molybdenum in enzymes of the *P. furiosus* AOR family.

Materials and methods

Growth of the organism and protein purification - *P. furiosus* (DSM 3638) was grown in an 8-L fermentor at 90 °C, under anaerobic conditions with starch as carbon source as

previously described [18]. For the cells regularly grown on tungstate, the media contained 10 µM sodium tungstate and 90 nM of molybdate, the latter as a contaminant from the yeast extract and from impurities in chemicals. For the molybdate-grown cells, a pre-culture without any tungstate was required. To remove traces of tungstate present in the cells of the inoculum, which was derived from regular tungstate-grown cells, 10 subsequent pre-cultures were made in medium containing 10 nM sodium tungstate and 10 µM sodium molybdate. The final culture, which contained effectively 10 nM tungstate, was used for the inoculation of the 8-L fermentor. Completely omitting tungstate from the media does not result in growth. After inoculation of the 8-L fermentor and 18 hrs running in batch mode, the culture was switched to continuous mode with a dilution rate of 0.3 h^{-1} [19] resulting in a wet weight of approximately 2 g/l .
FOR and WOR5 were purified from 175g cells (wet weight) under anaerobic conditions at 23 °C as previously described [11,12]. All buffers were repeatedly degassed and flushed with argon and contained 1 mM cysteine to scavenge traces of O_2. Cells were broken by osmotic shock upon dilution with 5 volumes 30 mM Tris-HCl, pH 8 containing 1 mM cysteine, 5 mM $MgCl_2$, 0.1 mg/L DNase I and 0.1 mg/L RNase.

Enzyme assays - Enzyme activities were routinely assayed at 60 °C, under anaerobic conditions, with aldehyde substrate and 1 mM methylviologen as the electron acceptor in 50 mM Epps buffer, pH 8.4. As described earlier, the following substrates were used (enzyme that exhibits highest activity on the mentioned aldehyde): crotonaldehyde (AOR) [10], formaldehyde (FOR) [11], glyceraldehyde-3-phosphate (GAPOR) [13].

Determination of cellular molybdenum and tungsten concentration - The relative amount of molybdenum or tungsten associated with proteins was determined by 3kDa centricon (Millipore) filtration of the cell free extract (CFE) and subsequently measuring metal concentrations in the CFE and in the filtrate by catalytic adsorptive stripping voltammetry [17]. The CFE was obtained from 5g *P. furiosus* cells that had been washed four times with 0.5 L 0.75 M NaCl, 20 mM Tris, pH 8.

Spectroscopy - EPR redox titrations were performed at room temperature under argon in 50 mM Hepes, pH 7.5 using 4 mg/ml (58 µM of monomer) FOR. The following dyes were added to a final concentration of 50 µM: N,N,N',N'-tetramethyl-p-phenylenediamine, 2,6-dichlorophenol indophenol, phenazine ethosulfate, methylene blue, resorufine, indigodisulfonate, 2-hydroxy-1,4-naphtaquinone, anthraquinone-2-sulfonate, phenosafranin, safranin O, neutral red, benzylviologen, methylviologen. Samples were first reductively titrated with sodium dithionite followed by oxidative titration with potassium ferricyanide. After equilibration at the desired potential a 0.2 mL sample was anaerobically transferred to an EPR tube and immediately frozen in liquid nitrogen. Potentials were measured with a platinum electrode and a Ag/AgCl reference electrode. All reported values are with respect to the normal hydrogen electrode (NHE).

A substrate/product (formaldehyde/formate) titration was performed at room temperature under argon in 50 mM Hepes, pH 7.5 using the same concentration of FOR (58 µM of monomer). The protein was incubated with formaldehyde and formate at the following ratio's (calculated potential): 1:99 (-472 mV), 1:9 (-502 mV), 1:1 (-532 mV), 9:1 (-562 mV), 99:1 -592 mV). Of each potential 0,2 ml sample was transferred into an EPR tube and frozen in liquid nitrogen.
X-band EPR spectra were recorded on a Bruker ER 200D spectrometer, using facilities and data handling as detailed elsewhere [20].

Other assays - Protein concentration was determined using the bicinchoninic acid assay method with bovine serum albumin as the standard. The tungsten and molybdenum content of proteins and cell free extract samples was determined by catalytic adsorptive stripping voltammetry [17]. Subunit molecular weight and degree of protein purity were determined with SDS-polyacrylamide gel electrophoresis on a Phast System (GE Healthcare) in 8-25% SDS.

Results and discussion

Uptake of molybdate and tungstate, and cell free extract enzyme activities

Cells grown on tungstate (W cells: 10 µM tungstate, 90 nM molybdate), respectively, molybdate (Mo cells:10 µM molybdate, 10 nM tungstate) were harvested and analyzed for their cellular group-6 oxoanion content. The results (figure 1) show that *P. furiosus* cells are able to take up both oxoanions to the same extent.

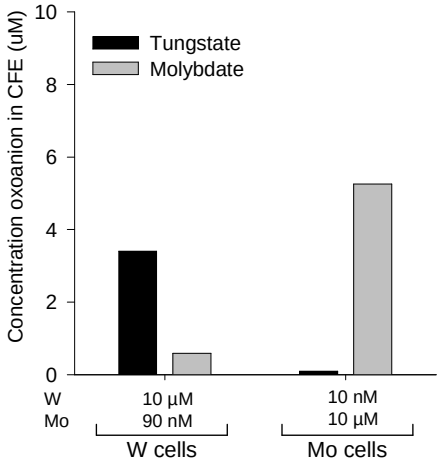

Figure 1. Molybdate and tungstate concentrations (µM) in cell-free extract of *P. furiosus* cells grown on medium containing10 µM tungstate and 90 nM molybdate (W cells) and 10 µM molybdate and 10 nM tungstate (Mo cells).

The cell-free extracts obtained from cells grown on excess of molybdate or tungstate were both examined for their total aldehyde oxidation activity using three representing substrates (formaldehyde, crotonaldehyde, and glyceraldehyde-3-phosphate) in order to estimate the levels of expression of the three most abundant and characterized aldehyde oxidoreductases in *P. furiosus*: AOR, FOR, and GAPOR (figure 2).

The results are similar as those previously reported by Adams and coworkers [15]: the specific activities of the aldehyde oxidoreductases were two or more orders-of-magnitudes lower in molybdate-grown cells, however, they were still detectable in the case of formaldehyde and crotonaldehyde oxidation. Surprisingly, no GAPOR activity could be detected although this enzyme is required for glycolysis. Formaldehyde and crotonaldehyde can serve as substrate for both FOR, AOR and WOR5, which makes it difficult to estimate expression levels of the separate enzymes on the basis of their specific activities. The formaldehyde-oxidation activity in the cell-free extract of the molybdate-grown cells was relatively higher than the oxidation activity on crotonaldehyde. Therefore, formaldehyde-oxidation activity became the target for protein purification, resulting in the isolation of FOR and WOR5 from both cell-free extracts containing both metals (table 1). The crotonaldehyde-oxidation activity co-eluted with the targeted formaldehyde-oxidation activity, suggesting that the initial activity on crotonaldehyde measured in CFE resulted from FOR and WOR5 and not from AOR [12].

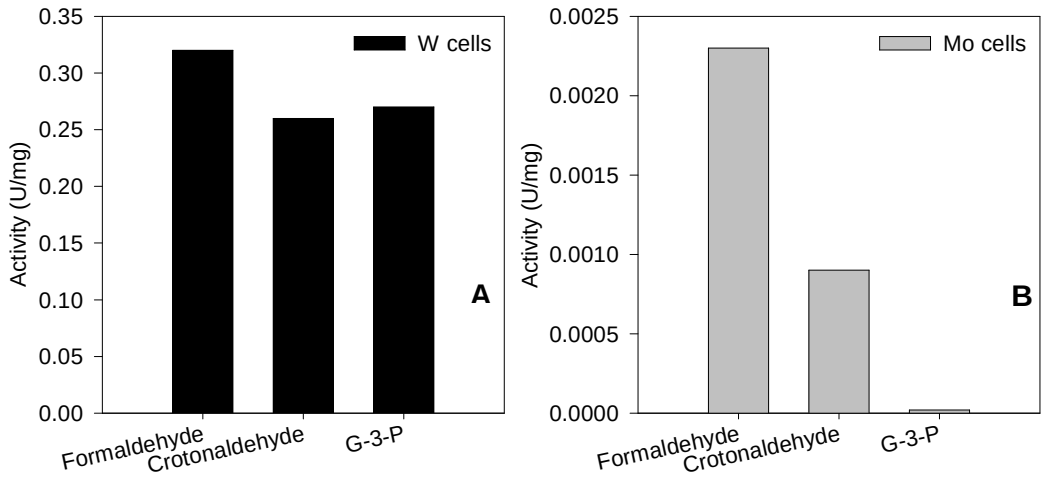

Figure 2. Specific activity of aldehyde oxidation for substrates formaldehyde, crotonaldehyde and glyceraldehyde-3-phosphate (G-3-P) in cell-free extracts of *P. furiosus* cells grown in media supplemented with tungstate (A) or molybdate (B).

Table 1. Purification table for FOR and WOR5 purified from cells grown on tungstate or molybdate. Activity (U) represents formaldehyde oxidation activity.

	CFE	Purified FOR			Purified WOR5		
Medium	**U/mg**	**U/mg**	**10^3 Mo/subunit**	**W/subunit**	**U/mg**	**Mo/subunit**	**W/subunit**
W	0.32	27	6.4	0.48	6.5	0.011	0.13
Mo	0.0023	1.25	57	0.02	0.95	0.23	0.017

Purification and activity of molybdenum and tungsten containing WOR5 and FOR

The purification table (table 1) and the data in figure 2 show a higher formaldehyde oxidation activity in the tungstate supplemented cells compared to the molybdate supplemented cells (140-fold). Also the metal content of the purified proteins varied between the two different supplementations (figure 3). Purified FOR from tungstate-grown cells exhibited a higher total metal incorporation (49% of the protein was purified in its holo-form) compared to the FOR purified from molybdate grown cells (8%). The holo-FOR isolated from the tungstate supplemented *P. furiosus* contained 99% tungsten whereas FOR purified from the molybdate supplemented cells contained 75% molybdenum (figure 3).

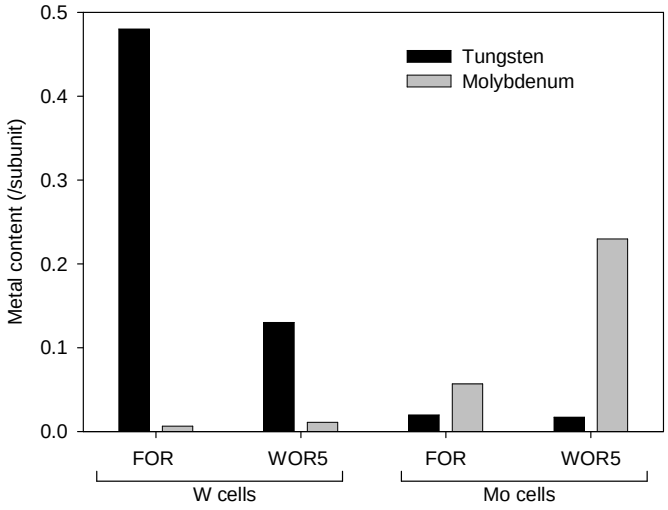

Figure 3. Metal content per subunit FOR and WOR5 isolated from *P. furiosus* cells grown on medium supplemented with tungstate or molybdate.

Surprisingly in the case of WOR5, the total metal incorporation was higher for the cells grown on molybdate: 24% of the total protein was purified containing a metal, of which 95% was molybdenum. In the tungstate supplemented cells only 15% of the WOR5 protein contained metal, most of it being tungsten (92%). In summary, both proteins were purified partly as apo-protein and partly as holo-protein containing both molybdenum and/or

tungsten. In the case of WOR5 a relatively higher molybdenum incorporation was observed compared to FOR.

It is commonly observed for these AOR enzymes that the ratio of metal per subunit is lower than the expected value of unity due to loss of the cofactor during the purification. This makes it difficult in these experiments to distinguish between apo-protein originating from a lack of molybdenum incorporation or from a loss of the metal during purification. However, it is assumed that the rate of metal-loss from the cofactor in a certain protein is independent of the incorporated metal. Therefore, we can compare the incorporation values for tungsten and molybdenum, under the different growing conditions, for the same protein.
By doing so, it can be concluded that, in cells grown on high molybdate, WOR5 has a higher tendency for molybdenum incorporation compared to FOR: in purified FOR almost no molybdenum was found (while the tungsten supplemented cells produced 49% holo-protein) whereas 23% of the WOR5 subunits actually contained molybdenum.
Correlating the specific activities of all enzyme preparations with the metal content gives an interesting and clear picture (table 2). In both enzymes and in all preparations the formaldehyde oxidation activity correlated well with the tungsten content even though in some cases the amount of incorporated tungsten was very low. From these results it can be concluded that the aldehyde oxidation is catalyzed by the enzyme that contains a tungsto-bispterin cofactor only, and that the molybdenum containing ones do not contribute to the observed activity. None of the preparations showed any activity for the reversed reaction; the reduction of the corresponding formic acid to formaldehyde (data not shown).

Table 2. Ratio of specific formaldehyde oxidation activity, ratio of incorporated tungsten per subunit, and ratio of incorporated molybdenum per subunit. The ratios were calculated from the data obtained for FOR and WOR5 preparations from the tungstate-supplemented cells versus those from the molybdate-supplemented cells.

	Specific activities		**W/ subunit**		**Mo/subunit**	
Enzyme	**FOR**	**WOR5**	**FOR**	**WOR5**	**FOR**	**WOR5**
W vs Mo	21.6	6.8	24	7.6	0.074	0.11

EPR Spectroscopy FOR

The total amount of purified WOR5 was not enough to study it with EPR spectroscopy and, therefore, EPR studies were only performed on FOR preparations containing molybdenum or tungsten. The g-values for the so called [21] mid-potential (gx = 1.922, gy = 1.942, gz = 1.973) and the low-potential (gx = 1.837, gy = 1.891, gz = 1.960) forms of tungsten-containing FOR are similar to the values reported in literature (gx = 1.926, gy = 1.946, gz = 1.977), (gx = 1.847, gy = 1.901, gz = 1.969) respectively [21]. The observation of characteristic hyperfine splitting caused by the presence of the ^{183}W isotope (nuclear spin I=1/2) further confirmed the incorporation of tungsten.

In the molybdenum-containing sample, novel signals were detected at similar potentials, therefore, they were named low and mid potential forms of molybdenum. The low potential molybdenum species was found only upon titration with the substrate formaldehyde. The maximal signal amplitude of the low potential molybdenum form was found at a potential of approximately -450 mV, similar to the potential of the maximal signal of the tungsten low potential species. The molybdenum mid-potential species was detected in a dye mediated redox titration between a potential of -250 mV to -20 mV (maximal signal around -150 mV). The g-values of these mid and low potential forms in molybdenum-containing FOR differ significantly from the ones reported for the tungsten-containing form. The overall intensity of the spectrum is also lower because of the substoichiometric incorporation of molybdenum, but comparison to simulated spectra, supports molybdenum incorporation.

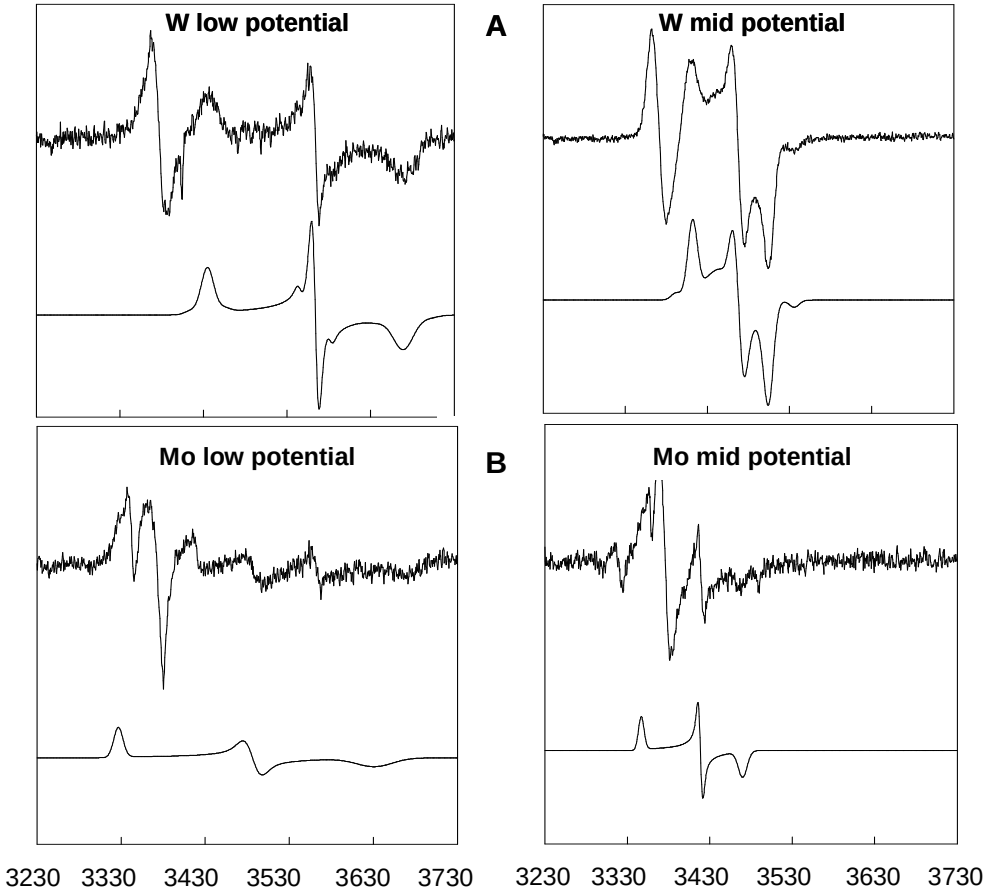

Figure 4. EPR spectra (upper line) and simulations (lower line) of mid (gx = 1.922, gy = 1.942, gz = 1.973) and low potential (gx = 1.837, gy = 1.891, gz = 1.960) tungsten signals in tungsten-containing FOR (A) and mid (gx = 1.942, gy = 1.971, gz = 2.012) and low potential (gx = 1.855, gy = 1.971, gz = 2.012) molybdenum signals in molybdenum-containing FOR (B).

Discussion and conclusion

We have shown that molybdenum can be incorporated in two enzymes of the AOR family in *P. furiosus*. The amount of incorporated molybdenum was found to be enzyme-dependent: more molybdenum was incorporated in WOR5 (0.23 Mo/subunit) than in FOR (0.06 Mo/subunit), and in AOR and GAPOR no incorporation could be detected.
By increasing the molybdate concentration in the medium by a factor of 100, the molybdate concentration in the CFE and the molybdenum incorporation in FOR increased both by a factor of 10. In WOR5, a 21-fold increase in the incorporation of molybdenum was observed, suggesting less selective metal incorporation for this enzyme.
However, *P. furiosus* is able to scavenge trace amounts of tungstate (10nM) from the molybdate supplemented medium, and to use it for the specific incorporation in the cofactor of WOR5 and FOR. It is unclear why *P. furiosus* uses the available tungsten for these two enzymes and not for AOR or GAPOR (the latter is required for glycolysis; the physiological role of the other AORs is still unknown). It would be interesting to analyze mRNA levels of *P. furiosus* cells grown on molybdate-supplemented media to verify whether the other AORs are indeed not expressed or whether their expression levels are below the detection limit of the activity measurement.
In summary, *P. furiosus* preferably uses tungstate for the incorporation of metal into the bis-pterin cofactor of the AOR enzymes. Tungsten cannot be easily replaced by molybdenum, but for some AOR enzymes it is possible to incorporate significant amount of molybdenum. However, these molybdenum containing AORs do not contribute to the observed aldehyde oxidation activity.
All these data together suggest the existence of a selective mechanism for tungsten incorporation in the pterin cofactor. Selective metal incorporation is thought to rely on the metal dependent hydrolysis of adenylylated MPT coupled to the metal insertion activity of Cnx1E (in plants) [22] or MoeA (in *E. coli*) [23]. Interestingly, two different genes for MoeA proteins are found in *P. furiosus* and a number of archaea and bacteria. It is tempting to speculate that the expression of two MoeA proteins forms the basis of metal selectivity, however, experimental data are required to corroborate this hypothesis (Chapter 4).

Acknowledgements

This research was supported by a grant from the Council for Chemical Sciences of the Netherlands Organization for Scientific Research (700.51.301).

References

[1] G. Schwarz, R.R. Mendel, Ann. Rev. Plant Biol. 57 (2006) 623.
[2] H.J. Cohen, R.T. Drew, J.L. Johnson, K.V. Rajagopalan, Proc. Natl. Acad. Sci. USA 70 (1973) 3655.
[3] L.J. Stewart, S. Bailey, B. Bennett, J.M. Charnock, C.D. Garner, A.S. McAlpine, J. Mol. Biol. 299 (2000) 593.
[4] J. Buc, C.-L. Santini, R. Giordani, M. Czjzek, L.-F. Wu, G. Giordano, Mol. Microbiol. 32 (1999) 159.
[5] M. Boll, B. Schink, A. Messerschmidt, P.M.H. Kroneck, Biol. Chem. 386 (2005) 999.
[6] R.U. Meckenstock, R. Krieger, S. Ensign, P.M.H. Kroneck, B. Schink, Eur. J. Biochem. 264 (1999) 176.
[7] M.O. Park, T. Mizutani, P.R. Jones, J. Bacteriol. (2007).
[8] A. Hochheimer, d. Linder, R.K. Thauer, R. Hedderich, Eur. J. Biochem. 242 (1996) 156.
[9] R.N. Schicho, L.J. Snowden, S. Mukund, J.B. Park, M.W.W. Adams, R.M. Kelly, Arch. Microbiol. 159 (1993) 380.
[10] S. Mukund, M.W. Adams, J. Biol. Chem. 266 (1991) 14208.
[11] R. Roy, S. Mukund, G.J. Schut, D.M. Dunn, R. Weiss, M.W.W. Adams, J. Bacteriol.181 (1999) 1171.
[12] L.E. Bevers, E. Bol, P.-L. Hagedoorn, W.R. Hagen, J. Bacteriol.187 (2005) 7056.
[13] S. Mukund, M.W.W. Adams, J. Biol. Chem. 270 (1995) 8389.
[14] R. Roy, M.W.W. Adams, J. Bacteriol.184 (2002) 6952.
[15] S. Mukund, M.W.W. Adams, J. Bacteriol.178 (1996) 163.
[16] L.E. Bevers, P.-L. Hagedoorn, G.C. Krijger, W.R. Hagen, J. Bacteriol.188 (2006) 6498.
[17] P.L. Hagedoorn, P. van't Slot, H.P. van Leeuwen, W.R. Hagen, Anal. Biochem. 297 (2001) 71.
[18] A.F. Arendsen, P.T. Veenhuizen, W.R. Hagen, FEBS Lett.368 (1995) 117.
[19] N. Raven, N. Ladwa, D. Cossar, R. Sharp, Appl. Microbiol. Biotech. 38 (1992) 263.
[20] A.J. Pierik, W.R. Hagen, Eur. J. Biochem.195 (1991) 505.
[21] E. Bol, L.E. Bevers, P.-L. Hagedoorn, W.R. Hagen, J. Biol. Inorg. Chem. 11 (2006) 999.
[22] A. Llamas, T. Otte, G. Multhaup, R.R. Mendel, G. Schwarz, J. Biol. Chem. 281 (2006) 18343.
[23] J.D. Nichols, K.V. Rajagopalan, J. Biol. Chem. 280 (2005) 7817.

Part III

Tungstoenzymes

Chapter 6

WOR5: A novel tungsten containing aldehyde oxidoreductase from *Pyrococcus furiosus* with a broad substrate specificity

Loes E. Bevers
Emile Bol
Peter-Leon Hagedoorn
Wilfred R. Hagen

Adapted from: Journal of Bacteriology 187 (2005) 7056-7061

Abstract

WOR5 is the fifth and last member of the family of tungsten containing oxidoreductases purified from the hyperthermophilic archaeon *Pyrococcus furiosus*. It is a homo-dimeric protein (subunit: 65 kDa) that contains one [4Fe-4S] cluster and one tungsto-bispterin cofactor per subunit. It has a broad substrate specificity with a high affinity for several substituted and non-substituted aliphatic and aromatic aldehydes with variable chain lengths. The highest catalytic efficiency of WOR5 is found for the oxidation of hexanal (V_{max} = 15.6 U/mg, K_M = 0.18 mM at 60 °C). Hexanal-incubated enzyme exhibits S = ½ EPR signals from $[4Fe\text{-}4S]^{1+}$ (g-values 2.08, 1.93, 1.87) and W^{5+} (g-values 1.977, 1.906, 1.855). Cyclic voltammetry of ferredoxin and WOR5 on an activated glassy carbon electrode shows a catalytic wave upon addition of hexanal, suggesting that ferredoxin can be a physiological redox partner. The combination of WOR5, FOR (formaldehyde oxidoreductase) and AOR (aldehyde oxidoreductase) forms an efficient catalyst for the oxidation of a broad range of aldehydes in *P. furiosus*.

Introduction

Pyrococcus furiosus is a strictly anaerobic, fermentative microorganism that grows optimally at 100 °C. It can use either peptides or carbohydrates as its carbon and energy source and it reduces elemental sulfur (S^0) to H_2S if present. The growth of *P. furiosus* is strictly dependent on the presence of tungsten [1]. Four tungsten enzymes have previously been purified from this organism, all of which are members of the aldehyde oxidoreductase (AOR) family. Complete genome analysis has revealed the presence of a gene encoding a putative fifth member of this family and two genes for two more W or Mo-enzymes assigned as putative formate dehydrogenases.

Three of the four AOR family enzymes have been purified and characterized in some detail: aldehyde ferredoxin oxidoreductase (AOR) [2], glyceraldehyde-3-phosphate ferredoxin oxidoreductase (GAPOR) [3] and formaldehyde ferredoxin oxidoreductase (FOR) [4]. AOR has a broad substrate specificity but appears to be most active on aldehydes derived from amino acids [2]. FOR has the highest activity on C1-C3 aldehydes [4], and both AOR and FOR are thought to play a role in peptide fermentation. In contrast, GAPOR is only known to convert the substrate glyceraldehyde-3-phosphate (GAP-3). It functions in glycolysis where it converts GAP-3 to 3-phosphoglycerate replacing glyceraldehyde-3 phosphate dehydrogenase and phosphoglycerate kinase in the unusual Emden-Meyerhof glycolysis [3].

A fourth tungsten-containing enzyme, WOR4, was more recently purified from *P. furiosus* grown in the presence of S^0 [5]. No activity could be identified yet, but the protein may play a role in S^0 reduction because it could not be purified in the absence of S^0 in the growth medium. From micro-array analysis it is known that the expression of WOR4 at the mRNA level is upregulated in cold-adapted cells that were grown for generations at 72 °C. Cells that were incubated for shorter periods at 72 °C (1-5 hours) showed a five-fold increase in the expression of the putative fifth tungsten containing enzyme WOR5 [6]. Also the adjacent ORF PF1479, coding for a 19 kDa protein with 16 cysteine residues that could bind multiple iron sulfur clusters, is upregulated to the same order of magnitude. This suggests a co-regulation of both proteins. The presence of four possible iron sulfur clusters in this protein associated with WOR5, indicates a role in electron transfer for the 19 kDa protein similar to the role of ferredoxin in the reactions catalysed by the other enzymes from the AOR family.

In the present study we describe the purification and characterization of WOR5. This enzyme was discovered in a side fraction during a standard FOR purification. During this purification all fractions were examined for formaldehyde and crotonaldehyde oxidation activity, to discriminate between fractions that contain FOR or AOR. Some fractions showed an unexpected ratio for these two activities. Further examination has lead us to the identification of WOR5 as a fifth aldehyde oxidoreductase with very broad substrate specificity.

Materials and methods

Growth of the organism and protein purification - *P. furiosus* (DSM 3638) was grown in an 8-L fermentor at 90 °C, under anaerobic conditions with starch as carbon source as previously described [7]. After 18 hrs running in batch mode, the culture was switched to continuous mode with a dilution rate of 0.3 h^{-1} [8] resulting in a wet weight of approximately 2 g/l. WOR5 was purified from 100 g cells (wet weight) under anaerobic conditions at 23 °C. All buffers were repeatedly degassed and flushed with argon and contained 1 mM cysteine to scavenge traces of O_2. Cells were broken by osmotic shock upon dilution with 5 volumes 30 mM Tris-HCl, pH 8 containing 1 mM cysteine, 5 mM $MgCl_2$, 0.1 mg/L DNase I and 0.1 mg/L RNase. Cell-free extract was loaded on a column of DEAE (Vc = 300 ml) fast flow sepharose, equilibrated with 20 mM Tris-HCl, pH 8. WOR5 eluted from the column between 175 and 270 mM NaCl with a gradient (1400 ml) from 0 to 500 mM NaCl. Fractions with WOR5 activity were combined and loaded onto a hydroxyapatite column (Vc = 120 ml) equilibrated with 5 mM potassium phosphate buffer, pH 7.5. WOR5 eluted from the column as 110 to 270 mM potassium phosphate was applied, using a gradient from 5 to 300 mM potassium phosphate in 500 ml. Fractions containing WOR5 activity were pooled and concentrated by ultrafiltration using an Amicon PM-30 membrane. The concentrated sample of WOR5 was applied to a Superdex-200 column (Vc = 320 ml), equilibrated with 20 mM Tris-HCl, pH 8, and 150 mM NaCl. Fractions containing WOR5 were combined, concentrated and washed to a maximal salt concentration of 50 mM NaCl before application to a Mono-Q column (Vc = 1 ml) equilibrated with 20 mM Pipes, pH 6.8. WOR5 eluted from the column at 72 to 85 mM NaCl using a gradient (60 ml) from 70 to 200 mM NaCl.

Enzyme assays - WOR5 activity was routinely assayed at 60 °C, under anaerobic conditions, with 5 mM hexanal as the substrate and 1 mM methylviologen as the electron acceptor in 50 mM Epps buffer, pH 8.4. Hexanal and other tested aldehydes were added to the assay mixture as a solution in 100% ethanol. The activities of AOR, GAPOR and FOR were determined as previously described [2-4]. The specific activities are on the basis of protein concentration.

Other assays - Protein concentration was determined using the bicinchoninic acid assay method with bovine serum albumin as the standard. The tungsten content of the purified WOR5 protein was determined by catalytic adsorptive stripping voltammetry [9]. Subunit molecular weight and degree of purity was determined with SDS-polyacrylamide gel electrophoresis on a Phast System (GE Healthcare) in 8-25% SDS. Iron and acid-labile sulfur were determined colorimetrically according to [10,11]. Metal analysis was carried out by diluting the protein sample up to a volume of 1.5 ml (0.2 % HNO_3) and introducing it in an inductively coupled plasma optical emission spectrometer (ICP-OES) Optima 4300 DV (Perkin Elmer, Norwalk, USA). Total element content was determined at 280.271 nm (Mg)

and 393.366 nm (Ca). Standard calibration curves between 0 and 1 mg/L were measured immediately after the sample and were used for final calculations.

Cyclic voltammetry - Cyclic voltammograms of *P. furiosus* ferredoxin and WOR5 were recorded with an Autolab PSTAT10 potentiostat. The electrochemical experiments were performed with a three electrode microcell using the method previously described [12]. The working electrode was a nitric acid activated glassy carbon disc. A micro platinum electrode was used as counter electrode and the potential was measured with reference to an Ag/AgCl electrode. A droplet with a volume of 25 µl containing 50 µM of ferredoxin in 25 mM Mops buffer, pH 7.2 and 7 mM of neomycin was placed on the working electrode. WOR5 was added to a final concentration of 5 µM and hexanal was added to a final concentration of 50 mM. The voltammograms were recorded at a scan rate of 10 mV/s at 60 °C.

Spectroscopy - X-band EPR spectra were recorded on a Bruker ER 200D spectrometer, using facilities and data handling as detailed elsewhere [13]. For the reduction of enzyme with substrate, a sample of WOR5 (120 µM) was incubated with hexanal (10 mM) for up to one hour at 60 °C. The UV-vis spectrum was recorded with a Hewlett Packard 8452A diode array spectrophotometer.

Results and discussion

Purification of WOR5

WOR5 was purified from cell free extract of *P. furiosus* by monitoring the ability of column fractions to catalyse the hexanal-dependent reduction of methylviologen. Cell free extract contained 0.36 U/mg of hexanal oxidizing activity (Table 1) and this is of the same order as the oxidizing activity of formaldehyde (0.34 U/mg) and crotonaldehyde (0.55 U/mg).

Table 1. Purification table of WOR5 from *P. furiosus*

	Protein (mg)	Activity (U)	Sp act (U/mg)	Recovery (%)	Purification (fold)
CFE	3394	1219	0.36	100	1
DEAE	1454	1202	0.83	99	2.3
HAP	411	811	1.97	67	5.5
SD-200	46	480	10.3	39	29
Mono-Q	5.3	83	15.6	6.8	43

FOR and AOR (not GAPOR) are also able to catalyse the oxidation of hexanal although at a much lower rate (Table 2). Therefore, the apparent WOR5 activity observed in the cell free extract is the sum of the hexanal oxidizing activities of FOR, AOR and WOR5. The specific

activities of FOR and AOR for the oxidation of hexanal were used in combination with the measured activity on formaldehyde and crotonaldehyde, to identify the presence of the three enzymes in fractions eluting from the columns. After the first DEAE column FOR (eluting at 100 mM NaCl) was readily separated from AOR and WOR5, and after the HAP column also AOR (7 mM KP_i) and WOR5 (110 mM KP_i) could be separated.
Approximately 5 mg of WOR5 was purified from 100 g wet weight of frozen *P. furiosus* cells. For comparison, the estimated yields of AOR, FOR, GAPOR and WOR4 per 100 g of cells are 23, 12, 6, and 2.5 mg, respectively [5].

Table 2. Specific activity of AOR, FOR and WOR5 for the oxidation of aldehydes, determined at 80 °C and with methylviologen as electron acceptor unless indicated otherwise.

Enzyme	Formaldehyde (50 mM) (U/mg)	Crotonaldehyde (0.2 mM) (U/mg)	Hexanal (5 mM) (U/mg)
AOR	9.2[a] (65 °C)	54[a]	3.1[c]
FOR	24[b]	0.59[b] (50 mM)	0.48[c]
WOR5	11.4[c]	0.93[c] (25 mM)	38[c]
WOR5 (60 °C)	4.7[c]	0.38[c] (25 mM)	15.6[c]

a) Determined by Mukund et al [2]
b) Determined by Roy et al [4]
c) This work

Molecular properties of WOR5

Purified WOR5 gave a single band in SDS-PAGE electrophoresis that corresponded to a molecular weight of 67 +/- 2 kDa (figure 1). The apparent molecular weight as determined by native PAGE was 135 +/- 5 kDa, suggesting that the enzyme is a homodimer (data not shown). The presence of a single subunit was confirmed by N-terminal sequence analysis, which resulted in a single sequence (MYAYNGKLLDVDLTREKVKEV) that matched for 100% with the N-terminus of ORF (PF1480, *wor5*) in the genome sequence of *P. furiosus*.

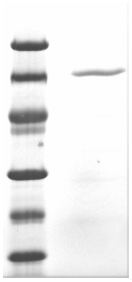

Figure 1. SDS-PAGE of purified WOR 5, lane 1: Low molecular weight markers from top: 94, 67, 43, 30, 20,14 kDa, lane 2: purified WOR 5.

The ORF *wor5* encodes a 64.9 kDa protein based on deduced amino acid sequence, which is in good agreement with experimental data (67 kDa). WOR5 has a high sequence identity with the other four members of the family: AOR (30%), FOR (34%), GAPOR (27%), and WOR4 (31%).

Purified WOR5 contained 0.13 +/- 0.05 g-atom of tungsten, 0.7 g-atom of magnesium, 1.4 g-atom of calcium, 2.8 +/- 0.3 g-atom of acid-labile sulfur and 3.0 +/- 0.1 g-atom of iron per g-atom subunit. Based on the translated protein sequence of WOR5 and its homology to the other members of the family, one [4Fe-4S] cluster and one tungsto-bispterin centre per subunit are expected for WOR5. The experimentally determined 0.13 g-atom of tungsten per subunit is perhaps due to loss of the cofactor during the purification.

Spectroscopy

The as-isolated WOR5 enzyme was EPR silent. Incubation with 10 mM hexanal substrate for one hour at 60 °C resulted in partial reduction of the prosthetic groups showing up as W(V) and $[4Fe\text{-}4S]^{1+}$ in the EPR as shown in Fig 2. At low temperature, 15 K, the spectrum was dominated by the iron-sulfur cluster; weak features of the partially saturated and overmodulated tungsten signal were also detected.

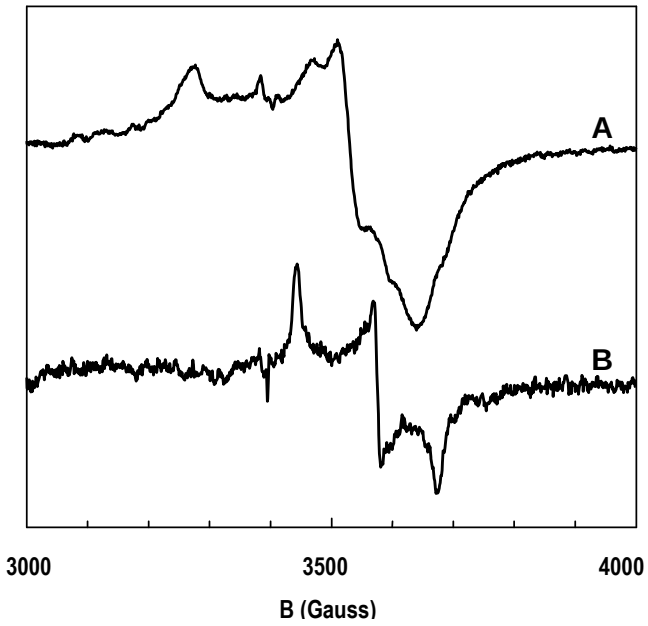

Figure 2. EPR spectra of the tungsten centre and the iron-sulfur cluster in substrate-reduced WOR5. The enzyme, 8 mg/ml, was incubated with 10 mM hexanal for 1 hour at 60 °C. Trace A is a low temperature spectrum (15 K) dominated by the signal from the $[4Fe\text{-}4S]^{1+}$ cluster; trace B is a high temperature spectrum (50 K) from W(V) in tungsto-bispterin. EPR conditions: microwave frequency, 9533 MHz; microwave power, 50 (A) and 200 (B) mW; modulation frequency, 100 kHz; modulation amplitude, 6.3 (A) and 3.2 (B) Gauss.

The iron-sulfur signal had approximate g-values 2.08, 1.93, 1.87, however, the spectral shape was rather broad and exhibited small extra peaks perhaps as the result of magnetic interaction. Possible origins of dipolar interaction are coupling between two cubanes of a protein dimer or coupling between a cubane and high-spin W(IV) within a subunit. No high-spin signals were detected suggesting that the cluster was purely S=1/2. In GAPOR [14] and FOR (our unpublished observation), the $[4Fe\text{-}4S]^{1+}$ cluster exists as a mixture of a S=1/2 and a S=3/2 ground state, and the cubane in AOR has been found to occur essentially only in the high spin state [15]. In oxidized WOR4 an unusual signal was assigned to a HiPIP-type of $[4Fe\text{-}4S]^{3+}$ -cluster [5].

Increasing the temperature from 15 K to 30 K resulted in the virtual broadening away of the iron-sulfur signal consistent with it being from a $[4Fe\text{-}4S]^{1+}$ cluster (not shown). A further increased to 50 K affords a single S=1/2 signal of W(V), which was non-saturable with microwave powers up to 200 mW. The g-values were 1.977, 1.906, 1.855. A ^{183}W hyperfine interaction (14.4% ; I=1/2) of approximate strength A ≅ 40 Gauss in all directions is just detectable as shoulders in figure 2B. Spin quantitation gave 0.45 spins per monomer of WOR5 for the cubane and 0.07 spins for W(V). The g-values of the tungsten signal are comparable to the g-values found for a tungsten signal at low redox potential in AOR (1.989, 1.901, 1.863, [15]). These comparable g-values indicate that the tungsten ion is present in a similar coordination in the bispterin cofactor. The tungsten signal at low redox potential in GAPOR has significantly lower g-values (1.948, 1.887, 1.831 [14]). In the EPR spectrum of WOR4 no tungsten signal could be detected [5].

The optical spectrum of WOR5 as isolated (see figure 3) shows a protein peak at 280 nm and a broad feature with a maximum at *circa* 390 nm, characteristic for iron-sulfur clusters of higher nuclearity such as cubanes. A shoulder is observed at approximately 320 nm. Extinction coefficients of ε_{390}=1.15 $mM^{-1}cm^{-1}$ and ε_{280}=6.44 $mM^{-1}cm^{-1}$ were determined from the UV-vis spectrum of WOR5 defining a purity index of A_{390}/A_{280} = 0.18.

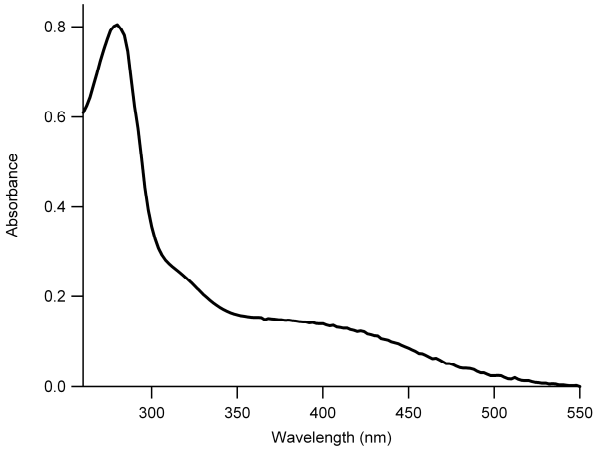

Figure 3. UV-vis absorption spectrum of *P. furiosus* WOR5. The protein concentration was 8 mg/ml in 20 mM Tris, pH 8.

Catalytic properties of WOR5

The enzyme was purified by monitoring the ability of fractions to catalyse the oxidation of hexanal and the reduction of methylviologen. In addition to hexanal WOR5 was able to utilize a range of aliphatic and aromatic aldehydes as substrates summarized in Table 3. The specific activity and K_M values were obtained by measuring the activity with methylviologen as electron acceptor at 60 °C at three different aldehyde concentrations (0.5, 5, 25 mM) in duplo, and fitting a Michaelis-Menten curve. The substrates can be divided in three classes based on K_M values. K_M < 0.5 mM was found for aldehydes where the carbonyl is attached to an aliphatic C atom. The degree of substitution of this beta C atom does not significantly influence the affinity or activity neither does the size of the aldehyde or the length of the side chain. The aromatic aldehydes with the carbonyl group directly attached to the phenyl-ring had K_M values between 1 and 5 mM. Crotonaldehyde and formaldehyde (both approximately K_M = 45 mM) were only oxidized at high concentrations. These activities and K_M values reflect a clear difference in substrate specificity between WOR5 and the other tungsten containing aldehyde oxidoreductases (Table 2). In its broad substrate specificity WOR5 clearly distinguishes itself from FOR and GAPOR, and the main difference between WOR5 and AOR is the low activity and affinity of the former for crotonaldehyde, which is one of the best substrates for AOR.

Table 3. Oxidation of aldehydes by WOR5 at 60 °C and methylviologen as electron acceptor. Substrate concentrations of 0.5, 5 and 25 mM were used to determine Michaelis constants unless indicated otherwise.

Substrate	V_{max} (U/mg)	K_M (mM)
Formaldehyde [b]	8.5 ± 1.0	45 ± 12
Crotonaldehyde [b]	1.1 ± 0.1	46 ± 6
Acetaldehyde [b]	0.34 ± 0.05	1.5 ± 0.2
Glutaraldehyde [a]	1.4 ± 0.1	9.4 ± 0.2
2-Methoxybenzaldehyde	15.1 ± 0.6	4.8 ± 0.6
Cinnamaldehyde	7.4 ± 1.6	1.6 ± 0.1
2-Naphthaldehyde(β)	7.7 ± 0.8	1.3 ± 0.1
Hexanal [a]	15.6 ± 1.8	0.18 ± 0.02
Hydratropaldehyde [a]	9.3 ± 0.7	0.12 ± 0.04
3-Phenylbutyraldehyde [a]	8.0 ± 0.6	0.42 ± 0.12
2-Ethylhexanal [a]	8.3 ± 1.5	0.17 ± 0.02
Isobutyraldehyde	11.8 ± 0.9	0.79 ± 0.03
2-Methylbutyraldehyde	7.7 ± 0.4	0.43 ± 0.09
2-Methylvaleraldehyde	12.7 ± 1.3	0.27 ± 0.03
Glyceraldehyde-3-phosphate	0.0	-

a) Substrate concentrations of 0.05, 0.5 and 5 mM were used to determine Michaelis constants. Higher concentrations caused solubility problems.
b) Substrate concentrations of 5, 25, 50 and 100 mM were used to determine Michaelis constants.

The temperature dependence of the specific activity of WOR5 for the oxidation of hexanal was determined from 30 °C to 100 °C (figure 4). Up to 80 °C the activities were fitted with an Arrhenius equation that describes reaction rate as a function of temperature. The maximum specific activity was measured at 80 °C. At temperatures higher than 80 °C the specific activity rapidly decreased in time, probably due to instability of the protein.

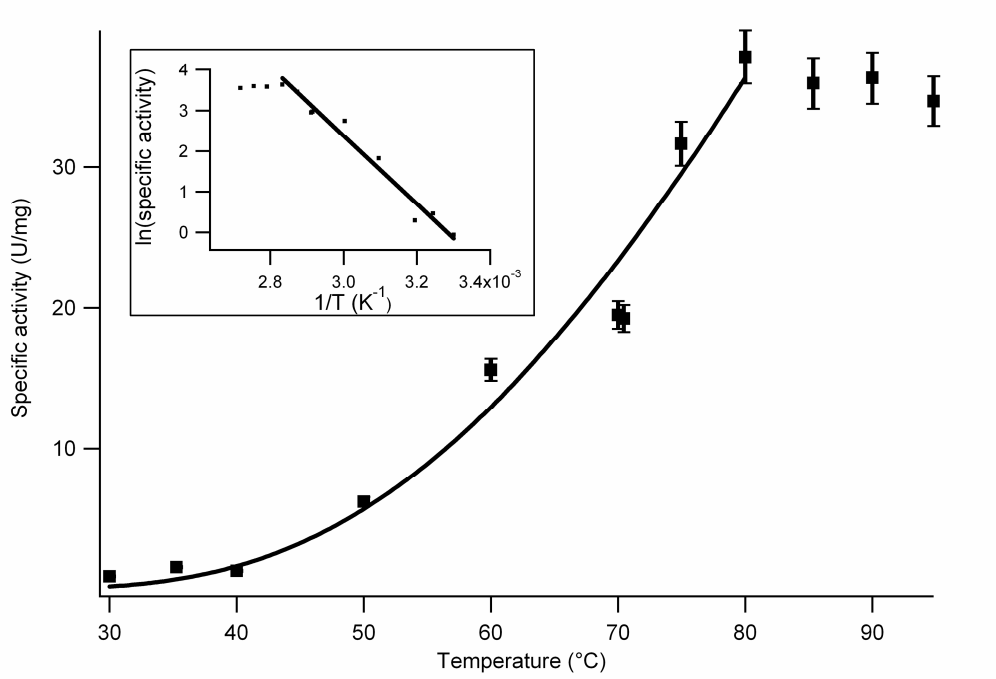

Figure 4. Temperature dependence of the hexanal oxidizing activity of WOR5. Activities have been fitted to the Arrhenius equation with an activation energy $E_a = 70 \pm 7$ kJ/mol.

In vitro reconstitution of electron transfer chain

The cyclic voltammogram of *P. furiosus* ferredoxin shows a reversible electron transfer between the ferredoxin and the activated glassy carbon electrode (figure 5) as observed earlier [14]. Addition of WOR5 or hexanal separately did not significantly change the voltammogram of ferredoxin. However, when hexanal plus WOR5 was added at 60 °C a catalytic wave appeared, showing that the enzyme is able to oxidize hexanal and transfer the electrons through the ferredoxin to the electrode. These results suggest that ferredoxin can be a physiological redox partner of WOR5 as for the other enzymes from the AOR family. However, the ORF PF1479 next to *wor5* on the genome encodes a protein with multiple iron-sulfur cluster binding motifs, which could also function as physiological partner protein.

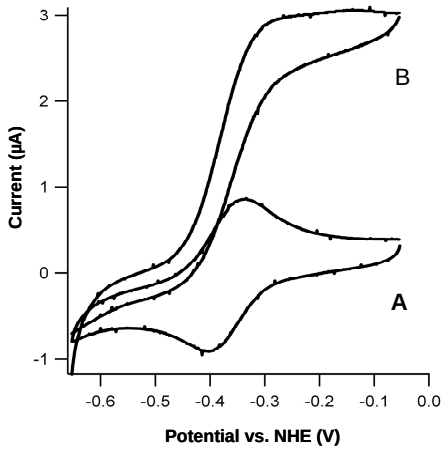

Figure 5. Cyclic voltammogram of *P. furiosus* ferredoxin in the presence of WOR5 without (A) and with hexanal at 60 °C (B). The droplet volume was 25 µl and contained 25 mM Mops buffer, pH 7.2, 7 mM neomycin, 50 mM ferredoxin, 5 µM WOR5 and 50 mM hexanal. The potential scan rate was 10 mV/s.

Sequence comparisons

A BLAST search [16] of the sequences of the aldehyde oxidoreductases from *P. furiosus* against the genomes of two other *Pyrococcus* species: *Pyrococcus horikoshii* [17] and *Pyrococcus abyssi* (http://www.genoscope.cns.fr/pab/) identifies homologs for AOR, FOR, GAPOR and FOR (Table 4). These four proteins all have homologs with sequence identities greater than 73%. All species have a putative fifth oxidoreductase, but these are mutually not very similar. In *P. horikoshii* there appear to be two additional proteins, but their genes are adjacent on the genome and probably form an αα' dimer and can therefore be considered as one protein. In Table 4, these fifth aldehyde oxidoreductases are compared with WOR5 to visualize the low homology between these enzymes and WOR5. In fact this fifth putative aldehyde oxidoreductase in both *P. horikoshii* and *P. abyssi* has more homology with *P. furiosus* AOR (approximately 40% sequence identity). From this genome comparison we can conclude that WOR5 is the only *P. furiosus* oxidoreductase that has no true homolog in one of the other *Pyrococcus* species. There are also no true homologues (identity greater than 40%) identified when the sequence of WOR5 is blasted against all the genomes collected in the Expasy database (http://www.expasy.org/tools/blast/).

Another remarkable feature of WOR5 is the sequence of its [4Fe-4S] binding motif. The motifs in FOR, AOR GAPOR all contain four cysteine residues ($Cxx(x)CxxxCx_nC$) that coordinate the [4Fe-4S] cluster. Only the last three are conserved in the sequence of WOR5, which could imply the presence of a [3Fe-4S] cluster. However, the EPR spectrum of WOR5 exhibits a clear signal of a $[4Fe\text{-}4S]^{1+}$ cubane cluster. Instead of the first cysteine there is an aspartate residue in the sequence of WOR5. Replacement of cysteine by an aspartate ligand was earlier observed in *P. furiosus* proteins namely the second cysteine of

the [4Fe-4S] cluster of ferredoxin [18] and the first cysteine of the [2Fe-2S] cluster in sulfide dehydrogenase (or ferredoxin:NAPD oxidoreductase) [19].

Table 4. Homolog genes of the five oxidoreductases from *P. furiosus* present in the genome sequences of *P. horikoshii* [17] and *P. abyssi* (http://www.genoscope.cns.fr/pab/) expressed as percentage of sequence identity between the deduced amino acid sequences of the genes.

P. furiosus	*P. horikoshii* Identity (gene)		*P. abyssi* Identity (gene)	
AOR	77%	(PH1019)	77%	(PAB0647)
FOR	88%	(PH1274)	88%	(PAB0798)
GAPOR	80%	(PH0457)	80%	(PAB1315)
WOR4	73%	(PH0028)	76%	(PAB2330)
WOR5	37%	(PH0891)	37%	(PAB2085)
	26%	(PH0892)		

Concluding remarks

With the purification of the fifth and presumably last member of the tungsten containing family of oxidoreductases from *P. furiosus*, a next challenge will be to elucidate their functions and mutual relations. It is an intriguing question why the cell needs at least four aldehyde oxidoreductase enzymes with relatively broad substrate specificities, expressed under similar conditions.

Acknowledgements

We thank Nahid Hasan for supplying the *P. furiosus* ferredoxin and Gerard Krijger of the Department of Radiation, Radionuclides and Reactors at the Delft University of Technology for performing the ICP-OES analysis. This research was supported by a grant from the Council for Chemical Sciences of the Netherlands Organization for Scientific Research (700.51.301).

References

[1] R.N. Schicho, L.J. Snowden, S. Mukund, J.B. Park, M.W.W. Adams, R.M. Kelly, Arch. Microbiol. 159 (1993) 380.
[2] S. Mukund, M.W. Adams, J. Biol. Chem. 266 (1991) 14208.
[3] S. Mukund, M.W.W. Adams, J. Biol. Chem. 270 (1995) 8389.
[4] R. Roy, S. Mukund, G.J. Schut, D.M. Dunn, R. Weiss, M.W.W. Adams, J. Bacteriol. 181 (1999) 1171.
[5] R. Roy, M.W.W. Adams, J. Bacteriol.184 (2002) 6952.
[6] M.V. Weinberg, G.J. Schut, S. Brehm, S. Datta, M.W.W. Adams, J. Bacteriol.187 (2005) 336.
[7] A.F. Arendsen, P.T. Veenhuizen, W.R. Hagen, FEBS Lett. 368 (1995) 117.
[8] N. Raven, N. Ladwa, D. Cossar, R. Sharp, Appl. Microbiol. Biotech..38 (1992) 263.
[9] P.L. Hagedoorn, P. van't Slot, H.P. van Leeuwen, W.R. Hagen, Anal. Biochem. 297 (2001) 71.
[10] P.E. Brumby, R.W. Miller, V. Massey, J. Biol. Chem. 240 (1965) 2222.
[11] A.J. Pierik, R.B. Wolbert, P.H. Mutsaers, W.R. Hagen, C. Veeger, Eur. J. Biochem. 206 (1992) 697.
[12] W.R. Hagen, Eur. J. Biochem. 182 (1989) 523.
[13] A.J. Pierik, W.R. Hagen, Eur. J. Biochem. 195 (1991) 505.
[14] P.L. Hagedoorn, J.R. Freije, W.R. Hagen, FEBS Lett. 462 (1999) 66.
[15] B.P. Koehler, S. Mukund, R.C. Conover, I.K. Dhawan, R. Roy, M.W.W. Adams, M.K. Johnson, J. Am. Chem. Soc. 118 (1996) 12391.
[16] S.F. Altschul, T.L. Madden, A.A. Schaffer, J. Zhang, Z. Zhang, W. Miller, D.J. Lipman, Nucl. Acids Res. 25 (1997) 3389.
[17] Y. Kawarabayasi, M. Sawada, H. Horikawa, Y. Haikawa, Y. Hino, S. Yamamoto, M. Sekine, S.-I. Baba, H. Kosugi, A. Hosoyama, Y. Nagai, M. Sakai, K. Ogura, R. Otsuka, H. Nakazawa, M. Takamiya, Y. Ohfuku, T. Funahashi, T. Tanaka, Y. Kudoh, J. Yamazaki, N. Kushida, A. Oguchi, K.-I. Aoki, T. Yoshizawa, Y. Nakamura, F.T. Robb, K. Horikoshi, Y. Masuchi, H. Shizuya, H. Kikuchi, DNA Res. 5 (1998) 55.
[18] L. Calzolai, C.M. Gorst, Z.-H. Zhao, Q. Teng, M.W.W. Adams, G.N. La Mar, Biochemistry 34 (1995) 11373.
[19] W.R. Hagen, P.J. Silva, M.A. Amorim, P.L. Hagedoorn, H. Wassink, H. Haaker, F.T. Robb, J. Biol. Inorg. Chem. 5 (2000) 527.

Chapter 7

Cellular localization and quaternary structure of WOR5

Loes E. Bevers
Nicolette Broers
Wilfred R. Hagen

Abstract

The hyperthermophilic archaeon *Pyrococcus furiosus* expresses five tungsten containing aldehyde oxidoreductases (AORs) of which at least four catalyze the oxidation of aldehydes (the activity of tungsten containing oxidoreductase number four (WOR4) is yet to be determined). They are able to transfer electrons from the substrate to the small, iron sulfur cluster containing protein ferredoxin. The AORs are monocistronic except for tungsten-containing oxidoreductase number five (WOR5), which is the only member of this family that has an adjacent gene (PF1479) encoding a putatively four [4Fe-4S] cluster binding protein, whose expression is fully co-regulated with the expression of WOR5 (Weinberg et al, 2005, J. Bact. 187, 336-348). A structural homology model of this PF1479 protein revealed a high structural similarity with iron-sulfur binding subunits of periplasmic molybdopterin containing proteins like *E. coli* formate dehydrogenase and periplasmic nitrate reductase. Based on these findings, a heterotetrameric structure for WOR5-PF1479 ($\alpha_2\beta_2$) is proposed. The β-subunit of this complex (PF1479) was cloned and expressed in *E. coli* as insoluble protein aggregate. EPR studies indicated the presence of [4Fe-4S] cluster(s) in the aggregated, non soluble protein fractions. Whole cell activity assays, based on the membrane permeability of different viologens, indicated a periplasmic localization of this WOR5-PF1479 complex in contrast to a cytoplasmic location of the other AORs.

Introduction

Pyrococcus furiosus is a hyperthermophilic archaeon, whose growth is fully dependent on the presence of tungstate. It uses the tungstate to incorporate tungsten into the active site of five aldehyde oxidoreductase (AOR) enzymes, which altogether comprise approximately 5% of the total cellular protein content. The complete AOR family from *P. furiosus* has been purified and characterized: aldehyde ferredoxin oxidoreductase (AOR) [2], glyceraldehyde-3-phosphate ferredoxin oxidoreductase (GAPOR) [3], formaldehyde ferredoxin oxidoreductase (FOR) [4], tungsten-containing oxidoreductase number four WOR4 [5], and most recently tungsten oxidoreductase number five (WOR5) [6]. Characteristic for these AORs is that they have broad, overlapping substrate specificities (table 1) except for GAPOR (which only converts glyceraldehyde-3-phosphate [3]), and WOR4 (for which no activity could be determined yet [5]).

Table 1. Specific activity of AOR, FOR and WOR5 for the oxidation of aldehydes (formaldehyde (50mM), crotonaldehyde (0.2mM), hexanal (5mM) and glyceraldehyde-3-phosphate (0.4mM)) , determined at 80 °C and with methylviologen as electron acceptor.

Enzyme	Formaldehyde (U/mg)	Crotonaldehyde (U/mg)	Hexanal (U/mg)	Glyceraldehyde-3-Phosphate (U/mg)
AOR	9.2[a] (65 °C)	54[a]	3.1[c]	0
FOR	24[b]	0.59[b] (50 mM)	0.48[c]	0
WOR5	11.4 [c]	0.93 [c] (25 mM)	38[c]	0
GAPOR	0	0	0	90[d]

a) Determined by Mukund et al [2]
b) Determined by Roy et al [4]
c) Determined by Bevers et al [6]
d) Determined by Mukund et al [7]

They all carry a non-nucleotide-modified tungsto-bispterin cofactor and are able to use ferredoxin as electron acceptor *in vitro* (not shown for WOR4). *In vivo*, the reduced ferredoxin is thought to serve as an electron donor for a transmembrane hydrogenase [8] and, in this way, contribute to the generation of a proton gradient that drives an ATP-synthase [9].

The physiological function of these AORs is still unknown. They are able to produce reducing equivalent in the form of reduced ferredoxin from aldehyde oxidation, but this is not likely to be their main function, since the amount of aldehydes is not expected to be sufficient to justify the large quantity of AORs present in the cell. Micro-array experiments have shown that mRNA levels of AORs are up-, or down-regulated during growth on peptides and maltose (WOR4, FOR and GAPOR) [10] and during cold shock stress experiments (WOR5, WOR4, AOR) [1]. Therefore, it is speculated that they play a role in peptide fermentation and/or stress response.

WOR5 distinguishes itself from the others in a special feature: it has an adjacent ORF (PF1479) on the genome, which is up- and down regulated in the same order of magnitude, suggesting a co-regulation of both proteins [1]. Interestingly, this PF1479 gene encodes a 19 kDa protein with 16 cysteine residues which are, based on protein sequence patterns, predicted to bind multiple iron sulfur clusters. The putative presence of four iron sulfur clusters strongly indicates a role for this protein in electron transfer, possibly similar to the role of the single-cubane ferredoxin in the reactions catalyzed by the other enzymes from the AOR family, none of which have a PF1479-like adjacent gene.
This chapter describes (i) an attempt to express and characterize the PF1479 gene product in *E. coli*, (ii) a sequence and structural homology study on PF1479 and WOR5 suggesting a heterotetrameric complex as native structure, and (iii) experimental evidence indicating a periplasmic cellular localization of this complex.

Materials and methods

Cloning, expression and purification of PF1479 – The gene PF1479 (*P. furiosus*) was amplified by PCR using *Pfx* polymerase (Invitrogen) and chromosomal DNA from *P. furiosus* as the template. Extraction of the chromosomal DNA was performed with phenol/chloroform/isoamylalcohol. PCR products were treated with *Taq* polymerase (Amersham Bioscience) for 10 min at 72 °C to obtain single 3'adenine overhangs for sub-cloning into the pCR®2.1-TOPO® vector (Invitrogen). The TOPO-construct was transformed into competent *E. coli* TOP10 cells (Invitrogen), the plasmid was isolated and after sequencing a positive fragment was cloned into the *Nde1* and *BamH1* sites of the pET15b (Novagen), resulting in a PF1479 fusion protein with an N-terminal his-tag. This construct was transformed into competent *E. coli* TP1000 cells for protein expression. These TP1000 cells containing pET15b-PF1479 were grown aerobically in L-broth or T-broth medium containing 100 µg/ml ampicillin. Protein synthesis was induced with an IPTG concentration ranging from 25 µM to 0.5 mM at an OD_{600} of 0.5. Cells were induced for 3, 5 or 18 hours at varying temperatures (16, 20, 25, 30 or 37 °C), harvested by centrifugation, washed with buffer A (20 mM Tris-HCl, pH 8.0, 10% glycerol and 250 mM NaCl) and lysed in the same buffer A (1 g of cells per 5 ml buffer) using a cell disruptor system (Constant systems). Cell-free extract was separated from the pellet (cell debris and inclusion bodies containing aggregated enzyme) and membranes by centrifugation for 20 min at 15.000 x g at 4 °C. The aggregated protein was solubilised under denaturing conditions in buffer B (20 mM Tris, pH 10.5, 4 M urea, 25 mM dithiotreitol (DTT)) and analysed with SDS-polyacrylamide gel electrophoresis on a Phast System (GE Healthcare) in 8-25% SDS.
Iron content was determined colorimetrically according to [11].

Spectroscopy - X-band EPR spectra were recorded on a Bruker ER 200D spectrometer, using facilities and data handling as detailed elsewhere [12]. For the reduction of the sample, concentrated pellet was incubated with dithionite (10 mM) for 5 minutes at 22 °C.

Structural prediction - Structural homology models were made for WOR5 and PF1479 based on the amino-acid sequence and a homologue of a known structure [13].

Cultivation *Pyrococcus furiosus* - *P. furiosus* (DSM 3638) was grown in a 50 ml batch culture, under anaerobic conditions with starch as carbon source as previously described [14]. Cells were harvested by centrifugation (for 10 minutes at 3000 x g) and resuspended in 0.5 ml anaerobic spent medium. This cell suspension was directly used for activity measurements (10 µl per 1 ml assay buffer).

Aldehyde oxidation assay - Aldehyde oxidation activities were assayed at 70 °C, under anaerobic conditions, in 25 mM EPPS, pH 8.0 (broken cells) or in 0.75 M NaCl, 100 mM EPPS, pH 8.0 (intact cells) using 3 mM benzylviologen or methylviologen, and, respectively, 0.2 mM crotonaldehyde, 50 mM formaldehyde, 5 mM hexanal, or 0.5 mM GAP as substrate. The assay buffer containing the cells and the viologen was pre-reduced using a 100 mM dithionite solution; subsequently, reduction of the viologen was followed by the increase of adsorption at 580 nm (BV) or 600 nm (MV) [2-4,6].

Results

Cloning, expression and purification of the β-subunit of WOR5

TP1000 cells transformed with pEt15b-PF1479, expressing the β-subunit as a 19.9 kD histag fusion protein, were induced under different conditions. In all the induction experiments a dark brown pellet of cells was obtained after centrifugation. After breaking the cells with the cell-disruptor system, the pellet (cell debris and inclusion bodies), the membrane fraction, and the soluble cell-free extract were analyzed with SDS PAGE. In all the performed experiments the recombinant fusion protein was localized in the pellet of the disrupted cells (figure 1). So far, the β-subunit could not be expressed as soluble protein in *E. coli.* That the protein in the pellet was indeed the histag-β-subunit fusion protein, was confirmed by its ability to bind to Ni-sepharose resin after solubilisation under denaturing conditions (data not shown). The addition of DTT to the buffer appeared to be crucial for solubilising the aggregated protein, which indicates the involvement of cysteine-to-cysteine di-sulfide bridge formation during the precipitation. The β-subunit contains 16 cysteines (putatively coordinating four [4Fe-4S] clusters) that become available for disulfide bond formation when the protein is (partly) present in its apo-form.

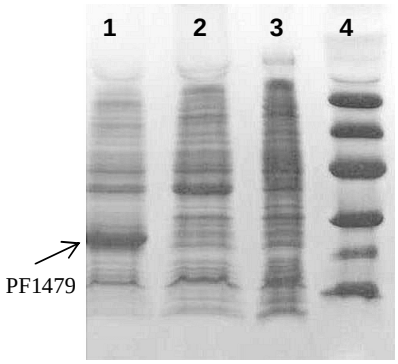

Figure 1. SDS-gel analysis of different cellular fractions of *E. coli* expressing the β-subunit. Lane 1: pellet after cell disruption, lane 2 membranes:, lane 3: soluble cell-free extract, lane 4: Low molecular weight marker: 94, 67, 43, 30, 20,14 kDa).

An EPR spectrum of the as isolated and reduced pellet was recorded (figure 2). The spectrum of the as isolated pellet did not result in any signal, which indicated the absence of $[3Fe\text{-}4S]^{+}$ clusters. The spectrum of the reduced sample gave a signal characteristic for a $[4Fe\text{-}4S]^{+}$ or a [2Fe-2S] cluster ($g\| = 2.03$, $g\perp = 1.94$) (figure 2). An iron and protein determination gave a ratio of 0.1 Fe per β-subunit, where 16 Fe per subunit is expected for the native holo-protein. There is an obvious substoichiometric incorporation of iron and, as a result, many cysteine residues are free to form disulfide-bonds which are proposed to be the cause of protein aggregation.

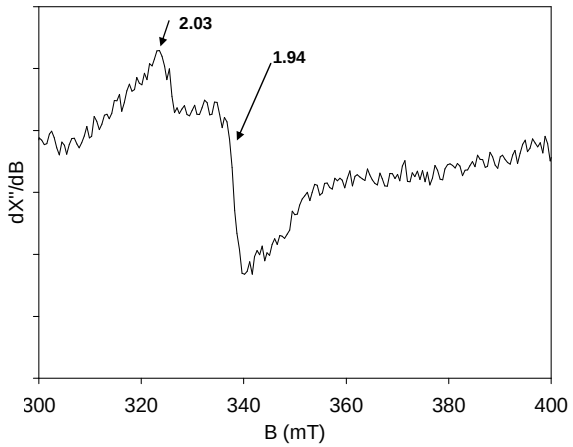

Figure 2. EPR spectrum of dithionite reduced cell pellet at a low temperature spectrum (22 K) dominated by the signal from $[4Fe\text{-}4S]^{1+}$ or [2Fe-2S] cluster(s). EPR conditions: microwave frequency, 9160 MHz; microwave power, 20 mW; modulation frequency, 100 kHz; modulation amplitude, 12.5 Gauss.

Sequence and structural alignments for the genes PF1479 and WOR5

The highest sequence homology with the PF1479 gene was found with hypothetical bacterial and archaeal proteins annotated as putative iron sulfur binding proteins (table 2). Interestingly, all these genes have a similar WOR5 homologue adjacent on the genome (table 2). In addition, all the homologues of WOR5 have a flanking gene encoding a PF1479 homologue. Interestingly, none of the other AORs in *P. furiosus* (or any other organisms), has a neighboring gene encoding a four [4Fe-4S] clusters binding protein.

PF1479 and its relatives are part of the superfamily of proteins containing four [4Fe-4S] cluster binding domains: all 16 cysteine residues are conserved in all homologues. Apparently, the proximity of these two genes is highly conserved in bacteria and archaea. In line with the earlier observed co-regulatory expression of WOR5 and PF1479 [1], these conserved genetic properties suggest a strong relation between the two proteins.

Table 2. Homologues of PF1479 ($< 10^{-15}$) in various bacteria, and archaea, and the adjacent gene encoding a WOR5 homologue.

Organism	**[4Fe-4S] binding domain Homologue**	**WOR5 homologue**
Archaea		
Pyrococcus furiosus	PF1479	PF1480
Thermofilum pendens	TpenDRAFT_1412	TpenDRAFT_1413
Pyrococcus abyssi	PAB2084	PAB2085
Pyrococcus horikoshii shinkaj OT3	PH0893	PH0892
Bacteria		
Moorella thermoacetica ATCC 39073	Moth_0153	Moth_0154
Polaromonas naphthalenivorans	Pnap_0048	Pnap_0049
Thermosinus carboxyivorans	TcarDRAFT_0817	TcarDRAFT_0818
Magnetospirillum magneticum	Amb2921	amb2922
Syntrophomonas wolfei subsp. Wolfei	Swol_1704	Swol_1703
Magnetospirillum magnetotacticum	Magn03009863	Magn03009864
Rhodoferax ferrireducens	Rfer_2851	Rfer_2850
Azoarcus sp. EbN1	ebA5004	ebA5005

Furthermore, PF1479 and PF1480 (WOR5) were recently recognized as one operon [15], which makes it very likely that they are expressed to become one protein complex built up from two different subunits. As WOR5 is known to form homodimers [6], the proposed native conformation is heterotetrameric ($\alpha_2\beta_2$): the α-subunit harbors the tungsto-bispterin cofactor (ORF PF1480) and the β subunit binds the four [4Fe-4S] clusters (ORF PF1479). From now on, we will refer to WOR5 as the protein in its heterotetrameric conformation.

A structural homology model for the β-subunit was made, based on its amino acid sequence and a homologue with a known structure [13]. The *E. coli* formate dehydrogenase subunit N

(FdnH) (1KQF) [16] was chosen from the PDB database as parental structure on which the PF1479 structure could be modeled with an e-value of 10^{-36} (figure 3A), indicating a reasonable similarity. We were able to assign the cysteines involved in the binding of the four [4Fe-4S] cluster by an overlay with the FdnH structure and its clusters (figure 3BC). In the structural alignment, depicted in figure 3A, it becomes clear that PF1479 is lacking the transmembrane helix that links the *E. coli* formate dehydrogenase to the membrane.

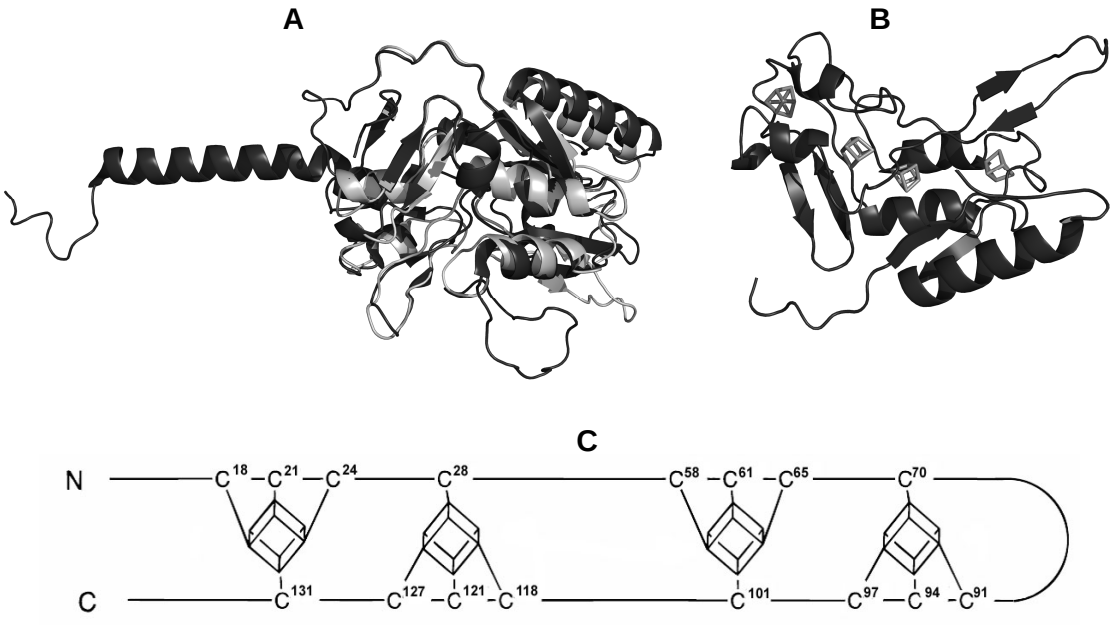

Figure 3. Homology modeling of PF1479. (A) Structural alignment of PF1479 and *E.coli* Fdh-N [13]. (B) Modeled structure of PF1479 with clusters taken from alignment with Fdh-N. (C) Highlighted cysteines involved in binding of various 4Fe-4S clusters.

E. coli formate dehydrogenase is a molybdopterin containing, periplasmic protein consisting of three subunits: the bis-MGD containing periplasmically oriented α-subunit (FdnG), the four [4Fe-4S] cluster containing β-subunit (FdnH), and the transmembrane, heme b containing γ-subunit (FdnI) [16]. Although the sequence homology between the bis-MGD containing α-subunit of formate dehydrogenase and the α-subunit of WOR5 is low, they both belong to the large family of tungsto- or molybdo-pterin containing enzymes. Alternative proteins, chosen by the structural homology program as possible parental structures are all four [4Fe-4S] carrying subunits of the following MGD containing proteins: *Aromatoleum aromaticum* ethylbenzene dehydrogenase (2IVF) [17], *Pelobacter acidigallici* pyrogallol-phloroglucinol transhydroxylase (1ti6_D) (contains 3 [4Fe-4S] clusters) [18], *E. coli* nitrate reductase (1Y4z) [19], and *Desulfovibrio gigas* tungsten containing formate dehydrogenase (1h0h_L) [20]. All these proteins form large complexes and, with the exception of the pyrogallol-phloroglucinol transhydroxylase, their catalytic subunits are all

found in the periplasmic space either linked to the membrane or as soluble protein. The hydrophobic transmembrane helix that links FdnH to the membrane is not present in the sequence of PF1479. There is also no other predicted membrane protein located on the genome in close proximity of PF1480 and PF1479. In addition, there is no practical evidence that WOR5 is associated to the membrane, as the α-subunit of WOR5 was purified as a soluble protein from *P. furiosus* [6] and the β-subunit was found in inclusion bodies as insoluble aggregate and not associated to the *E. coli* membrane fraction. Therefore, a transmembrane, or membrane linked localization of the WOR5 complex is unlikely.

On the contrary, a periplasmic localization seems an interesting hypothesis. First of all, it would explain WOR5's necessity to have its own 'ferredoxin like' β-subunit, as ferredoxin is a cytosolic protein. And secondly, a periplasmic expression of WOR5 distinguishes the protein from the very similar AOR and FOR, which goes some way towards answering the question why the cell expresses so many enzymes with similar substrate specificities.

In order to get an idea of the three-dimensional structure of the complex, a second structural homology model was made for the α-subunit of WOR5 (data not shown). *P. furiosus* AOR (1AOR) [21] was selected as parental structure with an e-value of 10^{-127}. The tungsten-bispterin cofactor, the [4Fe-4S]-cluster, and the dimerization are based on the alignment with the original AOR structure [21]. The only other available structure of a tungsto-bispterin enzyme is *P. furiosus* FOR, which has been co-crystallized with ferredoxin [22]. Based on aligning the [4Fe-4S] cluster from FOR with the [4Fe-4S] cluster from WOR5, and the [4Fe-4S] cluster from the docked ferredoxin with the [4Fe-4S] cluster closest to the N-terminal of PF1479 (Cys18, 21, 24 and 131), the modeled structure of the β-subunit was fitted into the modeled structure of the WOR5 dimer (figure 4). Because of steric hinder the PF1479 protein could only be oriented in one way.

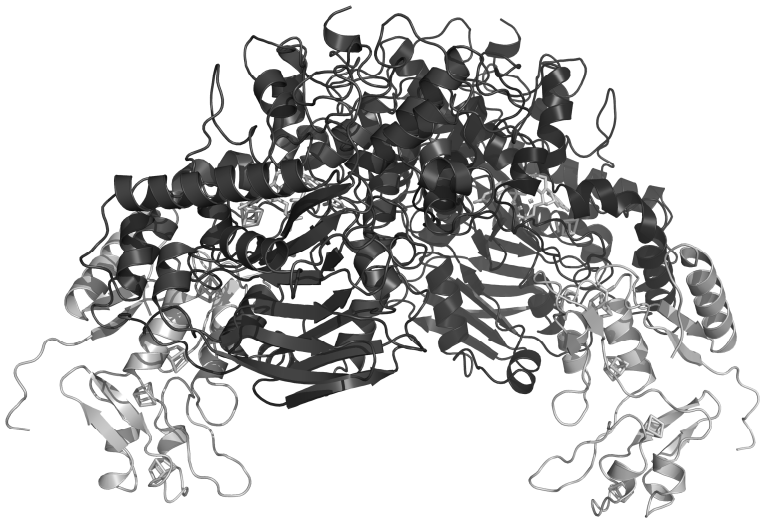

Figure 4. Modeled structure of heterotetrameric WOR5-PF1479 based on homology with *P. furiosus* AOR (α-subunit), *E. coli* Fdh-N (β-subunit) and FOR in complex with ferredoxin [22] (docking sites estimation) [13]. The iron sulfur cluster and tungsto-bispterin cofactor in the α-subunit are taken from the alignment with AOR.

Periplasmic activity assay

To verify the periplasmic localization of WOR5, an assay was designed based on earlier described experiments to determine the localization of periplasmic selenate reductase and nitrate reductase (NR) [23,24].

In this assay the enzyme activities are measured with membrane-impermeable methylviologen and membrane-permeable benzylviologen as electron acceptor. The principle is illustrated in figure 5. If an enzyme is able to convert the aldehyde substrate and subsequently reduce the methylviologen, the cellular localization of the protein must be periplasmic/outer cellular, because otherwise there is no access for the protein to the methylviologen. If the activity assay is performed with benzylviologen, both the intracellular and the extracellular proteins should be able to donate electrons and reduce the viologen upon oxidation of the substrate.

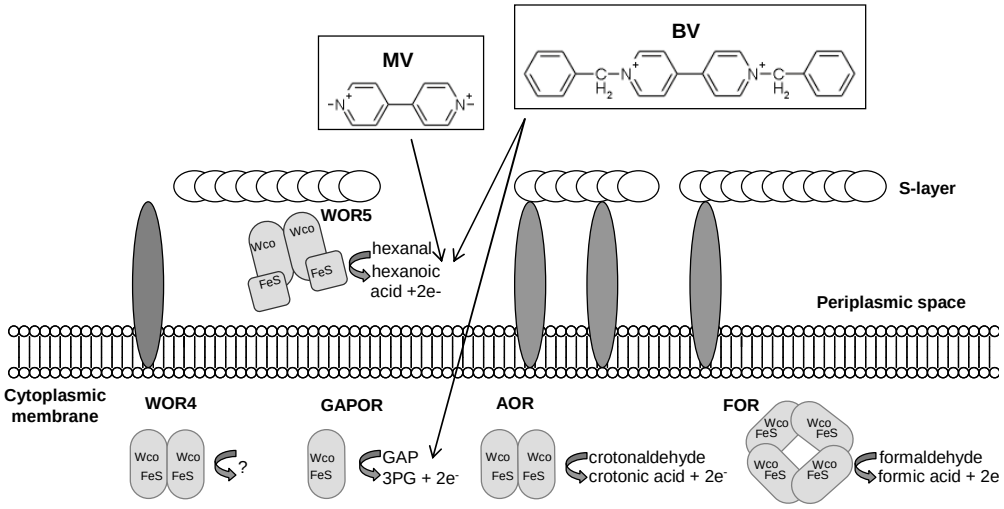

Figure 5. A schematic overview of a whole-cell assay, where the aldehyde oxidoreductase activities are measured with membrane-impermeable methylviologen or membrane-permeable benzylviologen as electron acceptor. The AORs are depicted in the cell according to their predicted cellular localization.

To interpret the results of this experiment, some additional complexities need to be taken into account. First of all, the substrate specificities of the enzymes are overlapping, so it is difficult to assign a certain activity to a specific enzyme (table 1). In addition, we know that the *in vitro* determined V_{max} and K_M differ per enzyme and per electron acceptor. For example, the specific activity of AOR for the oxidation of crotonaldehyde is higher when benzylviologen is used as electron acceptor, whereas FOR shows a higher formaldehyde activity in the presence of methylviologen.

Also the membrane permeability of the different substrates might differ: formaldehyde is less hydrophobic than hexanal and might therefore diffuse slower into the cell. Finally it is important to note that there are no data available for the (relative) expression levels of the different AORs, which make it impossible to predict the relative compartmental aldehyde oxidation activities.

With all these matters in mind, the aldehyde oxidation activity of intact cells and broken cells was determined for the four different aldehydes with both benzyl and methylviologen as electron acceptor. The results are depicted in figure 6AB.

With benzylviologen as electron acceptor, all aldehyde oxidation activities could be detected in intact cells (figure 6A). This indicates that the aldehyde substrates and benzylviologen are membrane-permeable and that it is possible to detect intracellular activities of the different AORs.

With methylviologen as electron acceptor, a periplasmic hexanal-oxidizing activity was measured (figure 6A) as well as a low oxidation activity on crotonaldehyde. No formaldehyde or GAP oxidation activity could be detected with this membrane-impermeable electron acceptor, indicating a cytosolic localization for the enzymes catalyzing these conversions (GAPOR and FOR). Hexanal is known to be the most effective substrate for WOR5 [6], therefore, the outer cellular hexanal-oxidizing activity suggests a periplasmic localization for WOR5. The detected extracellular crotonaldehyde activity could also be a result of the periplasmic localization for WOR5 because this enzyme can use crotonaldehyde as substrate as well (table 1). However, here the overlap in substrate specificity complicates the interpretation of the data: crotonaldehyde is known to be the best substrate for AOR. How can we exclude that periplasmically localized AOR is converting the crotonaldehyde and the hexanal?

The same aldehyde oxidation rates were measured in open cells to determine the increase of activity on the various substrates upon breaking of the cells. If a protein would be localized in the extracellular space, breaking the cells would not increase the activity nearly as much as when a protein is localized inside the cell. In the latter case, the step of diffusion of the aldehyde and benzylviologen into the cell has been eliminated upon breaking, and therefore the relative activity of cytosolic enzymes is expected to increase.

The results of the activity experiments in broken cells (figure 6B) show that indeed all the oxidation activities increase compared to the intact cell assay when benzylviologen was used as electron acceptor. However the increase of the hexanal-oxidation activity was significantly lower than the increase in activity on the other substrates (figure 6C), corroborating the extracellular localization of WOR5. On the contrary, there was a strong increase of crotonaldehyde activity with benzylviologen as electron acceptor upon breaking the cells, which indicates that this enzymatic activity was originally intracellular. The specific activity of AOR on crotonaldehyde with benzylviologen as electron acceptor is orders of magnitude higher than the specific activity of WOR5 for the combination of these two substrates. So taken this all together, AOR is concluded to be cytosolically localized and to be responsible for the intracellular oxidation of crotonaldehyde.

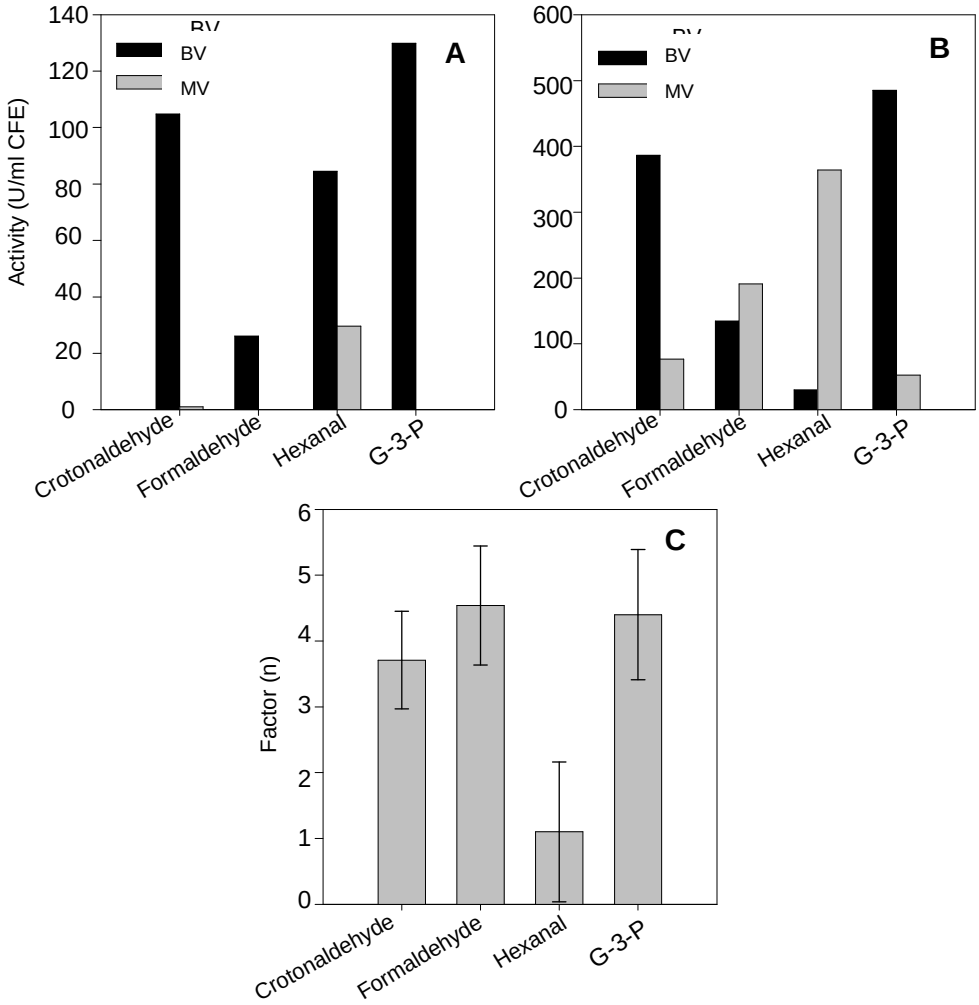

Figure 6. Aldehyde oxidation activity of intact (A) and broken cells (B) determined using membrane-impermeable methylviologen (grey) and membrane-permeable benzylviologen (black) as electron acceptors. Relative increase of aldehyde oxidation activity using benzylviologen as electron acceptor of broken cells compared to intact cells (C). Enzymes represent their most efficient aldehyde substrate: AOR (crotonaldehyde), FOR (formaldehyde), WOR5 (hexanal) and GAPOR (G-3-P).

In summary, WOR5 is proposed to be localized in the periplasm because of (i) the detected periplasmic hexanal activity and (ii) the small increase of this activity upon breaking of the cells. AOR, on the contrary, is proposed to be a cytosolic protein because of (i) the very low periplasmic crotonaldehyde-oxidation activity and (ii) the large increase of this activity upon breaking of the cells.

The aldehyde oxidation activities with methylviologen as electron acceptor also increased upon cell disruption (data not shown). However, these data are much more complicated to interpret as all activities are expected to rise because of the increased availability of methylviologen for all enzymes upon cell disruption.

Finally, we note that formaldehyde can also serve as substrate for WOR5 [6] and therefore we would expect to detect an extracellular formaldehyde-oxidation activity as well, especially because the specific oxidation activity of WOR5 for formaldehyde and crotonaldehyde is supposed to be similar to that determined in the *in vitro* assay on purified enzyme [6]. However, the conditions are different in this *in vivo* assay and perhaps for this reason the formaldehyde activity of WOR5 is too low to be detected.

Discussion and conclusion

Tungsten containing aldehyde oxidoreductases are intensively studied enzymes in particular with respect to their structural, spectroscopic, electrochemical and kinetic properties. However their physiological function is still unknown, which is intriguing because in organisms like *P. furiosus* these enzymes represent circa 5% of the whole proteome. Five different aldehyde oxidoreductases with partly overlapping substrate specificities have been purified from *P. furiosus*. In this chapter, we have made some proposals that distinguish WOR5 clearly from the other AORs regarding its quaternary structure and cellular localization. Based on the observed co-regulation with the adjacent four [4Fe-4S] cluster binding domain protein PF1479 [1], the alignment studies with structural homologues and the cellular localization assays, we propose that the gene products from *wor5* and PF1479 form a hetero tetrameric complex ($\alpha_2\beta_2$) that is located in the periplasmic space of the cell.
More experiments are required to confirm this hypothesis, especially *in vitro* and *in vivo* biochemical data on the heterodimer formation are lacking. For these experiments it would be convenient to obtain soluble β-subunit protein (PF1479) to perform *in vitro* binding studies with the α-subunit WOR5. However, the β-subunit might require an interaction with the α-subunit to enable the incorporation of the iron sulfur clusters. In that case, the absence of the tungsten containing α-subunit during the overexpression in *E. coli* might lead to the formation of apo-protein, resulting in many free cysteine residues which induce the misfolding. In addition to these cysteines that become available for 'random' disulfide bond formation, the absence of clusters by itself is also expected to have an impact on the protein structure. In a native, holo-form of the protein, the clusters are expected to play an important role in determining its overall fold: they can connect the N-terminus of the protein with the C-terminus thereby stabilizing the structure (figure 3C). This has been confirmed in nitrate reductase NarGH mutants, where a mutation of single cysteines in the H subunit (C184, C196, C227 or C223, homologous to C58, C70, C101 and C97 in PF1479) induced the loss of all metal centers, including the ones in the α-subunit. Also the double mutant, in which C247 and C244 were mutated into alanine or serine (C121, C118 in PF1479) had lost all metal centers [25,26]. These results suggest that the Fe-S clusters play an important structural role in nitrate reductase. They are thought to be built-in co-translationally in order to obtain the correct fold (Axel Magalon personal communication). The clusters in the β-subunit of WOR5 most likely play a similar structurally important role, and this, possibly in

combination with the absence of the α-subunit, could explain the observed aggregation of the apo-protein.
WOR5 was purified from *P. furiosus* as a homodimer (α_2) (chapter 6). It is quite possible that the high number of column steps required to purify the protein might have resulted in the loss of the β-subunit.
Examination of the amino acid sequence of both subunits of WOR5 and its homologues did not reveal any of the known signal peptides required for folded-protein translocation into the periplasmic space, which could confirm the periplasmic localization. In prokaryotes, the twin arginine translocation (Tat) system transports proteins in their folded state across the membrane [27]. All the substrates for this Tat-system contain the characteristic twin-arginine motif. Tat components are present in the genome of several archaea, however, in the genome of *P. furiosus* these genes are lacking [28,29].
So far, no translocation system for folded proteins has been identified in *P. furiosus* and other archaea that lack the Tat-system. These organisms might express other protein-translocation machineries that differ in their mechanism, subunit composition and recognition sequence [28-30]. There is no reason to assume that hyperthermophilic archaea, due to their environmental growing conditions, are not expressing complex, cofactor containing, proteins for translocation to their periplasmic space. For example, the hyperthermophilic *P. aerophilum* expresses a periplasmic membrane bound MGD-containing nitrate reductase (PAE2662) [31].
For many of the periplasmic molybdopterin containing enzymes no clear function has been described yet related to their cellular localization. For example, in the case of *E. coli* periplasmic nitrate reductase (Nap), no transcription promotors or conserved DNA sequences related to the nitrogen metabolism have been found [32]. Proposed roles for Nap are: denitrification [32] or playing a role in minimizing the cellular reducing power under aerobic growth conditions [33]. The physiological role of WOR5 remains elusive and the source of substrate aldehydes has also not been identified yet. Additional data on expression levels under different growth conditions might result in more clues on the physiological role of WOR5 and other AOR proteins.
And finally, the natural redox partner of the putative heterotetrameric WOR5 complex remains to be identified.

Acknowledgements

We thank Peter-Leon Hagedoorn for performing the EPR measurements. This research was supported by a grant from the Council for Chemical Sciences of the Netherlands Organization for Scientific Research (700.51.301).

References

[1] M.V. Weinberg, G.J. Schut, S. Brehm, S. Datta, M.W.W. Adams, J. Bacteriol.187 (2005) 336.
[2] S. Mukund, M.W. Adams, J. Biol. Chem. 266 (1991) 14208.
[3] S. Mukund, M.W.W. Adams, J. Biol. Chem. 270 (1995) 8389.
[4] R. Roy, S. Mukund, G.J. Schut, D.M. Dunn, R. Weiss, M.W.W. Adams, J. Bacteriol.181 (1999) 1171.
[5] R. Roy, M.W.W. Adams, J. Bacteriol.184 (2002) 6952.
[6] L.E. Bevers, E. Bol, P.-L. Hagedoorn, W.R. Hagen, J. Bacteriol.187 (2005) 7056.
[7] S. Mukund, M.W. Adams, J. Biol. Chem. 270 (1995) 8389.
[8] R. Sapra, M.F.J.M. Verhagen, M.W.W. Adams, J. Bacteriol.182 (2000) 3423.
[9] R. Sapra, K. Bagramyan, M.W.W. Adams, Proc. Natl. Acad. Sci. USA 100 (2003) 7545.
[10] G.J. Schut, S.D. Brehm, S. Datta, M.W.W. Adams, J. Bacteriol.185 (2003) 3935.
[11] A.J. Pierik, R.B. Wolbert, P.H. Mutsaers, W.R. Hagen, C. Veeger, Eur. J. Biochem. 206 (1992) 697.
[12] A.J. Pierik, W.R. Hagen, Eur. J. Biochem. 195 (1991) 505.
[13] P.A. Bates, L.A. Kelley, R.M. MacCallum, M.J. Sternberg, Proteins Suppl. 5 (2001) 39.
[14] A.F. Arendsen, P.T. Veenhuizen, W.R. Hagen, FEBS Lett. 368 (1995) 117.
[15] T.T. Tran, P. Dam, Z. Su, F.L. Poole, II, M.W.W. Adams, G.T. Zhou, Y. Xu, Nucl. Acids Res. 35 (2007) 11.
[16] M. Jormakka, S. Tornroth, B. Byrne, S. Iwata, Science 295 (2002) 1862.
[17] D.P. Kloer, C. Hagel, J. Heider, G.E. Schulz, Structure 14 (2006) 1377.
[18] A. Messerschmidt, H. Niessen, D. Abt, O. Einsle, B. Schink, P.M.H. Kroneck, Proc. Natl. Acad. Sci. USA 101 (2004) 11571.
[19] M.G. Bertero, R.A. Rothery, N. Boroumand, M. Palak, F. Blasco, N. Ginet, J.H. Weiner, N.C.J. Strynadka, J. Biol. Chem. 280 (2005) 14836.
[20] H. Raaijmakers, S. Macieira, J.M. Dias, S. Teixeira, S. Bursakov, R. Huber, J.J.G. Moura, I. Moura, M.J. Romao, Structure 10 (2002) 1261.
[21] M.K. Chan, S. Mukund, A. Kletzin, M.W.W. Adams, D.C. Rees, Science 267 (1995) 1463.
[22] Y. Hu, S. Faham, R. Roy, M.W.W. Adams, D.C. Rees, J. Mol. Biol. 286 (1999) 899.
[23] C.A. Watts, H. Ridley, K.L. Condie, J.T. Leaver, D.J. Richardson, C.S. Butler, FEMS Microbiol. Lett. 228 (2003) 273.
[24] L.C. Bell, D.J. Richardson, S.J. Ferguson, FEBS Lett. 265 (1990) 85.
[25] V. Augier, B. Guigliarelli, M. Asso, P. Bertrand, C. Frixon, G. Giordano, M. Chippaux, F. Blasco, Biochemistry 32 (1993) 2013.
[26] B. Guigliarelli, A. Magalon, M. Asso, P. Bertrand, C. Frixon, G. Giordano, F. Blasco, Biochemistry 35 (1996) 4828.
[27] B.C. Berks, F. Sargent, T. Palmer, Mol. Microbiol. 35 (2000) 260.
[28] G.W. Hutcheon, A. Bolhuis, Biochem. Soc. Trans. 31 (2003) 686.
[29] M. Pohlschroeder, M.I. Gimenez, K.F. Jarrell, Curr. Opin. Microbiol. 8 (2005) 713.
[30] S.-V. Albers, Z. Szabo, A.J.M. Driessen, Nat. Rev. Microbiol. 4 (2006) 537.
[31] S. Afshar, E. Johnson, S. De Vries, I. Schroder, J. Bacteriol.183 (2001) 5491.
[32] J. Gonzalez Pablo, G. Rivas Maria, D. Brondino Carlos, A. Bursakov Sergey, I. Moura, J.G. Moura Jose, J. Biol. Inorg. Chem. 11 (2006) 609.
[33] M.J.K. Ellington, G. Sawers, H.J. Sears, S. Spiro, D.J. Richardson, S.J. Ferguson, Microbiology 149 (2003) 1533.

Chapter 8

Redox Chemistry of Tungsten and Iron-Sulfur Prosthetic Groups in *Pyrococcus furiosus* Formaldehyde Ferredoxin Oxidoreductase

Emile Bol
Loes E. Bevers
Peter-Leon Hagedoorn
Wilfred R. Hagen

Adapted from: Journal of Biological Inorganic Chemistry 11 (2006) 999-1006

Abstract

Formaldehyde oxidoreductase (FOR) is one of the tungstopterin iron-sulfur enzymes of the five-membered family of aldehyde oxidoreductases in the hyperthermophilic archaeon *Pyrococcus furiosus*. In dye mediated equilibrium redox titrations the tungsten in active *P. furiosus* FOR is a two-electron acceptor, W(VI/IV). The intermediate, paramagnetic W(V) state can be trapped only by reduction with substrate, with consecutive one-electron intraprotein electron transfer to the single $[4Fe\text{-}4S]^{(2+;1+)}$ cluster and partial comproportionation of the tungsten over W(IV, V, VI); this is a stable state in the absence of an external electron acceptor. EPR spectroscopy reveals a single 'low-potential' W(V) spectrum with g_{xyz}-values 1.847, 1.898, 1.972, and a $[4Fe\text{-}4S]^{1+}$ cubane in a spin mixture of S=1/2 (10 %) and S=3/2 (90 %) of intermediate rhombicity (E/D=0.21, (g_{real} = 1.91). The development of this intermediate *in vitro* is slow even at elevated temperature and with a nominal 50:1 excess of substrate over enzyme presumably due to the very unfavorable hydratation equilibrium of the formaldehyde/ methylene glycol couple with $K_D \approx 10^3$. Rapid intermediate formation of enzyme at concentrations suitable for EPR spectroscopy (200 μM) is only obtained with extremely high nominal substrate concentration (1 M formaldehyde) which is followed by a slower phase of denaturation. The premise that the free formaldehyde, and not the methylene glycol, is the enzyme's substrate, implies that the K_M for formaldehyde is three orders-of-magnitude less that the previously reported value.

Introduction

The biochemistry of group-6 elements is unusual: the heavier congeners, Mo and W, are the only 4d and 5d metal ions with established biological role(s). They differ essentially from all other biologically relevant transition ions in having available, over a relatively narrow potential range, two oxidation states that differ by *two* units, namely +VI and +IV. This property is also well established in non-biological chemistry, where Mo and W are sometimes referred to as 'non-metals' to indicate that they behave somewhat like organic redox compounds, or electron-pair acceptors/donors, rather than single-electron accepting/donating transition metal ions. This basic property is reflected in the biological functioning of Mo- and W-enzymes, which, with very few exceptions, use mononuclear metal ion active sites to catalyze two-electron redox chemistry of organic compounds, e.g., $RHO + H_2O \leftrightarrow ROOH + 2[H]$, or of oxoanions, e.g., $XO_m^{n-} + H_2O \leftrightarrow XO_{m+1}^{n-} + 2[H]$, with X = N, Cl, S, As, Se. These reactions are also called O-atom transfers.

Pyrococcus furiosus is a strict anaerobe, fermentative, marine hyperthermophilic archaeon, whose growth is mandatorily dependent on the presence of tungstate [1,2]. Complete-genome analysis has revealed the presence of putative structural genes for five W-enzymes of the aldehyde oxidoreductase family. Three of these enzymes have been purified to apparent homogeneity and enzymatically characterized, namely homodimeric aldehyde oxidoreductase (AOR), homotetrameric formaldehyde oxidoreductase (FOR), and monomeric glyceraldehyde-3-phosphate oxidoreductase (GAPOR). A fourth putative W-associated oxidoreductase, WOR-4, has been purified but no activity could be identified yet [3]. Recently, a fifth enzyme, WOR-5, has been purified as a homodimer with high hexanal-oxidizing activity (chapter 6) [4]. Crystal structures have been determined of *P. furiosus* AOR (1AOR; [5]) and FOR (1B25; [6]) and tungsten L-edge EXAFS has been investigated for GAPOR [7]. Detailed redox chemical studies, monitored with spectroscopy, have been carried out for *P. furiosus* AOR and GAPOR, but not for FOR. However, the FOR of the close relative *Thermococcus litoralis* has been scrutinized spectroelectrochemically [8], and the protein sequence of this enzyme is 87% identical to that of *P. furiosus* FOR.

Molybdenum/tungsten enzymes can be classified into four subgroups that differ in terms of the structure of the active site: the sulfite oxidase family, the xanthine oxidase family, the dimethyl sulfoxide reductase family, and the aldehyde ferredoxin oxidoreductase (AOR) family [9]. The five known tungsten containing oxidoreductases (AOR, FOR, GAPOR, WOR4 and WOR5) from *P. furiosus* belong to the AOR family.

P. furiosus FOR is a tetrameric enzyme of 280 kDa molecular mass with each subunit containing one W center and one $[4Fe\text{-}4S]^{(2+;1+)}$ cluster. The tungstopterin of FOR consists of two pterin molecules and one tungsten atom. The two pterin molecules are further linked to each other by a magnesium ion. The tungsten atom in the enzyme as isolated is coordinated by the four dithiolene sulfur atoms and by one other ligand assumed to be an oxygen atom (1B25; [6]). FOR was purified by its ability to oxidize formaldehyde to formic acid (E_m = -530 mV at pH = 8) but it can also oxidize larger aldehydes [10].

The determination of the redox properties of Mo and W in enzymes is associated with a combination of experimental problems. Almost all Mo/W-enzymes contain other cofactors, notably flavins and/or iron-sulfur clusters, with relatively strong optical absorption. This makes EPR spectroscopy the method of choice for monitoring the redox properties of Mo/W-pterin. However, only the intermediate +V oxidation state, with S = 1/2, is readily detectable by EPR (theoretically the +IV state could be S = 1 but no experimental observation had been reported). The two subsequent reduction potentials $E_1'^0$(VI/V) and $E_2'^0$(V/IV) are usually quite close in value, and, in fact, frequently crossed over (i.e. $E_1 < E_2$) compliant with the 'non metal' nature of the elements. This means not only that the EPR signal is associated with an intermediate redox state (i.e. no signal for either fully oxidized or fully reduced enzyme) but also that the maximal signal intensity of the intermediate state is substoichiometric (e.g, for $E_1 \leq E_2$ the maximal intensity of the S = 1/2 signal ≤ 33%). Another series of problems stems from the relative fragility of the Mo/W active site, very frequently leading to modification in the course of enzyme purification, e.g., due to damage by molecular oxygen. Purified Mo/W-enzyme preparations often contain apoprotein. The holoprotein fraction can also consist of multiple forms, each of which may display a distinct Mo(V) or W(V) EPR signal. Finally, the associated iron-sulfur prosthetic group(s) in many cases has complex paramagnetism, and its spectra, as well as the radical spectra of flavins or pterins, overlap with that of Mo/W(V). Several of these problems are apparent in the extensive study of Dhawan et al. on the redox chemistry of FOR from *T. litoralis* [8]. We decided to have a closer look at the highly homologous FOR from *P. furiosus*.

Materials and Methods

Growth of the organism and protein purification - *Pyrococcus furiosus* (DSM 3638) was grown at 90 °C under anaerobic conditions with starch as carbon source, as previously described [11]. After 18 hours running in batch mode the culture was put to continuous mode with a dilution rate of 0.3 h^{-1} [12] resulting in a wet weight of approximately 2 g/l. Cells were broken by osmotic shock, diluting with 5 volumes 50 mM Tris/HCl, pH 8.0, containing, 0.1 mg/ml DNase I, 0.1 mg/ml RNase and 3 mM cysteine. A cell-free extract was obtained as the supernatant after 15 minutes centrifugation at 15,000 g.
Formaldehyde ferredoxin oxidoreductase was purified as reported previously [10]. Samples were anaerobically purified in 20 mM Tris/HCl buffer, pH 8.0. A final column (DEAE 1×10 cm) was used with a gradient of 15 column volumes up to a salt concentration of 200 mM NaCl.

Enzyme assays - Protein concentration was determined using the bicinchoninic acid method using bovine serum albumine as the standard. The tungsten concentration was determined by catalytic-adsorptive stripping voltammetry according to [13]. Activity was determined in an optical assay with 50 mM formaldehyde and 1 mM methyl viologen (ε_{600}=

12 $mM^{-1}cm^{-1}$) at pH 8.4 and T = 60 °C, where one unit is defined as two μmoles of viologen semiquinone formed per minute. Sulfide activation experiments were performed with excess sodium sulfide (20 mM) in 100 mM Tris/HCl buffer under anaerobic conditions.

Spectroscopy - EPR redox titrations were performed at room temperature under argon in 50 mM Hepes, pH 7.5 using 4 mg/ml (58 μM of monomer) FOR. The following dyes were added to a final concentration of 50 μM: N,N,N',N'-tetramethyl-p-phenylenediamine, 2,6-dichlorophenol indophenol, phenazine ethosulfate, methylene blue, resorufine, indigodisulfonate, 2-hydroxy-1,4-naphtaquinone, anthraquinone-2-sulfonate, phenosafranin, safranin O, neutral red, benzylviologen, methylviologen. Samples were first reductively titrated with sodium dithionite followed by oxidative titration with potassium ferricyanide. After equilibration at the desired potential a 0.2 mL sample was anaerobically transferred to an EPR tube and immediately frozen in liquid nitrogen. Potentials were measured with a platinum electrode and a Ag/AgCl reference electrode. All reported values are with respect to the normal hydrogen electrode (NHE). Substrate incubation experiments were performed at room temperature (22 °C) and at 60 °C. The enzyme was incubated with 10 mM formaldehyde for 30 sec before the sample was frozen in liquid nitrogen. The incubation was extended by thawing, incubating for a defined time, and freezing the sample until reduction was maximal as judged by EPR monitoring. The experiment was also done starting at 60 °C with 1 M formaldehyde.
X-band EPR-spectra were recorded on a Bruker ER 200D spectrometer, using facilities and data handling as detailed elsewhere [14]. The modulation frequency was always 100 kHz. High-spin EPR was analyzed with the usual spin Hamiltonian ($H = \beta B \cdot g \cdot S + D[S_z^2 - S(S+1)/3] + E(S_x^2 - S_y^2)$) in the weak-field limit using rhombograms [15]. Iron-sulfur EPR spectra were simulated as g-strain broadened effective S=1/2 spectra [16], and W(V) EPR was simulated as S=1/2 spectra with hyperfine broadening and splitting [17].

Results

Formaldehyde oxidation activity was found to vary significantly over samples purified from different batches. For redox spectroscopic studies two samples were chosen, prepared from two separate fermentations, that differed by an order of magnitude in specific activity at 60 °C (Table 1). The two samples will be denoted as high-activity FOR and low-activity FOR. No activity was observed when crotonaldehyde was used as a substrate which indicates the absence of AOR. Both preparations showed a single band around 67 kDa on a SDS-PAGE gel (not shown).

Table 1. Comparison of activities of FOR from *P. furiosus* and *T. litoralis*

	Spec act (U/mg)	Assay T (°C)	Electron acceptor	Rel. act. [(a)] (%)
P. furiosus				
FOR low activity [(b)]	3	60	MV	8
FOR high activity [(b)]	27	60	MV	71
FOR high activity + S^{2-} [(b)]	38	60	MV	100
FOR [(c)]	13	60	BV	34
FOR [(c)]	42	80	BV	34
FOR + S^{2-} [(c)]	85	80	BV	69
T. litoralis				
FOR [(d)]	6	80	MV	5
FOR + S^{2-} + dith [(d)]	48	80	MV	40

[(a)] Relative activity re-calculated for T = 60 °C and for methyl viologen as electron acceptor [(b)] this work, [(c)] [10], [(d)] [18]

A previous study on *T. litoralis* FOR [8] identified three different W(V) EPR signals, which were labeled 'high-potential', 'mid-potential', and 'low potential', with reference to the redox potential range in which the signals developed maximal amplitude. The present studies on *P. furiosus* FOR gives somewhat different results: a high potential signal was never found; a mid potential signal was found, but only in low-activity enzyme; a low potential signal was not found during equilibrium redox titrations, however, this signal does develop slowly upon incubation with excess reductant dithionite or with the substrate formaldehyde in the absence of mediator dyes (figure 1). The low potential signal is found in both the low-activity and the high-activity sample. The low potential signal from the dithionite reduced sample and the signal of the substrate reduced sample slightly differ in their g-values (Table 2). Furthermore, spectral simulation of the signal from formaldehyde-reduced enzyme shows a considerable decrease in linewidth (Table 2).

Table 2. EPR parameters of W(V) and $[4Fe\text{-}4S]^{1+}$ in *P. furiosus* FOR

	gx	Gy	gz	Ax[(a)]	Ay	Az	Wx[(b)]	Wy	Wz
W(V) mid potential	1.926	1.946	1.977	63	40	40	10	10	10
W(V) low potential (dithionite)	1.847	1.901	1.969	35[(c)]	35	35[(c)]	22	7.5	18
W(V) low potential (formaldehyde)	1.851	1.902	1.976	45	33	1[(c)]	14	6	10
High-spin [4Fe-4S] $\lvert m_S = \pm 3/2\rangle$	1.05	1.3	5.51				0.17	0.17	0.17
$\lvert m_S = \pm 1/2\rangle$	1.65	2.5	4.82				0.45	0.45	0.45
Low-spin [4Fe-4S] species-1	1.866	1.935	2.044				0.014	0.007	0.0085
Low-spin [4Fe-4S] species-2	1.848	1.902	2.065				0.012	0.0055	0.008

[(a)] ^{183}W hyperfine splitting in Gauss [(b)] linewidth in Gauss (for W signals) or in g-valve units (for Fe/S signals), [(c)] dummy values: no splitting observed.

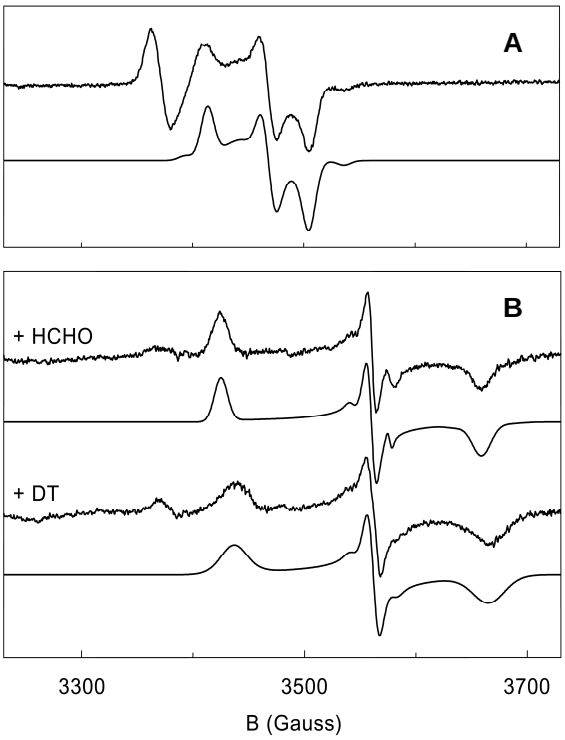

Figure 1. EPR spectra of the tungsten center in low-activity, as-isolated (A) and in high-activity, substrate/dithionite reduced (B) *P. furiosus* FOR. The enzyme, 12 mg/ml, was incubated with 10 mM dithionite or 10 mM formaldehyde for 45 minutes at 60 °C. Panel A is a spectrum of the mid-potential signal of the W(V) in tungsto-bispterin with the simulated spectrum; panel B shows spectra of the low-potential signal with the simulated spectrum of the W(V) in tungsto-bispterin. EPR conditions: microwave frequency, 9.43 MHz; microwave power, 32 mW; modulation amplitude, 4 Gauss, temperature, 40 K.

Upon reduction two $[4Fe\text{-}4S]^{1+}$ signals are found; a high spin (S=3/2) and a low spin (S=1/2) signal as shown in figure 2. The high-activity and the low-activity *P. furiosus* FOR give essentially identical $[4Fe\text{-}4S]^{1+}$ EPR. Fig. 2 shows simulations of the spectra on the basis of g-strain broadened effective S=1/2 systems. The effective g-values of the S=3/2 system fit the weak-field rhombogram [15] for g_{real} = 1.91 and E/D = 0.205, and the relative intensity of the subspectra is consistent with a small, positive D-value (D/hν ≈1). The real S=1/2 spectrum is simulated as a sum of two species with slightly different g-values. All spin-Hamiltonian parameters are summarized in Table 2. Quantitation on the basis of the simulated spectra affords a total spin count corresponding to circa one [4Fe-4S] cluster per FOR subunit. The fractions S=3/2 and S=1/2 that were found are 90 % and 10 %, respectively.

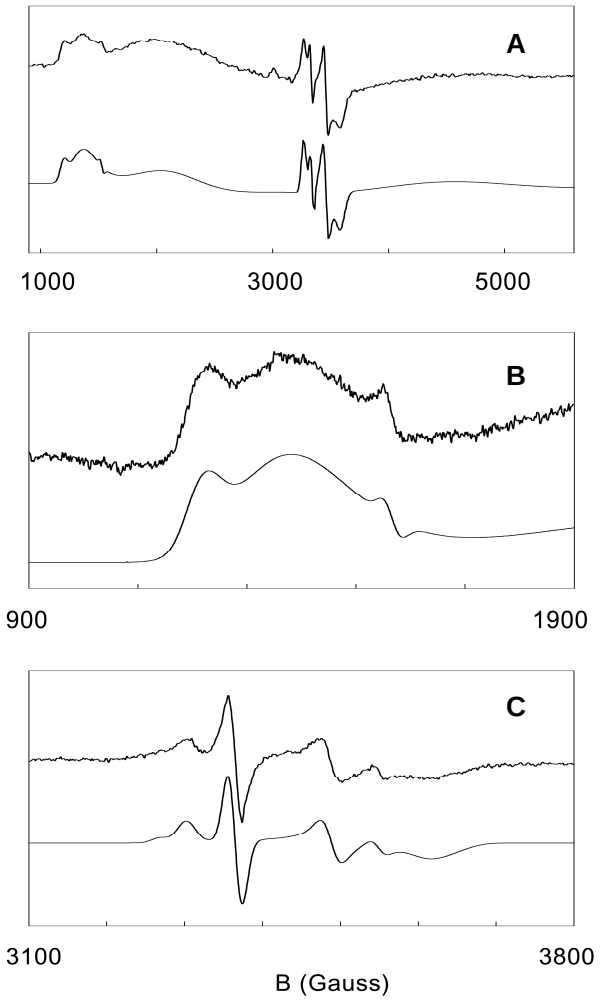

Figure 2. EPR spectra of the iron-sulfur cluster in dithionite reduced FOR. Trace A is an overview spectrum of the high spin (S=3/2) and partially saturated low spin (S=1/2) forms; trace B zooms in to the low-field part of the S=3/2 signal; trace C is a spectrum of the S=1/2 species under non-saturating conditions. EPR conditions: microwave frequency, 9.43 MHz; microwave power, 126 mW and (trace C) 2 mW; modulation amplitude, 8 Gauss and (trace C) 6.3 Gauss, temperature, 8.5 K and (trace C) 13 K.

Both high-activity and low-activity samples were used for dye mediated redox titrations at room temperature. The two preparations displayed the same properties for the [4Fe-4S] cluster. The S=3/2 signal intensity was monitored and plotted versus potential (figure 3). A midpoint potential of -330 mV for the $[4Fe\text{-}4S]^{(2+;+)}$ cluster was found for both samples. This is comparable to the midpoint potential of the [4Fe-4S] cluster found in *T. litoralis* of -368 mV.

Only the sample with the low specific activity showed a tungsten EPR signal that disappeared upon reduction with a E_m = -250 mV (figure 3b). The shape of the signal is reminiscent of that reported for *T. litoralis* FOR as the 'mid-potential' signal. However, the

value for the reduction potential is much lower than the E_m = -34 mV reported for the mid-potential W(V) signal of FOR from *T. litoralis*. With the high-activity *P. furiosus* FOR no mid-potential tungsten signal was detected. In *T. litoralis* FOR midpoint potentials of -280 and -335 mV were found during equilibrium titrations for a low potential tungsten species [8]. In the present study of *P. furiosus* FOR low potential tungsten signals were not observed in the equilibrium titrations.

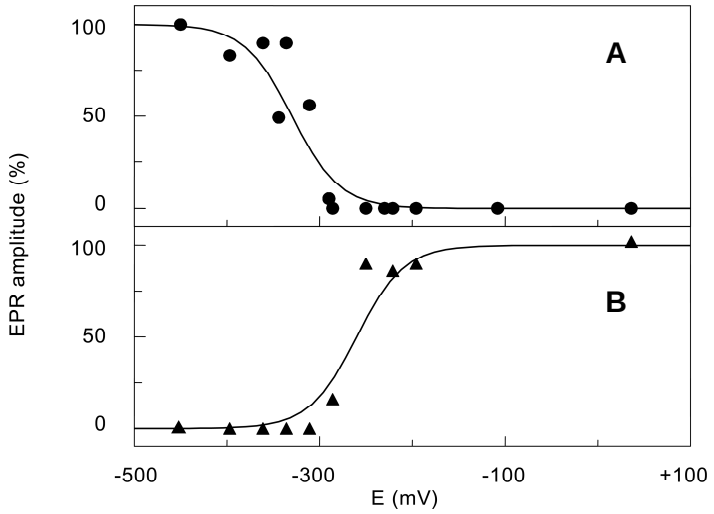

Figure 3. Dye mediated redox titrations of *P. furiosus* FOR. Trace A is the amplitude of the $[4Fe\text{-}4S]^{+}$ S=3/2 signal and is monitored at g = 5. Trace B is the amplitude of the W(V) mid-potential signal monitored at g = 1.94.

Low potential tungsten (V) signals slowly developed when FOR was incubated at room temperature with excess dithionite or formaldehyde in the absence of mediators. The EPR signals for dithionite versus formaldehyde reduced samples were significantly different (see figure 1). In figure 4 it can be seen that the substrate reacts faster with the enzyme than dithionite does. Within four minutes the protein (200 μM) reduced with 10 mM substrate reaches equilibrium ($k_{app} \approx 0.9$ min^{-1} assuming first-order kinetics) while this takes some 30 minutes for the dithionite-incubated sample ($k_{app} \approx 0.14$ min^{-1}). After equilibrium was reached the samples were heated to 60 °C and they were then flash-frozen and measured at different time intervals. After incubation at 60 °C with dithionite or with substrate for 60 minutes, the amount of EPR-detected tungsten increased to 10-20 % of the total amount of chemically determined W (cf the y-axis in figure 4). The rate of enzyme reduction is now similar with formaldehyde or with dithionite with $k_{app} \approx 0.12$ min^{-1} and 0.2 min^{-1}, respectively.

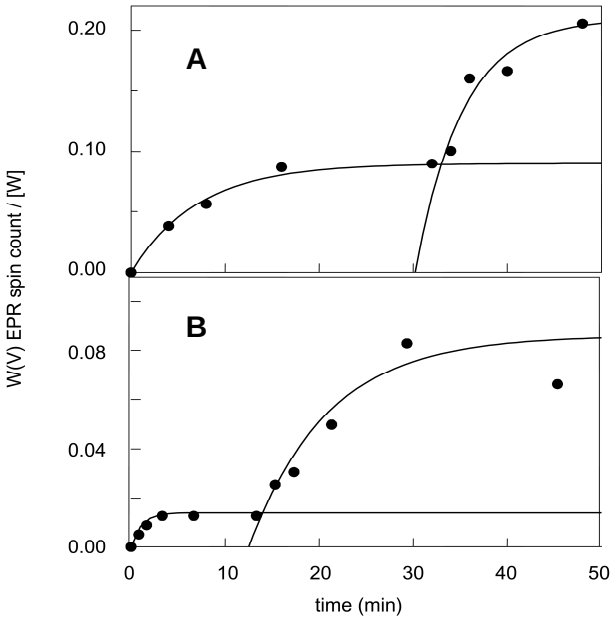

Figure 4. Kinetic reductions of *P. furiosus* FOR. Trace A is from enzyme reduced with dithionite and trace B from enzyme reduced with formaldehyde. The traces that start at t = 0 are from incubations at ambient temperature (22 °C); the second phase represents subsequent incubations at 60 °C.

Dithionite, $S_2O_4^{2-}$, is a notoriously slow reductant of metalloproteins, but the substrate formaldehyde should react rapidly with FOR. To check a possible influence of the hydration (and subsequent polymerization) equilibrium of formaldehyde, in a separate experiment the enzyme was incubated at 60 °C with 1 M of substrate. Following freezing after 2 minutes both the low-potential W(V) and the $[4Fe\text{-}4S]^{1+}$ EPR signals were fully developed. Incubation for another 10 minutes at 60 °C resulted in a slight turbidity, but after freezing no changes were observed in the EPR spectra. Upon re-thawing turbidity increased, and the protein precipitated.

Steady-state kinetics studies were performed to confirm that the free formaldehyde, and not the hydrated form, is the substrate. The K_M and k_{cat} values were determined at 20 °C and 80 °C (Table 3).

Table 3. K_M values of *P. furiosus* FOR for formaldehyde at different temperatures[(a)]

	Temperature (°C)	
	20	80
K_M^{app} (mM)[(b)]	40 ± 9	6 ± 3
K_M^{*} (µM)[(b,c)]	25 ± 5	33 ± 17
k_{cat} (s^{-1})[(b)]	14 ± 1.4	54 ± 5
K_M^{app} (mM)[(d)]		25

[(a)] Reactions were carried out in 50 mM EPPS buffer (pH 8.4) with benzyl viologen (3 mM) as the electron acceptor, [(b)] this work, [(c)] K_M value corrected for free formaldehyde, [(d)] [8,10]

The K_M^{app} (apparent K_M) values are high (millimolar) but comparable with a value reported earlier [8,10]. The values at 20 °C and 80 °C approximately differ by an order of magnitude. However, when corrected for the concentration of free formaldehyde, the K_M values at the two temperatures are identical within experimental error. No activity was detected with either methanol or formic acid as substrate.

Incubation of FOR (14 mg/mL) in 100 mM Tris/HCl (pH 8.0) buffer with excess sodium sulfide (20 mM) and sodium dithionite (20 mM) under anaerobic conditions led to an enhancement of the specific activity by 40 %. The enhancement occurs within seconds and lasts for at least 8 hours. When only sodium dithionite was added no significant enhancement was observed. Also, sodium dithionite was not required to enhance the activity in presence of sodium sulfide, showing that only sulfide is required for the activation process.

Discussion

The formaldehyde oxidoreductases of the two *Thermococcales*, *T. litoralis* and *P. furiosus*, share a very high sequence homology. Previously, the redox chemistry of the tungsten and iron-sulfur prosthetic groups of *T. litoralis* FOR has been extensively studied [8] and a routine check on the equivalent groups of *P. furiosus* FOR would seem to be sufficient as a control experiment for consistency. We found, however, the *P. furiosus* enzyme to differ from the *T. litoralis* enzyme on six counts. Part of these differences in redox properties appear to be related to differences in specific activity, but another part represents an unexpected diversity in view of the sequence homology. Below, the spectroelectrochemical differences between the two FOR enzymes are listed, followed by a discussion to what extent they are significant in terms of structure and enzymatic action.

(i) The EPR of the reduced cubane is common for this type of cluster in tungsten enzymes, namely, a mixture of S=3/2 of intermediate rhombicity and of S=1/2. Contrarily, the *T. litoralis* enzyme is uncommon in that it exhibits predominantly S=3/2 of extreme rhombicity.

(ii) A high-potential W(V) signal, as reported for *T. litoralis* FOR, is not found in *P. furiosus* FOR, neither in high-activity enzyme nor in low-activity enzyme;

(iii) A mid-potential W(V) signal is found in *P. furiosus* FOR but only in low-activity enzyme and with a reduction potential that is over 200 mV more negative than the value reported for the *T. litoralis* enzyme;

(iv) *T. litoralis* FOR activity was found to increase 8-fold over an eight-hours time course when incubated at room temperature with excess sulfide plus dithionite, with concomitant changes in the mid-potential and high-potential W(V) EPR signals [8]. Contrarily, *P. furiosus* FOR activity is only 1.4-times increased by sulfide incubation, and this occurs within seconds and does not require dithionite. The final activities of slowly activated

enzyme from *T. litoralis* versus rapidly activated enzyme from *P. furiosus* are comparable (cf Table 1);
(v) In previously reported equilibrium redox titrations of *T. litoralis* FOR a low potential W(V) signal with reduction potentials E_m = -280 mV and E_m = -335 mV was assigned to active enzyme. The potentials are somewhat high for an enzyme that reduces a low-potential ferredoxin (E_m is circa -350 mV in *P. furiosus* ferredoxin [19]), which in turn can donate electrons to a membrane-bound hydrogenase producing molecular hydrogen [20]. Contrarily, redox titrations of *P. furiosus* FOR did not reveal any low-potential W(V) signal suggesting that the potentials are significantly lower than -0.4 V and/or that the tungsten acts as a two-electron acceptor;
(vi) The low-potential W(V) signal was not generated in *T. litoralis* FOR by incubation with formaldehyde at 80 °C, and this was suggested to be due to the higher reduction potential values compared, e.g., to AOR, aldehyde oxidoreductase [8]. With *P. furiosus* FOR the signal does develop upon incubation with formaldehyde or with dithionite. This occurs both at room temperature and – more extensively – at 60 °C, and this would be consistent with a value for $E_m(W^V/W^{VI}) < 0.4$ V, and an even lower $E_m(W^{IV}/W^V)$ value.
The extreme rhombicity of the high-spin cubane in *T. litoralis* FOR is unprecedented, however, at this time the structural basis for this rhombicity and for fractional ratios of high-spin/low-spin mixtures is not known, therefore the observed difference (i) between the two enzymes remains to be explained.
In *T. litoralis* FOR a high-potential W(V) species was assigned to a W-trithiolene chelate resulting from oxidation and insertion of a sulfur ligand; a mid-potential W(V) species was proposed to be derived from dithiolene oxidation; the effect of sulfide was proposed to be an activation of a desulfo-form of the enzyme to an as yet unspecified structure. All this would be compatible with present results on the *P. furiosus* FOR (ii-iv) when one assumes that the latter is intrinsically less susceptible to degradation, so that the as isolated enzyme is already predominantly in the sulfide-activated form, and that the mid-potential and high-potential W(V) forms are less likely to occur in this more stable enzyme.
What remains are results on the low-potential W(V) species in which the two active enzymes appear to differ (iv-vi) at least in part. In redox titrations the species is observed in *T. litoralis* FOR, while it is not in *P. furiosus* FOR. This might be explained with the observation that upon sulfide activation the signal is no longer found in *T. litoralis* FOR, while the *P. furiosus* FOR used in the present work is hardly sulfide activatable apparently because it is already fully active. An important apparent inconsistency remains: it appears to be impossible to create the low-potential W(V) species in *T. litoralis* FOR by incubation with substrate at elevated temperature. In these experiments the substrate concentration and incubation time were not specified, and a possible explanation might be found in the unusual chemical properties of the substrate in aqueous solution.
Formaldehyde reacts with water to methylene glycol, and the latter polymerizes to poly(oxymethylene) glycols [21]. For the equilibrium constant (association constant) for the hydration of ‘free’ formaldehyde at ambient temperature several values have been reported,

which are all of the order of 10^3 [22-25], and so approximately 0.1% of a formaldehyde solution is indeed formaldehyde. The K_A is also temperature dependent such that the concentration of free formaldehyde at 80 °C is circa nine times that at 20 °C [24]. The rate constant for hydrolysis of methylene glycol [22,24] at high temperatures is sufficient to ensure that the concentration of free formaldehyde is essentially constant on the time scale of steady-state enzymology.

Formaldehyde is metabolized with *sub*-millimolar K_M by many organisms typically via formation of an adduct with a C_1-carrier (e.g., glutathione) followed by oxidation (e.g., to S-formylglutathione) with subsequent release of formate, cf [26]. We propose that when formaldehyde is used as substrate for the tungstoenzyme FOR the free formaldehyde is used and not the hydrated form or one of its polymerization products based on the following arguments: (1) the low-potential W(V) species develops rapidly only when the concentration of *free* formaldehyde is made superstoichiometric with respect to enzyme concentration; (2) FOR is a member of the AOR family of enzymes that all catalyze the oxidation of aldehydes; (3) The K_M^{app} for formaldehyde at 20 °C is approximately seven times higher than at 80 °C. This correlates well with the free formaldehyde concentration which is estimated to be circa nine times higher at 80 °C [24].

A practical implication of this proposal would be that magnetic spectroscopic studies have been done thus far with substoichiometric substrate concentrations. A fundamental implication would be that the K_M for free formaldehyde is actually circa three orders of magnitude less than the K_M reported for nominal formaldehyde. This indicates that FOR is very specific for formaldehyde oxidation and thus that FOR could be an effective scavenger of metabolically produced formaldehyde. On the other hand, from an evolutionary point of view the development of a catalyst for the activation of the hydrate (methylene glycol) would perhaps seem to make more sense. Even at 80 °C there is still 200 times more hydrate than free formaldehyde in aqueous solution. It is therefore probable that formaldehyde is not the 'real' substrate of FOR. Roy et al. proposed that the physiological substrate of FOR could be a C_5 di- or semialdehyde. However, the lowest K_M found by Roy et al. would still be two orders of magnitude greater than the K_M for free formaldehyde. With a K_M of 0.8 mM the catalytic competence of the enzyme for glutaricdialdehyde is still not very high. It is concluded that the physiological substrate(s) for FOR (and also for AOR, WOR4 and WOR5) still remains to be identified, and steady state kinetic studies on a broad spectrum of aldehydes are planned.

The results of the EPR monitored experiments with substrate incubation imply that formaldehyde reacts with oxidized enzyme having W(VI) and $[4Fe\text{-}4S]^{2+}$. A pair of electrons is transferred to the tungsten reducing it to W(IV), and this is followed by reduction of the cubane cluster by rapid electron rearrangement over the enzyme according to the reduction potentials of the product-bound complex. In order to pin down a more detailed and complete reaction mechanism, extensive pre-steady-state kinetic studies are under way.

Acknowledgements

This research was supported by a grant from the Council for Chemical Sciences of the Netherlands Organization for Scientific Research (700.51.301).

References

[1] R.N. Schicho, L.J. Snowden, S. Mukund, J.B. Park, M.W.W. Adams, R.M. Kelly, Arch. Microbiol. 159 (1993) 380.
[2] S. Mukund, M.W.W. Adams, J. Bacteriol. 178 (1996) 163.
[3] R. Roy, M.W.W. Adams, J. Bacteriol. 184 (2002) 6952.
[4] L.E. Bevers, E. Bol, P.L. Hagedoorn, W.R. Hagen, J. Bacteriol.187 (2005) 7056.
[5] M.K. Chan, S. Mukund, A. Kletzin, M.W. Adams, D.C. Rees, Science 267 (1995) 1463.
[6] Y. Hu, S. Faham, R. Roy, M.W. Adams, D.C. Rees, J. Mol. Biol. 286 (1999) 899.
[7] M.D. Clay, F.E. Jenney, Jr., H.J. Noh, P.L. Hagedoorn, M.W.W. Adams, M.K. Johnson, Biochemistry 41 (2002) 9833.
[8] I.K. Dhawan, R. Roy, B.P. Koehler, S. Mukund, M.W. Adams, M.K. Johnson, J. Biol. Inorg. Chem. 5 (2000) 313.
[9] M.K. Johnson, D.C. Rees, M.W. Adams, Chem. Rev. 96 (1996) 2817.
[10] R. Roy, S. Mukund, G.J. Schut, D.M. Dunn, R. Weiss, M.W. Adams, J. Bacteriol.181 (1999) 1171.
[11] A.F. Arendsen, P.T.M. Veenhuizen, W.R. Hagen, FEBS Lett. 368 (1995) 117.
[12] N. Raven, N. Ladwa, D. Cossar, R. Sharp, Appl. Microbiol. Biotech. 38 (1992) 263.
[13] P.L. Hagedoorn, P. van't Slot, H.P. van Leeuwen, W.R. Hagen, Anal. Biochem. 297 (2001) 71.
[14] A.J. Pierik, W.R. Hagen, Eur. J. Biochem. 195 (1991) 505.
[15] W.R. Hagen, Adv. Inorg. Chem. 38 (1992) 165.
[16] W.R. Hagen, D.O. Hearshen, L.J. Harding, W.R. Dunham, J. Magn. Reson. 61 (1985) 233.
[17] C. Holliger, A.J. Pierik, E.J. Reijerse, W.R. Hagen, J. Am. Chem. Soc. 115 (1993) 5651.
[18] S. Mukund, M.W. Adams, J. Biol. Chem. 268 (1993) 13592.
[19] P.L. Hagedoorn, M.C. Driessen, M. van den Bosch, I. Landa, W.R. Hagen, FEBS Lett. 440 (1998) 311.
[20] P.J. Silva, E.C.D. Van den Ban, H. Wassink, H. Haaker, B. De Castro, F.T. Robb, W.R. Hagen, Eur. J. Biochem. 267 (2000) 6541.
[21] I. Hahnenstein, H. Hasse, C.G. Kreiter, G. Maurer, Ind. Eng. Chem. Res. 33 (1994) 1022.
[22] I. Hahnenstein, M. Albert, H. Hasse, C.G. Kreiter, G. Maurer, Ind. Eng. Chem. Res 34 (1995) 440.
[23] Y.I. Tur'yan, Croatica Chem. Acta 73 (2000) 657.
[24] J.G.M. Winkelman, O.K. Voorwinde, M. Ottens, A.A.C.M. Beenackers, L.P.B.M. Janssen, Chem. Eng. Sci. 57 (2002) 4067.
[25] S.H. Hilal, L.L. Bornander, L.A. Carreira, QSAR & Combin. Sci. 24 (2005) 631.
[26] J.A. Vorholt, Arch. Microbiol. 178 (2002) 239.

Chapter 9

Concluding remarks and outlook

In this thesis several aspects of tungsten metabolism in *P. furiosus* have been explored: its tungstate transport system has been identified and characterized, studies on aspects of tungsten cofactor biosynthesis have been carried out and a new tungsten-containing aldehyde oxidoreductase (AOR), WOR5, has been purified and characterized. Overall, this study has contributed to a better understanding of different stages of tungsten metabolism in *P. furiosus*.

However, several issues remain to be solved. First of all, we have not been able to answer the questions why and how *P. furiosus* selectively incorporates tungstate instead of molybdate in the pterin cofactor of its AOR enzymes. We have excluded the transporter system as the only selective barrier, since the periplasmic binding protein WtpA is able to bind molybdate with a high affinity. Therefore, a step of metal selection is expected to take place during cofactor synthesis. We have done preliminary experiments in which MoeA proteins catalyze the oxoanion-dependent hydrolysis of MPT-AMP. These experiments need to be extended to determine the influence of the specific oxoanion on the rate of the hydrolysis reaction, in order to understand the role of the MoeA proteins in the process of selective metal incorporation.

Considering the remaining pathway of tungsten-cofactor synthesis, the mechanisms of bis-pterin formation and the optional nucleotide attachment also still need to be elucidated. These steps are also not understood for Moco biosynthesis.

We should also try to understand the ability of enzymes to discriminate between molybdate and tungstate on a molecular level. These oxoanions are very similar in their size and in their chemical properties, and at the current resolutions, no WtpA or ModA crystal structure has revealed any differences, e.g., bond lengths of the protein complexed with tungstate or molybdate. Apparently, a higher resolution measurement is required to explain the basis of affinity differences. In an attempt to reach this resolution, our laboratory has scheduled extended X-ray absorption fine structure (EXAFS) spectroscopy studies on the WtpA protein complexed with tungstate and molybdate. These studies will provide detailed information on the metal and its ligands in the first coordination shell, and might enable us to see differences in binding distances between the two oxoanions.

Returning to the cellular level, issues are still to be addressed in the fields of tungstate storage, the role of tungstate in regulation, and in the field of discovering new tungsten and molybdenum containing enzymes. As mentioned before, the genome of *P. furiosus* encodes two putative formate dehydrogenases that have never been purified. It would be interesting

to confirm that these enzymes indeed contain molybdenum or tungsten in a nucleotide-modified bis-pterin cofactor.

Future research might also include the development of an *in vivo* tungstoenzymes-expressing system. So far, it has not been possible to heterologously express tungsto-bispterin containing proteins in *E. coli*. However, the expression might be successful in a *mogA*/*moeA* host complemented with *P. furiosus* MoaB and MoeA1 or MoeA2 proteins. If the coupled expression of MoaB, MoeA1 or MoeA2, and a tungsten-containing AOR would afford holo-protein, mutational studies and bulk-protein production could be initiated. This would raise opportunities for technological exploration of these versatile enzymes.

Chapter 10

Summary
Samenvatting
Curriculum Vitae
List of Publications
Dankwoord

Summary

Tungsten is the heaviest element that exhibits biological activity (atomic number 74), when it is present in an enzyme. It is taken up by cells in the form of tungstate, and it is subsequently processed into an organic cofactor referred to as tungstopterin, which is found as active center in several enzymes. The first tungstoenzyme was isolated from an acetogenic *Clostridium* in 1983 and many others have followed since. The majority of the tungstoenzymes purified and characterized to date is isolated from (hyper)thermophilic anaerobic archaea. So far, no eukaryotic tungstoenzymes have been discovered.

Pyrococcus furiosus is a hyperthermophilic archaeon that grows anaerobically at an optimal temperature of 100 ˚C, strictly dependent on the presence of tungstate. The organism was originally isolated from a marine volcanic sediment in Italy, where both seawater tungsten concentration and temperatures are high. Over the last years, *P. furiosus* has become a model organism for hyperthermophiles, as many of its proteins have been the subject of research and its genome has been sequenced. Also regarding tungsten metabolism *P. furiosus* can be considered as a model: four tungsten containing aldehyde oxidoreductases were already characterized in some detail before the initiation of this study. The aim of this thesis project was to extend the knowledge on different aspects of tungsten metabolism in *P. furiosus* in particular on the tungstate uptake mechanism, tungsten cofactor synthesis, and to find new tungstoenzymes.

In chapter one of this thesis an overview is given on various aspects of the element tungsten, like its spectroscopic properties and its role in biological processes. Repeatedly, reference is made to the very similar, 'twin' element, molybdenum. The remaining of the thesis is divided into three parts, representing three different stages of tungsten metabolism in cells: part I describes the uptake of the metal by the cell; part II discusses the incorporation of tungsten into the pterin cofactor; and finally part III deals with the tungstoenzymes.

The first experimental data are presented in chapter two, in which the cloning, expression, purification, and characterization of the periplasmic binding protein of the tungsten ABC-transporter (WtpA) in *P. furiosus* are described. This protein was shown to bind tungstate with a very high affinity ($K_D \cong 17$ pM). It is also able to bind molybdate, however, with a 1000-fold lower affinity ($K_D \cong 11$ nM). This selectivity for tungstate was clearly shown in a tungstate-titration of WtpA saturated with molybdate, in which the tungstate efficiently replaced the molybdate in the binding pocket of the enzyme.

After the uptake of tungstate into the cell, the metal atom is inserted into a pterin cofactor in order to form tungstopterin. Prior to the step of metal insertion, the substrate, molybdopterin, needs to be activated by an adenyl transfer. In plants, this adenylylation step has previously been shown to be catalyzed by the Cnx1G protein, however, no archaeal homologues are found for this protein, and also in many bacterial genomes homologues are lacking. In chapter 3 we show that in *P. furiosus* the synthesis of adenylylated MPT (MPT-AMP) is catalyzed by the homohexameric MoaB protein. Subsequently, the reaction of the metal insertion is described in chapter 4 , where we show that MoeA1 and MoeA2 both

catalyze the tungstate and molybdate dependent hydrolysis of MPT-AMP. *In vivo* data on molybdenum incorporation in aldehyde oxidoreductase enzymes from *P. furiosus* are presented in chapter 5. When cells were grown on a 1000-fold excess of molybdate, molybdenum-containing formaldehyde oxidoreductase (FOR) and tungsten containing oxidoreductase number 5 (WOR5) could be purified, however, these molybdenum-substituted forms were not active.

In the last part of this thesis, two tungsten-containing enzymes are studied. Chapter 6 describes the purification and characterization of tungsten-containing oxidoreductase number five (WOR5). This newly characterized and putative last member of the AOR-family of *P. furiosus* has a very broad substrate specificity, exhibiting its highest catalytic activity on hexanal. Chapter 7 explores an interesting feature of WOR5: an attempt was made to clone, express and purify its adjacent gene (PF1479) encoding a putatively four [4Fe-4S] clusters binding protein. Based on structural homologies a heterotetrameric structure is proposed for the WOR5 and PF1479 proteins. In addition, whole-cell activity assays with different viologens as electron acceptor suggest a periplasmic localization for this complex. Chapter 8 presents an EPR study on the tungsten and iron-sulfur groups in *P. furiosus* formaldehyde oxidoreductase (FOR). It is also suggested that the K_M value for formaldehyde is three orders-of-magnitude less than previously reported, due to an unfavorable hydratation equilibrium which converts free formaldehyde, the actual substrate, into methylene glycol.

In a brief final chapter it is discussed what now ‘remains to be done’.

Loes E. Bevers

Samenvatting

Wolfraam is het zwaarste element uit het periodieke systeem dat biologische activiteit vertoont wanneer het aanwezig is in een enzym. Het wordt door cellen opgenomen in de vorm van wolframaat, en vervolgens wordt het ingebouwd in een organische cofactor die 'tungstopterine' wordt genoemd. Deze cofactor vormt het actieve centrum van verschillende enzymen.

Het eerste wolfraamenzym werd in 1983 gezuiverd uit een acetogeen *Clostridium* en daarna volgden er vele andere. Het grootste gedeelte van de tot op heden gezuiverde en gekarakteriseerde wolfraambevattende enzymen is geïsoleerd uit hyperthermofiele, anaerobe archaea. Tot nu toe is er nog geen wolfraam enzym ontdekt in een eukaryoot organisme.

Pyrococcus furiosus is een hyperthermofiel archaeon, dat optimaal groeit bij een temperatuur van 100 ˚C en dat zonder de aanwezigheid van wolframaat niet kan overleven. Het organisme werd voor het eerst ontdekt in zeevulkaansedimenten in Italië, waar zowel de watertemperatuur als de wolfraamconcentratie erg hoog zijn. De laatste jaren heeft *P. furiosus* zich steeds meer ontwikkeld als modelorganisme voor alle andere hyperthermofielen: er zijn al veel enzymen uit *P. furiosus* gezuiverd en onderzocht en ook het genoom is ontcijferd. We kunnen *P. furiosus* ook beschouwen als modelorganisme met betrekking tot het wolfraammetabolisme: aan het begin van deze studie waren al vier wolfraambevattende aldehyde oxidoreductase enzymen uit *P. furiosus* gezuiverd en gekarakteriseerd.

Het doel van dit proefschrift was het vergroten van de kennis over verschillende aspecten van wolfraammetabolisme in *P. furiosus* zoals: het cellulaire wolframaattransportmechanisme, de wolfraamcofactor synthese en het ontdekken van nieuwe wolfraam bevattende eiwitten.

In hoofdstuk 1 van dit proefschrift wordt een overzicht gegeven van verschillende bio-anorganische, spectroscopische en biologische eigenschappen van het element wolfraam. Regelmatig wordt verwezen naar het soortgelijke element: molybdeen. Het vervolg van het proefschrift is opgedeeld in drie gedeelten die ieder een ander stadium van het wolfraammetabolisme beschrijven; deel I begint met de cellulaire opname van het metaal, deel II behandelt de incorporatie van het wolfraam in de pterine cofactor en in deel III komen de wolfraambevattende enzymen aan bod.

De eerste experimentele data worden gepresenteerd in hoofdstuk 2, waarin het cloneren, het tot expressie brengen en het karakteriseren van het periplasmatische bindingseiwit van de wolframaat ABC transporter (WtpA) uit *P. furiosus* wordt beschreven. De experimentele data laten zien dat het eiwit wolframaat kan binden met een hele hoge affiniteit ($K_D \cong 17$ pM). Het eiwit is ook in staat om molybdaat te binden, hoewel die affiniteit 1000 maal lager is ($K_D \cong 11$ nM). De selectiviteit voor wolframaat werd bevestigd in een wolframaat-titratie van het molybdaat-gebonden eiwit. Bij deze titratie verving wolframaat, zeer efficiënt, alle gebonden molybdaat op de bindingsplaatsen in het enzym.

Nadat het wolframaat in de cel is opgenomen, wordt het metaalatoom ingebouwd in een pterine cofactor om het biologisch actieve 'tungstopterine' te verkrijgen. Voordat het metaal ingebouwd kan worden, moet het substraat, de pterine, geactiveerd worden door middel van een adenyl-modificatie. In planten wordt deze adenylyleringsstap gekatalyseerd door het Cnx1G enzym, maar zowel in de genomen van archaea als in de genomen van vele bacteriën is geen homoloog voor het Cnx1G eiwit aanwezig. In hoofdstuk 3 laten we zien dat de synthese van geadenylyleerd MPT (MPT-AMP) in *P. furiosus* gekataliseerd wordt door het homohexamere eiwit MoaB. Vervolgens komt de stap waarin het metaal wordt ingebouwd aan bod in hoofdstuk 4. Daar laten we zien dat de eiwitten MoeA1 en MoeA2 allebei de molybdaat- en wolframaat- afhankelijke hydrolyse van MPT-AMP katalyseren. *In vivo* data van de incorporatie van molybdaat in *P. furiosus* aldehyde oxidoreductase enzymen worden gepresenteerd in hoofdstuk 5. Uit cellen gegroeid op een 1000 maal overmaat aan molybdaat, konden molybdaatbevattend formaldehyde oxidoreductase (FOR) en wolfraam oxidoreductase nummer vijf (WOR5) worden gezuiverd. Deze molybdaat gesubstitueerde vormen waren echter niet actief.

In het laatste gedeelte van dit proefschrift, worden de wolfraambevattende eiwitten bestudeerd. Hoofdstuk 6 beschrijft de ontdekking, de zuivering en de karakterisering van het wolfraambevattende oxidoreductase nummer vijf (WOR5). Dit nieuw gekarakteriseerde, en mogelijk laatste lid van de AOR-familie in *P. furiosus* heeft een brede substraatspecificiteit. De hoogste activiteit werd echter gemeten wanneer hexanal als substraat aanwezig was. Hoofdstuk 7 belicht een interessant aspect van WOR5: er wordt een poging gedaan het naburige gen (PF1479), dat waarschijnlijk een vier [4Fe-4S] clusters bindend eiwit is, te kloneren en tot expressie te brengen. Op basis van structurele homologieën wordt een heterotretramere structuur voor WOR5 en PF1479 voorspeld. Daarnaast geven activiteitsmetingen aan hele cellen, met verschillende viologenen als electronenacceptor, aan dat het complex waarschijnlijk is gelokaliseerd in het periplasma. Hoofdstuk 8 beschrijft een EPR studie naar de wolfraam en ijzer-zwavel groepen in *P. furiosus* formaldehyde oxidoreductase (FOR). Daarnaast wordt voorgesteld dat de K_M waarde voor formaldehyde drie orden van grootte lager is dan eerder vermeld. Dit komt door een ongunstig hydratatieevenwicht waarin vrije formaldehyde, het eigenlijke substraat, omgezet wordt in methyleen glycol.

In een kort laatste hoofdstuk wordt bediscussieerd welke experimenten gedaan zouden moeten worden in de toekomst.

Loes E. Bevers

Curriculum Vitae

Loes Elizabeth Bevers werd geboren op 29 maart 1978 in Nijmegen. In 1996 behaalde ze haar gymnasium diploma aan het Coornhert gymnasium te Gouda, waarna ze direct begon aan een studie Scheikunde aan de Universiteit Utrecht. Haar afstudeerstage werd uitgevoerd in het 'Centre of Biomembranes and Lipid Enzymology' (CBLE) onder begeleiding van professor K.W.A. Wirtz en dr. A.P.M. de Brouwer. In augustus 2001 studeerde zij *cum laude* af in de richting Biochemie, waarna ze in september begon aan de post doctorale opleiding 'Advanced study in Biotechnology' aan de Technische Universiteit Delft. Deze studie rondde zij in september 2003 af met een onderzoek naar 'Edible films' uitgevoerd bij de afdeling Biotechnologie, Unilever Research Vlaardingen, onder begeleiding van dr. H.T.W.M. van der Hijden.

In oktober 2003 begon ze aan haar promotieonderzoek bij de Sectie Enzymology aan de Technische Universiteit Delft onder begeleiding van promotor professor W.R. Hagen. Een deel van haar onderzoek heeft ze uitgevoerd in het laboratorium van Professor G. Schwarz in het Instituut voor Biochemie van de Universiteit Keulen. De resultaten van haar promotieonderzoek zijn in dit proefschrift beschreven.

Na haar promotie zal ze werkzaam blijven als post-doc binnen de groep van prof. W.R. Hagen en zal ze gaan werken aan een geheel ander onderwerp: 'de enzymatische conversie van onverzadigde vetzuren naar hydroxy vetzuren'.

List of publications

- Loes E. Bevers, Peter-Leon Hagedoorn, Wilfred R. Hagen, 'The Bioinorganic chemistry of tungsten', *Coordination Chemistry Reviews, 2008, in press.*

- Loes E. Bevers, Peter-Leon Hagedoorn, José A. Santamaria-Araujo, Axel Magalon, Wilfred R. Hagen, Guenter Schwarz, 'The function of MoaB proteins in the biosynthesis of the molybdenum and tungsten cofactors', *Biochemistry*, 2008, 47: 949-956.

- Loes E. Bevers, Peter-Leon Hagedoorn, Gerard C. Krijger, and Wilfred R. Hagen,'Tungsten transport protein A (WtpA) in *Pyrococcus furiosus*: the first member of a new class of tungstate and molybdate transporters', *Journal of Bacteriology*, 2006, 188:6498-6505.

- Emile Bol, Loes E. Bevers, Peter-Leon Hagedoorn and Wilfred R. Hagen,'Redox Chemistry of Tungsten and Iron-Sulfur Prosthetic Groups in *Pyrococcus furiosus* Formaldehyde Ferredoxin Oxidoreductase' *Journal of Biological Inorganic Chemistry*, 2006, 11(8):999-1006.

- Loes E. Bevers, E. Bol, Peter-Leon Hagedoorn, Wilfred R. Hagen, 'WOR5, a novel tungsten-containing aldehyde oxidoreductase from *Pyrococcus furiosus* with a broad substrate specificity', *Journal of Bacteriology*, 2005, 187(20):7056-61.

Dankwoord

Ten slotte wil ik graag van de gelegenheid gebruik maken om iedereen te bedanken die een bijdrage heeft geleverd aan het tot stand komen van dit proefschrift. Ik wil beginnen met het bedanken van mijn promotor. Fred, ik ben je erg dankbaar voor de manier waarop je het mij mogelijk maakte om mijn promotie onderzoek uit te voeren. Je gaf me de vrijheid om mijn eigen keuzes te maken. Ik wil je bedanken voor je wetenschappelijke input en feedback die je op ieder moment bereid was te geven. Het heeft me vaak verbaasd waar je, ogenschijnlijk rustig, de tijd vandaan haalde met al dat werk, dat vele reizen, en al die vragende studenten en AIO´s op de achtergrond. Ik heb ontzettend veel van je geleerd in de afgelopen vier jaar en ik ben blij dat ik dat nog twee jaar als postdoc kan blijven doen.
Secondly, I would like to thank my collaborator from the University of Cologne, Guenter Schwarz. We have started our successful collaboration at the Gordon conference in Oxford, and two years later we were able to present our results at the next one in New London. Guenter, I want to thank you for giving me the opportunity to work in your lab in Cologne and for teaching me many things. I feel really lucky to have been able to work with you.
Terug in Delft wil ik graag Peter-Leon en Emile bedanken, met wie ik veel heb samengewerkt. Emile met name voor het werk dat we samen hebben gedaan aan FOR en WOR5, en Peter-Leon voor zijn wetenschappelijke input.
Dan mijn enige student, Nicolette. Jouw inbreng heeft zowel inhoudelijk als visueel heel erg bijgedragen aan hoofdstuk 7, bedankt daarvoor!
Ook Simon wil ik graag bedanken. Je interesse en inbreng in vele inspirerende wetenschappelijke discussies hebben me vaak aan het denken gezet en op nieuwe ideeën gebracht.
Natuurlijk wil ik ook mijn andere collega's en oud collega's bij Enzymology bedanken voor al hun gezelligheid, interesse en behulpzaamheid: Nahid, Barbara, Laura, Ana, Angela, Inga, Alidin, Alexey, Elena, Aida, Sandra, Jaap, Jana, Linda, Marieke, Daan, Urjan, Peter, Dirk, en Frankie, bedankt daarvoor!
Speciaal wil ik Marc en mijn paranimf Esengül noemen. Wat Marc is voor de eiwitzuiveringen is Esengül voor het cloneren. Jullie zijn twee onmisbare experts binnen Enzymologie! Ik heb het geluk gehad om met jullie allebei te mogen werken en ik heb echt ontzettend veel geleerd van jullie kennis en ervaring en de vele trouble-shoot sessies. En nog een speciaal woord van dank voor Esengül voor het ontwerpen en schilderen van de kaft van dit proefschrift.
Natuurlijk wil ik ook andere collega's binnen het Kluyverlab bedanken: Ann-Charlotte, Mirjam, Udo, Wouter, Marije, Daan, Merle, Janine, Frieda, Marlene, Lies, Ger, Sjaak, Jos, Joop, Astrid, Robert en de mannen van de werkplaats, bedankt voor al jullie hulp en gezelligheid!
Tijdens mijn promotie heb ik de mogelijkheid gehad om samen te werken met verschillende mensen binnen en buiten de TU Delft. Ik wil Gerard Krijger bedanken voor de samenwerking op het IRI, and of course my colleagues at the University of Cologne who

were always willing to help me and who were made my stays there so very pleasant: Simona, Katrin, Jose, Birthe, Iris, Oliver and Jenni, thank you! I would also like to thank Axel Magalon from the Laboratoire de Chimie Bactérienne (IBSM, CNRS) in Marseille for our succesfull collaboration on the MoaB project.

Naast mijn onderzoek heb ik me met veel plezier ingezet voor de belangen van de promovendi aan de TU Delft samen met mijn collega's in het bestuur van Promood. Ik wil met name Frederik de Wit, Rudy Negenborn en Koen van Dam voor deze fijne samenwerking bedanken.

Mijn andere paranimf en oud-studiegenoot Jolein, wil ik ook graag bedanken. Natuurlijk als vriendin, maar bij deze vooral ook als collega-AIO. Bedankt voor de goede raad die je me hebt gegeven als ervaringsdeskundige op vele gebieden!

Tot slot wil ik mijn familie bedanken. Toon, Beppie, Emma, Miguel en Esteban. Jullie steun, interesse en vaak inspirerende andere kijk op mijn onderzoek zijn erg belangrijk geweest en hebben me op veel verschillende manieren geholpen. Heel erg bedankt voor alles!